ESA-WPP-345
December 2016

Proceedings of the

30th European Space Thermal Analysis Workshop

ESA/ESTEC, Noordwijk, The Netherlands

5–6 October 2016

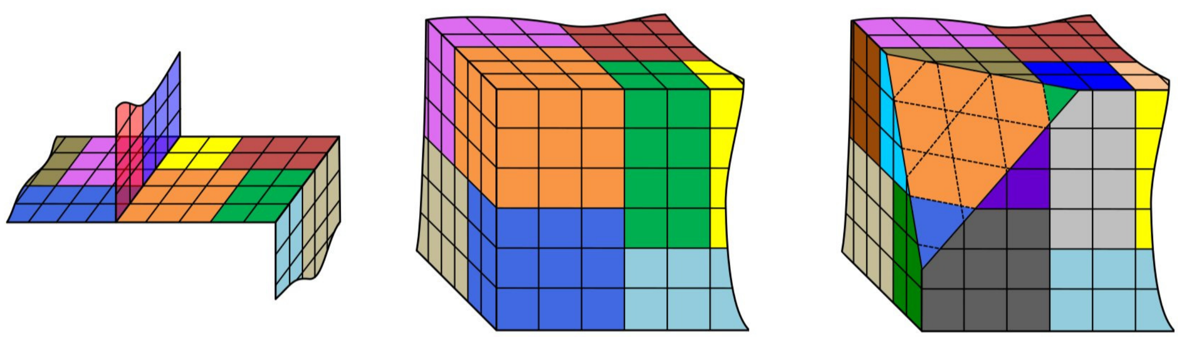

courtesy: University of Liège

European Space Agency
Agence spatiale européenne

Abstract

This document contains the presentations of the 30th European Space Thermal Analysis Workshop held at ESA/ESTEC, Noordwijk, The Netherlands on 5–6 October 2016. The final schedule for the Workshop can be found after the table of contents. The list of participants appears as the final appendix. The other appendices consist of copies of the viewgraphs used in each presentation and any related documents.
Proceedings of previous workshops can be found at http://www.esa.int/TEC/Thermal_control under 'Workshops'.

⇒ Please note that text like this are clickable hyperlinks in the document.
⇒ This document contains video material. By (double) clicking on picture of a video the movie file is copied to disk and then played with an external viewer. This has been tested with Adobe Reader 9 in Windows and Linux using vlc as external viewer. Other pdf readers may not work automatically. As a last resort the user can manually extract the movie attachment from the file and play it separately.

Contents

Appendices

Programme Day 1

9:00 Registration

9:45 **Opening address**
Wolfgang Supper (ESA/ESTEC, The Netherlands)

9:50 **Welcome and introduction**
Harrie Rooijackers (ESA/ESTEC, The Netherlands)

10:00 **GENETIK+** — Near-real time thermal model correlation using genetic algorithm
Guillaume Mas (CNES, France)

10:25 **World Space Observatory-Ultraviolet** — Thermal Analysis of Spacecraft Electronics
Samuel Tustain (RAL Space, United Kingdom)

10:50 **Thermal mapping on Bepicolombo's Mercury Planetary Orbiter (MPO) using SINASIV**
Claudia Terhes & Simon Appel (ESA/ESTEC, The Netherlands)

11:15 Coffee break in the Foyer

11:45 **Correlation of MLI Performance Measurement with a Custom MATLAB Tool**
Lars Tiedemann & Peter Lindenmaier (HPS GmbH, Germany)
João Pedro Loureiro (HPS Lda., Portugal)

12:10 **Solar Orbiter STM Thermal Testing and Correlation**
Scott Morgan (Airbus Defence and Space, United Kingdom)

12:35 **Automated thermal model correlation**
Martin Trinoga (Airbus Safran Launchers, Germany)

13:00 Lunch in the ESTEC Restaurant

14:00 **The challenges of modelling helium gas conduction and helium seal interfaces in ESATAN-TMS r7**
Nicole Melzack (RAL Space, United Kingdom)

14:25 **Improved integrated way of post-processing thermal result data**
Henri Brouquet (ITP Engines UK Ltd, United Kingdom)

14:50 **Thermal modelling of thruster nozzles and plumes for planetary landers**
Hannah Rana & Andrea Passaro (ESA/ESTEC, The Netherlands)

15:15 **Thermal experiments on LISA Pathfinder's Inertial Sensors**
Ferran Gibert (University of Trento, Italy)

15:45 Coffee break in the Foyer

16:15 **Quasi-autonomous spacecraft thermal model reduction**
Germán Fernández Rico (Max Planck Institute for Solar System Research, Germany)
Isabel Pérez Grande & Ignacio Torralbo (Universidad Politécnica de Madrid, Spain)

16:40 **Space Thermal Analysis through Reduced Finite Element Modelling**
Lionel Jacques
(Space Structures and Systems Laboratory, University of Liège & Centre Spatial de Liège, Belgium)
Luc Masset & Gaetan Kerschen (Space Structures and Systems Laboratory, University of Liège, Belgium)

17:05 **VEGA Launch Vehicle** — Improved Fluidic Thermal Prediction Model
P. Perugini & David Moroni & Matteo Tirelli (Avio S.p.A., Italy)

17:30 Social Gathering in the Foyer

19:30 Dinner in *Blu Beach*

Programme Day 2

9:00 **SYSTEMA — THERMICA**
Timothée Soriano & Antoine Caugant (Airbus Defense and Space SAS, France)

9:45 **Gas conduction and convection modelling techniques for the ExoMars Rover**
Joshua Katzenberg (Airbus Defence and Space, United Kingdom)

10:10 **Modelling of complex satellite manoeuvres with ESATAN-TMS**
Nicolas Bures (ITP Engines UK Ltd, United Kingdom)

10:35 **pyTCDT (TCDT 2.0)** — A flexible and scriptable toolbox for thermal analyses.
Marco Giardino & Andrea Tosetto (Blue Engineering, Italy)
James Etchells & Harrie Rooijackers (ESA/ESTEC, The Netherlands)

11:00 Coffee break in the Foyer

11:30 **A comprehensive integration methodology based on cosimulation** — Integration of thermal management in early phases of an electronic / electrical design
Benoit Triquigneaux & M.Bareille & Julien Pouzin & Laurent Labracherie & J.Vidal
(ALTRAN Technologies, France)

11:55 **THERM3D / e-Therm GMM (conductive) and TMM generation of thermo-mechanical antenna support designed for ALM**
Patrick Connil & Jean Paul Dudon & Thierry Basset & Patrick Hugonnot (TAS, France)
François Brunetti (DOREA, France)

12:20 **Development towards 3D thermography**
Gianluca Casarosa (ESA/ESTEC, The Netherlands)

12:45 **Data exchange for thermal analysis** — a status update
James Etchells & Duncan Gibson & Harrie Rooijackers & Matthew Vaughan (ESA/ESTEC, The Netherlands)

13:00 Closure

13:00 Lunch in the ESTEC Restaurant

Opening address

Good Morning Ladies and Gentlemen
Dear Colleagues and Friends

On behalf of the European Space Agency, I have the pleasure to welcome all of you to this 30th edition of the Space Thermal Analysis Workshop here at ESTEC and I would like to express a warm welcome to all participants coming from various ESA Member States and a number of other countries.

30th anniversary ! That is quite an achievement and also a sort of record.

It started out as the ESATAN workshop in 1985 with 38 attendants and was promoted and organized by my now retired colleague Charles Stroom with the aim

- to introduce the ESATAN space thermal analysis tool to the European thermal community as a replacement for SINDA
- and to create a forum to exchange information and experience between users and developers

The second workshop was held in 1987 and called "ESATAN Users Meeting". After the third one in 1989, the workshop has been taking place every year since that time.

I unfortunately did not attend the first two workshops in 1985 and 1987 - as I only joined the Agency in December of 1987. But then I had the pleasure to attend many of the 28 workshops over the years.

Looking back at the development of space thermal analysis there has been quite some changes and a lot of progress.

From tools like CBTS, VWHEAT (with VUFACT, RADCON, ROHCAT), VUVU, MATRAD, Manip, Polytan, ESABASE, ESARAD to today's ESATAN-TMS, EcoSim, Thermica/Thermisol, TMG and others with powerful pre- and post-processing tools and advanced GUI's make the life of the thermal engineer easier.

However, a word of warning from an old thermal engineer - any software tool is only as good as the engineer sitting on the other side of the terminal. Experience and thermal engineering knowledge is still very much needed prior to switching on the computer and using any of these tools. And the experience and knowledge is even more needed when looking at the results!

Over the years, the scope of the workshop has significantly evolved, as ESA's approach to the thermal tools also evolved.

The workshop objectives today are:

- to promote the exchange of views and experiences amongst the users of European thermal analysis tools and related methodologies
- to provide a forum for contact between end users and software developers
- to present new features of thermal tools and solicit feedback for development
- to present innovative methodologies, standardisation activities.

Let me also say a few words on statistics:

Over the last 30+ years we have had - including this year's - close to 600 presentations and almost 2000 registered external participants, some of them attending many workshops over the years. I want to sincerely thank all participants and authors, past and present.

This year again more than 100 participants have registered, which confirms the interest and important role of Thermal Software & Analysis Methods to the space community. For us, this is a clear sign of appreciation and a confirmation of the usefulness of this workshop and it also clearly demonstrates the continued need for such events to exchange information and to strengthen further cooperation on the subject as well as to provide recommendations for future developments.

I also want to take the occasion to thank all my colleagues - Harrie, Duncan and also the Conference Bureau - who have worked hard to prepare and organise these workshops.

I hope you will find this event both enjoyable and rewarding and I want to wish you all a very fruitful and interesting workshop.

Let me now hand over to my colleague Harrie Rooijackers, the organiser of the workshop, who will provide you with some details on the logistics.

Wolfgang Supper
Head of Thermal Division

Appendix A

Welcome and introduction

Harrie Rooijackers
(ESA/ESTEC, The Netherlands)


esa
30th European Space Thermal Analysis Workshop
Harrie Rooijackers
2016-10-05
ESA UNCLASSIFIED – For Official Use
ESA UNCLASSIFIED - For Official Use
European Space Agency

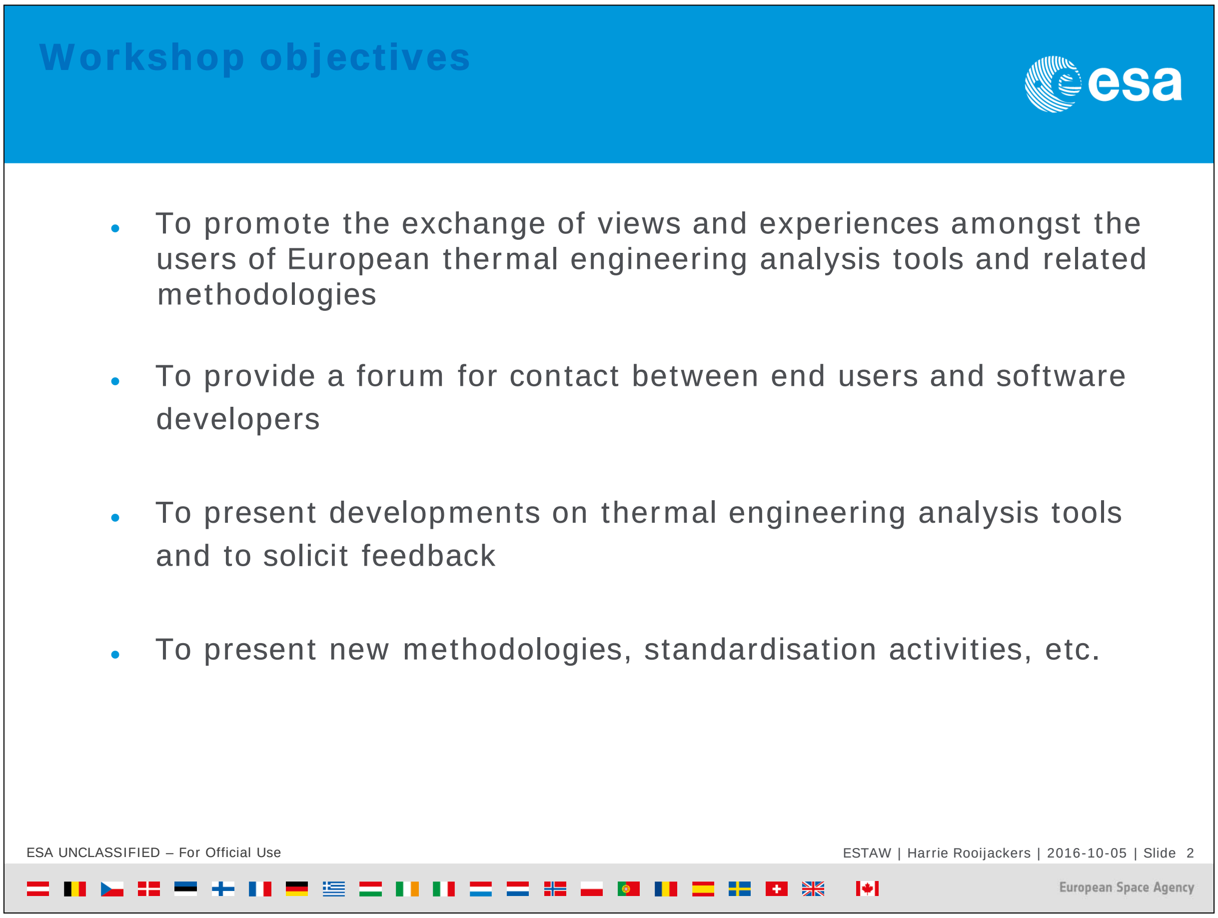
Workshop objectives
esa
• To promote the exchange of views and experiences amongst the users of European thermal engineering analysis tools and related methodologies
• To provide a forum for contact between end users and software developers
• To present developments on thermal engineering analysis tools and to solicit feedback
• To present new methodologies, standardisation activities, etc.
ESA UNCLASSIFIED – For Official Use
ESTAW | Harrie Rooijackers | 2016-10-05 | Slide 2
European Space Agency

ESA Team

esa

Benoit Laine — Head of Section
James Etchells
Duncan Gibson
Harrie Rooijackers
Matthew Vaughan

Workshop organised by the
Thermal Analysis and Verification Section TEC-MTV
with help from the ESA Conference Bureau

ESA UNCLASSIFIED – For Official Use

ESTAW | Harrie Rooijackers | 2016-10-05 | Slide 3

European Space Agency

Programme

esa

- Two-day programme
- Presentations of 25 min, including 5 minutes for questions and discussions
- Presenters:
  If not done already please leave your presentation (PowerPoint or Impress and PDF file) with Harrie before the end of Workshop.
- No copyrights, please!
- Workshop Proceedings will be supplied to participants afterwards, on the Web.

ESA UNCLASSIFIED – For Official Use

ESTAW | Harrie Rooijackers | 2016-10-05 | Slide 4

European Space Agency

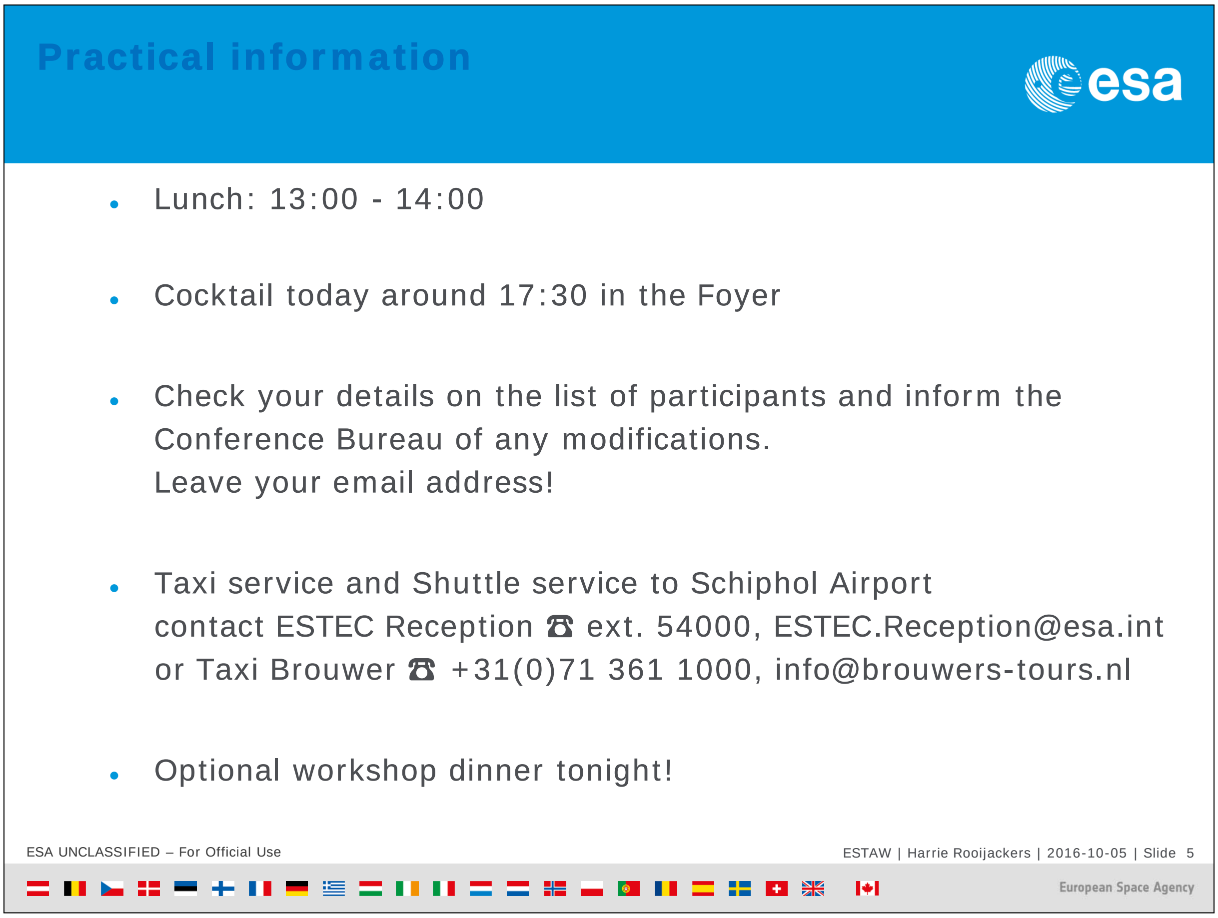
Practical information
esa
Lunch: 13:00 - 14:00
Cocktail today around 17:30 in the Foyer
Check your details on the list of participants and inform the Conference Bureau of any modifications.
Leave your email address!
Taxi service and Shuttle service to Schiphol Airport
contact ESTEC Reception ☎ ext. 54000, ESTEC.Reception@esa.int
or Taxi Brouwer ☎ +31(0)71 361 1000, info@brouwers-tours.nl
Optional workshop dinner tonight!
ESA UNCLASSIFIED – For Official Use
ESTAW | Harrie Rooijackers | 2016-10-05 | Slide 5
European Space Agency

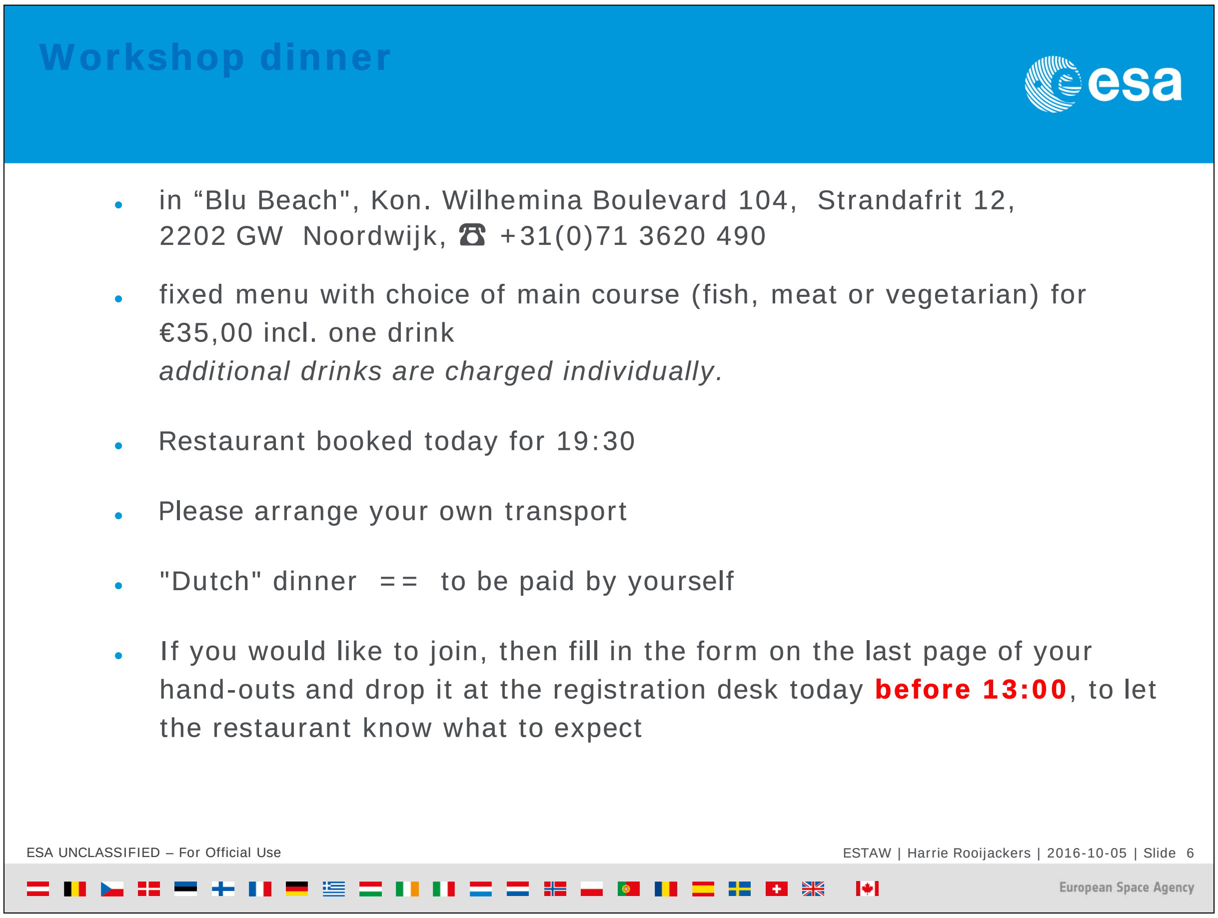
Workshop dinner
esa
in “Blu Beach", Kon. Wilhemina Boulevard 104, Strandafrit 12,
2202 GW Noordwijk, ☎ +31(0)71 3620 490
fixed menu with choice of main course (fish, meat or vegetarian) for €35,00 incl. one drink
additional drinks are charged individually.
Restaurant booked today for 19:30
Please arrange your own transport
"Dutch" dinner == to be paid by yourself
If you would like to join, then fill in the form on the last page of your hand-outs and drop it at the registration desk today before 13:00, to let the restaurant know what to expect
ESA UNCLASSIFIED – For Official Use
ESTAW | Harrie Rooijackers | 2016-10-05 | Slide 6
European Space Agency

Blu Beach

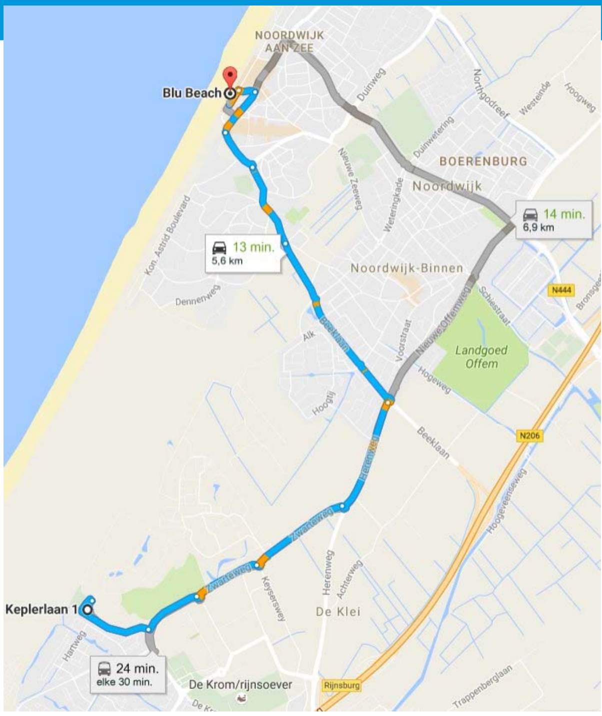

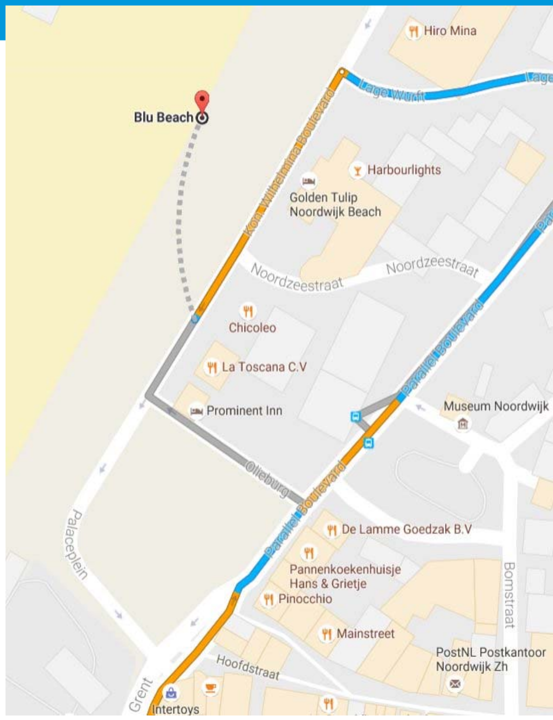

ESA UNCLASSIFIED – For Official Use

ESTAW | Harrie Rooijackers | 2016-10-05 | Slide 7

European Space Agency

ICES

- The 47th International Conference on Environmental Systems (ICES) will be held 16-20 July 2017, Charleston, South Carolina, USA.
- Deadline for submitting abstracts: 7 November, 2016
- For details see: https://www.ices.space

ESA UNCLASSIFIED – For Official Use

ESTAW | Harrie Rooijackers | 2016-10-05 | Slide 8

European Space Agency


Workshop
esa
Current workshop:
21 very interesting presentations covering:
• Range of general applications
• New tools
• Existing thermal tools
• Enhancements
• Applications
• User experiences
Next year:
31st workshop, 24-25 October 2017
ESA UNCLASSIFIED – For Official Use
ESTAW | Harrie Rooijackers | 2016-10-05 | Slide 9
European Space Agency

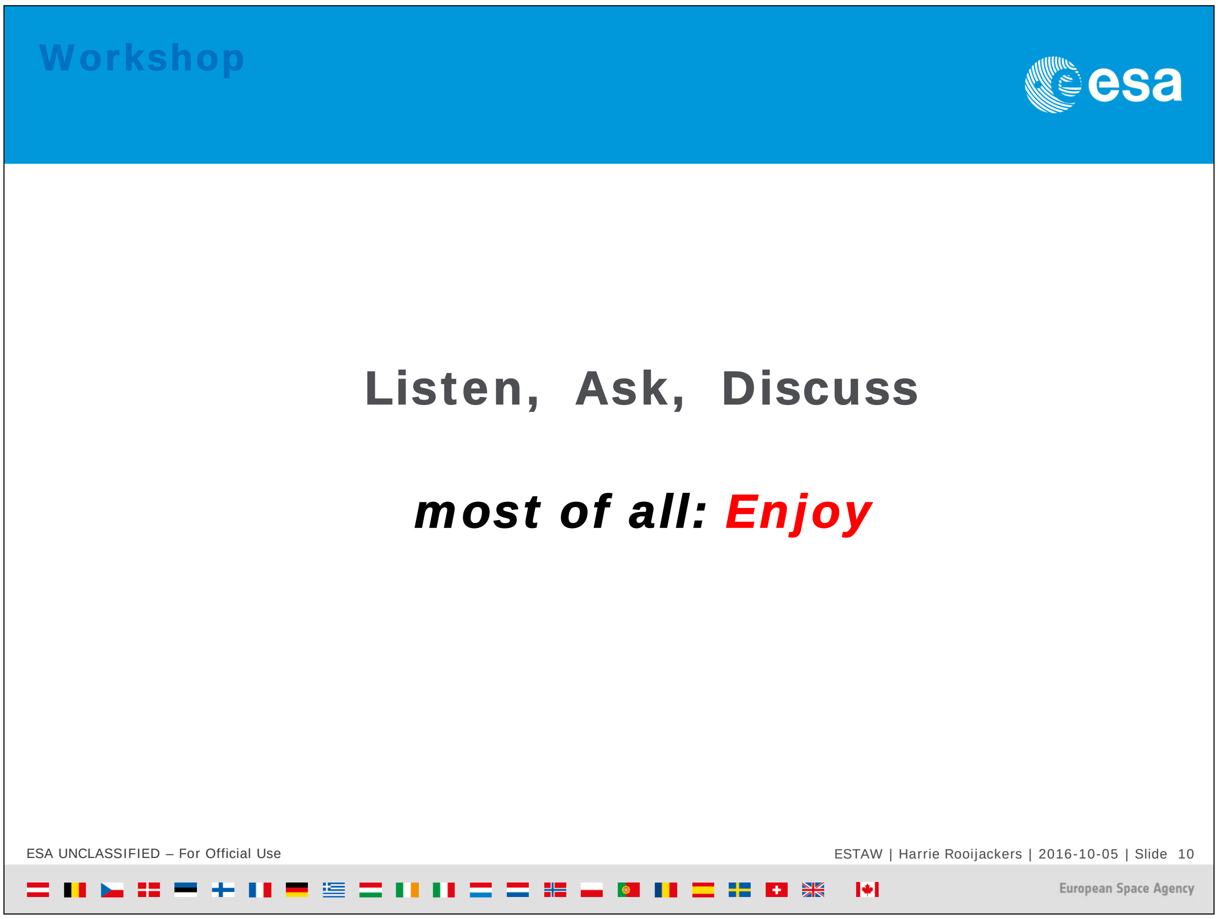
Workshop
esa
Listen, Ask, Discuss
most of all: Enjoy
ESA UNCLASSIFIED – For Official Use
ESTAW | Harrie Rooijackers | 2016-10-05 | Slide 10
European Space Agency

Appendix B

GENETIK+

Near-real time thermal model correlation using genetic algorithm

Guillaume Mas
(CNES, France)

Abstract

Using the recent improvements of GENETIK+, CNES tool that couple genetic algorithm to SYSTEMA, a new method dedicated to thermal test follow-up and explotation has been developed and validated.
This method, based on the previous development on analytical model reduction using genetic algorithm, offers the possibility to perform thermal sensors time extrapolation and near-real time thermal model correlation.
First tested on simple example, the method has been applied during real thermal test in CNES facilities.
The objective of the presentation is to:

- Present the method
- Show the potential of this method on real example

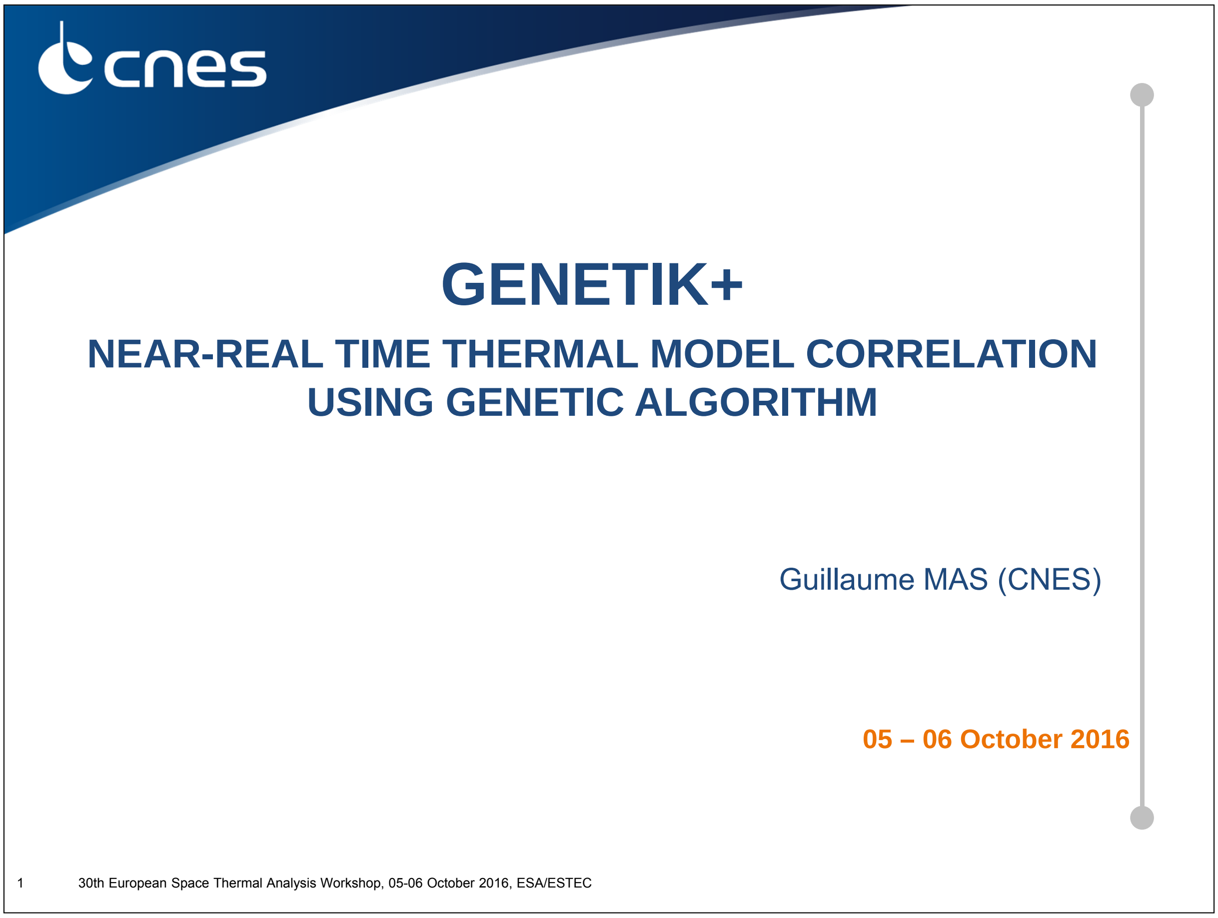
cnes
GENETIK+
NEAR-REAL TIME THERMAL MODEL CORRELATION
USING GENETIC ALGORITHM
Guillaume MAS (CNES)
05 – 06 October 2016
1
30th European Space Thermal Analysis Workshop, 05-06 October 2016, ESA/ESTEC

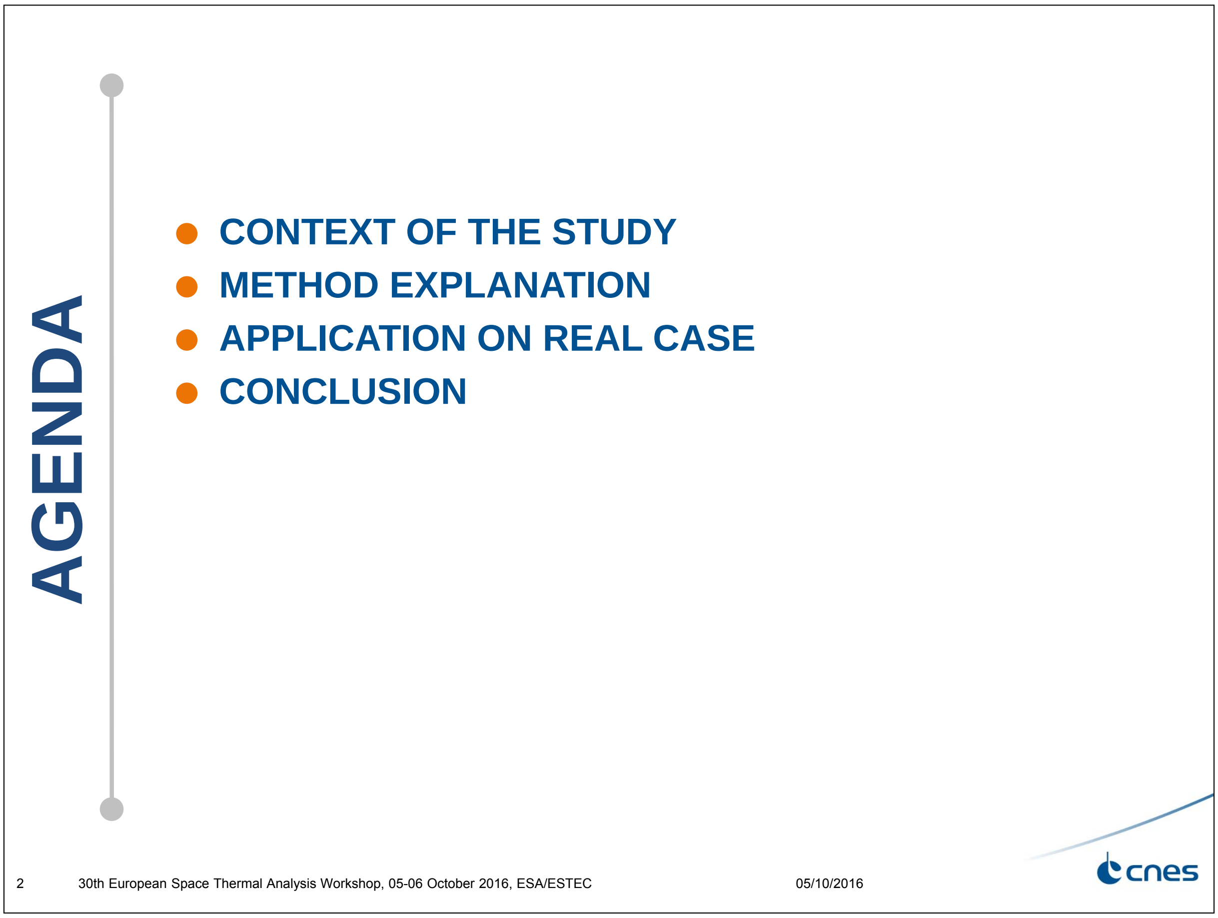
AGENDA
CONTEXT OF THE STUDY
METHOD EXPLANATION
APPLICATION ON REAL CASE
CONCLUSION
2
30th European Space Thermal Analysis Workshop, 05-06 October 2016, ESA/ESTEC
05/10/2016
cnes

AGENDA

- **CONTEXT OF THE STUDY**
- METHOD EXPLANATION
- APPLICATION ON REAL CASE
- CONCLUSION

3 30th European Space Thermal Analysis Workshop, 05-06 October 2016, ESA/ESTEC 05/10/2016

CONTEXT OF THE STUDY

Since 2005 GENETIK+ is developed by CNES :

- Allow to couple Systema with genetic algorithm
- 2015 upgrades:
  - Post processing module for full exploitation of results
  - Investigation of genetic algorithm possibilities at each step of TCS development

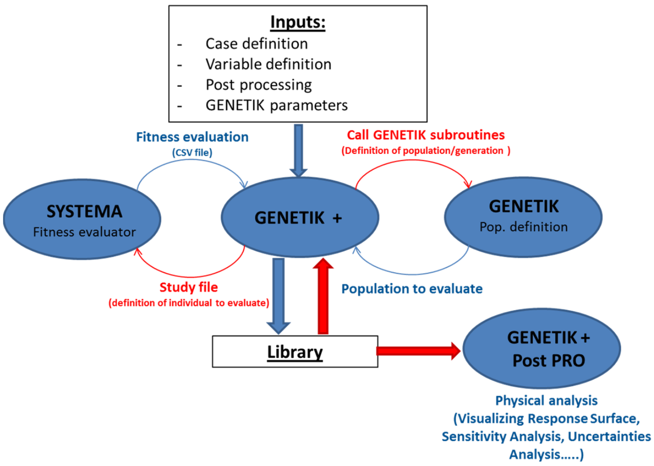

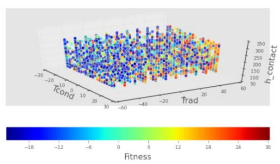

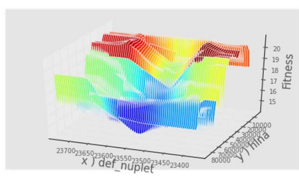

4 30th European Space Thermal Analysis Workshop, 05-06 October 2016, ESA/ESTEC 05/10/2016

CONTEXT OF THE STUDY

How Genetic algorithms can be used for thermal test follow-up:

- Test follow-up is based on preliminary test predictions
  - Performed using model not yet correlated …
  - Most of the time predictions are far away from test conditions
  - No simple way to update test predictions during the test (access to thermal software, computation time,…)
- Thermal engineer need a simple tool for:
  - Time extrapolation to estimate duration before phase ending
  - Start investigation on which parameters to adjust for model to test correlation
- One flexible and simple solution:
  - Provide an analytical formula for each thermal sensor

$$Temperature_{TC} = f(time, parameters)$$

5 30th European Space Thermal Analysis Workshop, 05-06 October 2016, ESA/ESTEC 05/10/2016 cnes

AGENDA

- CONTEXT OF THE STUDY
- **METHOD EXPLANATION**
- APPLICATION ON REAL CASE
- CONCLUSION

6 30th European Space Thermal Analysis Workshop, 05-06 October 2016, ESA/ESTEC 05/10/2016 cnes

METHOD EXPLANATION

How to obtain a simple analytical formula:

- Simple example – aluminium bar
  - Test control parameters: radiative environment temperature, conductive interface temperature
  - Thermal model parameters: thermal conductivity, specific heat capacity, contact coefficient

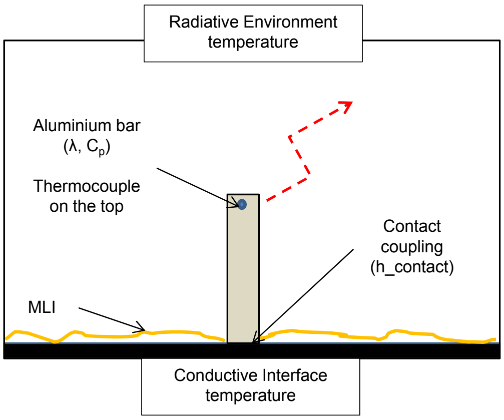

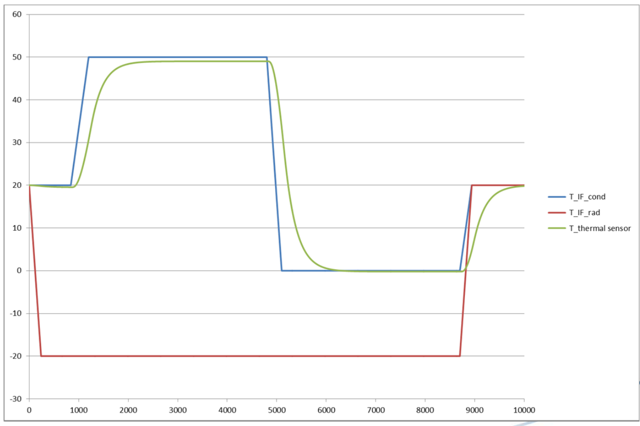

METHOD EXPLANATION

Problem simplification:

- Thermocouple = Thermal Node
- Heat equation = First order non linear system
- Hypothesis : TC thermal behavior ≈ First order linear system
  - Radiative fluxes << conductive fluxes
  - Conductive couplings constants over temperature
- F.O.L.S response to step : $f(t) = a.G.\left(1 - e^{-t/\tau}\right)$
  - a : Step amplitude
  - G : steady state Gain
  - τ : Time constant

METHOD EXPLANATION

Problem simplification:

- Superposition principle → TC = Multi inputs single output system

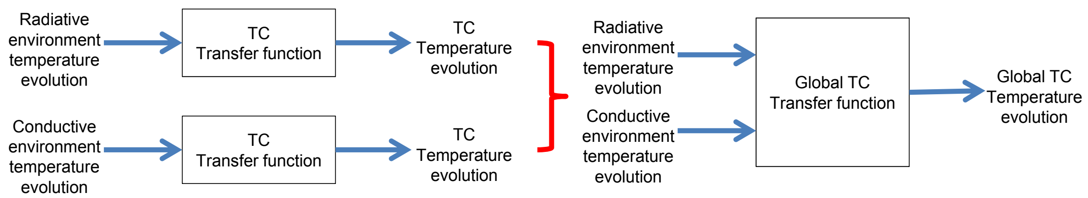

- Superposition principle → 1 single formula for each thermocouple

$$T_{TC}(t) = \sum_i G_i . a_i . \left(1 - e^{-t/\tau_i}\right)$$

  - ✦ a_i : Step amplitude of the input
  - ✦ G_i : steady state Gain corresponding to the input variation
  - ✦ τ_i : Time constant corresponding to the input variation

9 30th European Space Thermal Analysis Workshop, 05-06 October 2016, ESA/ESTEC 05/10/2016 cnes

METHOD EXPLANATION

Problem simplification:

- Step discretization of inputs:

$$T_{TC}(t) = \sum_i T_{TC}(t-1)_i + \left(T_{TC}(\infty)_i - T_{TC}(t-1)_i\right).\left(1 - e^{-t/\tau_i}\right)$$

  - ✦ $T_{TC}(\infty)_i$, steady state response for each contributor computed at time *t*
  - ✦ τ_i time constant for each contributor

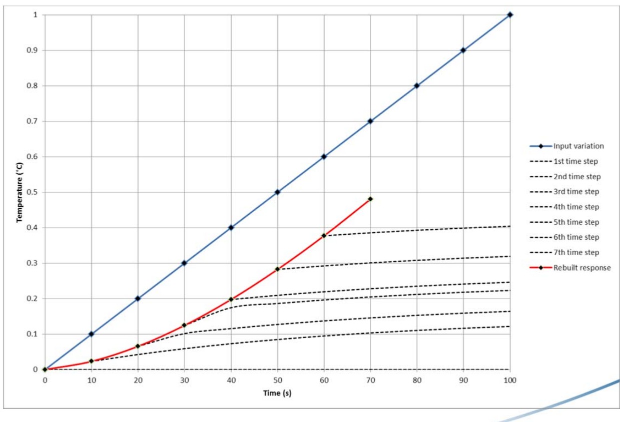

10 30th European Space Thermal Analysis Workshop, 05-06 October 2016, ESA/ESTEC 05/10/2016 cnes

METHOD EXPLANATION

Problem simplification:

- Dependency of $T_{TC}(\infty)$ and τ_i to model parameters (λ, h, mC_p...)...

$$T_{TC}(t, param.) = \sum_i T_{TC}(t-1, param.)_i + \left(T_{TC}(\infty, param.)_i - T_{TC}(t-1, param.)_i\right).\left(1 - e^{-t/\tau(param.)_i}\right)$$

- To obtain the global analytical response
  - $T_{TC}\infty$: Steady state response to all the parameters variation
  - τ_i: Time constant to the test control parameters variation

11 30th European Space Thermal Analysis Workshop, 05-06 October 2016, ESA/ESTEC 05/10/2016

METHOD EXPLANATION

How GENETIK+ can be used to obtain the global analytical response:

- In the simple example → need to obtain:
  - $T_{TC}\infty = f\left(T_{conductive\_IF}, T_{radiative\_IF}, \lambda, h_{contact}, C_p\right)$
  - $\tau_{conductive\_IF} = f\left(T_{radiative\_IF}, \lambda, h_{contact}, C_p\right)$
  - $\tau_{radiative\_IF} = f\left(T_{conductive\_IF}, \lambda, h_{contact}, C_p\right)$

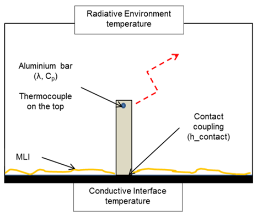

- GENETIK+ is used to smartly explore the space of solutions
  - Genetic algorithm will focus on most variable areas → Minimize number of calculation cases
  - 2 optimization searches (min/max) to well characterize the space of solution
- GENETIK+ Post processing module is used to extract the space of solution analytical formula
  - Polynomial interpolation
  - Coupled terms simplification → Sensitivity analysis (Sobol index)

12 30th European Space Thermal Analysis Workshop, 05-06 October 2016, ESA/ESTEC 05/10/2016

METHOD EXPLANATION

First results with nominal value of model parameters:

- Computed results vs. test data

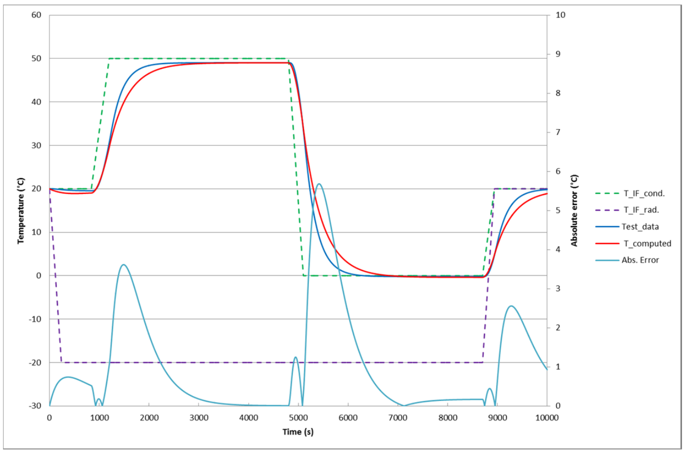

	λ	$h_{contact}$	C_p
Test data	146 W.m-1.K-1	625 W.m-2.K-1	875 J.K-1.kg-1
Initial values	100 W.m-1.K-1	500 W.m-2.K-1	800 J.K-1.kg-1

13 30th European Space Thermal Analysis Workshop, 05-06 October 2016, ESA/ESTEC 05/10/2016

METHOD EXPLANATION

Parameters correlation during test:

- GENETIK+ used to find the best set of parameters → Reduce global error
  - First iteration after 840 s.

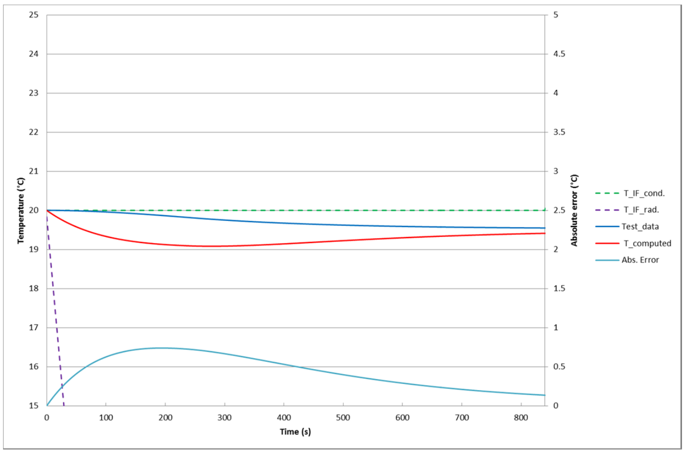

	λ	$h_{contact}$	C_p
Test data	146 W.m-1.K-1	625 W.m-2.K-1	875 J.K-1.kg-1
Initial values	*100 W.m-1.K-1*	*500 W.m-2.K-1*	*800 J.K-1.kg-1*
First iteration	200 W.m-1.K-1	850 W.m-2.K-1	810 J.K-1.kg-1

	Initial value	First iteration
Mean error (over 840s.)	0.6°C	0.44°C

14 30th European Space Thermal Analysis Workshop, 05-06 October 2016, ESA/ESTEC 05/10/2016

METHOD EXPLANATION

Parameters correlation during test:

- GENETIK+ used to find the best set of parameters → Reduce global error
  - Second iteration after 4800 s.

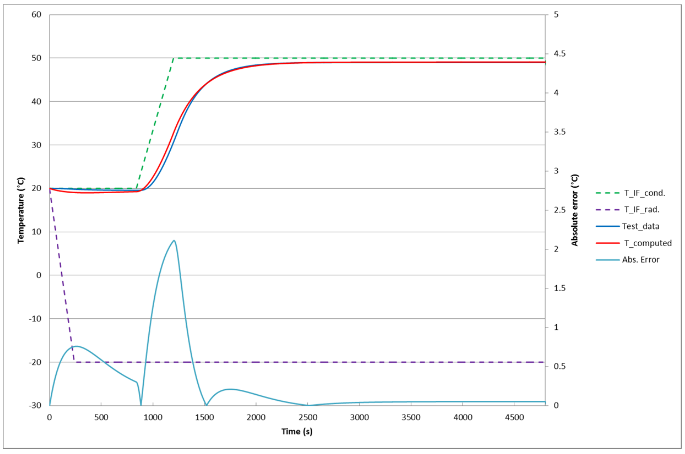

	λ	$h_{contact}$	C_p
Test data	146 $W.m^{-1}.K^{-1}$	625 $W.m^{-2}.K^{-1}$	875 $J.K^{-1}.kg^{-1}$
Initial values	*100 $W.m^{-1}.K^{-1}$*	*500 $W.m^{-2}.K^{-1}$*	*800 $J.K^{-1}.kg^{-1}$*
First iteration	*200 $W.m^{-1}.K^{-1}$*	*850 $W.m^{-2}.K^{-1}$*	*810 $J.K^{-1}.kg^{-1}$*
Second iteration	150 $W.m^{-1}.K^{-1}$	600 $W.m^{-2}.K^{-1}$	830 $J.K^{-1}.kg^{-1}$

	Initial value	2nd iteration
Mean error (over 4800s.)	0.76°C	0.29°C

15 30th European Space Thermal Analysis Workshop, 05-06 October 2016, ESA/ESTEC 05/10/2016

METHOD EXPLANATION

Parameters correlation during test:

- GENETIK+ used to find the best set of parameters → Reduce global error
  - Final iteration after 10000 s.

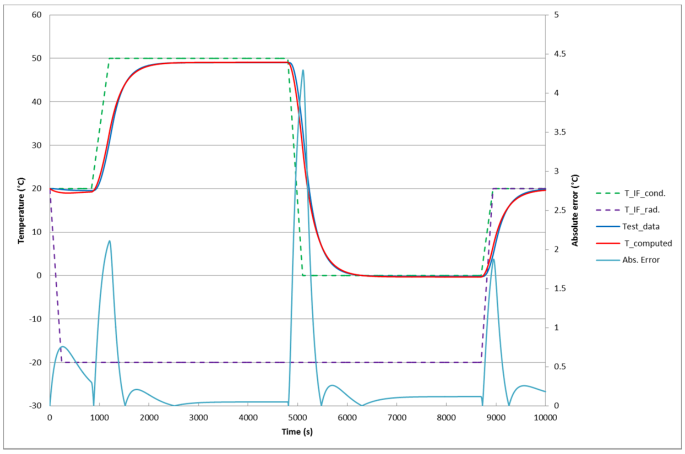

	λ	$h_{contact}$	C_p
Test data	146 $W.m^{-1}.K^{-1}$	625 $W.m^{-2}.K^{-1}$	875 $J.K^{-1}.kg^{-1}$
Initial values	*100 $W.m^{-1}.K^{-1}$*	*500 $W.m^{-2}.K^{-1}$*	*800 $J.K^{-1}.kg^{-1}$*
First iteration	*200 $W.m^{-1}.K^{-1}$*	*850 $W.m^{-2}.K^{-1}$*	*810 $J.K^{-1}.kg^{-1}$*
Second iteration	*150 $W.m^{-1}.K^{-1}$*	*600 $W.m^{-2}.K^{-1}$*	*830 $J.K^{-1}.kg^{-1}$*
Final iteration	146 $W.m^{-1}.K^{-1}$	625 $W.m^{-2}.K^{-1}$	875 $J.K^{-1}.kg^{-1}$

	Initial value	Final iteration
Mean error (over 10000s.)	1.05°C	0.38°C

16 30th European Space Thermal Analysis Workshop, 05-06 October 2016, ESA/ESTEC 05/10/2016

METHOD EXPLANATION

Method summary:

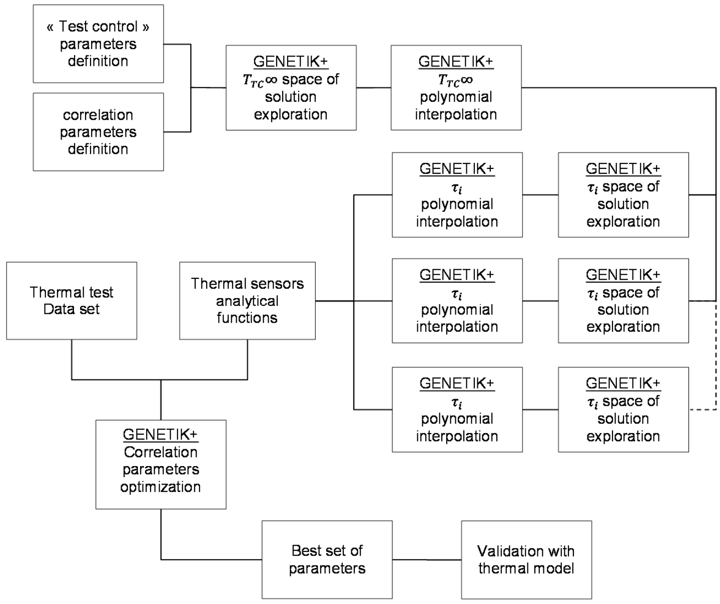

17 30th European Space Thermal Analysis Workshop, 05-06 October 2016, ESA/ESTEC 05/10/2016 cnes

AGENDA

- CONTEXT OF THE STUDY
- METHOD EXPLANATION
- **APPLICATION ON REAL CASE**
- CONCLUSION

18 30th European Space Thermal Analysis Workshop, 05-06 October 2016, ESA/ESTEC 05/10/2016 cnes

APPLICATION ON REAL CASE

Method tested during thermal test in CNES facilities:

- PHU instrument - TARANIS payload : Thermal balance test in CNES facilities

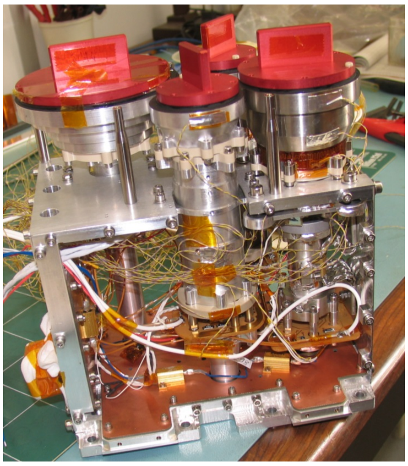

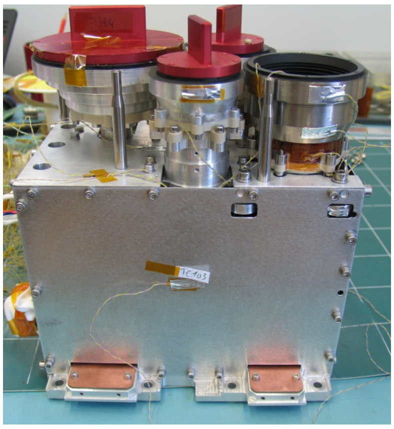

19 30th European Space Thermal Analysis Workshop, 05-06 October 2016, ESA/ESTEC 05/10/2016 cnes

APPLICATION ON REAL CASE

Method tested during thermal test in CNES facilities:

- Focus on electronics, box and only 1 optical head (21 TC)
- Thermal model quite detailed corresponding to phase C ≈ 300 nodes
- 13 parameters taken into account:
  - 4 “test control” parameters: Conductive and radiative environment, heat dissipation, heating line
  - 9 thermal model parameters: λ, contact coefficients,…
  - No parameter concerning thermal inertia
- Global computation time to obtain 21 functions = 120 hours (24 000 calculation cases)
  - $T_{TC}\infty \approx 40^h$ - 8000 calculation cases
  - $\tau_i \approx 20^h$ - 4000 calculation cases → 80h to compute 4 τ

20 30th European Space Thermal Analysis Workshop, 05-06 October 2016, ESA/ESTEC 05/10/2016 cnes

APPLICATION ON REAL CASE

Method tested during thermal test in CNES facilities:

- Preliminary results after model correlation with GENETIK+

	TC location	Min abs. error	Max abs. Error		Global mean abs. error
			Global	Without transient phases	
1	TRP	0°C	2.1°C	<0.5°C	0.3°C
2	Box	0°C	3.6°C	2°C	1.2°C
3	Electronic	0°C	1.8°C	<0.5°C	0.4°C
4	PH1	0.1°C	5.2°C	<3°C	1.9°C
5	PH1 electronic	0°C	7.6°C	<2°C	1.3°C
6	PH1	0°C	3.6°C	<2.5°C	0.9°C
7	PH1	0°C	6.1°C	<2.5°C	1.6°C
8	PH1	0°C	23.7°C	<8°C	5.5°C

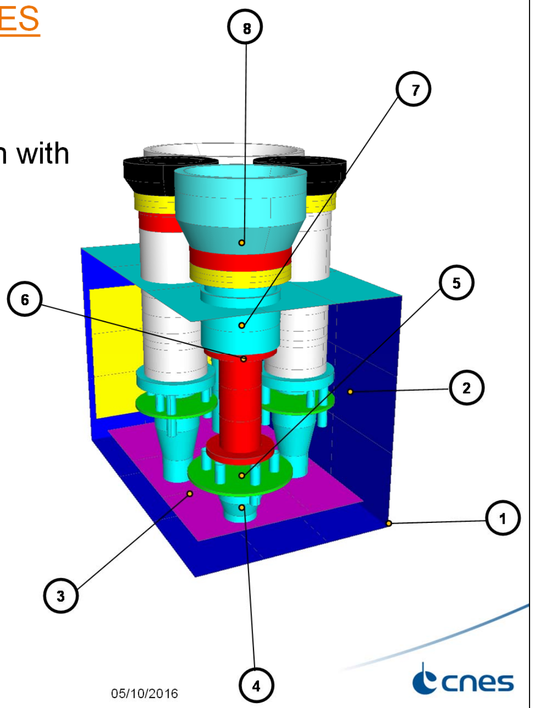

21 30th European Space Thermal Analysis Workshop, 05-06 October 2016, ESA/ESTEC 05/10/2016 cnes

APPLICATION ON REAL CASE

Method tested during thermal test in CNES facilities:

- Results after model correlation with GENETIK+

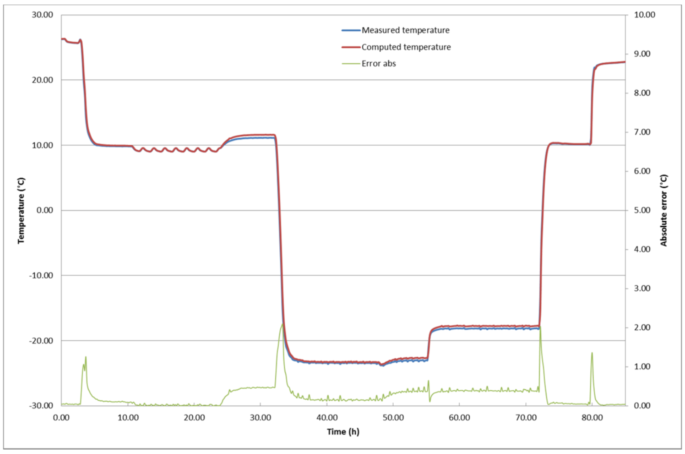

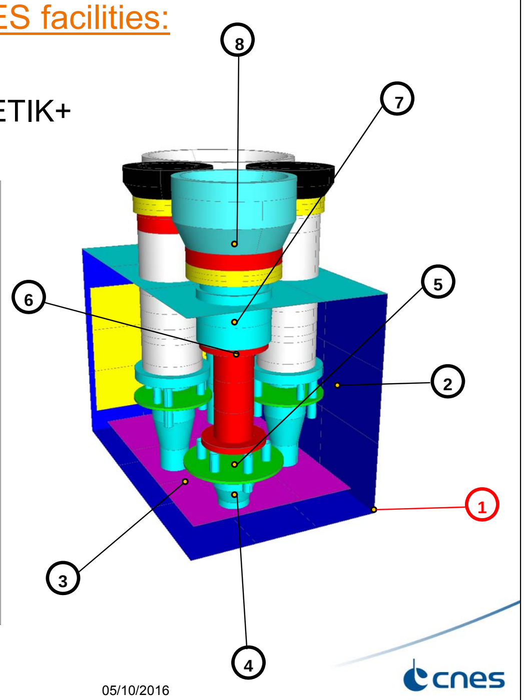

22 30th European Space Thermal Analysis Workshop, 05-06 October 2016, ESA/ESTEC 05/10/2016 cnes

APPLICATION ON REAL CASE

Method tested during thermal test in CNES facilities:

- Results after model correlation with GENETIK+

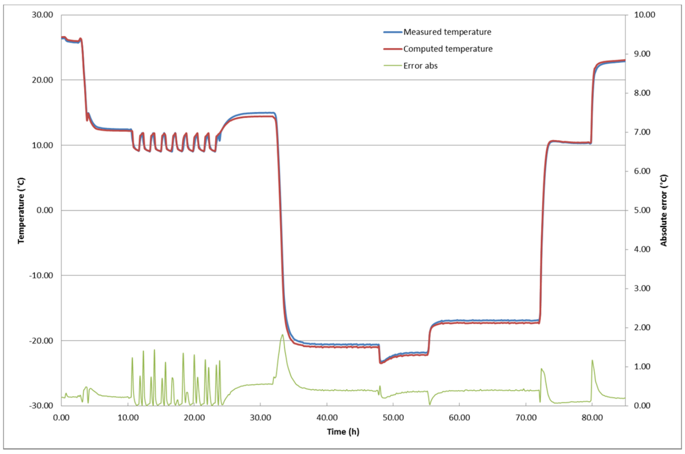

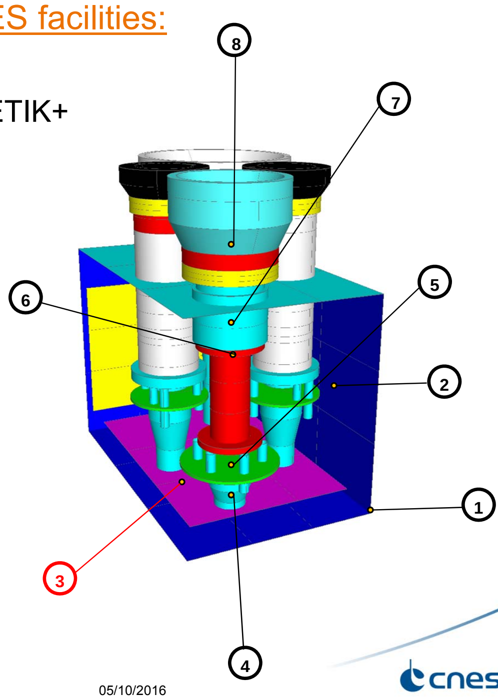

APPLICATION ON REAL CASE

Method tested during thermal test in CNES facilities:

- Results after model correlation with GENETIK+

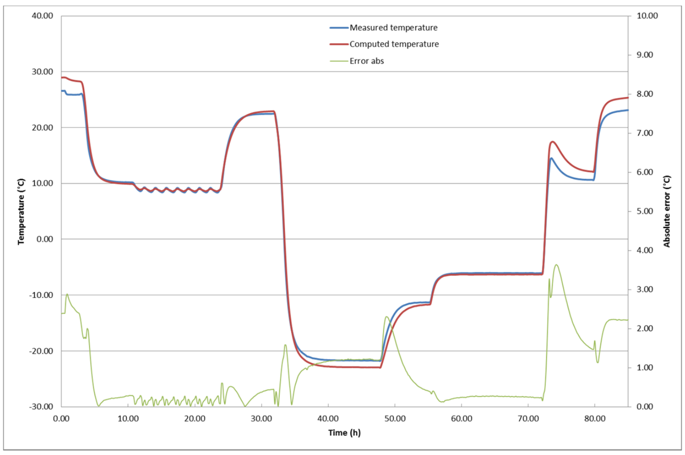

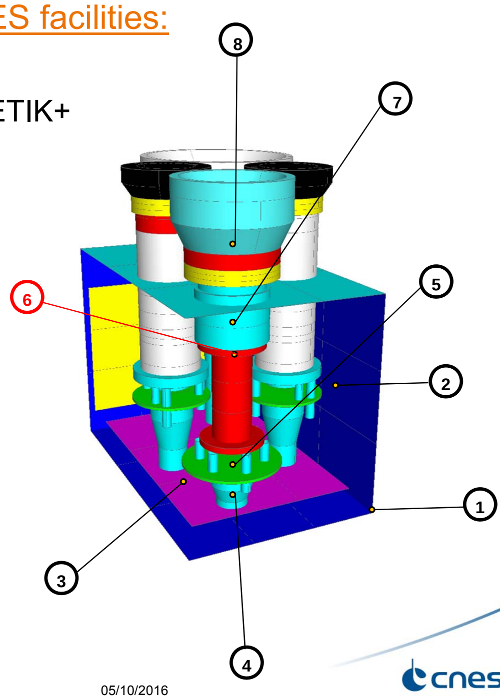

APPLICATION ON REAL CASE

Method tested during thermal test in CNES facilities:

- Results after model correlation with GENETIK+

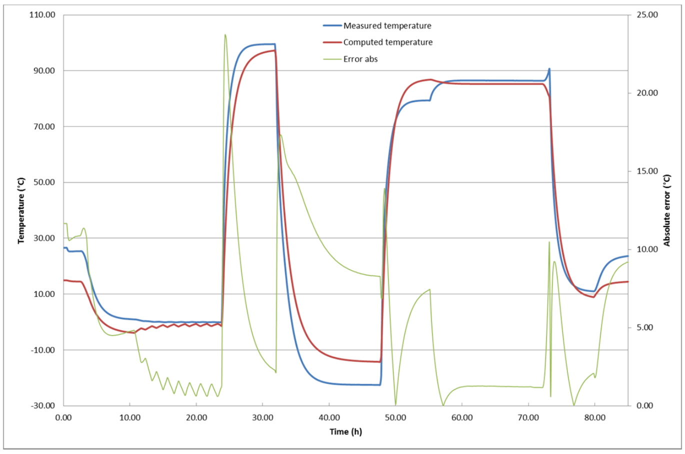

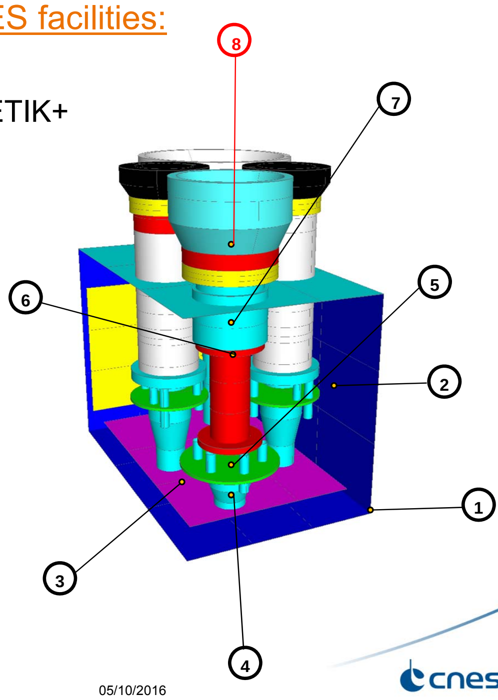

25 30th European Space Thermal Analysis Workshop, 05-06 October 2016, ESA/ESTEC 05/10/2016

AGENDA

- CONTEXT OF THE STUDY
- METHOD EXPLANATION
- APPLICATION ON REAL CASE
- **CONCLUSION**

26 30th European Space Thermal Analysis Workshop, 05-06 October 2016, ESA/ESTEC 05/10/2016

CONCLUSION

Conclusions:

- Based on the 2015 works on analytical reduction → new method developed for thermal test follow-up
- GENETIK+ used to obtain the analytical function of thermocouple thermal behaviour
- Time extrapolation with simple formula gives good results
- Possibility to use GENETIK+ to perform model correlation during the test (only few seconds for each calculation case)

- Some improvements :
  - Interpolation method to be upgrade (limited to 4th order)
  - Impact of calculation case density on interpolated function accuracy → to be studied
  - Improvement of the methodology for correlation using GENETIK+ (multi criteria optimization)

27 29th European Space Thermal Analysis Workshop, 03-04 November 2015, ESA/ESTEC 04/11/2015 cnes

Appendix C

World Space Observatory-Ultraviolet
Thermal Analysis of Spacecraft Electronics

Samuel Tustain
(RAL Space, United Kingdom)

Abstract

The World Space Observatory-Ultraviolet (WSO-UV) is an upcoming mission led by Roskosmos that aims to provide a major space observatory operational at ultraviolet wavelengths. RAL Space is working in collaboration with e2v on the World Space Observatory UV Spectrographs (WUVS) instrument, with RAL Space being primarily responsible for the design, build and testing of the Camera Electronics Box (CEB) that drives the instrument.

This work at RAL Space follows on from previous electronics box projects on spacecraft such as the NASA Solar Dynamics Observatory (SDO) and the Geostationary Operational Environmental Satellite R Series (GOES-R). Thermal analysis of the CEB provides a difficult challenge, since in order to be meaningful the analysis must capture the hot spots within the electronics that are caused by high power dissipating components on the printed circuit boards. The thermal characteristics of these components are often poorly defined, which therefore introduces uncertainty in the results. The requirement to de-rate component temperature limits in accordance with product assurance standards such as ECSS adds additional challenge, since it significantly reduces any thermal margin within the design.

With the dissipated heat loads generated by on-board electronics expected to steadily increase as hardware becomes more sophisticated, these are issues that are likely to become more prevalent for future space missions. This talk will examine the rationale behind the modelling of the CEB, discuss possible thermal management solutions and describe the ways in which uncertainty is being defined and accounted for within the analysis.

World Space Observatory-Ultraviolet (WSO-UV)

Thermal Analysis of Spacecraft Electronics

WSO - UV

Samuel Tustain
Spacecraft Thermal Engineer
STFC Rutherford Appleton Laboratory

30th European Space Thermal Analysis Workshop, 5th-6th October 2016

Science & Technology Facilities Council | RAL Space | e2V

RAL Space

Outline

- WSO-UV Overview
- WUVS Instrument
- Camera Electronics Box (CEB)
- Heritage
- Analysis
- Uncertainty and Mitigation Strategies
- Testing
- Future

WSO-UV Overview

- Also known as Spektr-UV
- Led by Roskosmos, with European involvement
- Launch currently planned for 2021
- Key objectives:
  - Continue to provide UV observation post-Hubble
  - To improve on Hubble
  - Study formation and evolution of our galaxy
  - Study exoplanet atmospheres and transits
- Contains a suite of instruments, including the WSO-UV Spectrographs (WUVS)
  - e2v are designing the cryostat and CCD assembly, RAL Space are designing the camera electronics box (CEB)

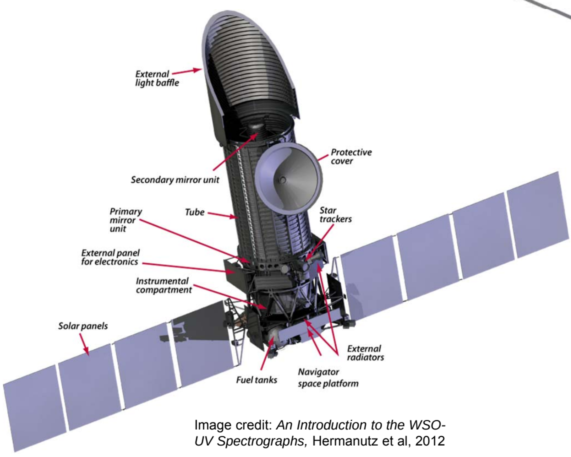

Image credit: *An Introduction to the WSO-UV Spectrographs,* Hermanutz et al, 2012

WUVS Instrument

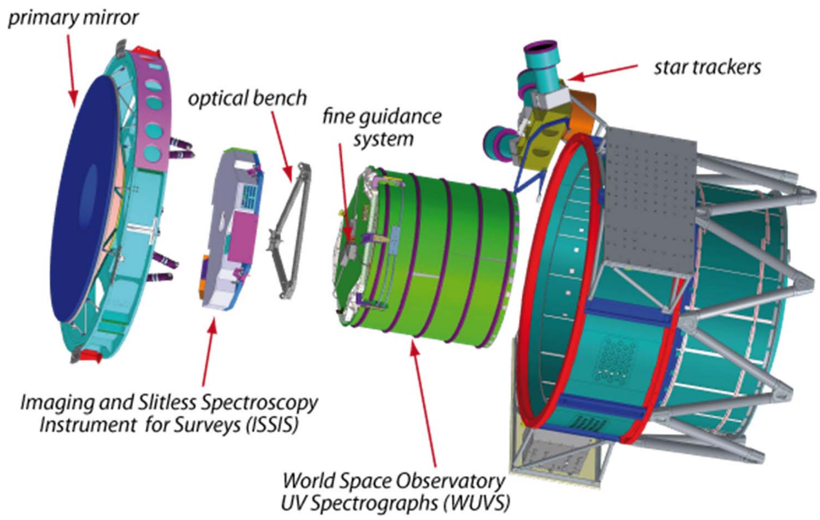

Image credit: WSO-UV Spanish Team Web Page: *http://www.wso-uv.es/index.php?id=12*

WUVS Instrument

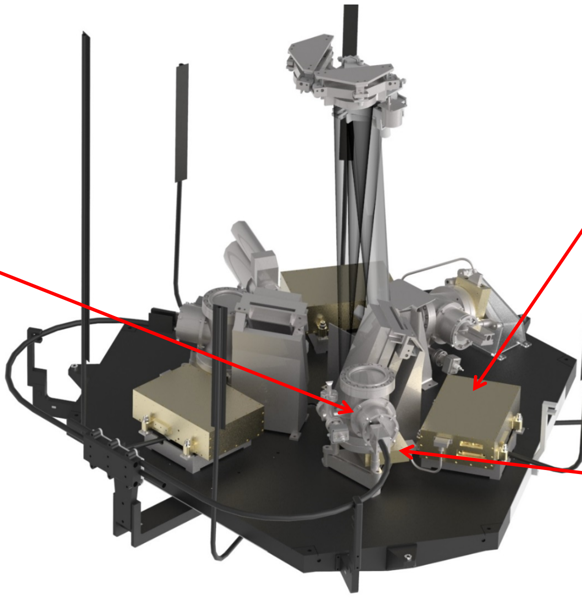

RAL Space Heritage

- NASA Solar Dynamics Observatory (SDO)
  - Provided flight electronics for two of three instruments
- NASA Geostationary Operational Environmental Satellite – R Series (GOES-R)
- Initially planned to re-use the GOES-R design for the WSO CEB
  - Unfeasible due to ITAR restrictions

Image credit: NASA

GOES-R Camera Electronics Box

Image credit: NASA

RAL Space

Camera Electronics Box (CEB)

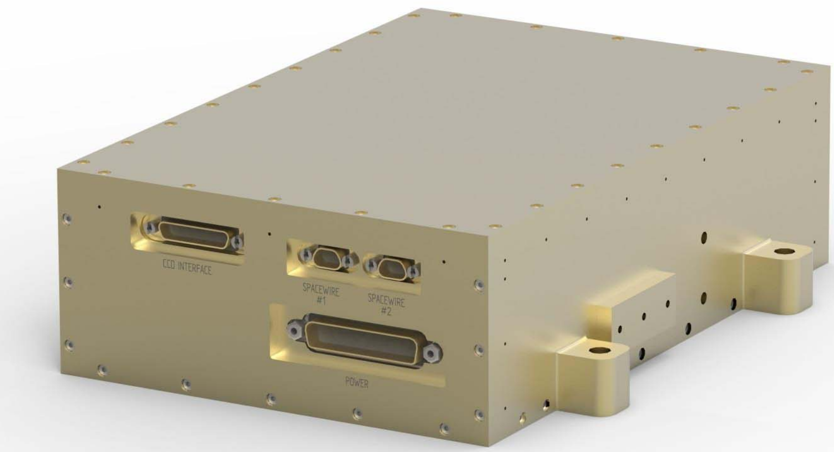

RAL Space

Camera Electronics Box (CEB)

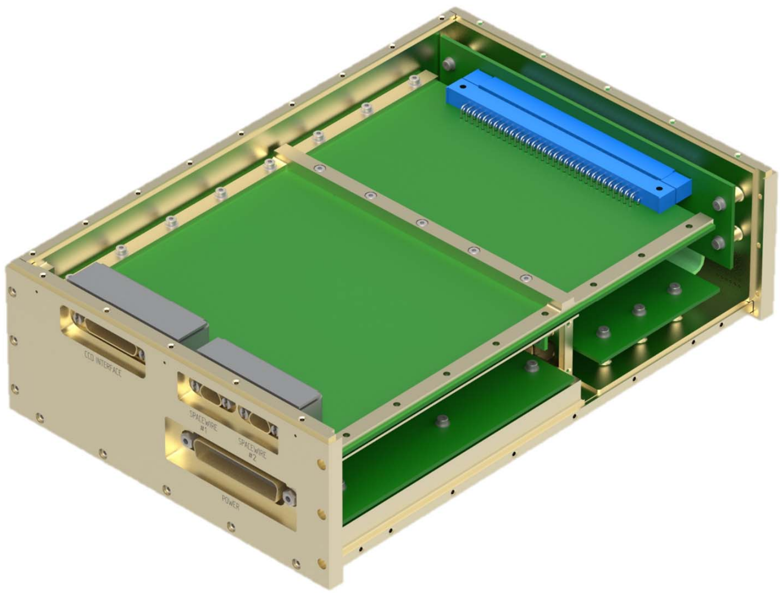

Camera Electronics Box (CEB)

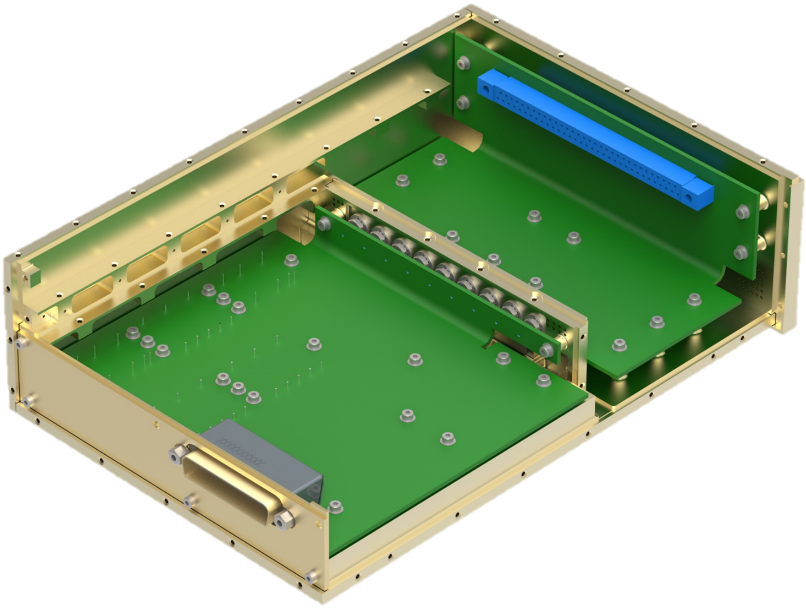

Thermal Challenges

- The CEB sits on a thermal plate that varies between -25 ºC and 50 ºC during the mission
- The total power dissipation for the CEB is 14.7 W
  - This must be conducted away via the base
  - Radiated heat flows to/from the CEB are assumed negligible
- The PCB components have defined temperature limits, which are then de-rated by 40 ºC according to ECSS standards
- Compliance with this must be analytically demonstrated, with qualification and uncertainty margins included
- The analysis must therefore capture the hot spots on the CEB caused at the components

Thermal Model

- Constructed using ESATAN-TMS r7sp2
- Submodels representing the structure and each of the PCBs
- Simple 'Enclosure' type radiative case to capture radiative couplings
- Conservative modelling rationale
  - Lots of uncertainty in modelling PCB components

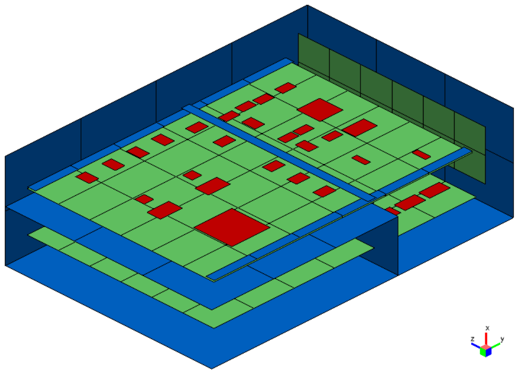

PCB Modelling

- In-plane thermal conductivity is calculated as a function of copper thickness (t_{Cu}) and overall thickness (t_{Ov}):

$$k = 385\frac{t_{Cu}}{t_{Ov}} + 0.87$$

Experimental Determination of Thermal Conductivity of Printed Wiring Boards, K. Azar and J.E Graebner, 1996

- Through-thickness conductance is ignored due to low thickness
- Conformance coating (ε = 0.878) is assumed

RAL Space

Component Modelling

- Components with either large surface area or large power dissipation are modelled.
  - Smaller components are accounted for by applying their dissipations directly to the PCB
- Each component comprised of junction (where heat is generated) and casing.
  - Junction-to-case conductance generally found in datasheets (although not always!)
  - Case-to-board conductance rarely found, and therefore estimated

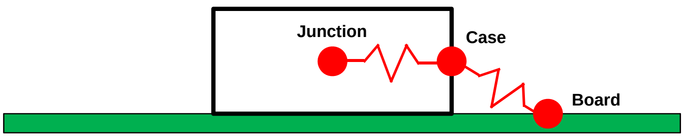

RAL Space

Case-to-board Conductance

- Estimated based on the number of pins and pin dimensions:

$$G = \frac{kA}{L} \times n$$

- Kovar (16 $Wm^{-1}K^{-1}$) assumed for all pins
- Area and number of pins varies from component to component
- Pin lengths are estimated based on the bending jig that RAL uses

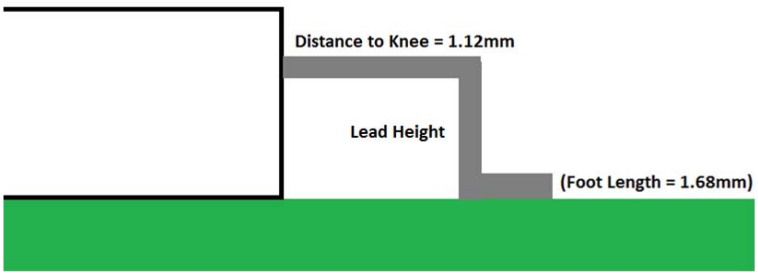

Uncertainty

- There are large uncertainties in this method, due to a lack of information from component manufacturers
- Characterising this in simple terms is difficult, because it varies from component to component
- In accordance with MIL-STD-1540, an uncertainty margin of +17 ºC has been applied
  - Based on experimental data
  - General practice on instrument projects until a thermal balance test has been performed

Results

This uncertainty presents issues, as some of the components are predicted to be within this margin during the hottest case (thermal plate at 50 ºC)

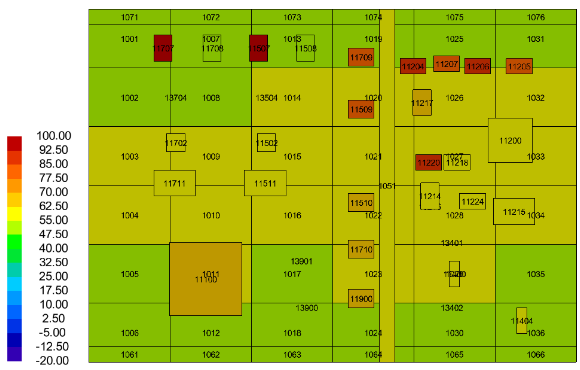

Component	Case Temperature (ºC)	Junction Temperature (ºC)	Derated Maximum Junction Temperature (ºC)	Junction Margin (ºC)
IC100	66.2	70.9	85	14.1
IC200	62.2	62.7	85	22.3
IC204	87.9	95.6	110	14.4
IC205	84.6	91.6	110	18.4
IC206	88.2	95.9	110	14.1
IC207	83.7	90.3	110	19.7
IC214	56.4	56.4	85	28.6
IC215	57.3	58.2	85	26.8
IC217	68.6	69.3	110	40.7
IC218	60.2	60.8	110	49.2
IC220	88.0	95.3	110	14.7
IC224	59.2	59.8	110	50.2
IC400	61.5	62.8	85	22.2
IC404	60.6	61.9	85	23.1
IC502	59.4	65.4	110	44.6
IC507	94.5	97.0	110	13.0
IC508	54.4	54.4	110	55.6
IC509	79.7	81.2	110	28.8
IC510	67.9	68.6	110	41.4
IC511	60.4	63.1	85	21.9
IC702	59.1	65.1	110	44.9
IC707	94.2	96.7	110	13.3
IC708	53.9	53.9	110	56.1
IC709	78.4	79.8	110	30.2
IC710	68.5	69.3	110	40.7
IC711	60.1	62.8	85	22.2
IC900	68.9	69.7	110	40.3

RAL Space

Mitigation Strategies

- Thermal filler
  - Improves case-to-board conductance, and analysis suggests significant temperature reductions
  - However it's messy and complicates the assembly process
- Testing
  - Conduct a thermal balance case during qualification thermal vacuum testing
  - Determines suitability of uncertainty margin

RAL Space

Testing

- Test carried out last month on Engineering Qualification Model (EQM)
- Thermocouples attached to problematic components
- Results demonstrate compliance with requirements, and components were cooler than the analysis predicted
  - Analysis too pessimistic?
  - Uncertainty approach unsuitable?

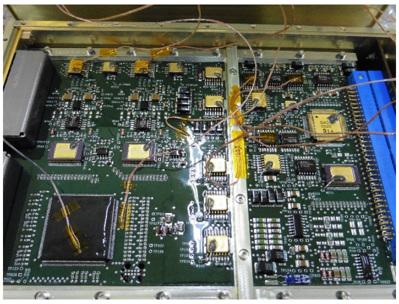

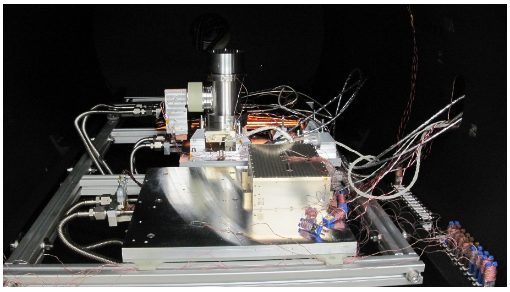

RAL Space

Future

- The thermal balance case has confirmed that thermal filler is not required for the flight model
- Correlation of thermal model required
- Future approach for uncertainty is challenging
  - Root sum squared (RSS)? $\Delta T_i = \sqrt{\sum_{k=1}^{n_p} \left(\Delta T_{p,k}\right)_i^2}$
  - Difficult to accurately characterise individual sources of uncertainty

RAL Space

Contact Details

Samuel Tustain
Thermal Engineering Group
Email: samuel.tustain@stfc.ac.uk
www.ralspace.stfc.ac.uk

Appendix D

Thermal mapping on Bepicolombo's Mercury Planetary Orbiter (MPO) using SINASIV

Claudia Terhes Simon Appel
(ESA/ESTEC, The Netherlands)

Abstract

Bepicolombo mission to Mercury poses complex problems in terms of environment aspects, and its effect on the structural behaviour of the spacecraft.
In order to analyse the spacecraft thermal elastic distortions cause by Mercury's harsh environment, the thermal node temperatures were mapped and interpolated on the structural finite element model using SINAS software.
This presentation will describe the work that has been done so far:

- Temperatures mapping onto the MPO finite element model;
- Challenges regarding the gradients areas and embedded heat pipes;
- Discrepancies between thermal and structural model and how they can be reduced.

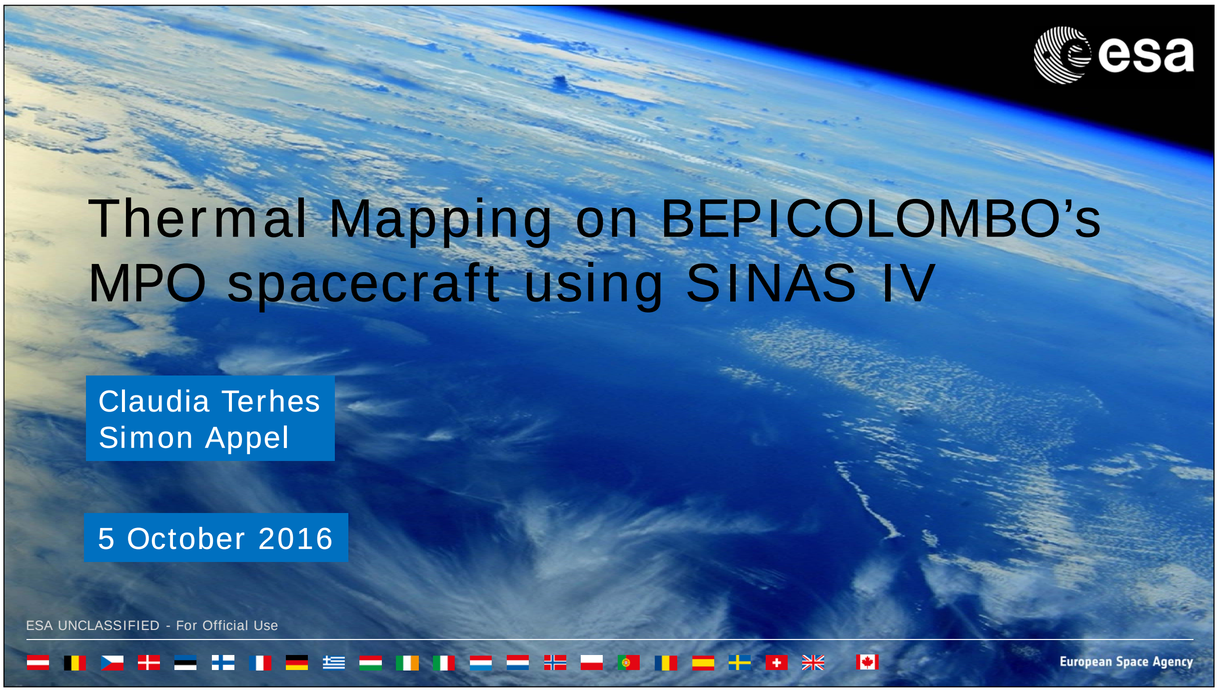
Thermal Mapping on BEPICOLOMBO's MPO spacecraft using SINAS IV
Claudia Terhes
Simon Appel
5 October 2016
ESA UNCLASSIFIED - For Official Use
European Space Agency

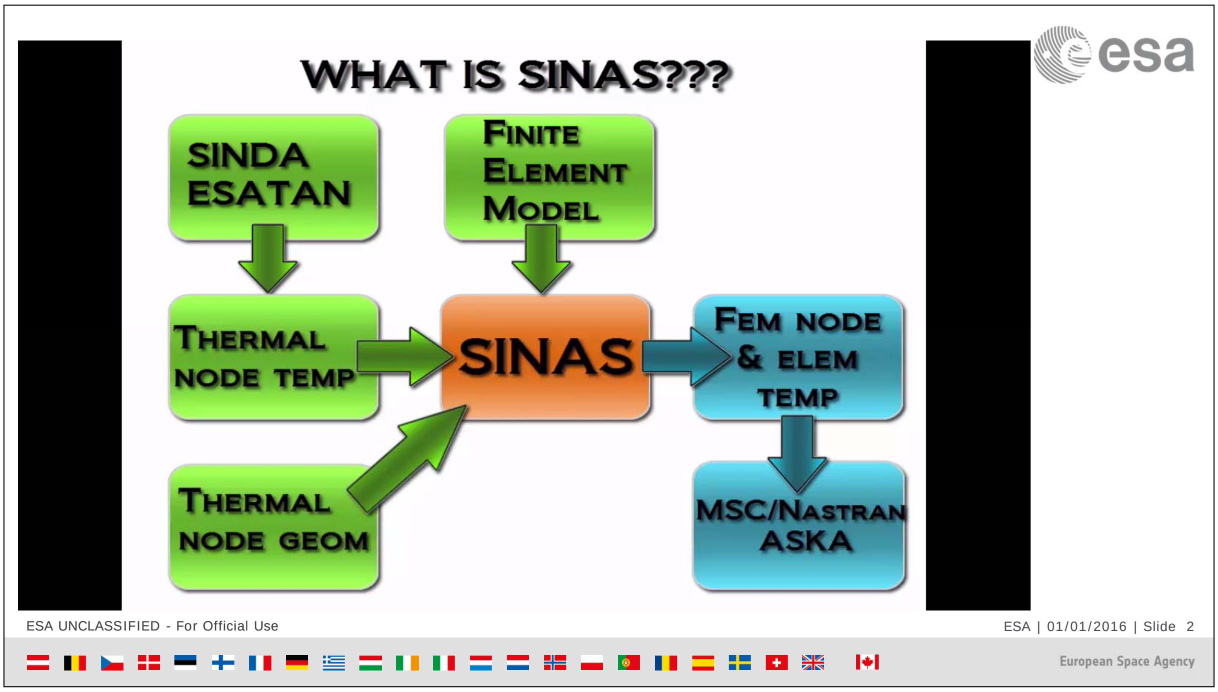
WHAT IS SINAS???
SINDA ESATAN
FINITE ELEMENT MODEL
THERMAL NODE TEMP
SINAS
FEM NODE & ELEM TEMP
THERMAL NODE GEOM
MSC/NASTRAN ASKA
ESA UNCLASSIFIED - For Official Use
ESA | 01/01/2016 | Slide 2
European Space Agency

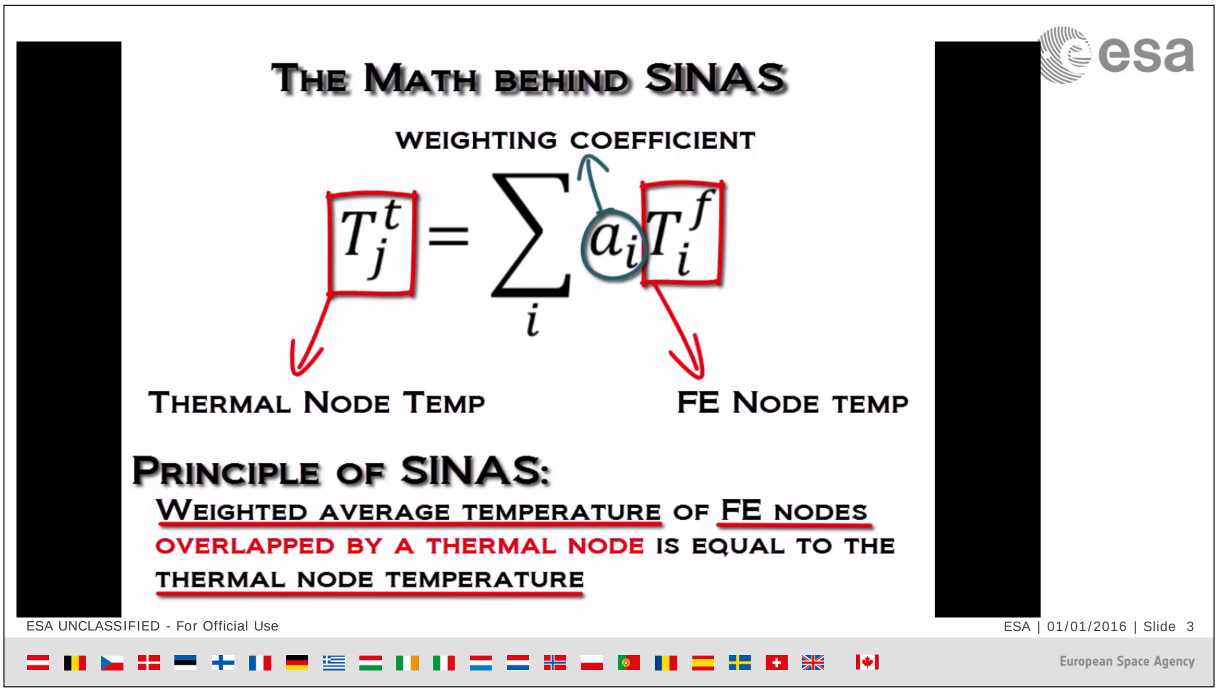
THE MATH BEHIND SINAS
WEIGHTING COEFFICIENT
$T_j^t = \sum_i a_i T_i^f$
THERMAL NODE TEMP
FE NODE TEMP
PRINCIPLE OF SINAS:
WEIGHTED AVERAGE TEMPERATURE OF FE NODES OVERLAPPED BY A THERMAL NODE IS EQUAL TO THE THERMAL NODE TEMPERATURE
ESA UNCLASSIFIED - For Official Use
ESA | 01/01/2016 | Slide 3
esa
European Space Agency

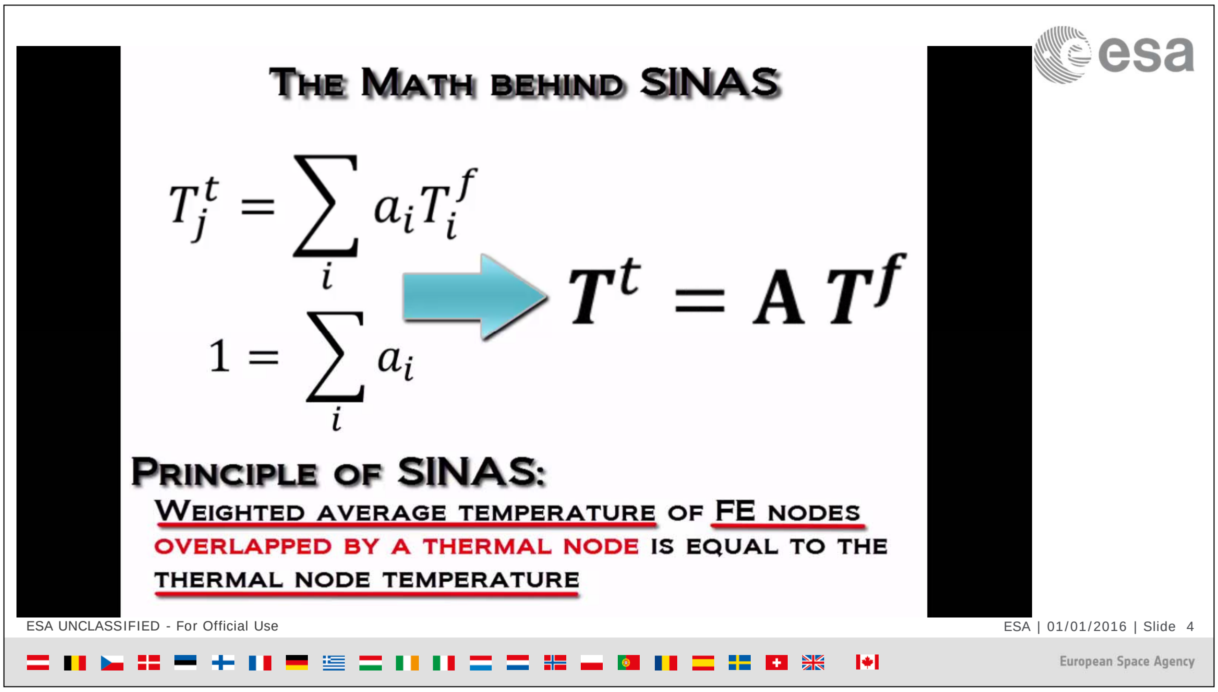
THE MATH BEHIND SINAS
$T_j^t = \sum_i a_i T_i^f$
$1 = \sum_i a_i$
$\boldsymbol{T^t = A\,T^f}$
PRINCIPLE OF SINAS:
WEIGHTED AVERAGE TEMPERATURE OF FE NODES OVERLAPPED BY A THERMAL NODE IS EQUAL TO THE THERMAL NODE TEMPERATURE
ESA UNCLASSIFIED - For Official Use
ESA | 01/01/2016 | Slide 4
esa
European Space Agency

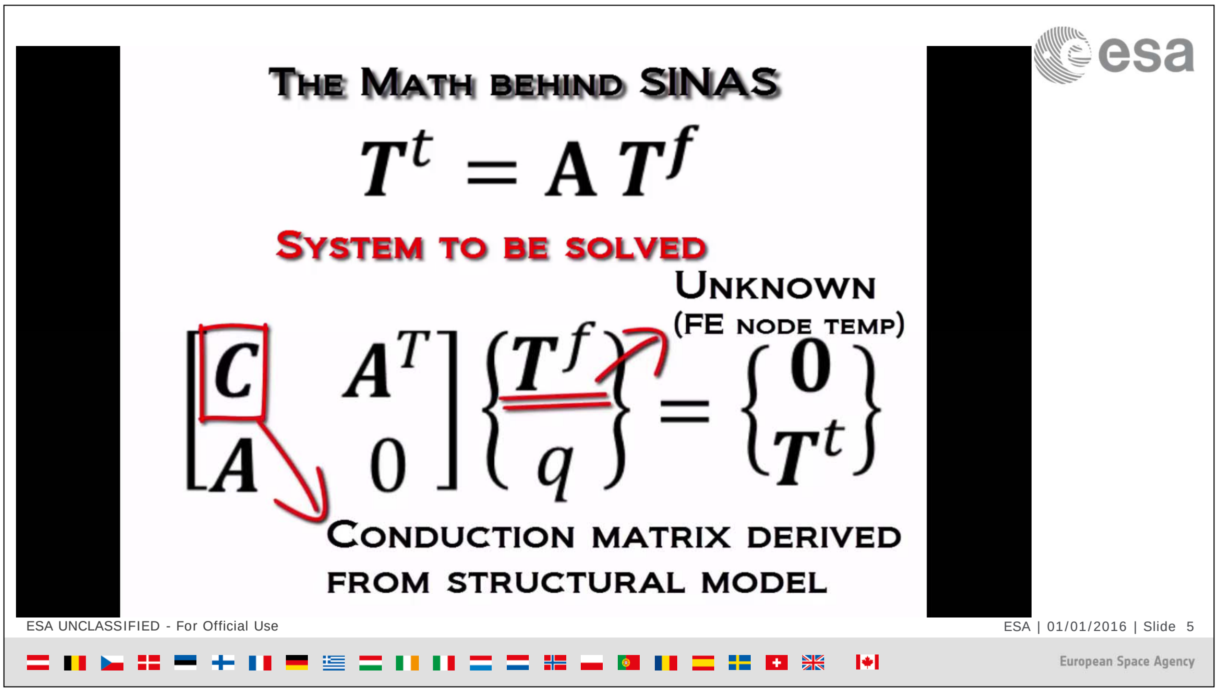
esa
The Math behind SINAS
$T^t = A\,T^f$
System to be solved
Unknown
(FE node temp)
$\begin{bmatrix} \boxed{C} & A^T \\ A & 0 \end{bmatrix} \begin{Bmatrix} T^f \\ q \end{Bmatrix} = \begin{Bmatrix} 0 \\ T^t \end{Bmatrix}$
Conduction matrix derived
from structural model
ESA UNCLASSIFIED - For Official Use
ESA | 01/01/2016 | Slide 5
European Space Agency

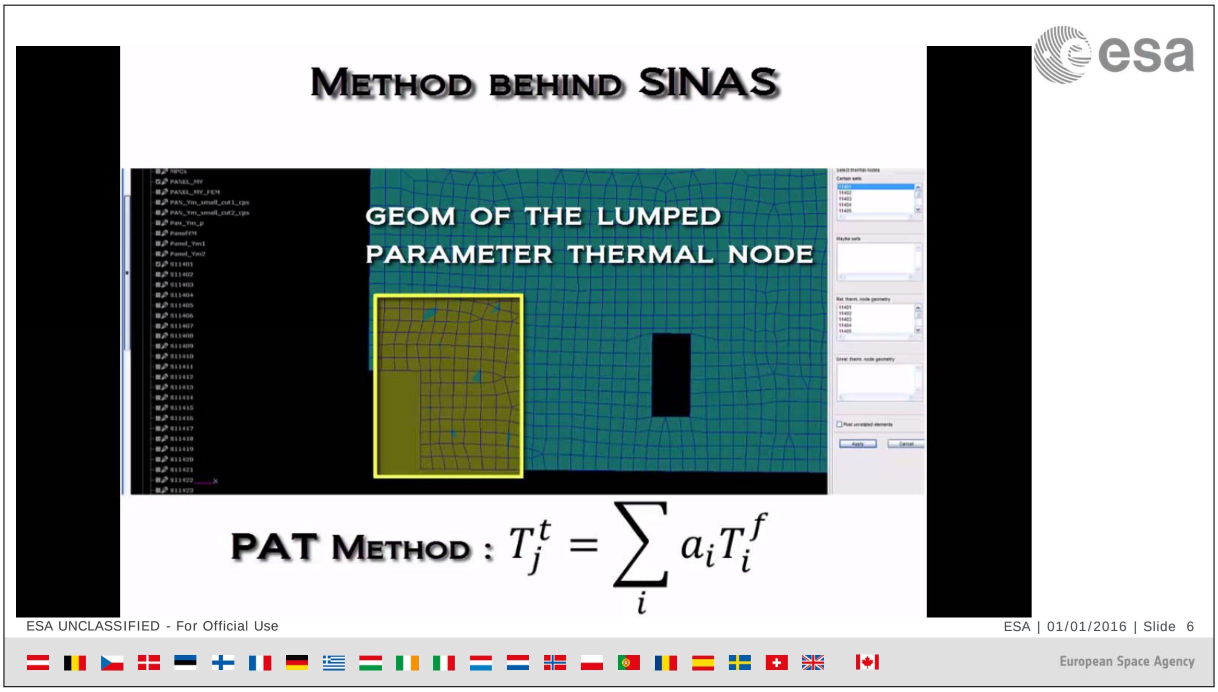
esa
Method behind SINAS
GEOM OF THE LUMPED
PARAMETER THERMAL NODE
PAT Method : $T_j^t = \sum_i a_i T_i^f$
ESA UNCLASSIFIED - For Official Use
ESA | 01/01/2016 | Slide 6
European Space Agency

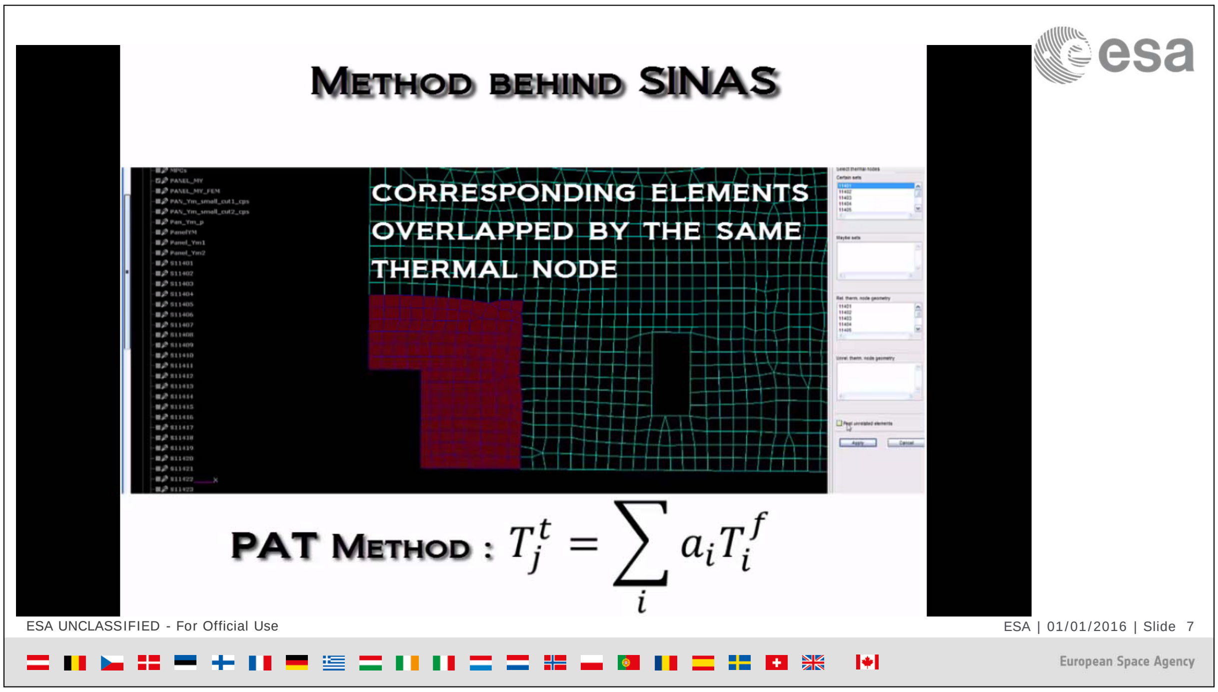
METHOD BEHIND SINAS
CORRESPONDING ELEMENTS OVERLAPPED BY THE SAME THERMAL NODE
PAT METHOD : $T_j^t = \sum_i a_i T_i^f$
ESA UNCLASSIFIED - For Official Use
ESA | 01/01/2016 | Slide 7
European Space Agency

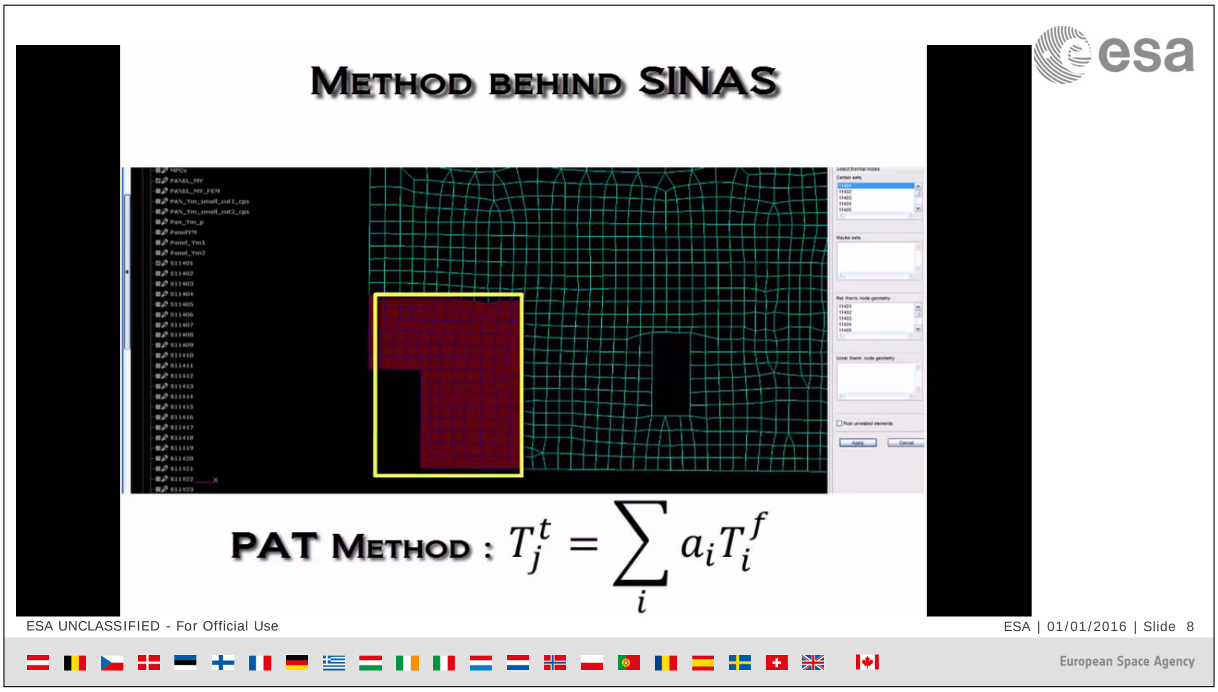
METHOD BEHIND SINAS
PAT METHOD : $T_j^t = \sum_i a_i T_i^f$
ESA UNCLASSIFIED - For Official Use
ESA | 01/01/2016 | Slide 8
European Space Agency

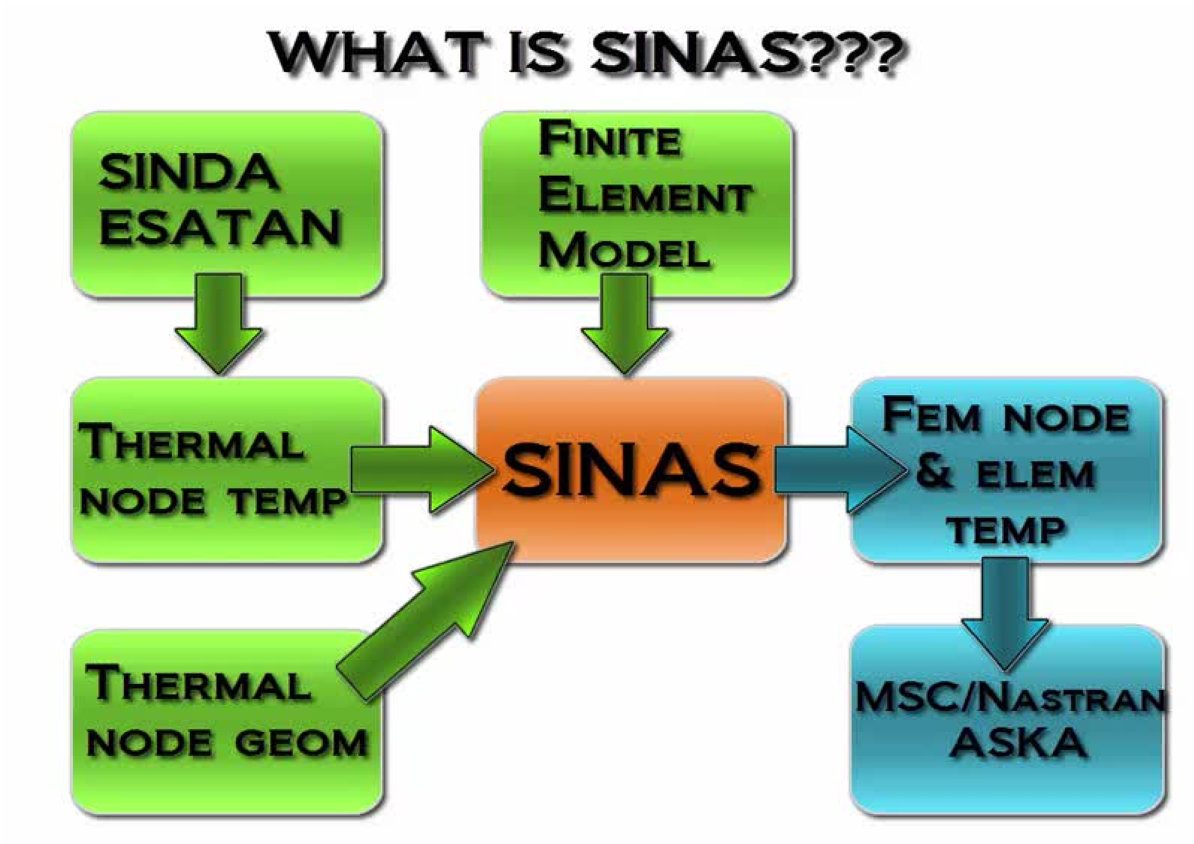

Save the attachment to disk or (double) click on the picture to run the movie.

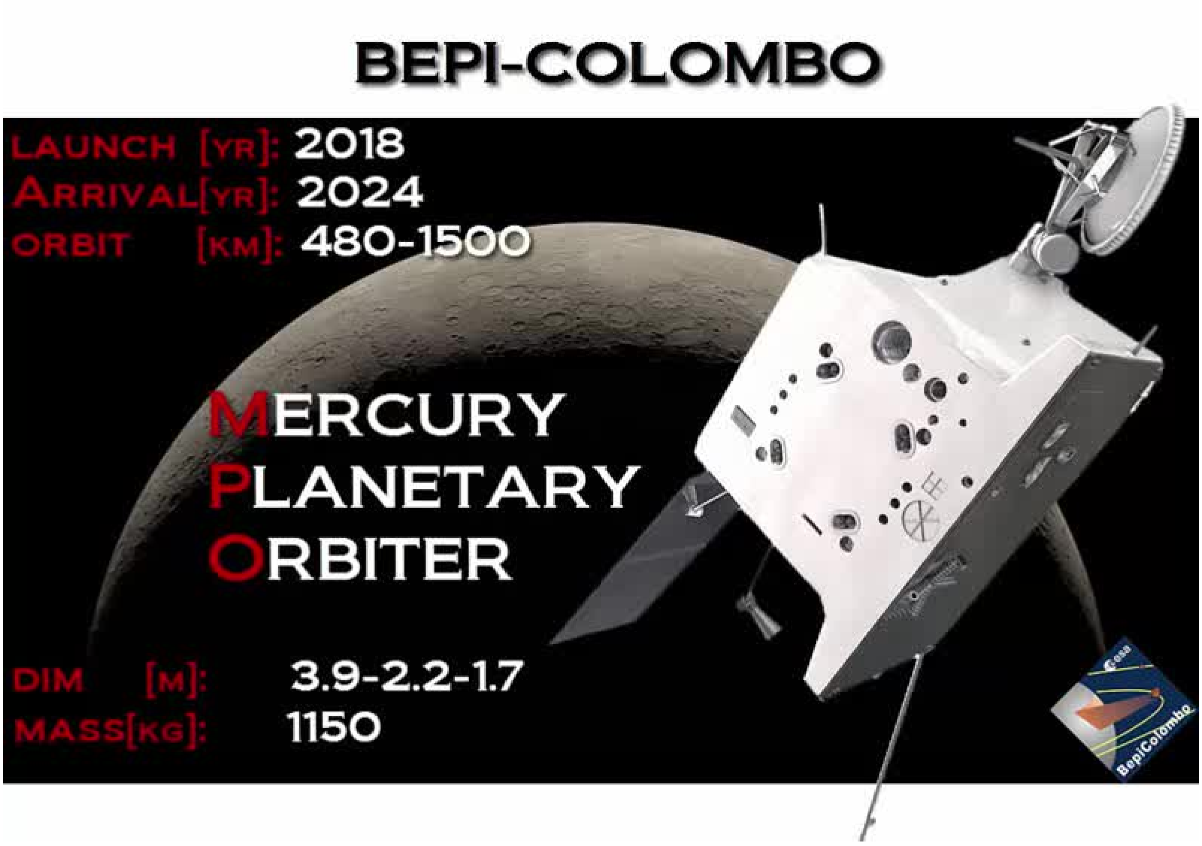

Save the attachment to disk or (double) click on the picture to run the movie.

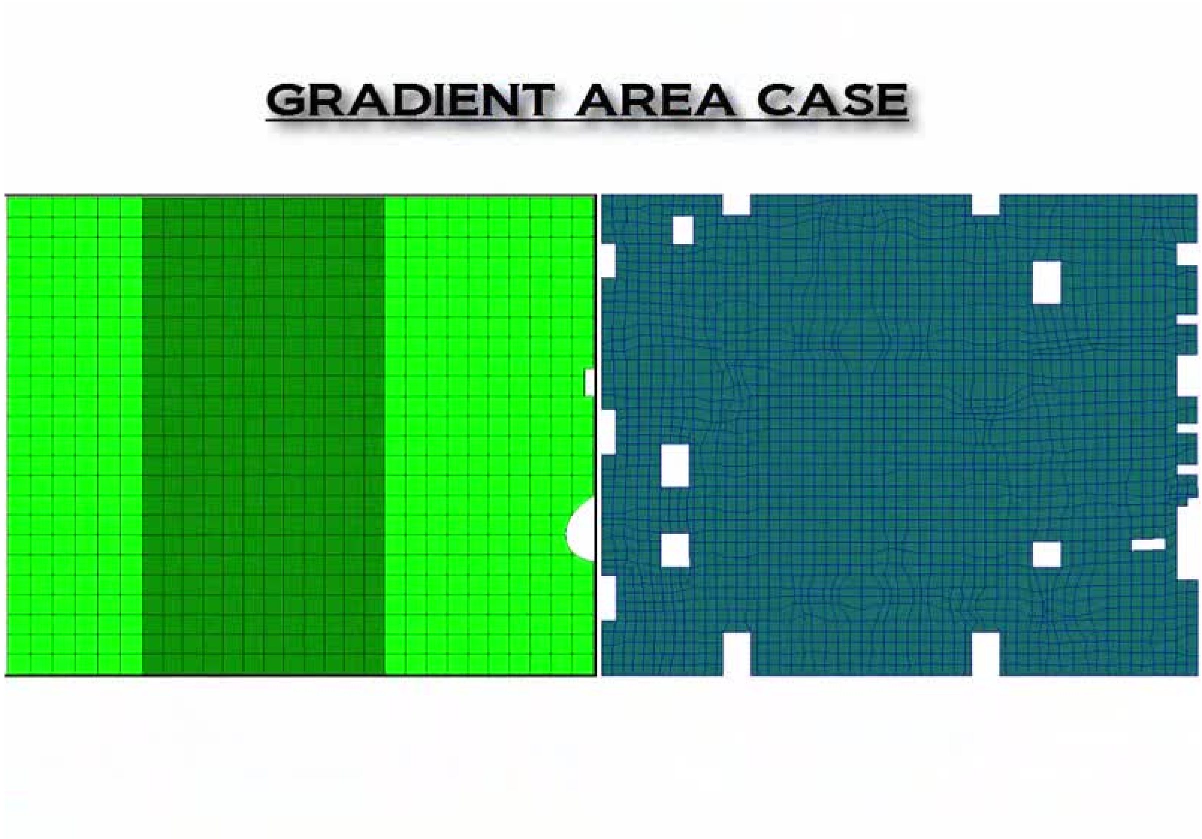

Save the attachment to disk or (double) click on the picture to run the movie.

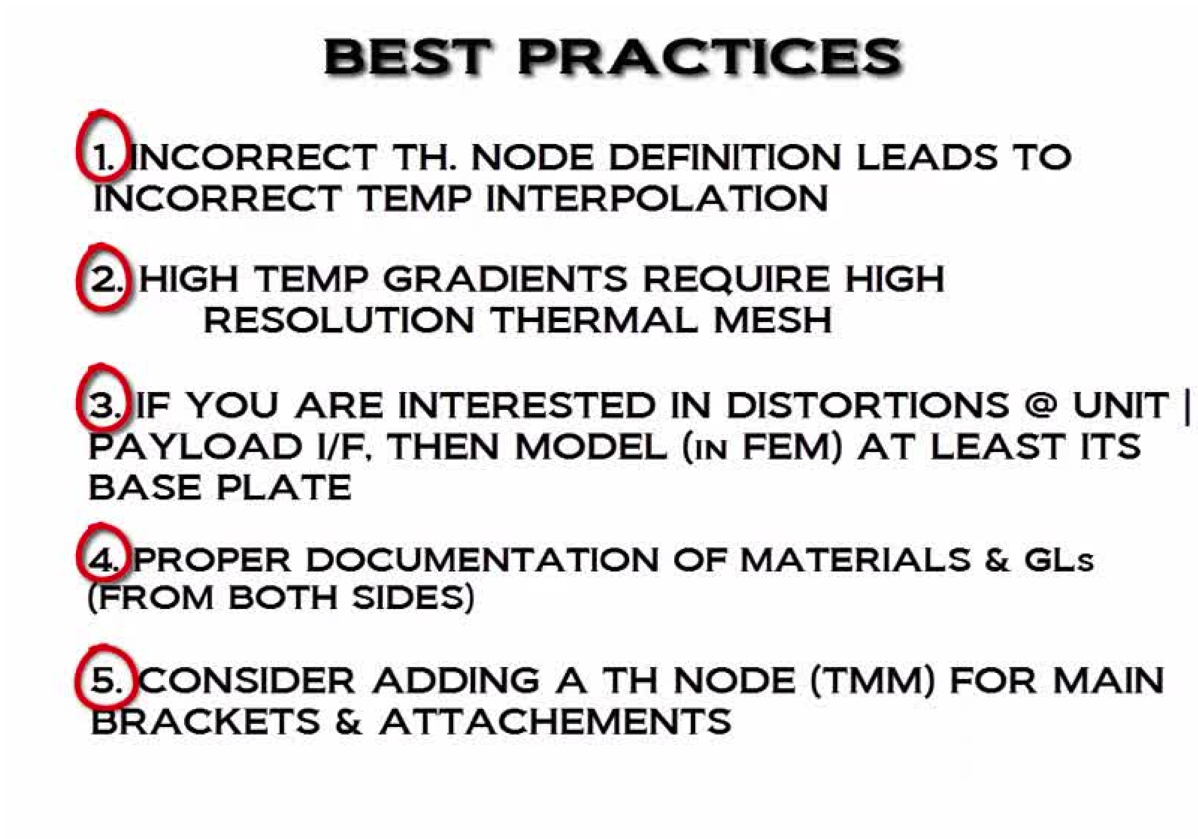

Save the attachment to disk or (double) click on the picture to run the movie.

Appendix E

Correlation of MLI Performance Measurement with a Custom MATLAB Tool

Lars Tiedemann   Peter Lindenmaier
(HPS GmbH, Germany)

João Pedro Loureiro
(HPS Lda., Portugal)

Abstract

HPS has conducted MLI performance measurements at ESA ESTEC. The results where correlated using a custom MATLAB thermal modelling tool. With the tool it is possible to solve transient non-geometrical thermal problems allowing extremely quick parameter analyses. The tool was extremely useful for explaining unexpected test results.

MLI performance is measured with standardized test setups in a thermal vacuum chamber. The MLI specimen encloses a heater plate with controlled temperature and known heat output. The heater plate with the MLI wrapping is surrounded by a thermal shroud with controlled temperature. The thermal performance is then deduced from the temperature measurements of the inner MLI layer and the outer MLI layer assuming that the MLI is in thermal equilibrium (steady state).

The results obtained from the MLI performance measurement where not as expected and showed some irregularities which could not be explained initially. In order to verify the test results, transient simulations with a detailed model of the test setup where conducted using a custom MATLAB tool for thermal modelling.

The tool models each MLI layer with realistic properties including surface emissivity, specific heat capacity, density, thickness and area. Spacer material in between MLI layers is considered by introducing conductive contributions between adjacent layers taking into account the compression of the MLI.

The mathematical model applied could in fact reproduce the unexpected test results. The model clearly shows that the observed effects are due to the fact that the MLI has not achieved a thermal equilibrium even after 24 hours. The simulation achieved a steady state after setting the dwell time to 10^4 hours. In steady state, the thermal performance values where as expected.

The applied mathematical model could in fact explain the measurement results which where not as expected in the beginning. The reason for the deviation could be identified to be a transient problem. Finally, steady-state values for the MLI performance measurements could be obtained by extending the simulated dwell time. However, it is worthwhile discussing whether steady-state performance values are in fact helpful for modelling realistic MLI blankets or if it would be better to create a new set of thermal performance values that also considers transient effects which MLI has in reality.

HPS High Performance Space Structure Systems GmbH GERMANY

Correlation of MLI Performance Measurement with Custom Matlab Tool

30th European Space Thermal Analysis Workshop

Dr. Lars Tiedemann

ESTEC|October 5th 2016

HPS High Performance Space Structure Systems GmbH GERMANY

CORRELATION OF MLI PERFORMANCE

Contents

05.10.2016 Page 2

HPS High Performance Space Structure Systems GmbH GERMANY

CORRELATION OF MLI PERFORMANCE

MLI on external surfaces

eROSITA: integration of blankets in September 2012 (picture: HPS)

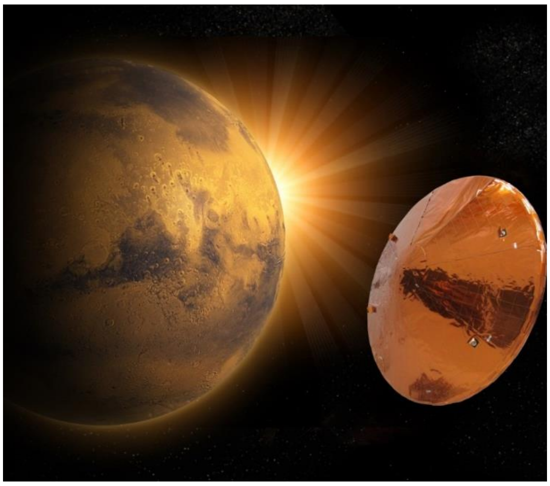

EDM module of ExoMars 2016 completely equipped with MLI by HPS (picture: HPS)

05.10.2016 Page 3

HPS High Performance Space Structure Systems GmbH GERMANY

CORRELATION OF MLI PERFORMANCE

Internal MLI

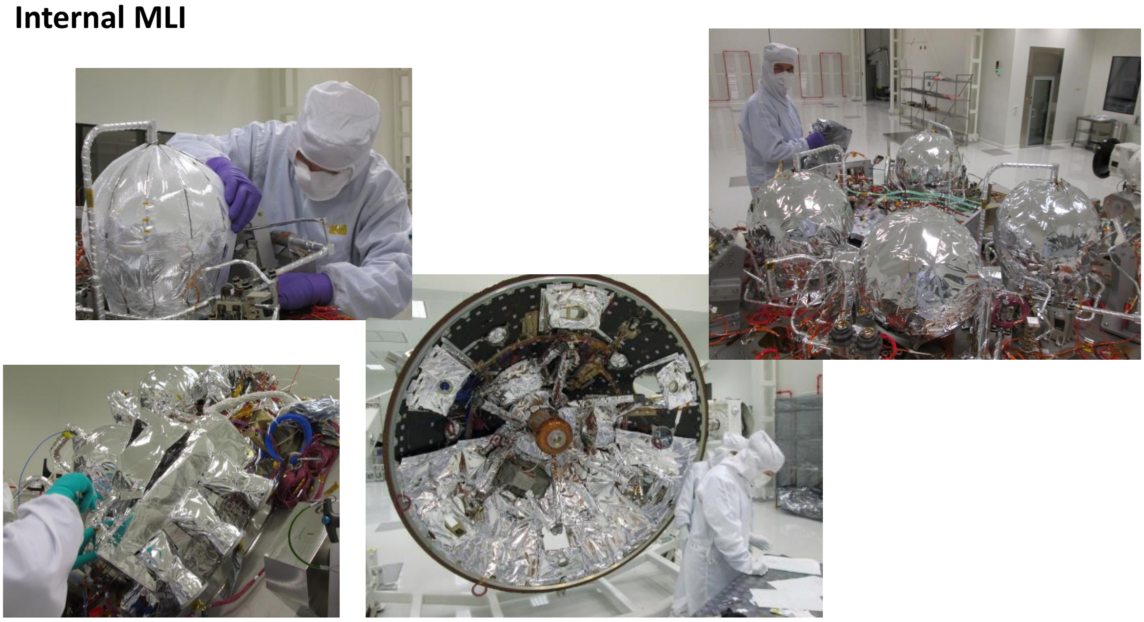

Exomars 2016 EDM internal MLI

05.10.2016 Page 4

HPS High Performance Space Structure Systems GmbH GERMANY

CORRELATION OF MLI PERFORMANCE

Instrument MLI

LRI OBA MLI: cut-outs for optics and cables

NOMAD instrument MLI: small covers for instrument optics

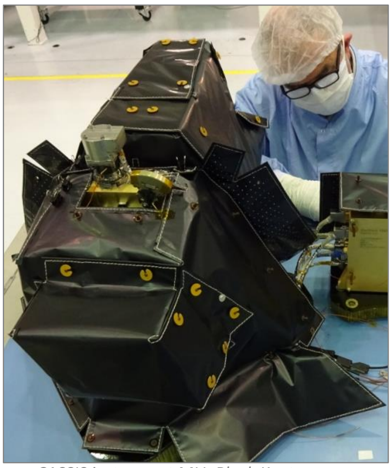

CASSIS instrument MLI: Black Kapton, non-perforated, sewed

05.10.2016 Page 5

HPS High Performance Space Structure Systems GmbH GERMANY

CORRELATION OF MLI PERFORMANCE

Factors influencing MLI performance

- Number MLI layers
- Size of blankets
- Edges
- Foldings
- Type of spacer
- Groundings
- Attachments
- Sewings
- ➢ Blanket perimeter vs. area
- ➢ Blanket compression

No (significant) influence:

- Perforation
- Outside optical properties

05.10.2016 Page 6

HPS High Performance Space Structure Systems GmbH GERMANY

CORRELATION OF MLI PERFORMANCE

MLI Performance

Heat exchange with effective emissivity

$$Q = 4\,\sigma\,A\,\varepsilon_{eff}\,T_m^3\,(T_h - T_c)$$

Mean Temperature

$$4\,T_m^3 = \frac{T_h^4 - T_c^4}{T_h - T_c} = \left(T_h^2 + T_c^2\right)\cdot(T_h + T_c)$$

Effective conductivitv

$$h_{eff} = 4\,\varepsilon_{eff}\,\sigma\cdot T_m^3$$

Ideal effective emissivity

$$\varepsilon_{eff,ideal} = \frac{1}{N-1}\cdot\frac{\varepsilon}{2-\varepsilon}$$

Heat exchange in ESARAD/ESATAN

$$q = GL\cdot(T_h - T_c) + GR\cdot\sigma\,\left(T_h^4 - T_c^4\right)$$

Q heat

σ Stefan-Boltzmann

A area

T_m mean temperature

T_h Temperature hot side

T_c Temperature cold side

N Number of MLI layers

ε_{eff} effective emissivity (function of T_m)

h_{eff} effective conductivity (function of T_m)

GL conductivity value (const.)

GR radiation value (const.)

05.10.2016 Page 7

HPS High Performance Space Structure Systems GmbH GERMANY

CORRELATION OF MLI PERFORMANCE

Effective conductivity according to ESA handbook

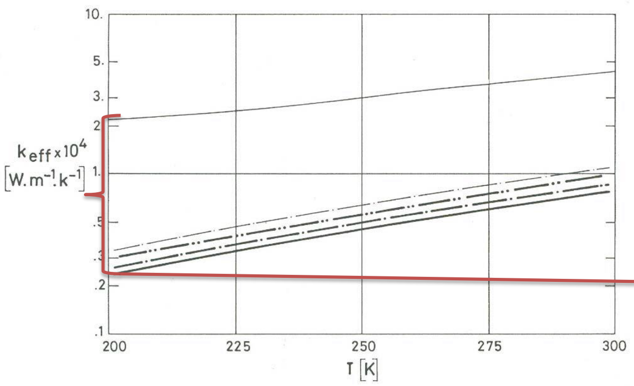

Key	Eq.	N	tx10² [m]	Other	Highlights
	[6-9]	22	2,92	$\varepsilon_1 = \varepsilon_2 = 0{,}02$	ε Effects
	[6-12]			$\varepsilon_C = \varepsilon_H = 0{,}02$ $\alpha_C = \alpha_H = 0{,}2$	α/ε Effects
				$\varepsilon_C = \varepsilon_H = 0{,}02$ $\alpha_C = \alpha_H = 0{,}6$	
	[6-13]			$\varepsilon = 0{,}02$, $T_H = 300$ K $C_1 = 6{,}79 \times 10^{-13}$ $C_2 = 5{,}39 \times 10^{-10}$	Solid Conduction Effects
	Figure 6-63, clause 6.11			Mylar Single Aluminized Dimpled $p < 0{,}5\text{x}10^{-3}$ Pa	Practical System

source: ECSS-E-HB-31-01 Part 7A, p. 117

x10 difference between theory and practical system

05.10.2016 Page 8

HPS High Performance Space Structure Systems GmbH GERMANY

CORRELATION OF MLI PERFORMANCE

The Doennecke-Method

$$\varepsilon_{eff} = \left(1.36\cdot10^{-4}\frac{1}{4\,\sigma\,T_m^2} + 1.21\cdot10^{-4}\cdot T_m^{\frac{2}{3}}\right)\cdot f_N\cdot f_A\cdot f_P$$

$$f_N = 4.5465\cdot N^{-0.501}$$

$$f_P = 0.3252\cdot P + 0.6729 \quad ; \quad \varepsilon = 0.03 \quad \text{Sheldahlgold}$$

$$f_P = 0.2685\cdot P + 0.73 \quad ; \quad \varepsilon = 0.04 \quad \text{SheldahlVDA}$$

$$f_A = 3 \quad ; \quad A < 0.05m^2$$

$$= 0.6638 \quad ; \quad A > 3m^2$$

$$= 1/10^{(0.373\cdot\log_{10}A)} \quad ; \quad 0.05m^2 < A < 3m^2$$

Doenecke (1993): Survey and Evaluation of Multilayer Insulation Heat Transfer Measurements;
David G. Gilmore: Spacecraft Thermal Control Handbook

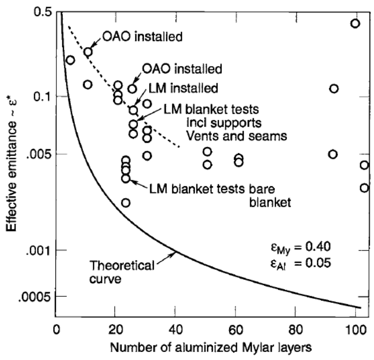

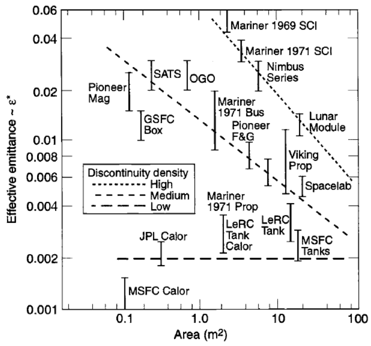

05.10.2016 Page 9

HPS High Performance Space Structure Systems GmbH GERMANY

CORRELATION OF MLI PERFORMANCE

MLI performance measurement test setup

Calorimeter plate

Test specimen

Test area

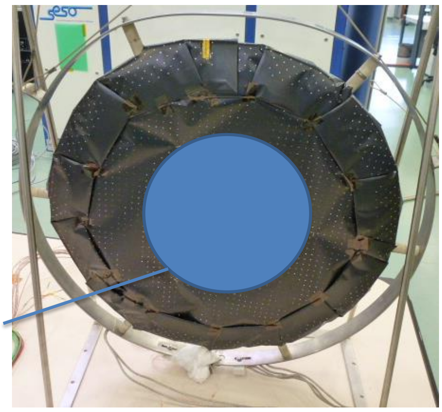

Guard heater

Edges covered to reduce edge effects

05.10.2016 Page 10

HPS High Performance Space Structure Systems GmbH GERMANY

CORRELATION OF MLI PERFORMANCE

Test results

Case	T_hot [°C]	T_cold [°C]	T_av [°C]	P [W]
1	-62.52	-180.75	-121.635	0.045
2	26.14	-92.25	-33.055	0.079
3	57.39	-31.56	12.915	0.169
4	98.7	14.39	56.545	0.272
5	179.04	58.21	118.625	0.443

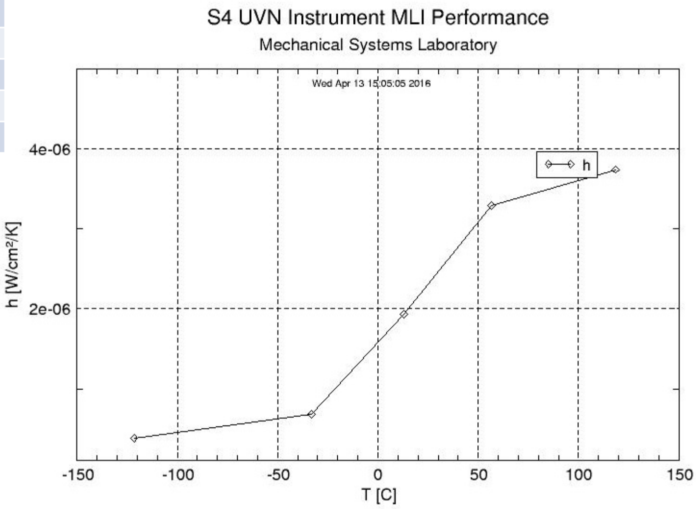

s-shape?

05.10.2016 Page 11

HPS High Performance Space Structure Systems GmbH GERMANY

CORRELATION OF MLI PERFORMANCE

Theoretical curves

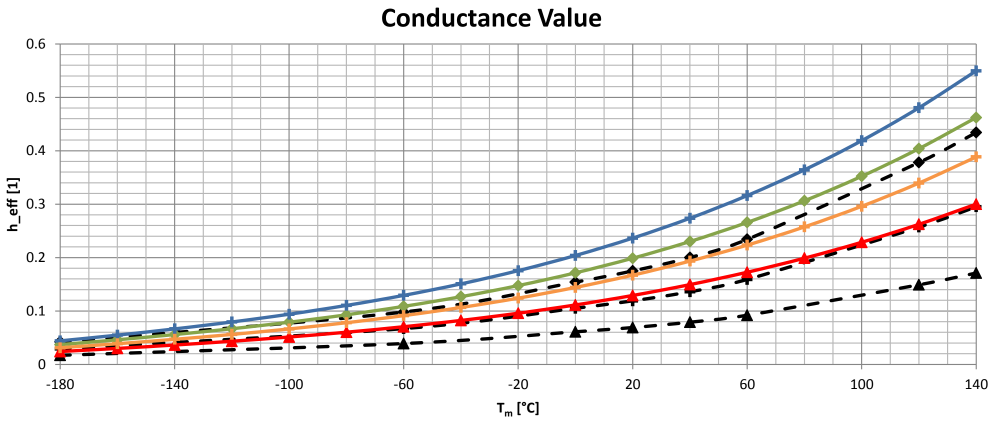

$h = h(T_m)$, but the curves are never s-shaped
→ detailed correlation required

05.10.2016 Page 12

HPS High Performance Space Structure Systems GmbH GERMANY

CORRELATION OF MLI PERFORMANCE

MATLAB thermal modeling tool description

- Class architecture
- Solver class
  - solves 0-dimensional thermal problems
  - definition of arbitrary nodes: node name, capacity, initial temperature, heat dissipation
  - definition of radiative couplings and conductive couplings between nodes
  - assembles matrices and solves ODE

$$-C \cdot \dot{T} + K \cdot T + E \cdot T^4 + Q = 0$$

  - transient solution
  - stores results as vectors t, T
  - methods for heat transfer calculation
- MLI Performance test class
  - heater power, area (const.), optical properties
  - defines MLI nodes (input: N)
  - perforation taken into account (area fraction)
  - conduction through spacer taken into account
  - spacer fraction =1: spacer is perfect conductor, =0: no conduction
  - methods for result plots, post solving analysis etc.

05.10.2016 Page 13

HPS High Performance Space Structure Systems GmbH GERMANY

CORRELATION OF MLI PERFORMANCE

Mathematical model for test correlation

test setup

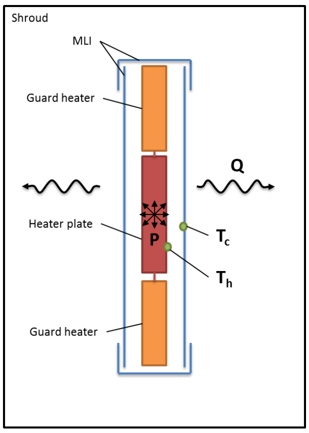

model architecture

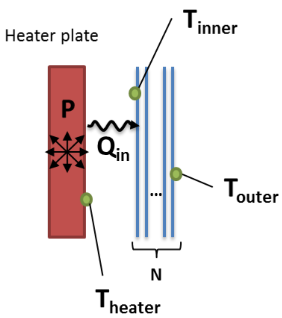

Node Name	Properties
Heater	q_{in}= ½ P A= 0.049087 m² (diameter: 250mm) ε=0.90 to MLI
MLI1	Black Kapton 1-VDA, perforated ε=0.85 to heater ε=0.035 to next MLI layer
MLI2	Kapton or Mylar, 2-VDA ε=0.035 to next/previous MLI layer
…	…
MLIn	Black Kapton 1-VDA, perforated ε=0.035 to previous MLI layer $T=T_c$=const.

$$\varepsilon_{eff,heater} = \frac{P}{\sigma\, A\, ({T_{heater}}^4 - {T_{outer}}^4)}$$ test assumption

$$\varepsilon_{eff,MLI} = \frac{Q_{in}}{\sigma\, A\, ({T_{inner}}^4 - {T_{outer}}^4)}$$ calculated by model

05.10.2016 Page 14

HPS High Performance Space Structure Systems GmbH GERMANY

CORRELATION OF MLI PERFORMANCE

Correlation results

- Modeled time 24 hours (as tested)
- Temperatures match measurements <0.6K
- S-shape in h_{eff} curve could be reproduced very well
- Q_{in} and P are not equal!
- ➢ MLI not in steady state
- ➢ what happens in steady state?

Case	Q_in	P
1	0.03352122	0.02234146
2	0.06042269	0.03960077
3	0.06333031	0.08446073
4	0.08147294	0.1361239
5	0.17390231	0.22154237

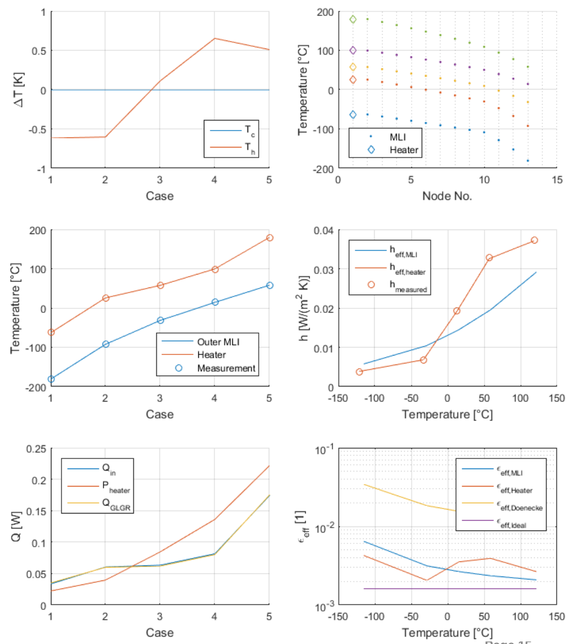

05.10.2016

Page 15

HPS High Performance Space Structure Systems GmbH GERMANY

CORRELATION OF MLI PERFORMANCE

Correlation results 2

- Modeled time 10^4 hours (simulated)
- Temperatures do not match measurements
- S-shape in h_{eff} curve is gone!
- Q_{in} and P are now equal!
- ➢ MLI is now in steady state!

Case	Q_in	P
1	0.02234267	0.02234146
2	0.03960075	0.03960077
3	0.08456646	0.08446073
4	0.13616629	0.1361239
5	0.22152256	0.22154237

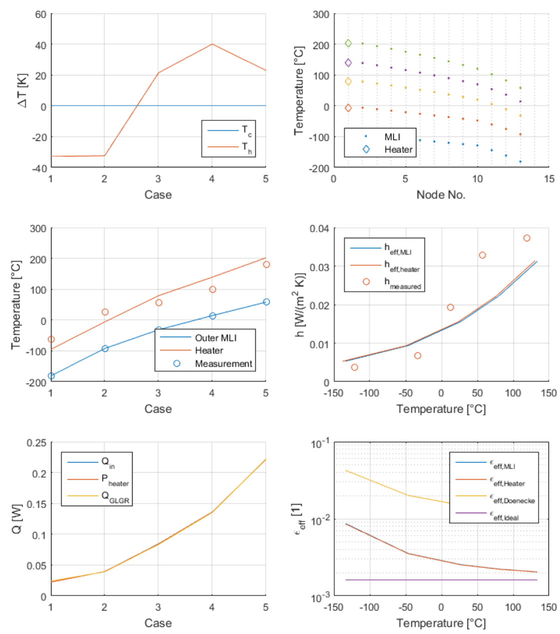

05.10.2016

Page 16

HPS High Performance Space Structure Systems GmbH GERMANY

CORRELATION OF MLI PERFORMANCE

Conclusion

- Tested MLI has excellent insulation capabilities
- very low heater power are applied <50mW for low temperatures, <1W for high temperatures
- only small temperature changes observed in measurements after a few hours, however
- small heat influx has small impact on MLI layer temperatures
- leading to the wrong conclusion that the MLI is in equilibrium

05.10.2016 Page 17

HPS High Performance Space Structure Systems GmbH GERMANY

CORRELATION OF MLI PERFORMANCE

Fundamental problems of MLI performance measurements

Deriving performance parameters from measurements

- Heat influx cannot be measured directly, only temperatures
- Equilibrium assumption is fragile (thermal capacity, low power levels, low coupling)
- Innermost and outermost layer do not change temperature, but the inner layers still do
- Increasing dwell time has a direct cost effect

Possible test improvements

- add purge gas (GN2 purging, turbo pumps off) to accellerate temperature adaption, then add turbos to achieve desired pressure
- constant heater power instead of controlled temperature
- higher power levels

MLI performance forecast for real life applications

- Test setup is idealized
- MLI geometry has a significant impact on performance
- Discrepancy between real MLI and theory is up one order of magnitude

05.10.2016 Page 18

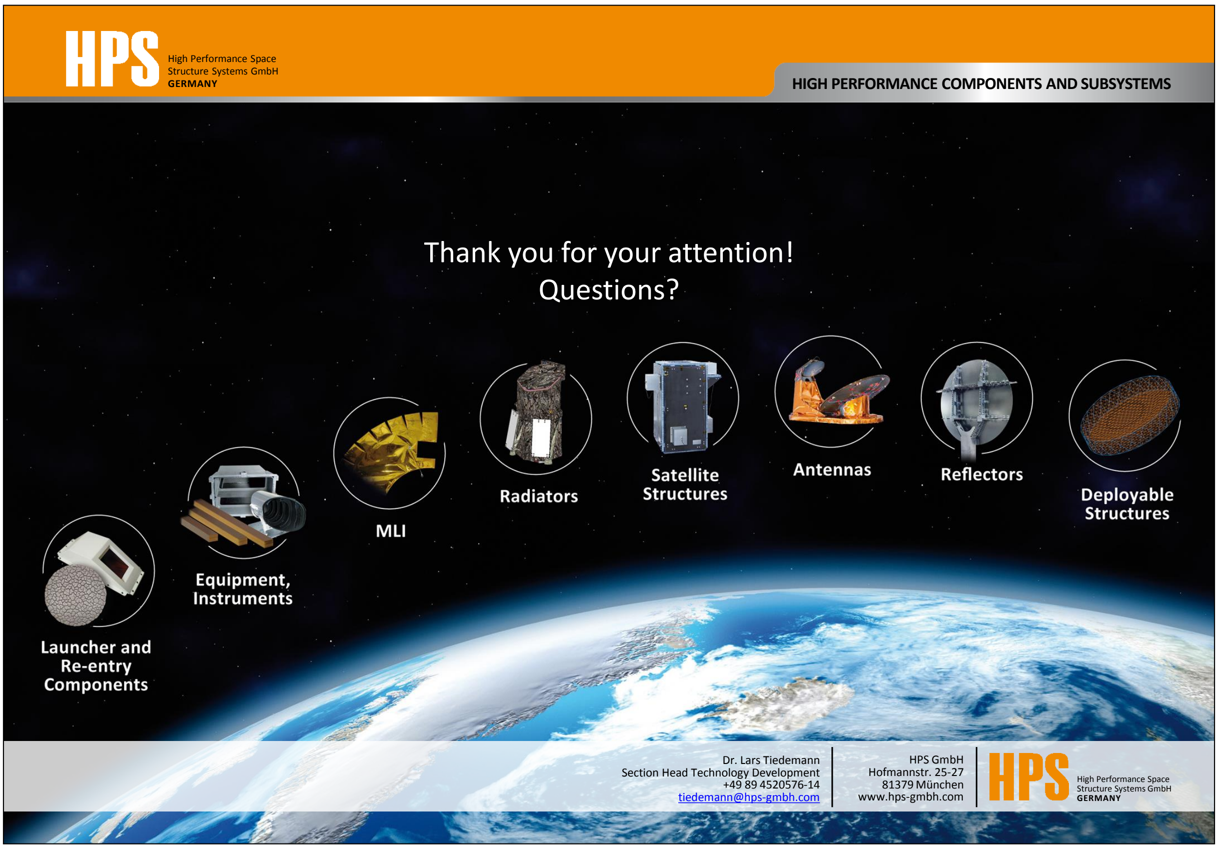
HPS
High Performance Space
Structure Systems GmbH
GERMANY
HIGH PERFORMANCE COMPONENTS AND SUBSYSTEMS
Thank you for your attention!
Questions?
Launcher and Re-entry Components
Equipment, Instruments
MLI
Radiators
Satellite Structures
Antennas
Reflectors
Deployable Structures
Dr. Lars Tiedemann
Section Head Technology Development
+49 89 4520576-14
tiedemann@hps-gmbh.com
HPS GmbH
Hofmannstr. 25-27
81379 München
www.hps-gmbh.com
HPS
High Performance Space
Structure Systems GmbH
GERMANY

Appendix F

Solar Orbiter STM Thermal Testing and Correlation

Scott Morgan
(Airbus Defence and Space, United Kingdom)

Abstract

Solar Orbiter is an ESA mission which will explore the Sun and the heliosphere closer than ever before. One of the main design drivers for Solar Orbiter is the thermal environment, determined by a total irradiance of 13 solar constants (17500 W/m^2), due to the proximity to the Sun. As part of the thermal design and validation process, the Solar Orbiter STM platform thermal balance test was performed in the IABG test facility in November- December 2015. This presentation will describe the Thermal Balance Test performed on the Solar Orbiter STM and the activities performed to correlate the thermal model and to show the verification of the STM thermal design.

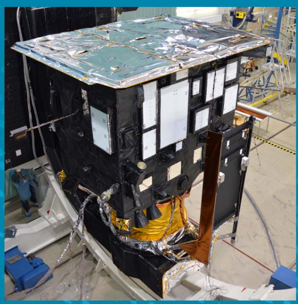
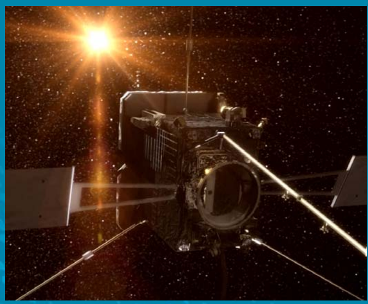
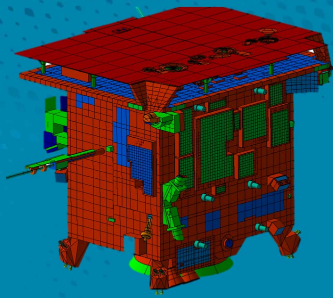

Thermal Test Campaign of the Solar Orbiter STM

Scott Morgan

5th October 2016

Overview

- Solar Orbiter Spacecraft
- Thermal Test Overview
- Test Article
- Test Set-Up
- Test Description
- Correlation Activities
- Conclusions

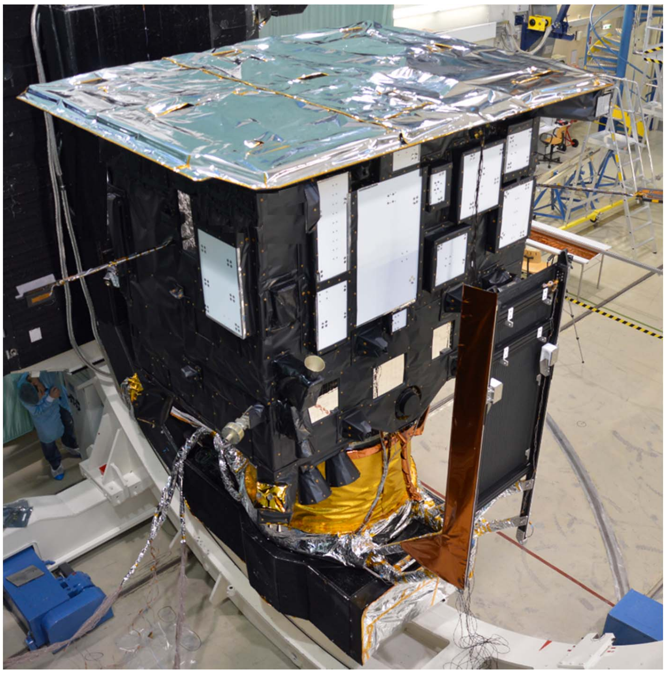

2

Thermal Test Campaign of the Solar Orbiter STM

Solar Orbiter Spacecraft

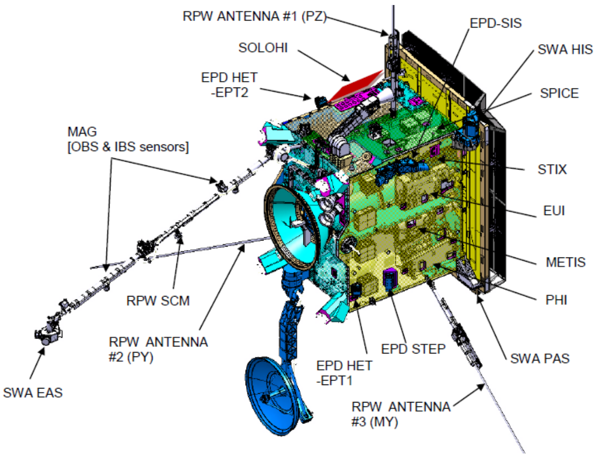

Mission Facts:

- Launch Date : October 2018
- Orbits Sun at distances between 0.28AU (perihelion) and 1.47AU (aphelion)
- Cruise Phase (3 years) – Nominal Mission Phase (3.8 years) – Extended Mission Phase (2.5 years)

Spacecraft Features:

- Heatshield to protect against 17,500 W.m^{-2} solar flux at perihelion, sized to offer complete Sun shielding of the platform within an 8° half-cone.
- High Gain Antenna which is articulated to enable communication with Earth throughout the mission
- Instrument boom to isolate magnetically sensitive instrument from the rest of the spacecraft

3

Thermal Test Campaign of the Solar Orbiter STM

Thermal Test Overview

Test Location: IABG, Munich

Test Objectives:

- Verify and Correlate Platform Thermal Model
- Demonstrate adequacy of spacecraft level thermal control, payload radiator assemblies and MLI
- Verify thermal power requirements in relation to heater consumption needed for TCS

Items Excluded from Test:

- Instrument boom, HGA and solar arrays
- The HGA and solar array effect on the spacecraft is simulated using IR heater plates
- Spacecraft heatshield has undergone its own STM campaign . To meet the objectives of the spacecraft level STM, it was sufficient to use a heated plate to simulate the heat flux from the rear of the heat shield.

4

Thermal Test Campaign of the Solar Orbiter STM

Test Article - I

Truncated RPW antenna (full antenna would not fit in chamber when deployed)

Thermally representative heat shield dummy

-Y solar array simulator

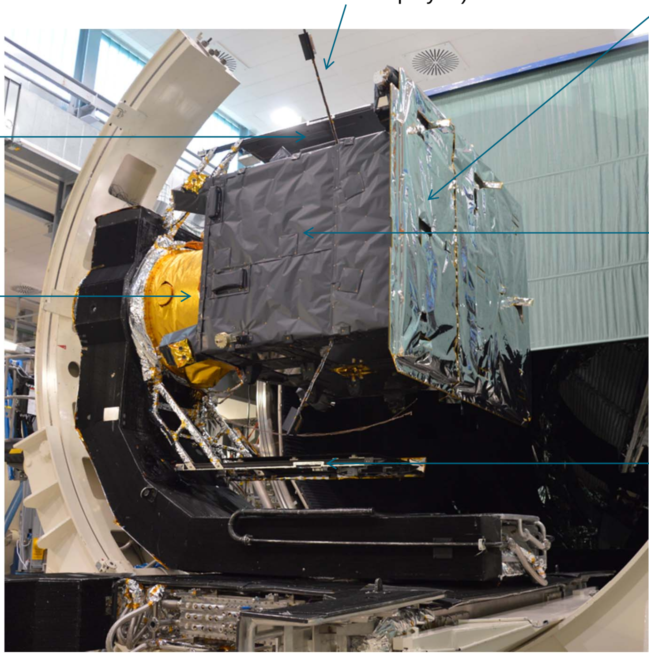

Spacecraft Platform STM

Thermal Test Adapter

+Y solar array simulator

5

AIRBUS DEFENCE & SPACE

Thermal Test Campaign of the Solar Orbiter STM

Test Article - II

- Heatshield thermal dummy (see image on right)
  - Consists of four aluminium plates assembled together, painted black with heaters located as shown. Front (non-SC facing side) of heatshield covered with MLI to ensure heat rejection is directed towards spacecraft
  - Purpose of heatshield thermal dummy is to provide radiative and conductive fluxes to the spacecraft which are comparable with those expected in flight at 0.28AU

Heatshield thermal dummy

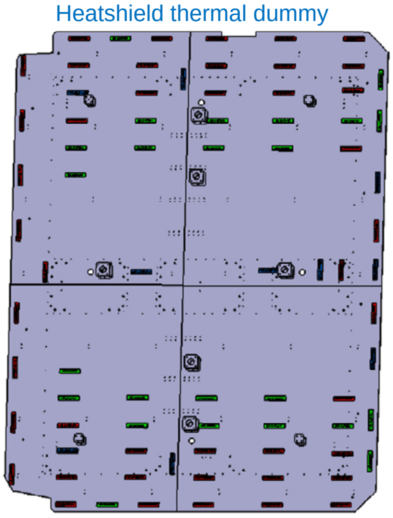

6

AIRBUS DEFENCE & SPACE

Thermal Test Campaign of the Solar Orbiter STM

Test Article - III

STM thermal hardware was installed to represent the flight TCS design:

- Flight representative MLI to insulate platform external walls and battery
- Flight representative platform radiators
- 8 flight representative stood off radiators (SORA) located on –Y and +Z panels
- Thermal filler for improved thermal contact between unit baseplates and SC panels
- Heatpipes for SORA and some platform units (PCDU and RIU)
- TCS heaters to represent operation flight heaters that will be used to protect equipment interfaces in flight

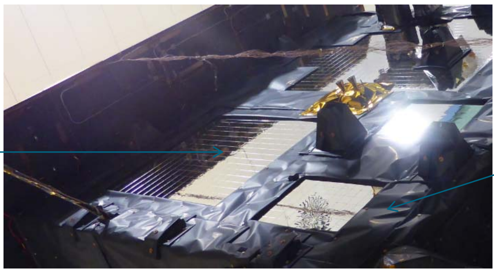

7

AIRBUS DEFENCE & SPACE

Thermal Test Campaign of the Solar Orbiter STM

Test Article IV – Stood-Off Radiator Assembly (SORA)

- The five internal remote sensing instruments have very stringent temperature requirements.
- Some must be kept below -60°C when in operational mode at 0.28AU.
- To enable efficient radiator design, the radiator panels are decoupled from the spacecraft panel via isostatic feet.
- To achieve efficient heat transfer from the instrument interfaces to the radiator, they are connected via flexible thermal straps and rigid bars using pyrolytic graphite with aluminium end-fittings
- To meet STM schedule, it was decided that two flexible and two rigid bars would be represented. These simulate the full chain from payload instrument interface to radiator. All other strap interfaces are simulated using a heated interface blocks.

+Y SORA integrated

8

AIRBUS DEFENCE & SPACE

Thermal Test Campaign of the Solar Orbiter STM

Test Set-Up

- Thermocouples (TC)
  - Approx. 400 thermocouples in total
  - For MTDs, one TC was located on the TRP and two or more on the panel around the baseplate to enable temperature gradients between the unit and panel and within the panel itself to be resolved
  - TCs also located along the heatpipes beneath the PCDU and RIU
- Heaters
  - Approx. 173 heater circuits
  - Four categories:
    - Test heaters (approx. 90) to simulate heat dissipated due to operation of the equipment
    - Flight heaters for TCS (approx. 75) to represent those heaters which are used to maintain equipment within temperature limits
    - Heaters located on IR simulators to represent the radiative environment presented to the SC radiators due to external components such as the solar array, HGA etc.
    - Guard heaters to prevent unwanted conductive heat loss through the test facility interfaces (mechanical and electrical).

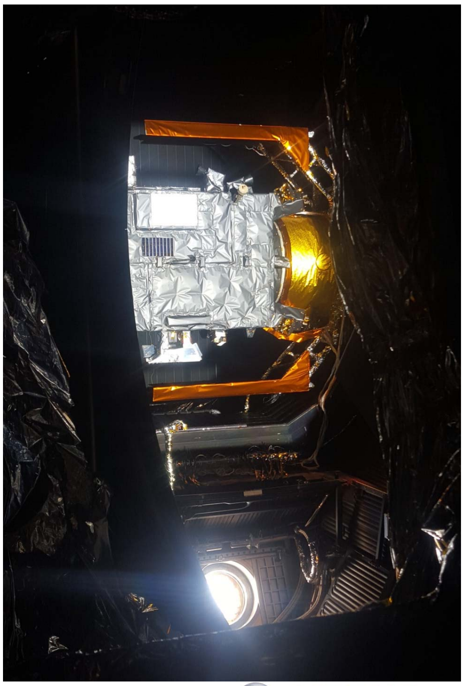

9

AIRBUS DEFENCE & SPACE

Thermal Test Campaign of the Solar Orbiter STM

Test Description

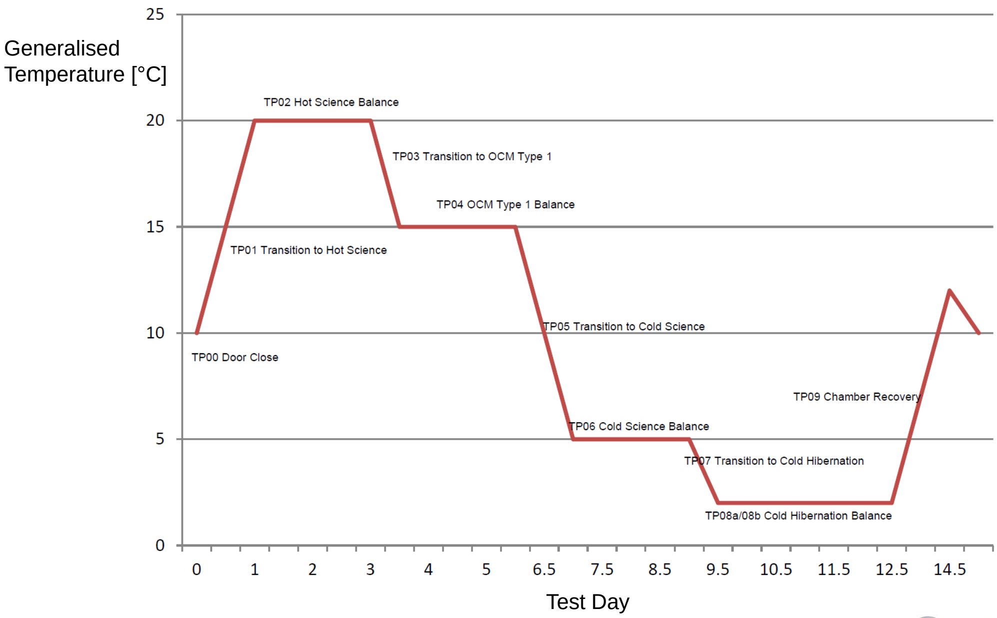

10

AIRBUS DEFENCE & SPACE

Thermal Test Campaign of the Solar Orbiter STM

Correlation Activities - I

- A correlation activity was performed after the event, aiming to correlate all four balance phases
- The correlation procedure was performed in ESATAN TMS
- The first step of the correlation involved the parameterisation of key values within the model, such as
  - Interface couplings
  - MLI couplings
  - Optical properties

- The data from the test was then sanitised. This involved:
  - Removal of data for spurious or failed thermocouples
  - Averaging TC data where there was significant noise (non twisted pair cables)
  - Exponential based extrapolation of TC data for high capacity units

- Next, any large deviations between predictions and test were investigated

11

AIRBUS DEFENCE & SPACE

Thermal Test Campaign of the Solar Orbiter STM

Correlation Activities - II

The main model updates coming out of the correlation activity are:

- Geometric Mathematical Model:
  - Position and thermo-optical properties of the Solar Array simulator
  - Orientations and thermo-optical properties of RPW antenna MTDs
  - Correction of SADM MLI
  - Correction of position of EPD HET +Y bracket
  - Modification of the LVA internal MLI
  - OSR emissivity (small reduction)

- Thermal Mathematical Model:
  - Improved modelling of PHI HE1 heatpipe
  - Corrected conductive couplings between SWA electronics box, SPICE electronics box and EPD with radiators
  - Improved modelling of TWT doublers
  - Instrument conductive couplings of star trackers and thrusters
  - Propellant tank MLI couplings

The above changes are all minor – overall the correlation of most elements of the thermal model was good without need for modification.

12

AIRBUS DEFENCE & SPACE

Thermal Test Campaign of the Solar Orbiter STM

Correlation Results

The final status of the correlation is stated below:

	Hot Science	Hot OCM	Cold Science	Cold Hibernation	Requirement
Temp deviation test vs TMM (±5°C)	97.7%	94.6%	95.5%	93.8%	
Temp deviation test vs TMM (±8°C)	100.0%	99.4%	100.0%	99.4%	
Temp mean deviation [°C]	0.61	-0.25	0.05	0.91	2.0
Temp standard deviation [°C]	2.07	2.44	2.33	2.45	3.0

The table above shows that both the mean temperature deviation and the standard deviation of thermocouple measurements are within limits in all four balance phases

The vast majority of internal units show good adherence to the above requirement. Areas which were difficult to correlate were:

- Propulsion tanks
- Optics unit feet
- SORA

The most difficult case to correlate is TP04 (off-pointing, Sun illumination case). For most TCs the TMM predicts hotter than measured in test.

13

AIRBUS DEFENCE & SPACE

Thermal Test Campaign of the Solar Orbiter STM

Conclusions and Next Steps

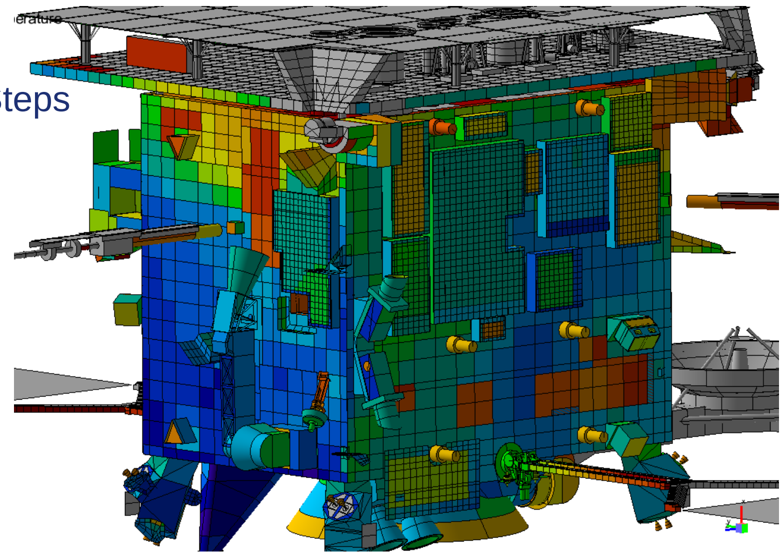

Conclusions:

- STM thermal balance test for Solar Obiter was performed between 23rd November and 2nd December 2015
- 98% thermocouples reached stabilisation in all test phases
- Good level of correlation has been achieved with minor modifications made to thermal model

Next Steps:

- Feedback from the SC STM correlated thermal model will be implemented in the SC flight model. Together with integration of thermal models from the major subsystems (Heat shield, HGA solar arrays), the thermal model will then be in a position to inform the Solar Orbiter PFM Thermal Campaign.

14

AIRBUS DEFENCE & SPACE

Appendix G

Automated thermal model correlation

Martin Trinoga
(Airbus Safran Launchers, Germany)

Abstract

An essential part in the development of a spacecraft is the establishment of a thermal model for the thermal design and the temperature predictions during the operation phase. In order to improve the accuracy of the temperature predictions, all thermal spacecraft models need to be correlated with measurements from thermal tests or if available thermal flight data. Since 2013 a new tool for an automated model correlation is under development with the name TAUMEL. With this newly developed tool written in MATLAB(R) programming language it will be possible to correlate thermal models from ESATAN-TMS automatically. For the validation several different thermal models from real flight hardware such as various test models were used. A first insight was already given in the 28th European Space Thermal Analysis Workshop in October 2014. Within the last two years a significant progress was mastered. Especially the functionality and user-friendliness was improved in the last period and lead to a promising tool for an effective automated thermal model correlation. On this conference the latest status, highlights and results which were treated during the past development will be presented.


Automated thermal model correlation
Martin Trinoga
Airbus Safran Launchers GmbH
Bremen / Germany
06.10.2016
AIRBUS SAFRAN LAUNCHERS
30th european space thermal analysis workshop @ ESTEC

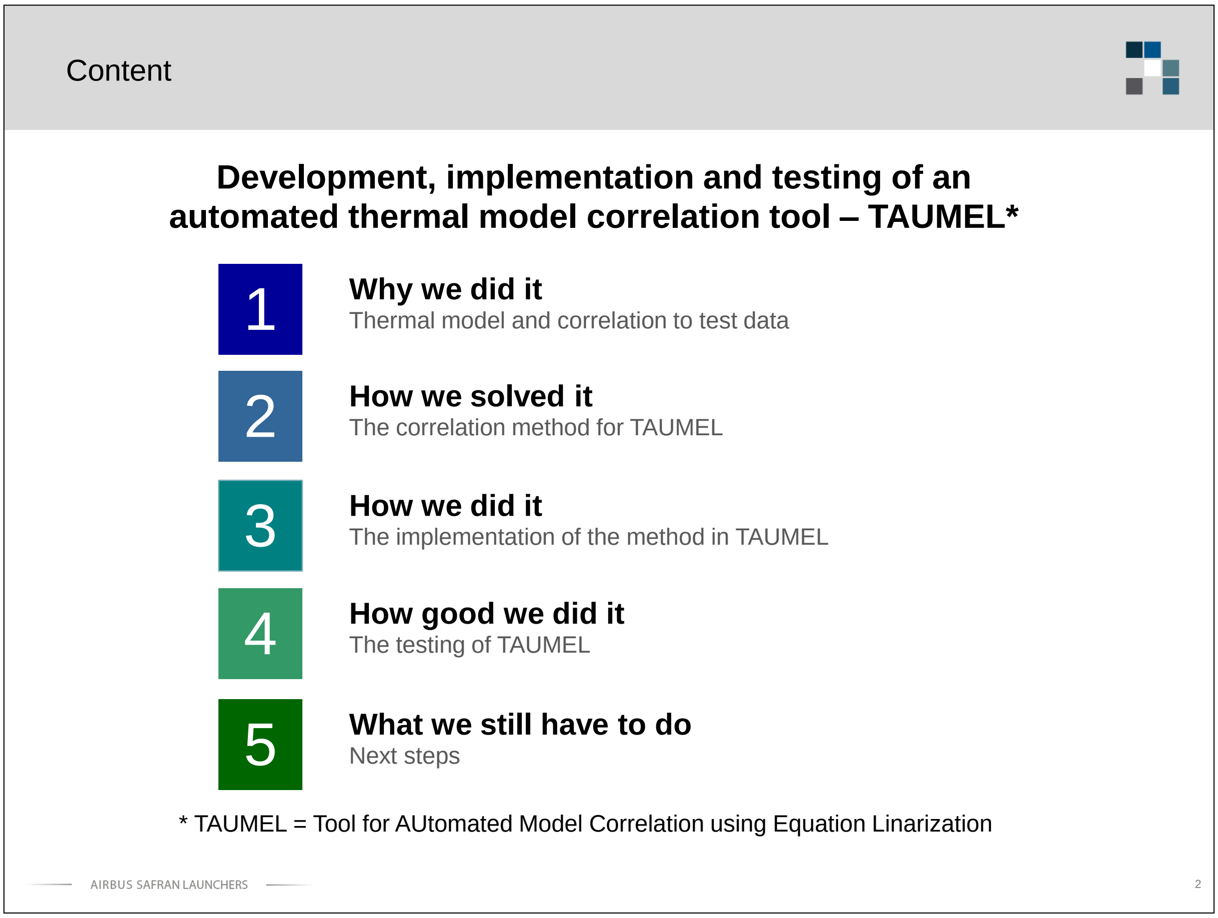
Content
Development, implementation and testing of an automated thermal model correlation tool – TAUMEL*
1 Why we did it
Thermal model and correlation to test data
2 How we solved it
The correlation method for TAUMEL
3 How we did it
The implementation of the method in TAUMEL
4 How good we did it
The testing of TAUMEL
5 What we still have to do
Next steps
* TAUMEL = Tool for AUtomated Model Correlation using Equation Linarization
AIRBUS SAFRAN LAUNCHERS
2

1 Why we did it

Thermal model and correlation to test data

AIRBUS SAFRAN LAUNCHERS 3

1) Why we did it

TMM

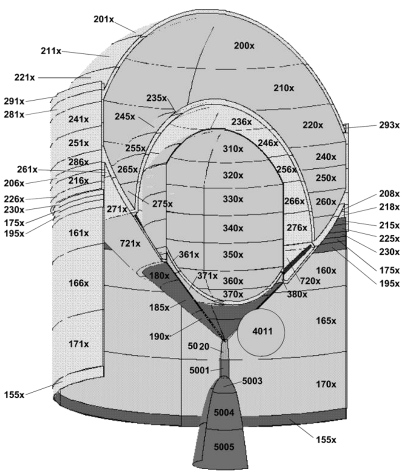

Goodness of fit

$$\begin{bmatrix} T_{model,1} \\ \vdots \\ T_{model,n} \end{bmatrix} \leftrightarrow \begin{bmatrix} T_{test,1} \\ \vdots \\ T_{test,n} \end{bmatrix}$$

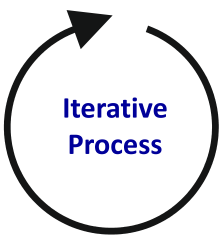

Test

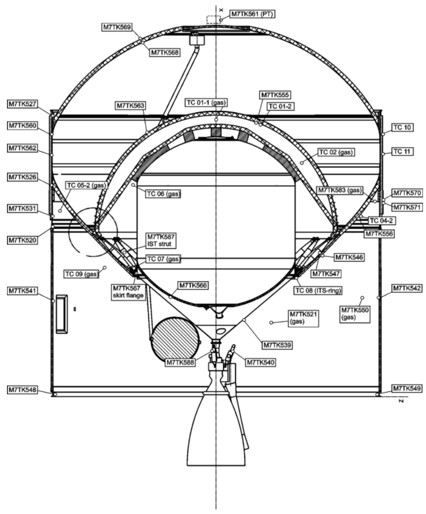

Correlation: **Modification of a thermal model (TMM) to fit the node temperatures and the measurement temperatures**

AIRBUS SAFRAN LAUNCHERS 4

2 How we solved it

The correlation method for TAUMEL

AIRBUS SAFRAN LAUNCHERS 5

2) How we solved it (our solution)

Parameterized model

Initial TMM

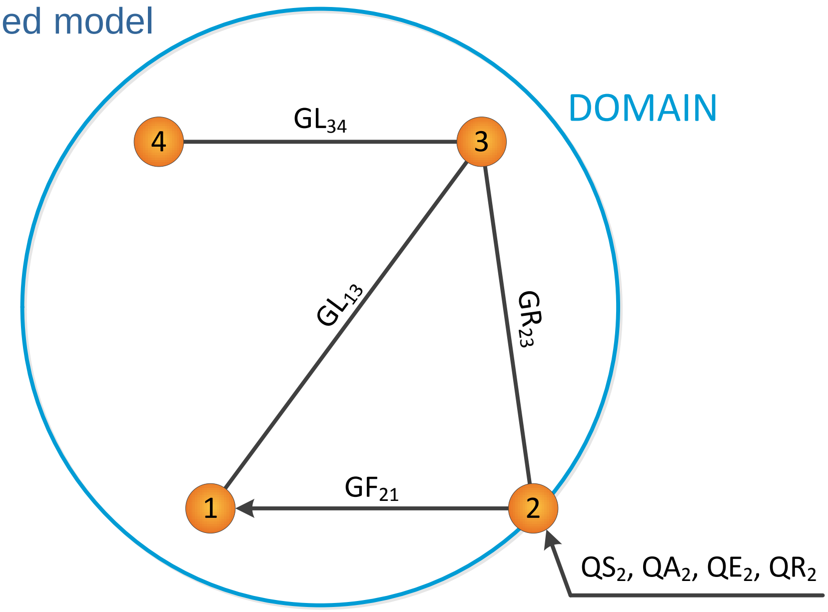

AIRBUS SAFRAN LAUNCHERS 6

2) How we solved it (our solution)

Parameterized model

Modified TMM

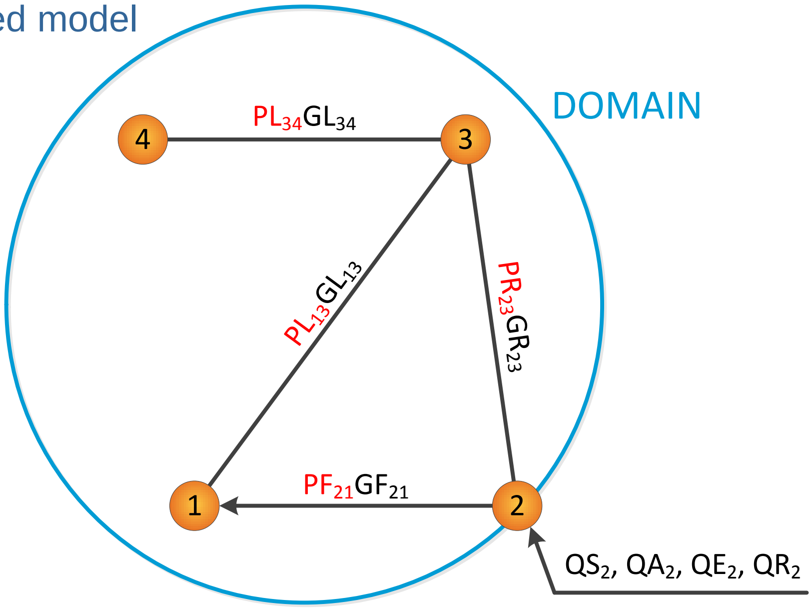

Variation of parameters ←→ Variation of conductors

AIRBUS SAFRAN LAUNCHERS 7

2) How we solved it (our solution)

Linearized parameterized solver

1

$$C_i\dot{T}_i = \sum_{i\neq j} GL_{ij}(T_j - T_i) + \sigma \sum_{i\neq k} GR_{ik}((T_k)^4 - (T_i)^4) + \dot{Q}_{B,i} \qquad \forall i$$

- Read the governing equation solved by the TMM
- Selection of a time step t_0

2

$$C_i\dot{T}_i^r = \sum_{i\neq j} \boldsymbol{PL_{ij}} GL_{ij}(T_j - T_i) + \sigma \sum_{i\neq k} \boldsymbol{PR_{ik}} GR_{ik}((T_k)^4 - (T_i)^4) + \dot{Q}_{B,i} \qquad \forall i$$

- Introduction of Parameters by the user

3

$$0 = \sum_{i\neq j} \boldsymbol{PL_{ij}} GL_{ij}(T_j - T_i) + \sigma \sum_{i\neq k} \boldsymbol{PR_{ik}} GR_{ik}(T_k - T_i) + \dot{Q}_{B,i} + \dot{Q}_{\dot{T}} + \dot{Q}_L \qquad \forall i$$

- Linearization of the equation and opimization of Parameters

AIRBUS SAFRAN LAUNCHERS 8

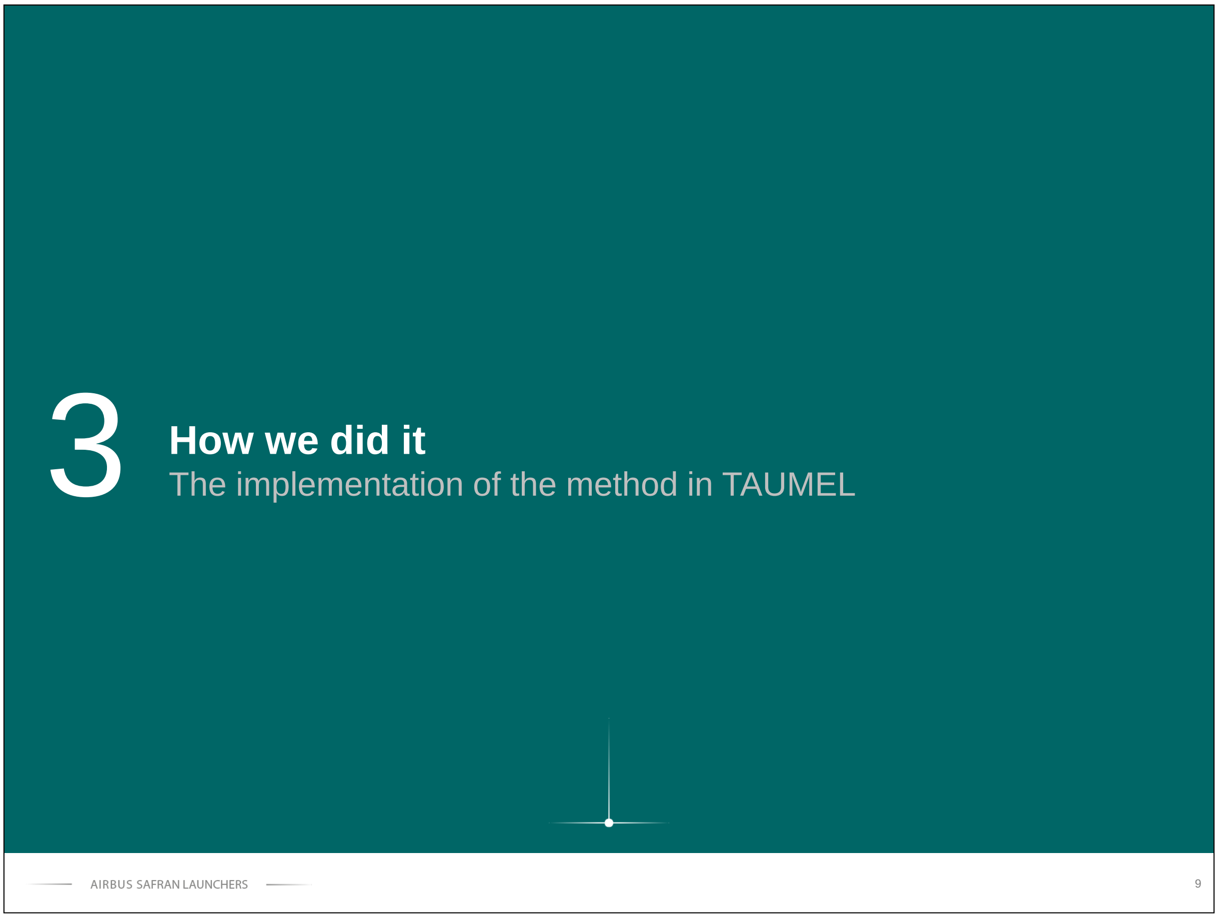
3
How we did it
The implementation of the method in TAUMEL
AIRBUS SAFRAN LAUNCHERS
9

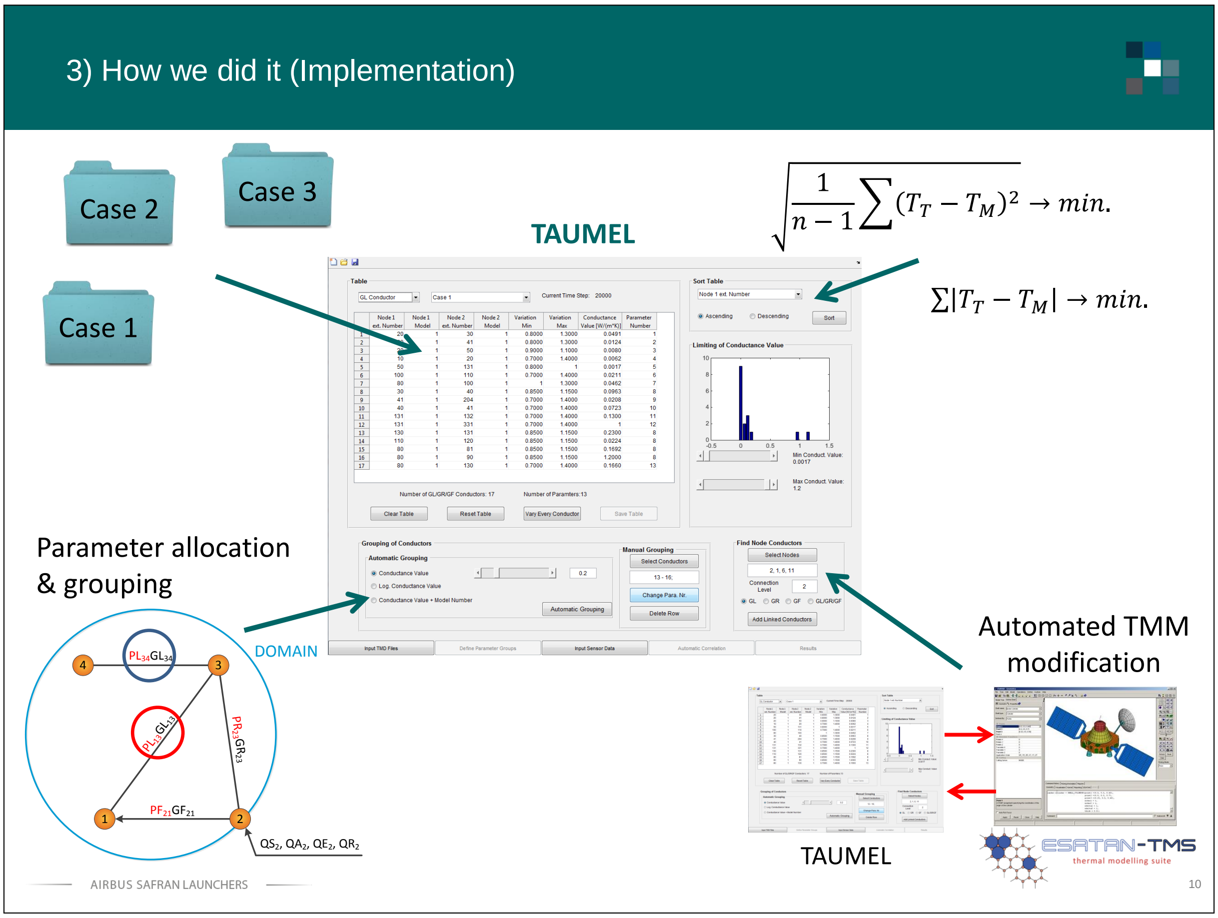
3) How we did it (Implementation)
Case 2
Case 3
Case 1
TAUMEL
$\sqrt{\frac{1}{n-1}\sum(T_T - T_M)^2} \rightarrow min.$
$\sum|T_T - T_M| \rightarrow min.$
Parameter allocation
& grouping
DOMAIN
Automated TMM
modification
TAUMEL
ESATAN-TMS
thermal modelling suite
AIRBUS SAFRAN LAUNCHERS
10

4 How good we did it

The testing of TAUMEL

AIRBUS SAFRAN LAUNCHERS 11

4) How good we did it (Testing)

Test model 1N-Thruster

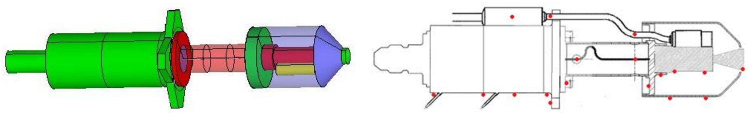

- Measurements coverage of 66% of model nodes
- Already existing conventional correlation for comparison
- Small model:
    - 45 diffusion nodes
    - 234 conductors

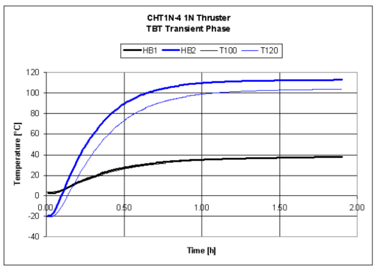

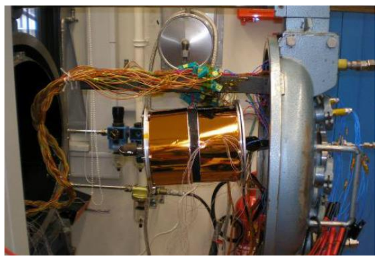

AIRBUS SAFRAN LAUNCHERS 12

4) How good we did it (Testing)

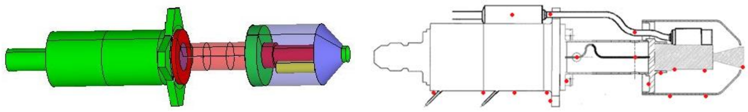

Node Nr	Node Description	Sensor Temp. [°C]	ESATAN-TMS (uncorr.) Temp. [°C]	Abs. Diff [°C]
10	Nozzle	179	215	36
20	TCA Housing	190	225	35
30	TCA Flange Rim	165	199	34
40	TCA Flange Main	150	137	13
70	TCA Housing_Cov	118	107	11
80	Hea_Bar_Flg_Rim	55	47	8
90	FCV Flange	51	46	5
100	Hea_Bar_Low	70	89	19
120	Hea_Bar_Upp	138	136	2
130	FCV_H/B	54	47	7
131	FCV_Mid	57	54	3
132	FCV_Sup	58	57	1
133	FCV_Tubing	52	54	2

Mean Absolute Deviation: 13,483 K ☹

AIRBUS SAFRAN LAUNCHERS 13

4) How good we did it (Testing)

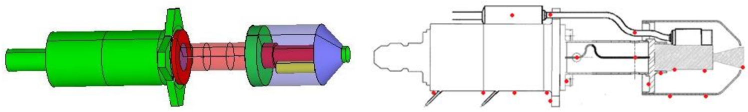

Node Nr	Node Description	Sensor Temp. [°C]	TAUMEL Temperature [°C]	Abs. Diff [°C]
10	Nozzle	179	179	0
20	TCA Housing	190	187	3
30	TCA Flange Rim	165	165	0
40	TCA Flange Main	150	140	10
70	TCA Housing_Cov	118	117	1
80	Hea_Bar_Flg_Rim	55	52	3
90	FCV Flange	51	51	0
100	Hea_Bar_Low	70	70	0
120	Hea_Bar_Upp	138	138	0
130	FCV_H/B	54	54	0
131	FCV_Mid	57	57	0
132	FCV_Sup	58	58	0
133	FCV_Tubing	52	54	2

Mean Absolute Deviation: 1,602 K☺

AIRBUS SAFRAN LAUNCHERS 14

4) How good we did it (Testing)

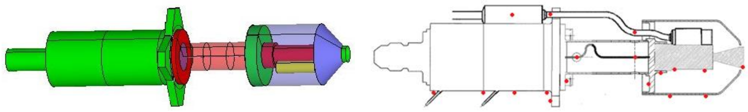

Node Nr	Node Description	Sensor Temp. [°C]	ESATAN-TMS (corr.) Temp. [°C]	Abs. Diff [°C]
10	Nozzle	179	181	2
20	TCA Housing	190	189	1
30	TCA Flange Rim	165	166	1
40	TCA Flange Main	150	140	10
70	TCA Housing_Cov	118	117	1
80	Hea_Bar_Flg_Rim	55	52	3
90	FCV Flange	51	51	1
100	Hea_Bar_Low	70	69	1
120	Hea_Bar_Upp	138	138	0
130	FCV_H/B	54	54	0
131	FCV_Mid	57	57	0
132	FCV_Sup	58	58	0
133	FCV_Tubing	52	54	2

Mean Absolute Deviation: 1,695 K☺

AIRBUS SAFRAN LAUNCHERS 15

4) How good we did it (Testing)

Correlation Strategy

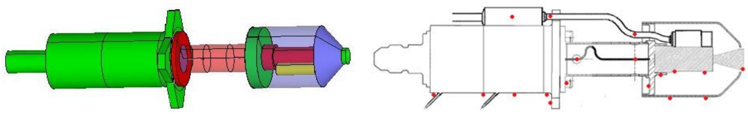

Run	Description of Strategy	MAD [K]
0		13,48
1	All linear conductors GL (0.7 – 1.3)	7,42
2	All GLs +- 0.3	5,32
3	All GLs +- 0.3	3,53
4	All GLs +- 0.2	2,98
5	Nodes 40 and 70: GRs added to variation	2,60
6	All GLs and selected GRs +- 0.2	2,45
7	All GLs and selected GRs +- 0.2	2,30
8	Node 20: GRs on node 20 added to variation	2,29
9	All GLs and selected GRs +- 0.2	2,10
10	All GLs and selected GRs +- 0.2	1,86
11	All GLs and selected GRs +- 0.2	1,73
12	All GLs and selected GRs +- 0.2	1,60

AIRBUS SAFRAN LAUNCHERS 16

4) How good we did it (Testing)

Evolution of goodness of fit

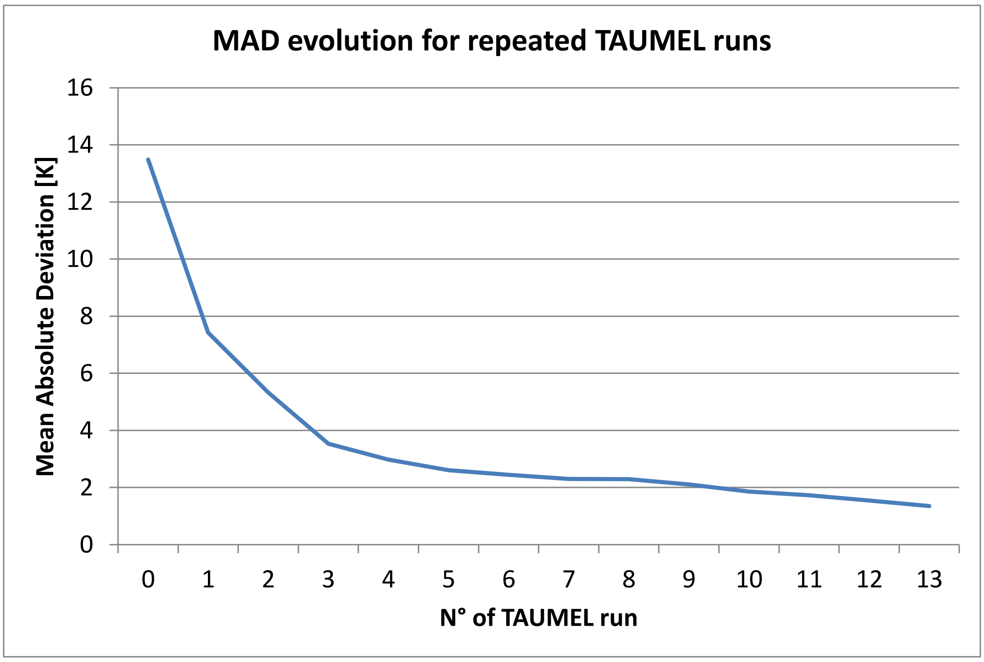

AIRBUS SAFRAN LAUNCHERS 17

4) How good we did it (Testing)

Evolution of parameters

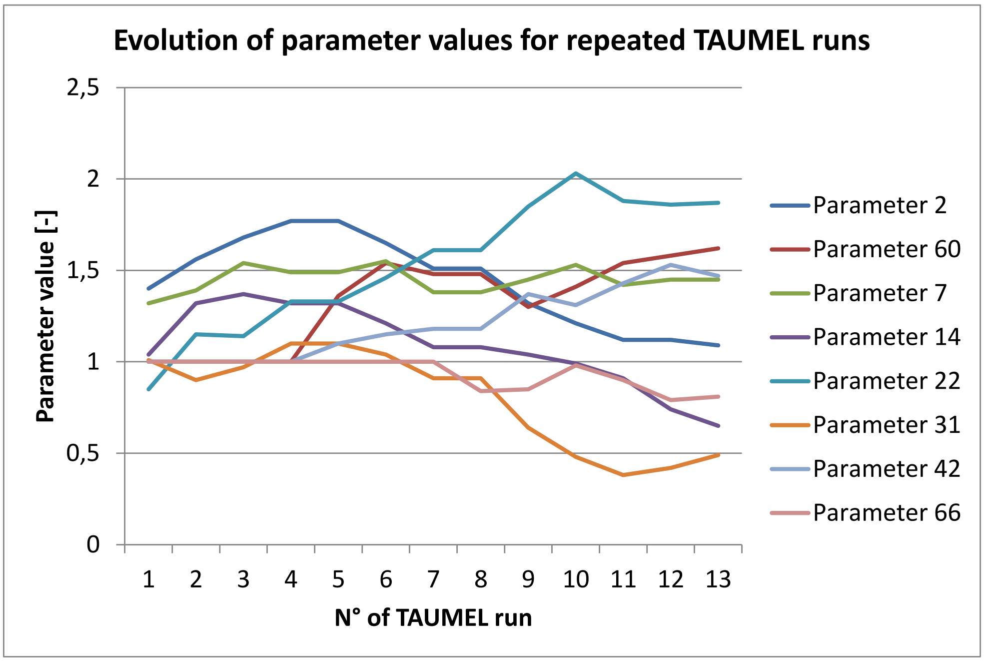

AIRBUS SAFRAN LAUNCHERS 18

4) How good we did it (Testing)

Benchmarking

Model	Number of Cycles	Number of Iterations	Number of Nodes	Processing Time [s]
1-N-Thruster	100	100	45	25
20-N-Thruster	100	100	144	60
ESC-A	100	100	1467	201
A5ME US	100	100	~23000	~1h

Experience:
~10 repetitions of the correlation for optimized results

Model	Preparation* [min]	Process [min]	Total correlation time (assessed)
1-N-Thruster	60	8	~1h
20-N-Thruster	90	20	~2h
ESC-A	120	67	~3h
A5ME	300	600	~15h

Nota: 1-N-Thruster conventional correlation ~4 Weeks of iterations

AIRBUS SAFRAN LAUNCHERS 19

5 What we still have to do

Next steps

AIRBUS SAFRAN LAUNCHERS 20

5) Next steps

- Test of TAUMEL from non-involved people (only with user-manual).
- Enabling to correlate Systema/Thermica models with TAUMEL.
- Code documentation – e.g. flow chart.
- Function for assessment of conductor correlation impact.
- Documentation of current verification, validation and results.

External usage of TAUMEL

- <u>ASL is interested in external usage</u>!
  However, we want to be involved in the correlation process in order to see if new thermal models lead to new unknown problems.
- <u>No verification</u> according to commercial software foreseen.

AIRBUS SAFRAN LAUNCHERS 21

6 Backup Slides

AIRBUS SAFRAN LAUNCHERS 23

6) Backup Slides

New approach overview

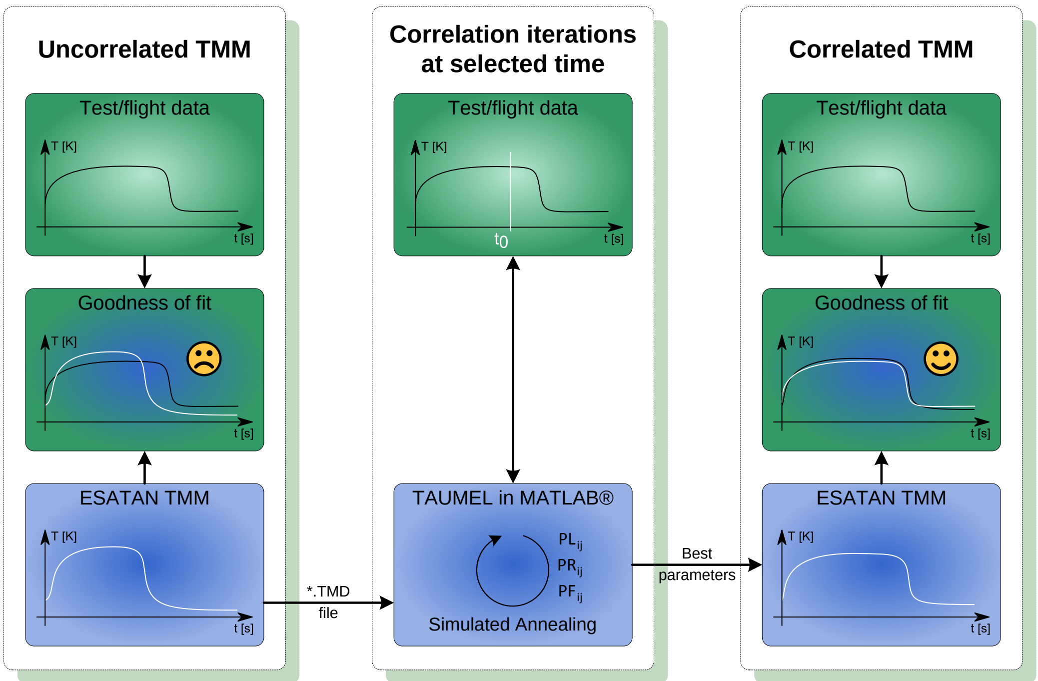

AIRBUS SAFRAN LAUNCHERS 24

6) Backup Slides

TAUMEL GUI

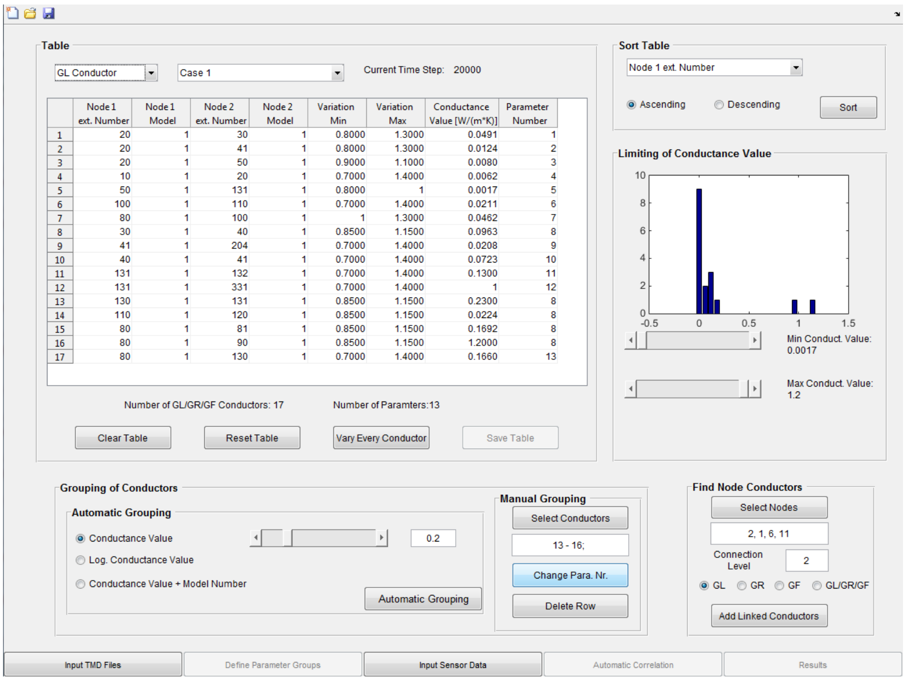

AIRBUS SAFRAN LAUNCHERS 25

6) Backup Slides

Calculation times

Model	Without GR improvement-term	Without GR improvement-term (2 calculations)	ESATAN-TMS (transient calculation)
1-N-Thruster (45 nodes)	0.0015 s	0.0018 s	38.3s
VINCI (170 nodes)	0.0033 s	0.0043 s	7m, 29s
ESC-A (1467 nodes)	0.0132 s	0.0214 s	2m, 36s
A5ME (~23000 nodes)	0.3336 s	0.6213 s	>4h

Slide 19

AIRBUS SAFRAN LAUNCHERS 26

Appendix H

The challenges of modelling helium gas conduction and helium seal interfaces in ESATAN-TMS r7

Nicole Melzack
(RAL Space, United Kingdom)

Abstract

The Meteosat series of spacecraft are meteorological satellites, providing a range of data that inform weather forecasts across Europe. Two instruments going on the MTG (Meteosat Third Generation) satellites will be calibrated using the blackbody targets that are being designed at RAL Space.

Modelling of the ground based blackbody calibration targets was done in ESATAN-TMS r7. The targets use a helium gas gap heat switch as the main aspect of the thermal control system. This talk will cover the challenges involved in modelling the gas conduction, and will present the current implementation.

Other aspects of the design, such as determining the conductance across a complex interface involving a helium seal will also be discussed. This presentation will also touch on the correlation of the thermal model post prototype testing.

The challenges of modelling helium gas conduction and helium seal interfaces in ESATAN-TMS r7

Nicole Melzack, RAL Space, STFC

RAL Space

European Space Thermal Analysis Workshop
5-6th October 2016

Science & Technology Facilities Council

RAL Space

Outline

- Meteosat
- Blackbodies
- Design overview
- Thermal challenges
  - Helium Conduction
  - Helium seal interface
- Next steps

Meteosat

MFG 1979—2011

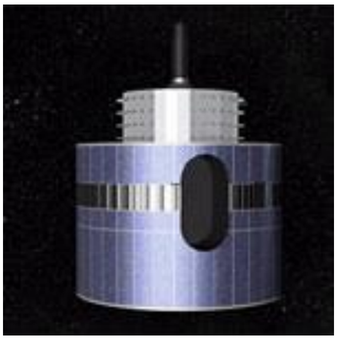

Image credit: ESA

MSG 2002—2019

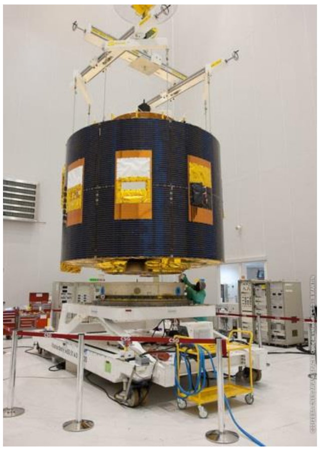

Image credit: ESA

MTG 2018—2038

Image credit: Eumetsat

MTG

- MTG-S
  - IRS (Infra-red Sounder) by OHB
- MTG-I
  - FCI (Flexible Combined Imager) by TAS-F

- Two sets of customer requirements
  - One calibration blackbody design

Blackbody calibration target

- Target of accurately known temperature and high (~1) emissivity
- Precisely controlled
  - Better than instrument can measure
- Used to calibrate instrument
- Often a baseplate surrounded by a baffle

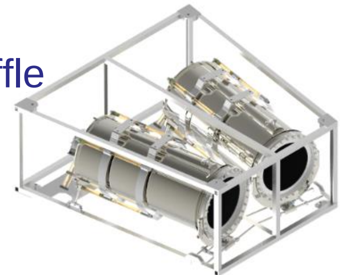

Calibration blackbody

MTG blackbodies thermal challenges

- **Large operating temperature range**
  - **100–370 K**
- Small temperature gradient requirements
- Transition between temperatures in 0.1 K steps
- Transition 16 K in 30 minutes
- 3 kW power limit

RAL Space

Helium gas gap

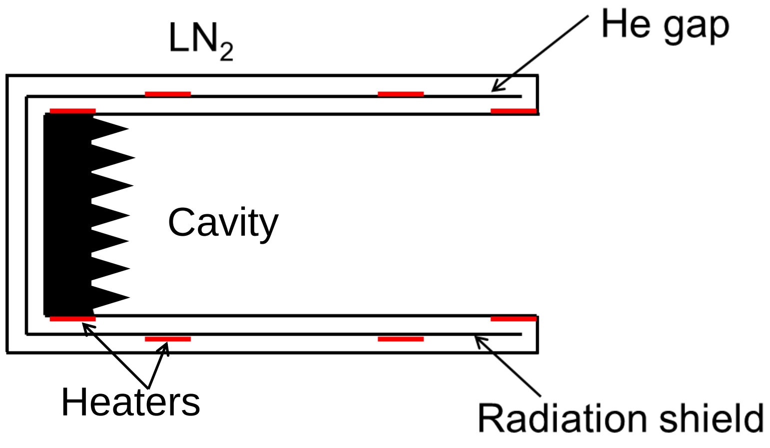

RAL Space

Helium conductivity in a gas gap

Helium thermal conductivity in a helium gas gap

$$k(T) = k_{bulk}(T) \cdot \left(1 + \frac{8}{3} \cdot \frac{k_{bulk}(T) \cdot T}{e \cdot p \cdot \sqrt{3 \cdot R \cdot T}} \cdot \left(\frac{1}{\alpha_1} + \frac{1}{\alpha_2} - 1\right)\right)^{-1}$$

k_{bulk} is the bulk conductivity of He
T is temperature
e is the gap thickness
p is the pressure of the gas
R is the specific gas constant
α is the thermal accommodation factor

Equation from:
'Active-mirror-laser-amplifier thermal management with tuneable helium pressure at cryogenic temperatures', A. Lucianetti et al., Optics Express, Vol 19, Issue 13, pp. 12766 – 12780, 2011.

Helium pressure and thermal conductivity

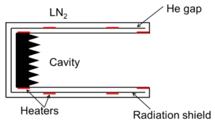

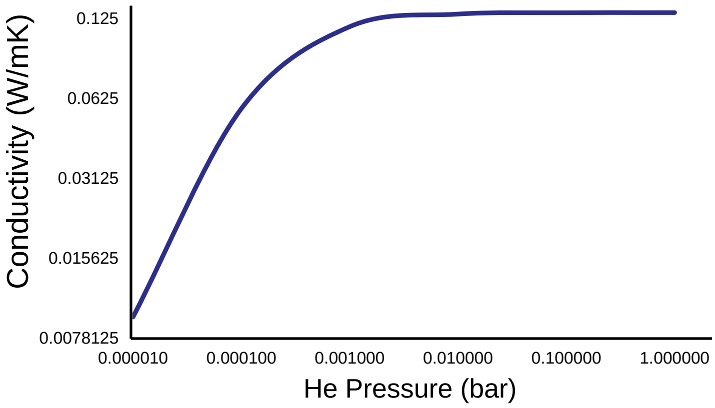

Main thermal modelling challenges

- **Helium conductivity**
- Helium seal interface

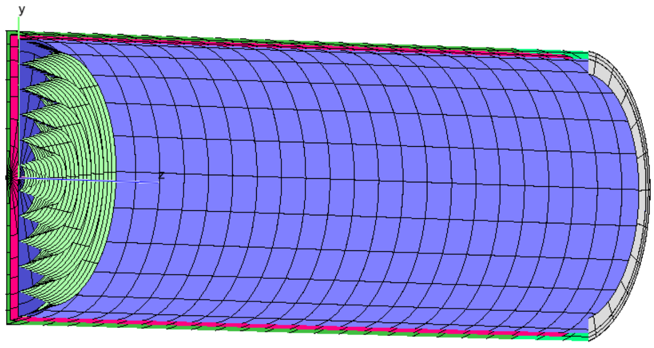

RAL Space

Helium gas conduction modelling

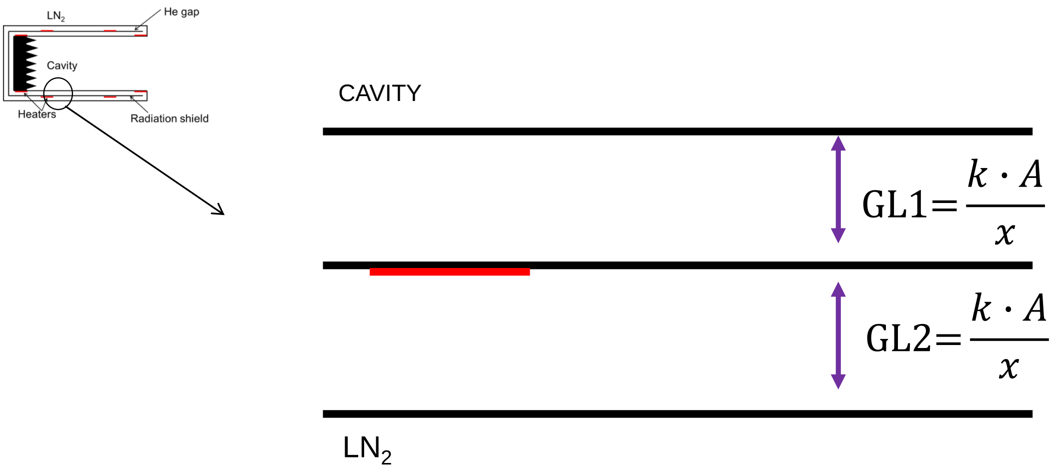

$$GL1 = \frac{k \cdot A}{x}$$

$$GL2 = \frac{k \cdot A}{x}$$

$$k(T) = k_{bulk}(T) \cdot \left(1 + \frac{8}{3} \cdot \frac{k_{bulk}(T) \cdot T}{e \cdot p \cdot \sqrt{3 \cdot R \cdot T}} \cdot \left(\frac{1}{\alpha_1} + \frac{1}{\alpha_2} - 1\right)\right)^{-1}$$

RAL Space

Helium gas conduction in ESATAN

```
$LOCALS
# GENCODE LOCALS - DO NOT REMOVE
#


      $REAL

####  FOR 0.025 mbar intermediate He pressure unhash below

                #Modelling of Helium Gas Conductance - conductivity value
        GL1=5.0;        # k = 0.021563  at 0.025 mbar
        GL2=5.206052;
        GL3=0.514395;
        GL4=0.2214;
####  FOR 1 bar He pressure unhash below

    #   GL1 = 16.60581;      # based on k =0.071 at 1 bar
    #   GL2 = 17.29014;
    #   GL3 = 1.708;
    #   GL4 = 0.735;

      $CHARACTER
```

RAL Space

Helium gas conduction in ESATAN

```
# applying gas conduction values between radiation shield and cavity
FOR KL1 = 11000 TO 11527 DO
    KL2 = KL1 + 11000;
    GL(KL2,KL1)= GL1/528;
END DO

# applying gas conduction values between radiation shield and LN2 jacket
FOR KL1 = 21000 TO 21479 DO
    KL2 = KL1 + 7000;
    GL(KL1,KL2) = GL2/480;
END DO
```

RAL Space

Three He pressure set points needed

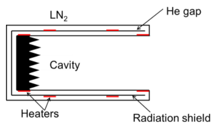

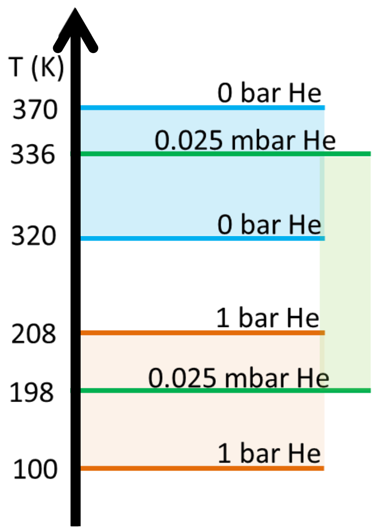

Helium conduction – limitations of equation

- Temperature of helium
- Perpendicular conduction modelled only
- Gas gap modelled O(1mm) much larger than conventional gas gaps
- Larger surface area than a conventional gas gap heat switch
- Curved surface

Dynamic helium gas conduction

```
# applying gas conduction values between radiation shield and cavity
    DO I = 11000,11527,1
       J = I + 11000
       KL1 = INTNOD(CURRENT,I)
       KL2 = INTNOD (CURRENT,J)
       XKL3 = (GETT(KL1) + GETT(KL2))/2  # average temperature (T of He)
       XKL4 = INTRP1 (XKL3,He_T_v_k,1)  # bulk conductivity from array
       XKL5 = XKL4*((1+(8/3*XKL4*XKL3/e1/press/(3*8314/4.0026*XKL3)**0.5*(1/alf +1/alf-1)))**(-1)) # k value in gas gap
       XKL6 = XKL5*0.00245662 / e1 *XKL7
       CALL SETGL(CURRENT,KL2,KL1,XKL6 )   # GL value based on average area of node
   END DO
```

Helium gas conduction modelling

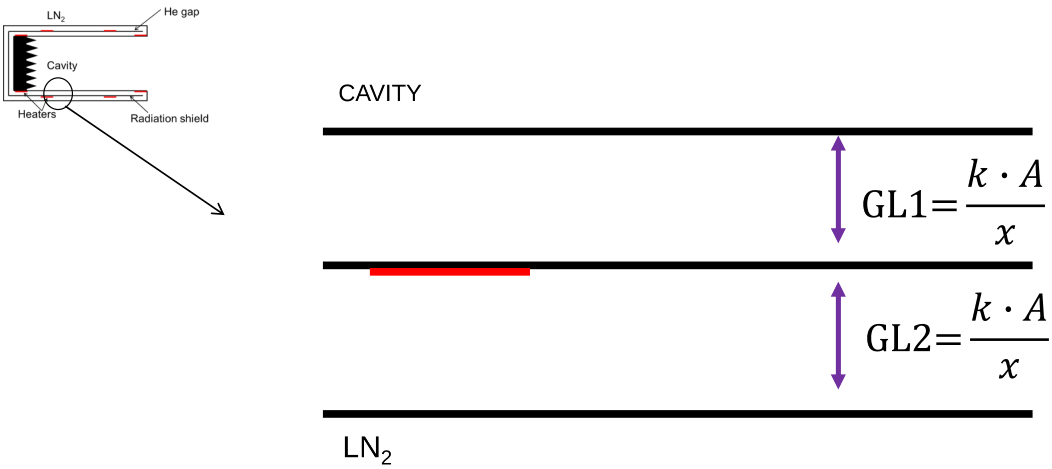

Breadboard Model Testing

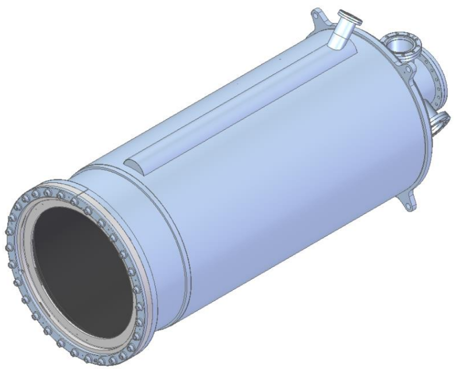

RAL Space

Helium conduction from testing

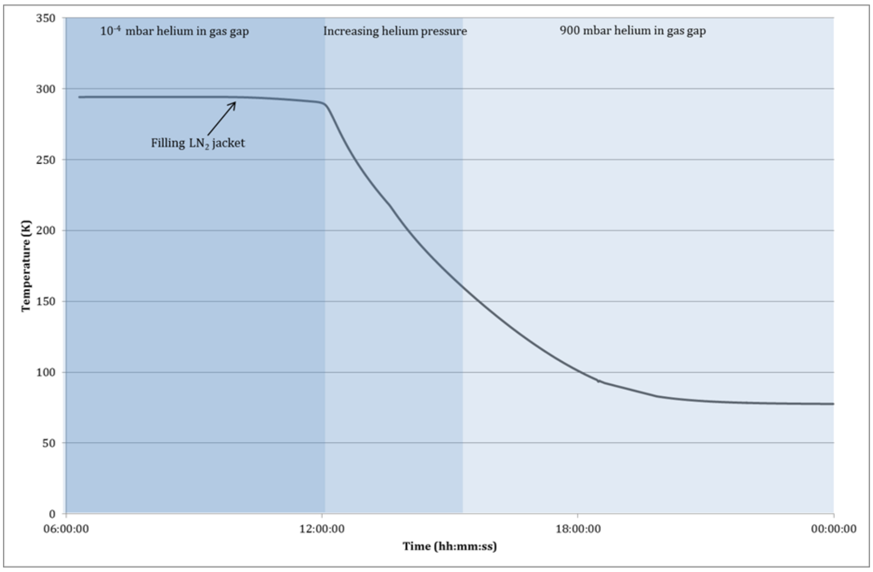

RAL Space

Main thermal modelling challenges

- Helium conductivity
- **Helium seal interface**

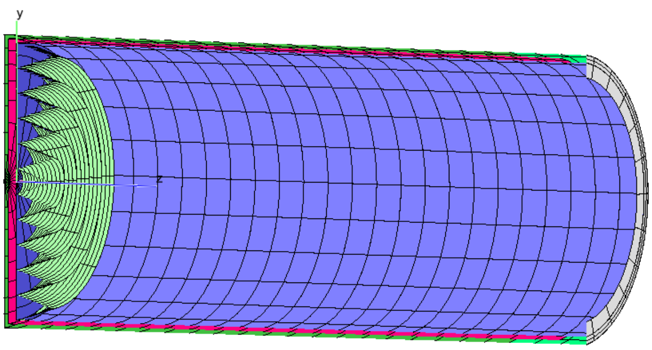

Helium seal interface

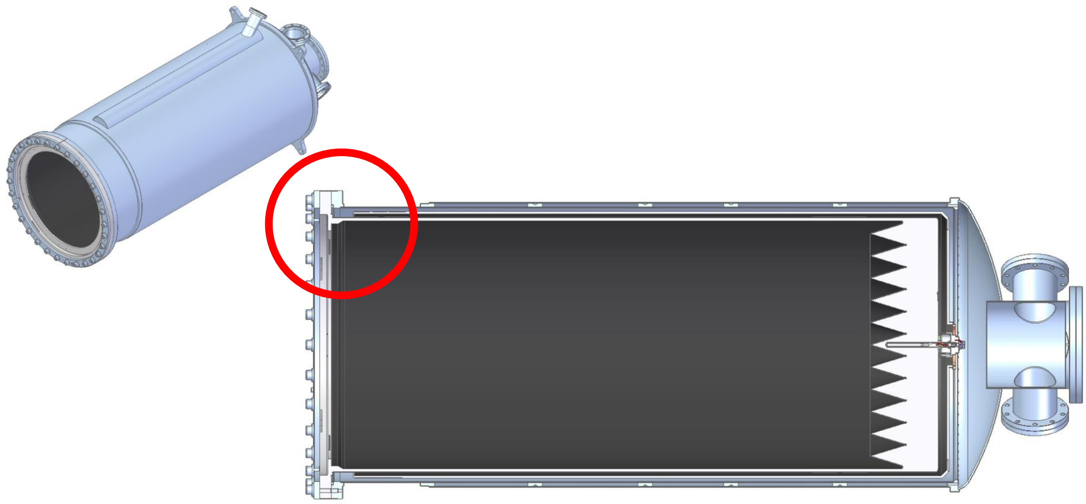

Helium seal interface

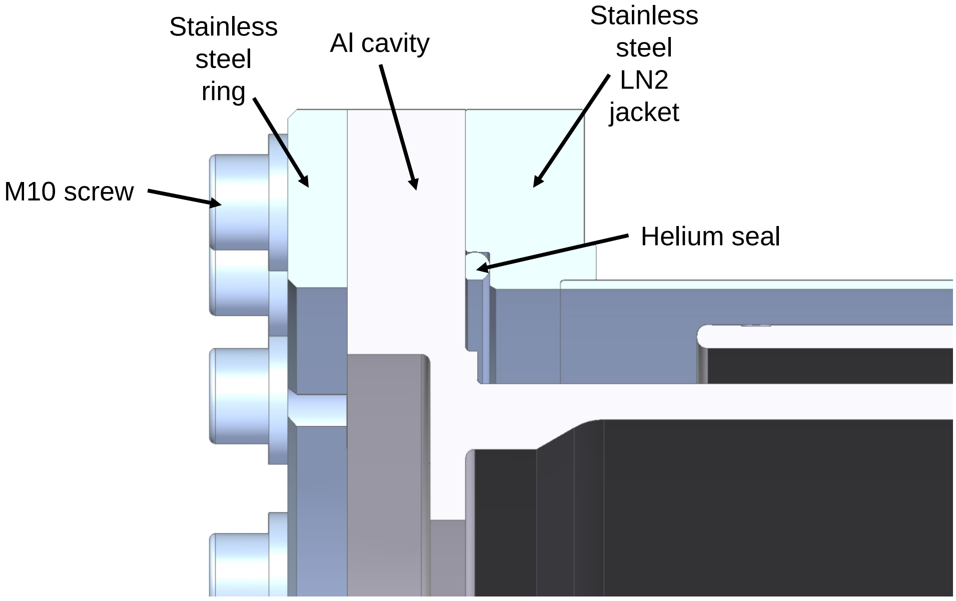

Helium seal interface

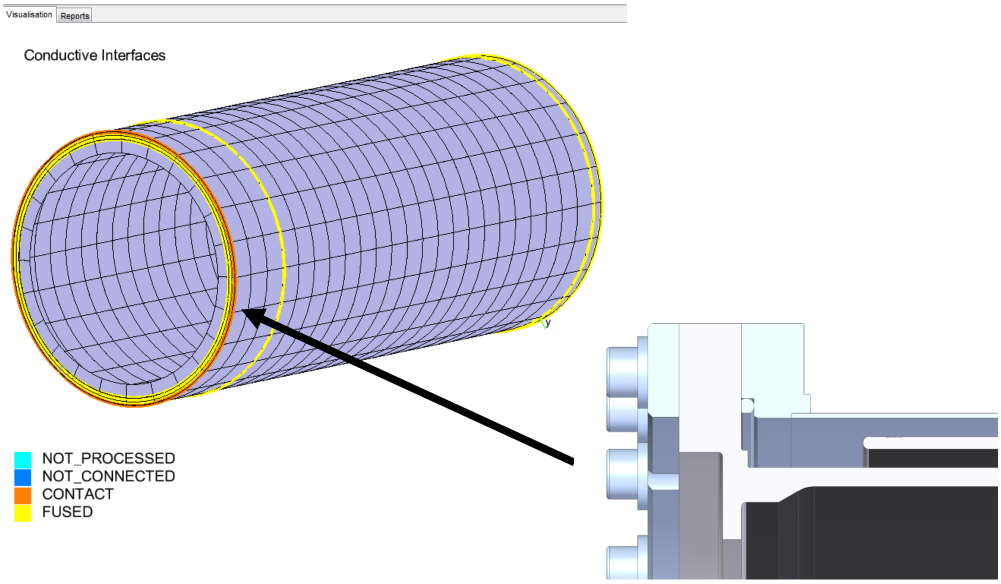

Dummy seal interface

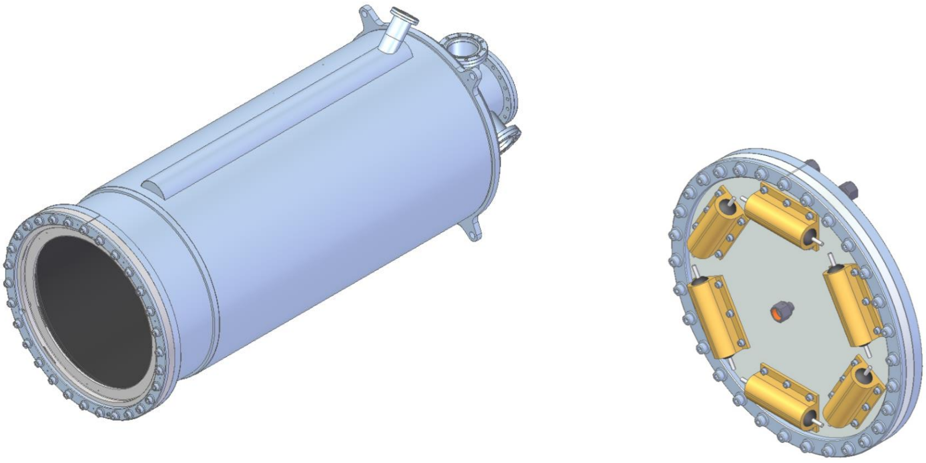

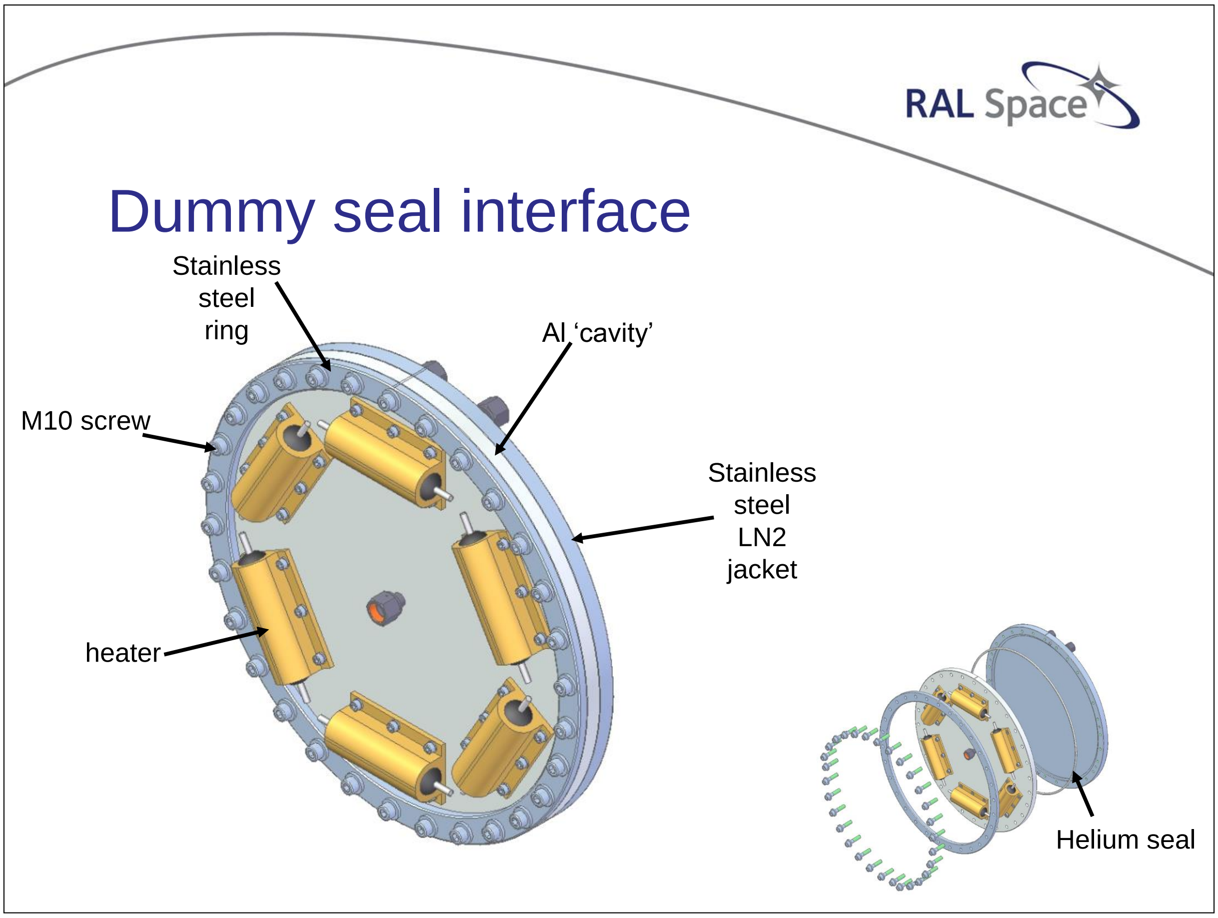
RAL Space
Dummy seal interface
Stainless steel ring
Al 'cavity'
M10 screw
Stainless steel LN2 jacket
heater
Helium seal

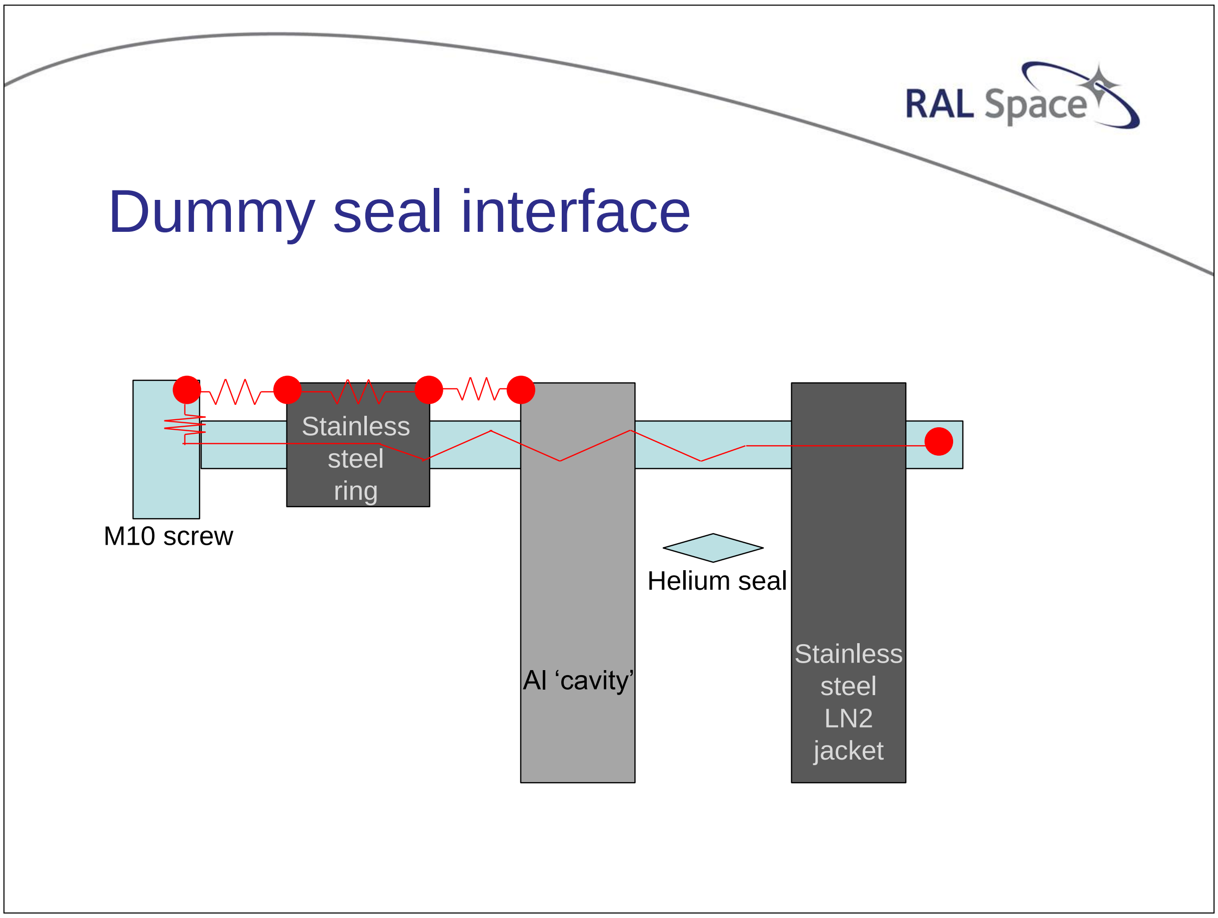
RAL Space
Dummy seal interface
Stainless steel ring
M10 screw
Helium seal
Al 'cavity'
Stainless steel LN2 jacket

Next steps

- Using model to improve bulk temperature changes
  - Modelling transient ‘helium assisted’ cooldowns
- Performing helium seal test
  - Verifying the conductive path through the interface, and correlating model further with findings

Thank you

Nicole Melzack, RAL Space, STFC
Email: Nicole.Melzack@stfc.ac.uk
Tel: +441235 567147

European Space Thermal Analysis Workshop
5-6th October 2016

Appendix I

Improved integrated way of post-processing thermal result data

Henri Brouquet
(ITP Engines UK Ltd, United Kingdom)

Abstract

Post-processing and reporting of the thermal results is a significant part of the overall thermal modelling process. Clear presentation of results not only helps towards the understanding of the thermal behaviour of the model, but also helps towards model validation.
This presentation focuses on how ESATAN-TMS helps the thermal engineer work efficiently, removing the burden of repetitiveness by making the process fully automatic and integrated within a single interface.

ESATAN-TMS
thermal modelling suite

Improved integrated way of post-processing thermal result

Henri Brouquet

30th European Thermal & ECLS Software Workshop
5 – 6 October 2016, ESA/Estec, Noordwijk, The Netherlands

ESATAN-TMS
thermal modelling suite

Introduction / Background

Requirements → Demo → Questions

- Post-processing and reporting of the thermal results is a significant part of the overall thermal modelling process
  – Repetitive manual process
  – Disconnected from the main geometrical model
  – Model validation is therefore difficult to perform
  – Error prone and time wasting
- Complexity of thermal models has increased significantly over the years

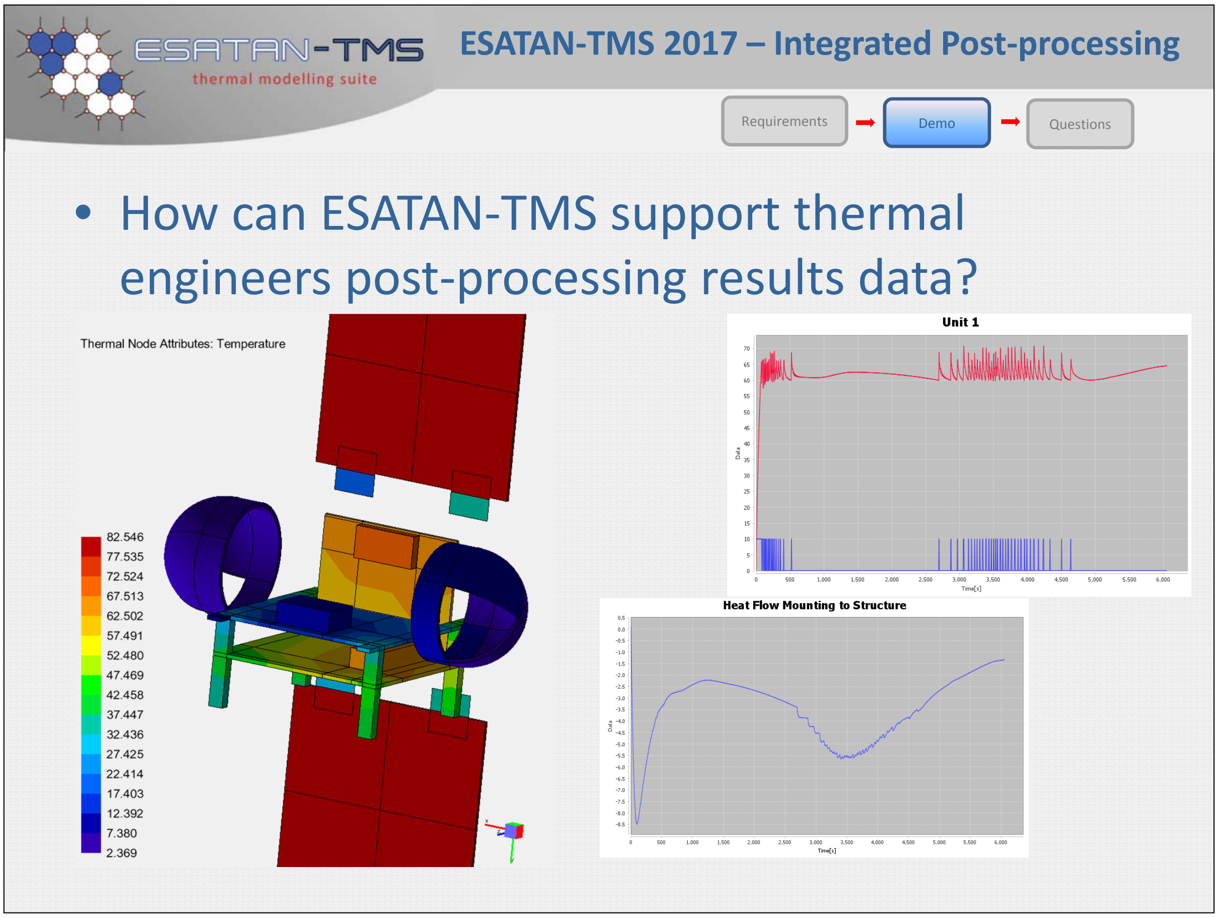
ESATAN-TMS
thermal modelling suite
ESATAN-TMS 2017 – Integrated Post-processing
Requirements
Demo
Questions
• How can ESATAN-TMS support thermal engineers post-processing results data?
Thermal Node Attributes: Temperature
82.546
77.535
72.524
67.513
62.502
57.491
52.480
47.469
42.458
37.447
32.436
27.425
22.414
17.403
12.392
7.380
2.369
Unit 1
Heat Flow Mounting to Structure

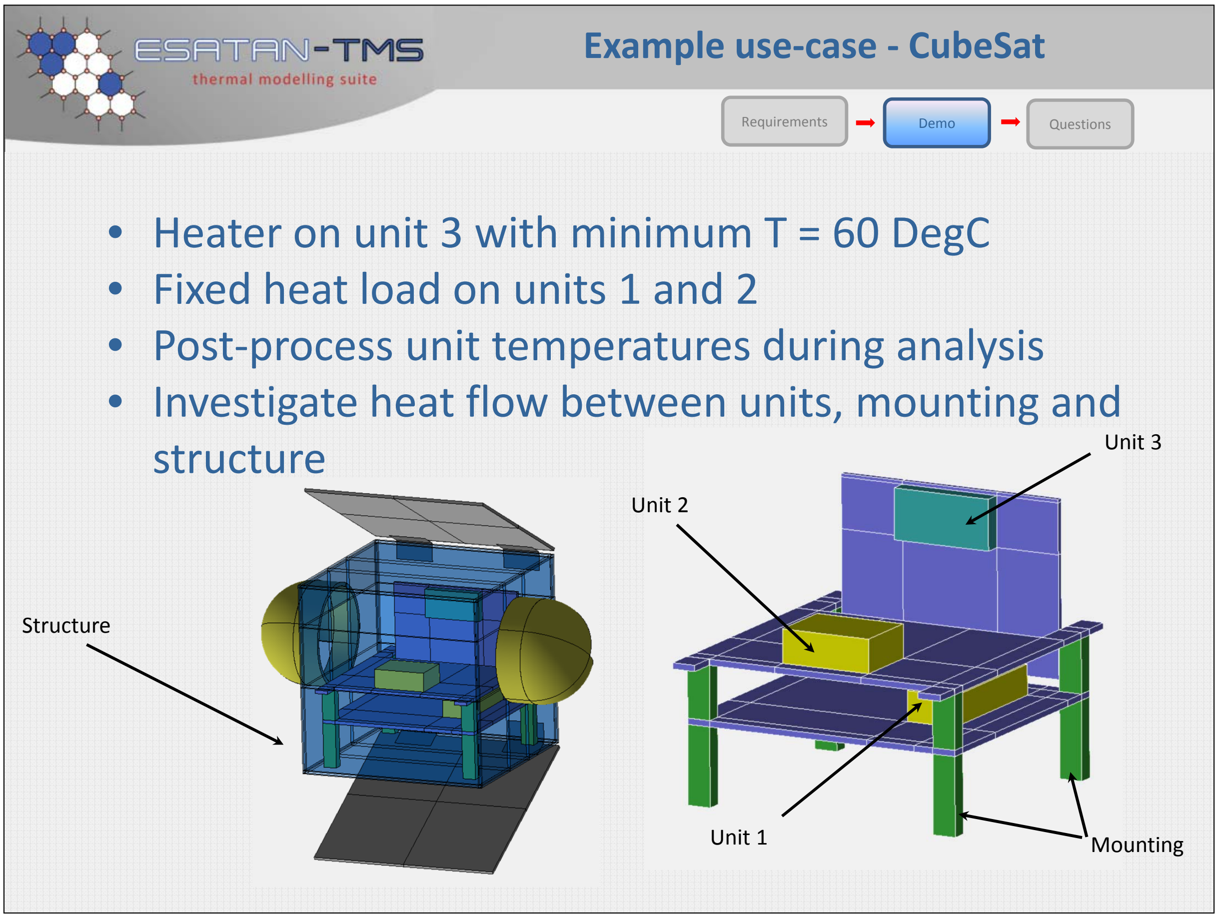
ESATAN-TMS
thermal modelling suite
Example use-case - CubeSat
Requirements
Demo
Questions
• Heater on unit 3 with minimum T = 60 DegC
• Fixed heat load on units 1 and 2
• Post-process unit temperatures during analysis
• Investigate heat flow between units, mounting and structure
Structure
Unit 2
Unit 3
Unit 1
Mounting

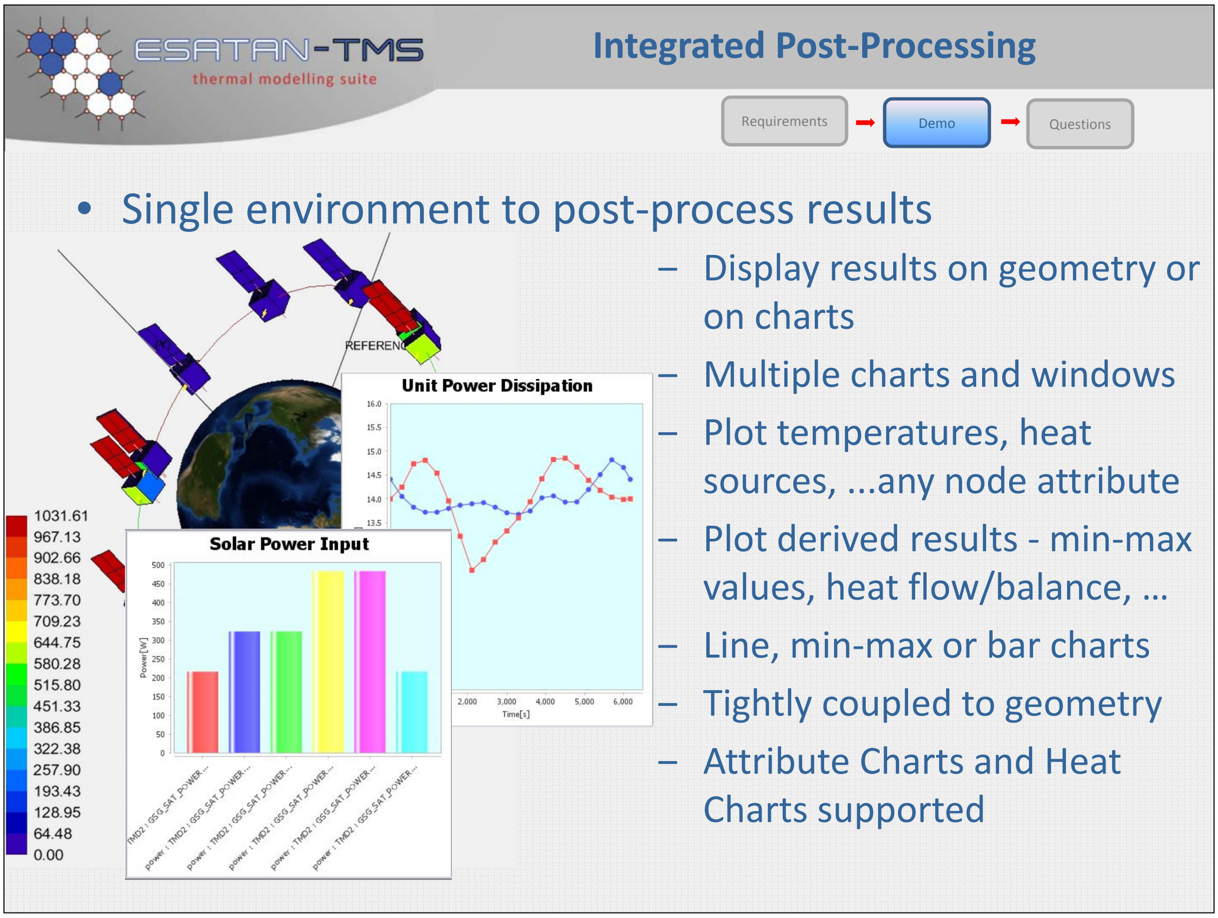
ESATAN-TMS
thermal modelling suite
Integrated Post-Processing
Requirements
Demo
Questions
• Single environment to post-process results
– Display results on geometry or on charts
– Multiple charts and windows
– Plot temperatures, heat sources, ...any node attribute
– Plot derived results - min-max values, heat flow/balance, ...
– Line, min-max or bar charts
– Tightly coupled to geometry
– Attribute Charts and Heat Charts supported
REFERENC
Unit Power Dissipation
Solar Power Input
1031.61
967.13
902.66
838.18
773.70
709.23
644.75
580.28
515.80
451.33
386.85
322.38
257.90
193.43
128.95
64.48
0.00

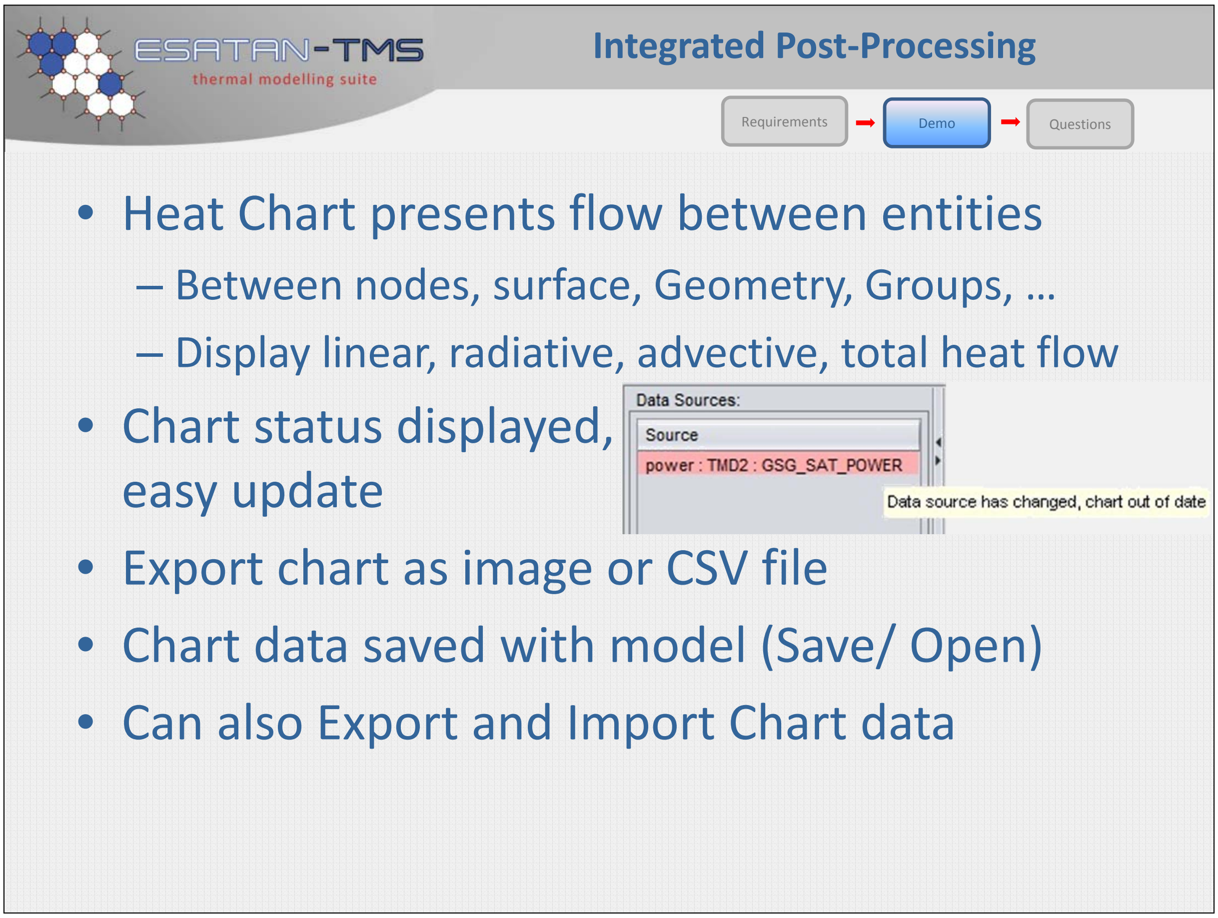
ESATAN-TMS
thermal modelling suite
Integrated Post-Processing
Requirements
Demo
Questions
• Heat Chart presents flow between entities
– Between nodes, surface, Geometry, Groups, …
– Display linear, radiative, advective, total heat flow
• Chart status displayed, easy update
Data Sources:
Source
power : TMD2 : GSG_SAT_POWER
Data source has changed, chart out of date
• Export chart as image or CSV file
• Chart data saved with model (Save/ Open)
• Can also Export and Import Chart data

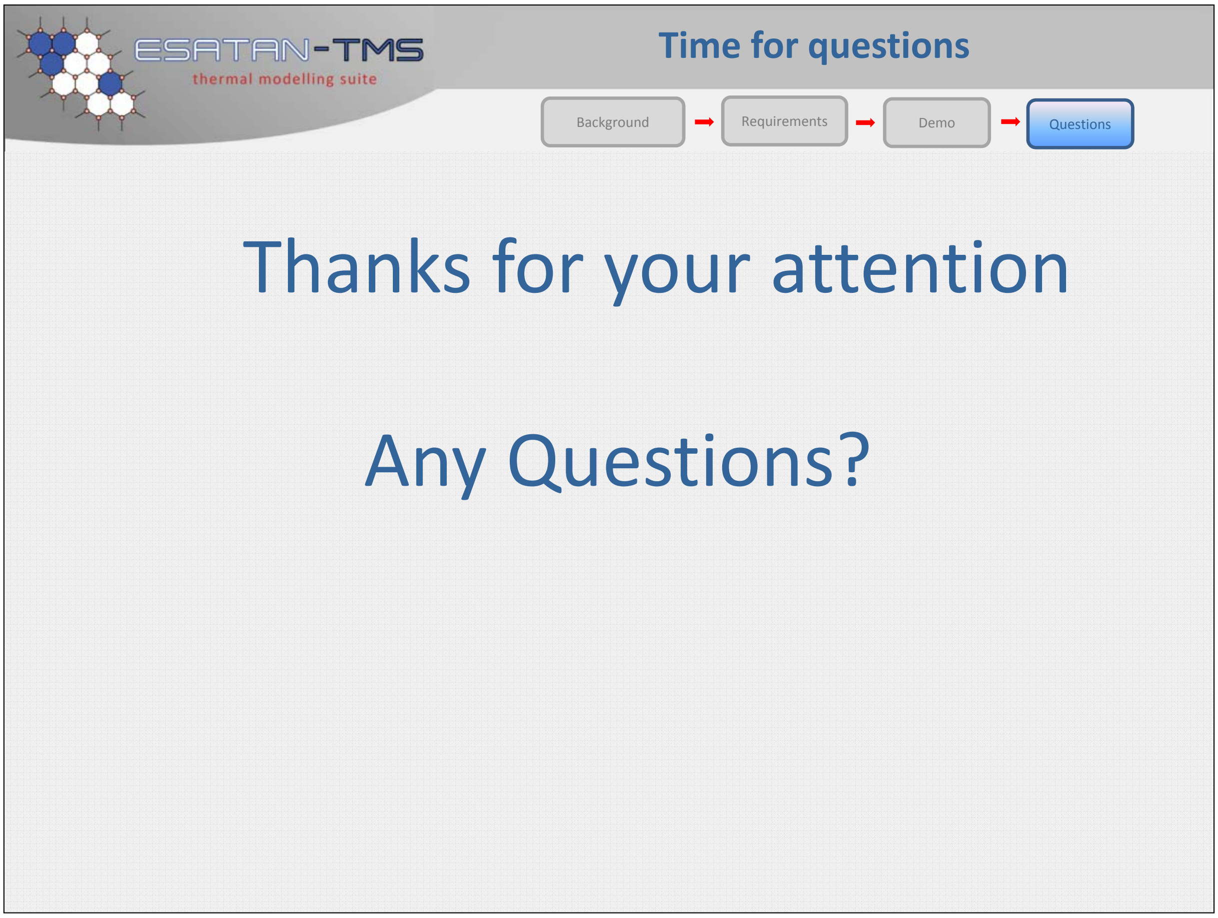
ESATAN-TMS
thermal modelling suite
Time for questions
Background
Requirements
Demo
Questions
Thanks for your attention
Any Questions?

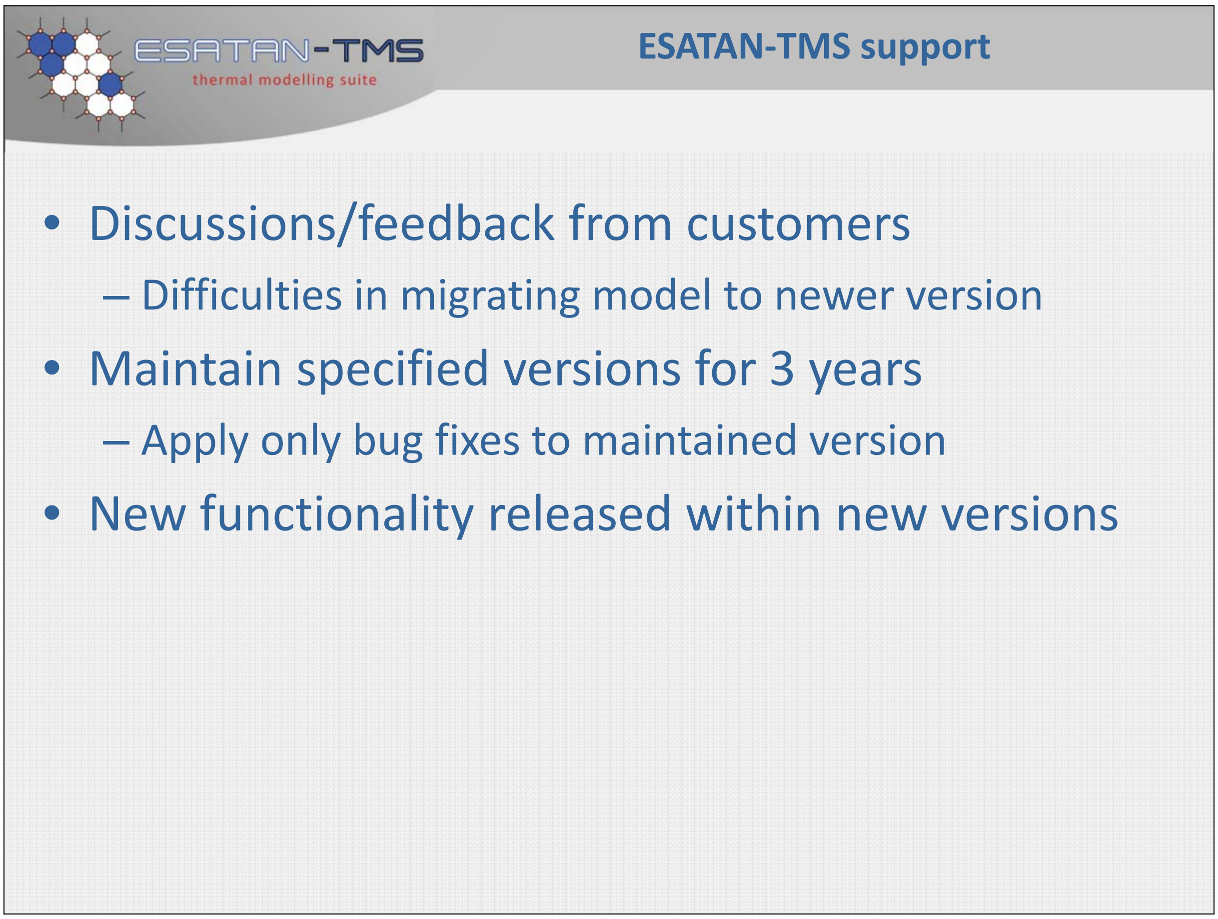
ESATAN-TMS
thermal modelling suite
ESATAN-TMS support
• Discussions/feedback from customers
– Difficulties in migrating model to newer version
• Maintain specified versions for 3 years
– Apply only bug fixes to maintained version
• New functionality released within new versions

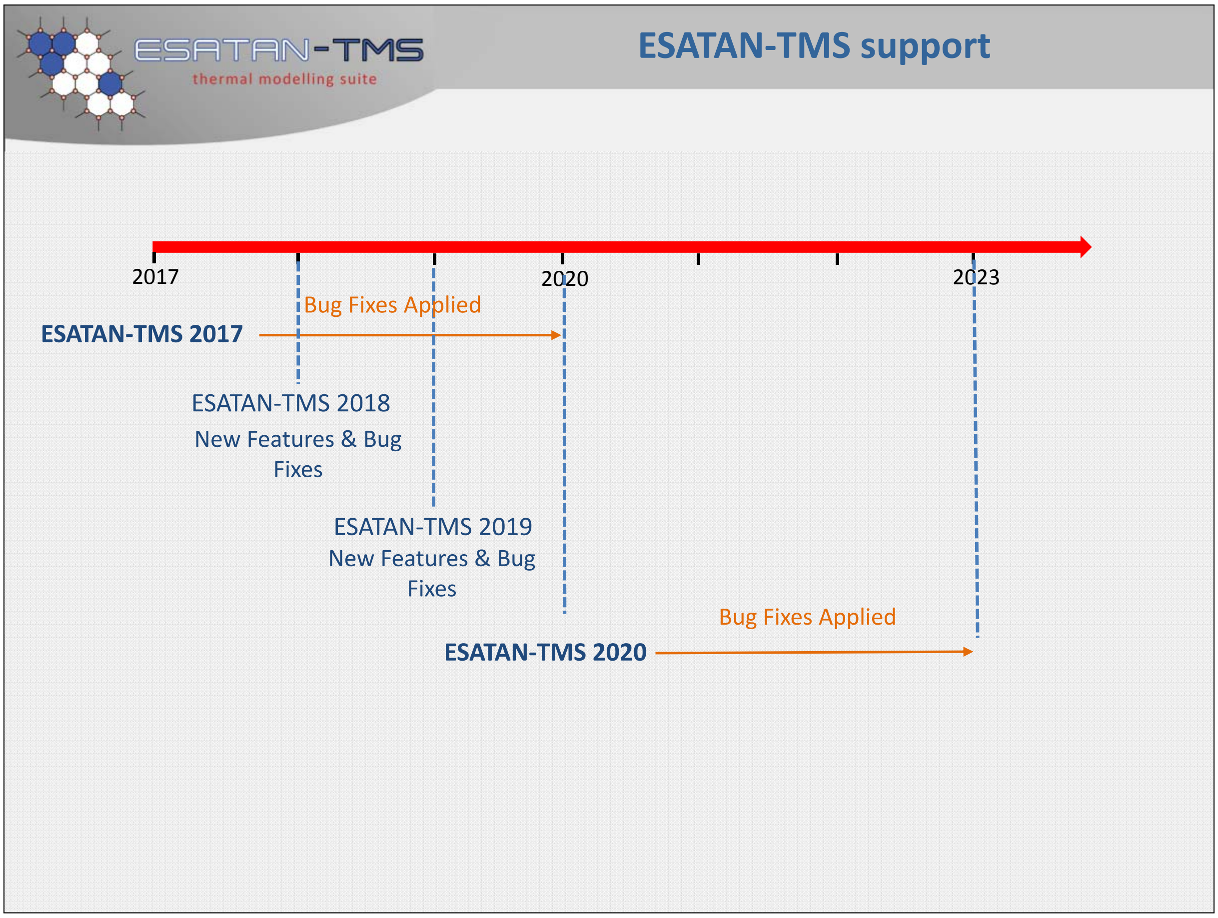
ESATAN-TMS
thermal modelling suite
ESATAN-TMS support
2017
2020
2023
Bug Fixes Applied
ESATAN-TMS 2017
ESATAN-TMS 2018
New Features & Bug Fixes
ESATAN-TMS 2019
New Features & Bug Fixes
Bug Fixes Applied
ESATAN-TMS 2020


ESATAN-TMS
thermal modelling suite
www.esatan-tms.com

Appendix J

Thermal modelling of thruster nozzles and plumes for planetary landers

Hannah Rana Andrea Passaro
(ESA/ESTEC, The Netherlands)

Abstract

Future planetary landers will embark optical sensors (e.g. cameras and imaging LIDAR) which will feed data to navigation and hazard avoidance systems, to enable safe and precise landing. These sensors may be located in proximity to thruster nozzles which, during landing, may reach temperatures around 1000K. It is therefore important to model the radiative fluxes impingent on the cameras due to the thruster as well as the plume created. Geometrically modelling the plume was achieved by establishing a mathematical model of the setup, and the emissivities of a series of truncated cones of the plume were determined. The thruster and plume were then modelled in ESATAN-TMS and the thermal impact was studied during landing phase. A preliminary engineering design was considered for the LIDAR and camera, and an overall methodology for thermally modelling thrusters and their plumes was established.

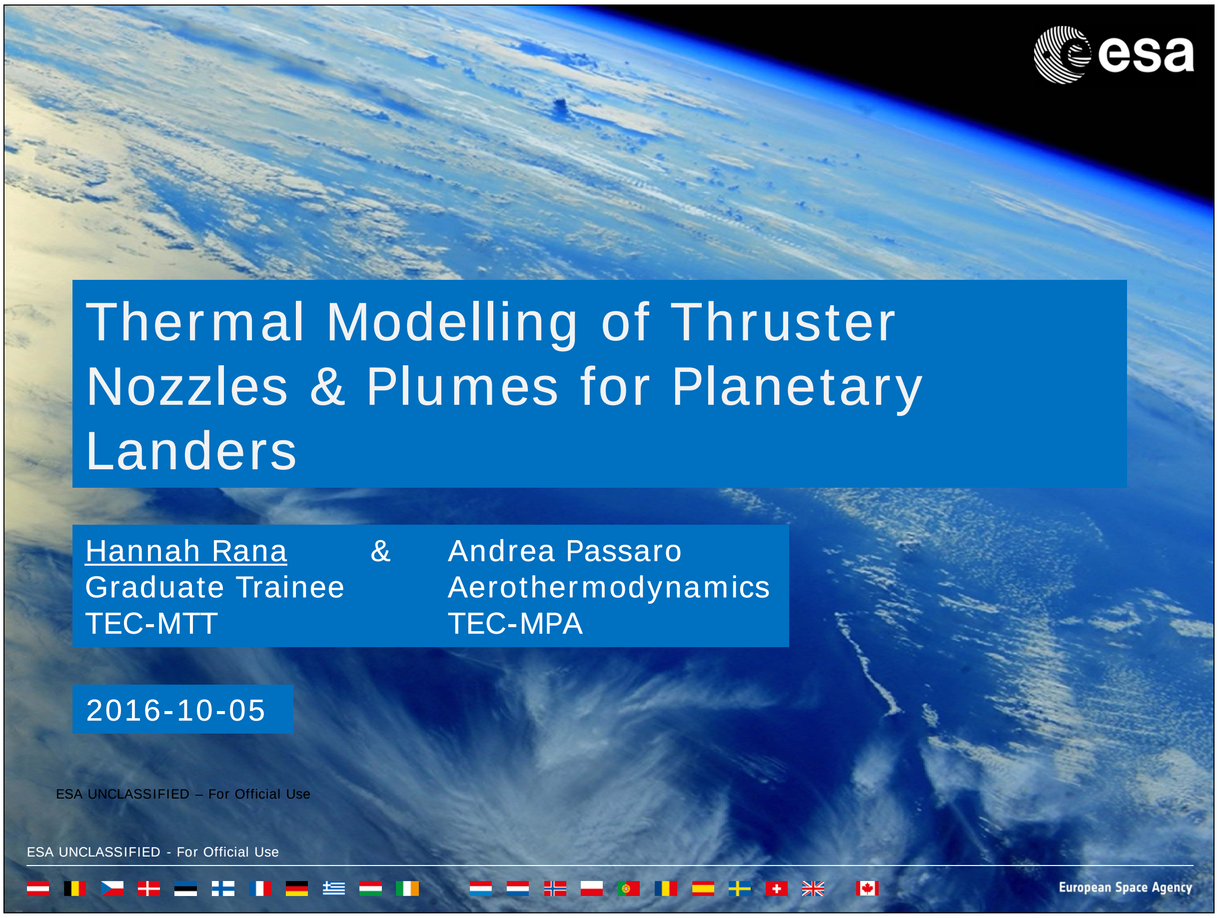
esa
Thermal Modelling of Thruster Nozzles & Plumes for Planetary Landers
Hannah Rana & Andrea Passaro
Graduate Trainee
TEC-MTT
Aerothermodynamics
TEC-MPA
2016-10-05
ESA UNCLASSIFIED – For Official Use
ESA UNCLASSIFIED - For Official Use
European Space Agency

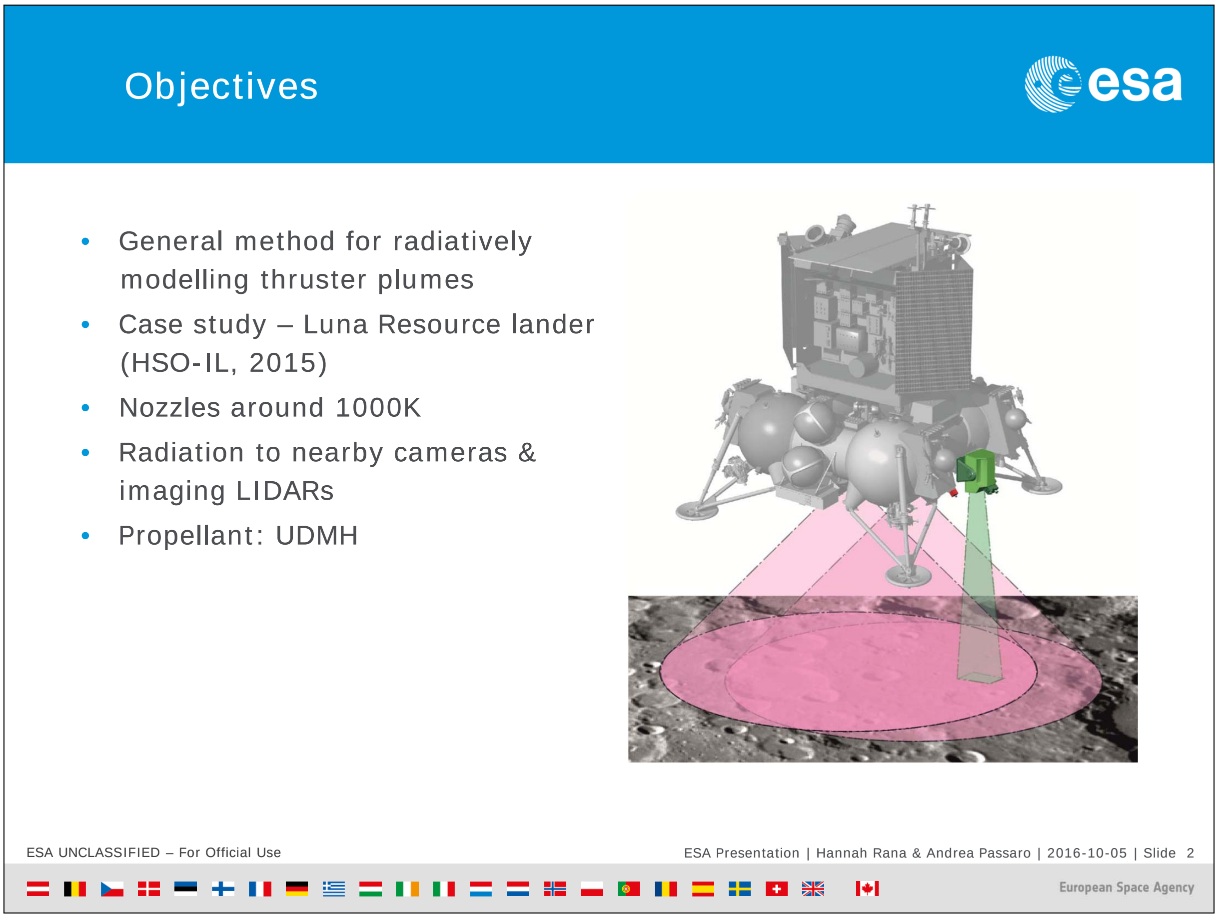
Objectives
esa
• General method for radiatively modelling thruster plumes
• Case study – Luna Resource lander (HSO-IL, 2015)
• Nozzles around 1000K
• Radiation to nearby cameras & imaging LIDARs
• Propellant: UDMH
ESA UNCLASSIFIED – For Official Use
ESA Presentation | Hannah Rana & Andrea Passaro | 2016-10-05 | Slide 2
European Space Agency

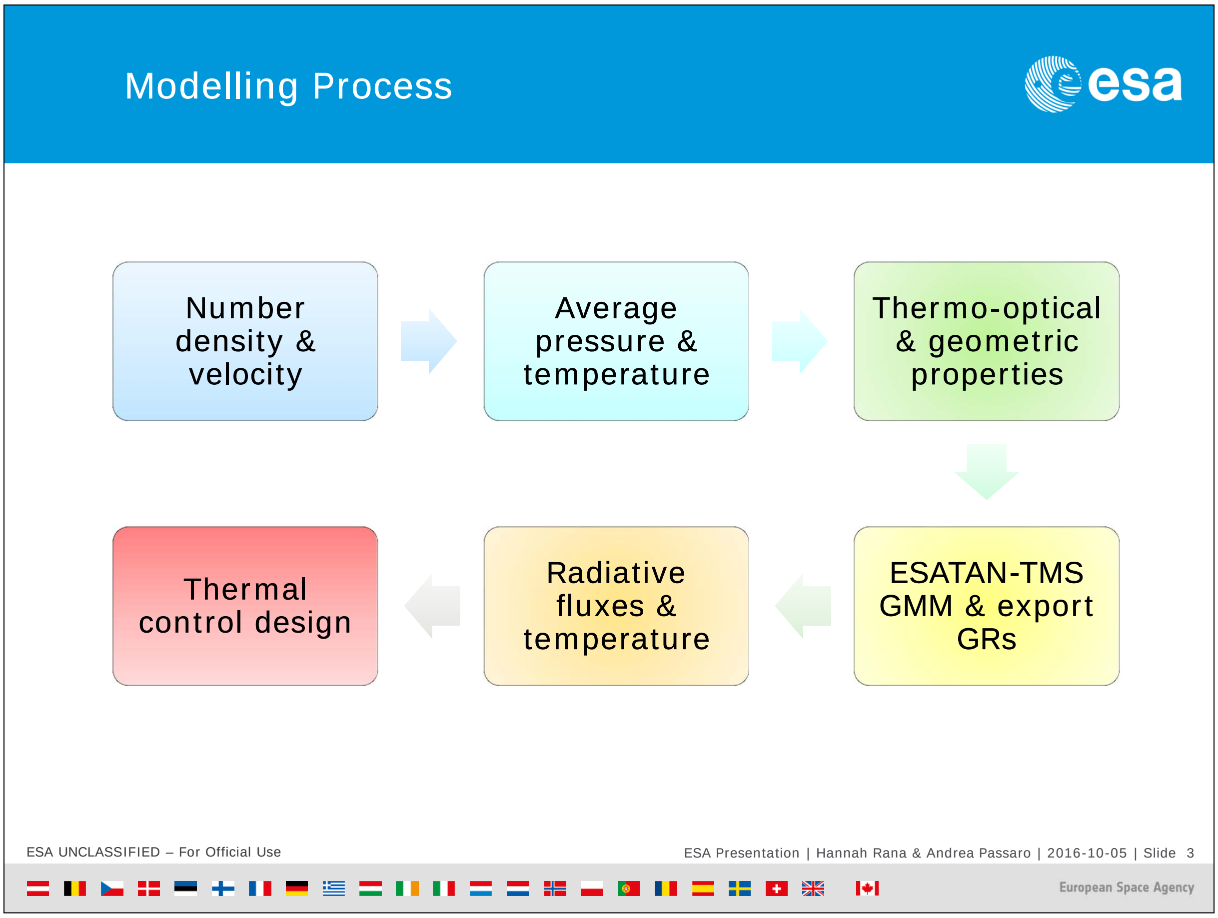
Modelling Process
esa
Number density & velocity
Average pressure & temperature
Thermo-optical & geometric properties
ESATAN-TMS GMM & export GRs
Radiative fluxes & temperature
Thermal control design
ESA UNCLASSIFIED – For Official Use
ESA Presentation | Hannah Rana & Andrea Passaro | 2016-10-05 | Slide 3
European Space Agency

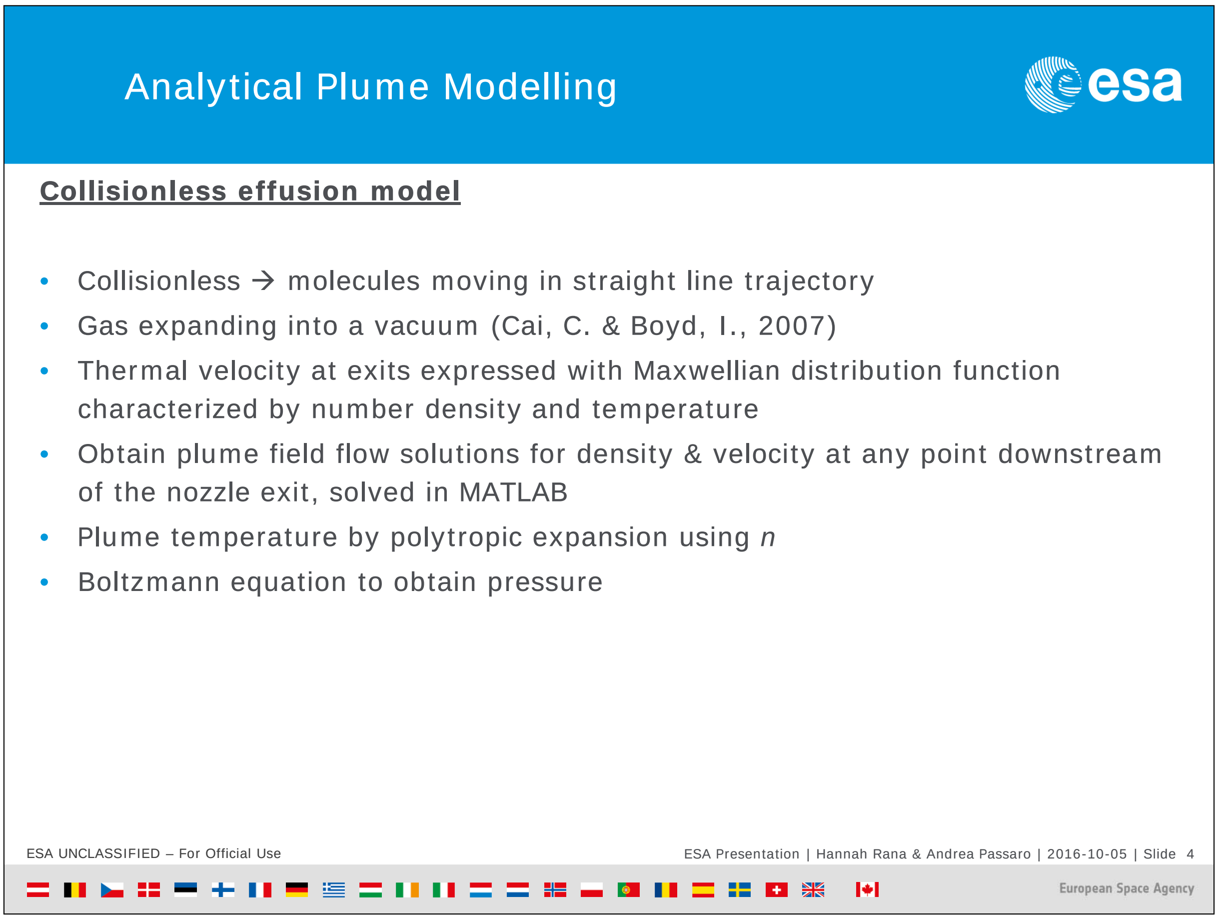
Analytical Plume Modelling
esa
Collisionless effusion model
• Collisionless → molecules moving in straight line trajectory
• Gas expanding into a vacuum (Cai, C. & Boyd, I., 2007)
• Thermal velocity at exits expressed with Maxwellian distribution function characterized by number density and temperature
• Obtain plume field flow solutions for density & velocity at any point downstream of the nozzle exit, solved in MATLAB
• Plume temperature by polytropic expansion using n
• Boltzmann equation to obtain pressure
ESA UNCLASSIFIED – For Official Use
ESA Presentation | Hannah Rana & Andrea Passaro | 2016-10-05 | Slide 4
European Space Agency

Analytical Plume Modelling

esa

Inputs:

- Nozzle exit radius (m)
- Thrust (N)
- Exhaust velocity (m/s)
- Isentropic expansion coefficient
- Temperature of nozzle (K)
- Average atomic mass of flow (g/mol)

Number Density along Plume Length

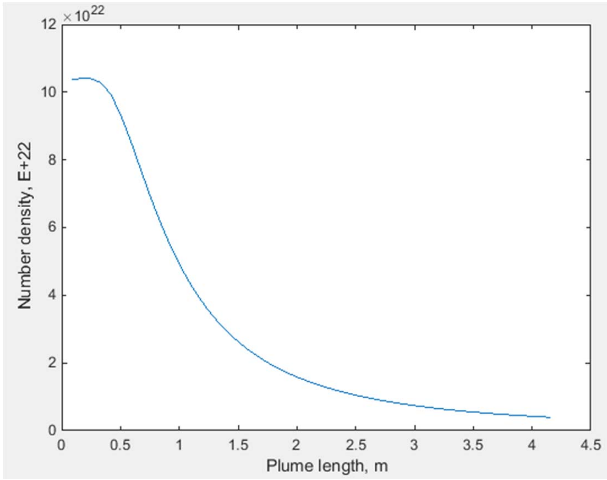

ESA UNCLASSIFIED – For Official Use

ESA Presentation | Hannah Rana & Andrea Passaro | 2016-10-05 | Slide 5

European Space Agency

Analytical Plume Modelling

esa

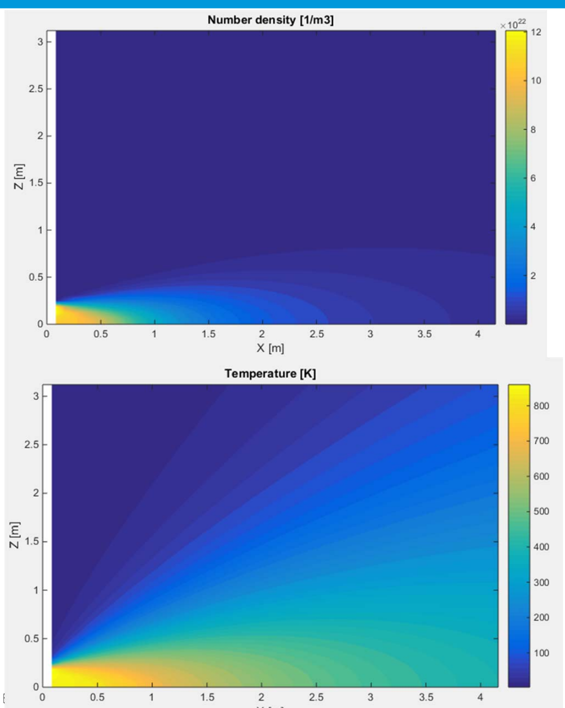

Parameter	Value
Nozzle temperature	840.5 K
Cone 1 temperature	605.1 K
Cone 2 temperature	394.5K
Average plume pressure	258.7 Pa

ESA Presentation | Hannah Rana & Andrea Passaro | 2016-10-05 | Slide 6

European Space Agency

Analytical Plume Modelling

- **Gaseous emissivity-Temperature correlations**
- Charts established based on Leckner's correlations (Howell et al., 2016)
- Inputs required/assumptions:
    - Average pressure & temperature
    - Composition of combustion products
    - H_2O and CO_2 for IR emittance only

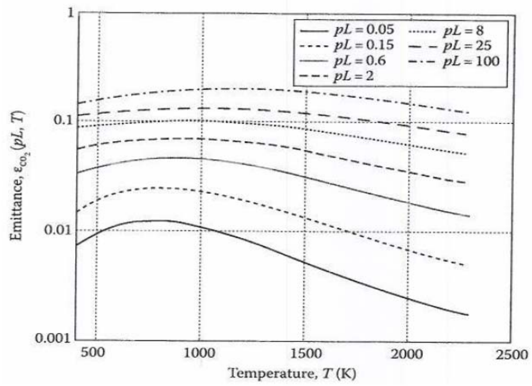

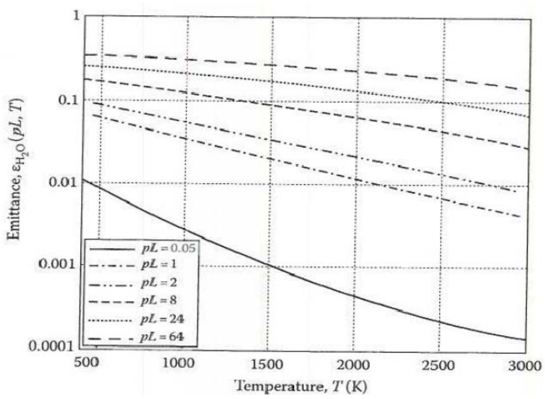

ESA UNCLASSIFIED – For Official Use

ESA Presentation | Hannah Rana & Andrea Passaro | 2016-10-05 | Slide 7

European Space Agency

Analytical Plume Modelling

- The LIDAR and Camera 2 are modelled as black critical surfaces.

Nozzle	Value
Length	0.64m
Temperature	840.5K
Emissivity	0.6
Cone 1	**Value**
Length	0.83m
Temperature	605K
Emissivity	0.0181
Cone 2	**Value**
Length	1.25m
Temperature	395K
Emissivity	0.0041

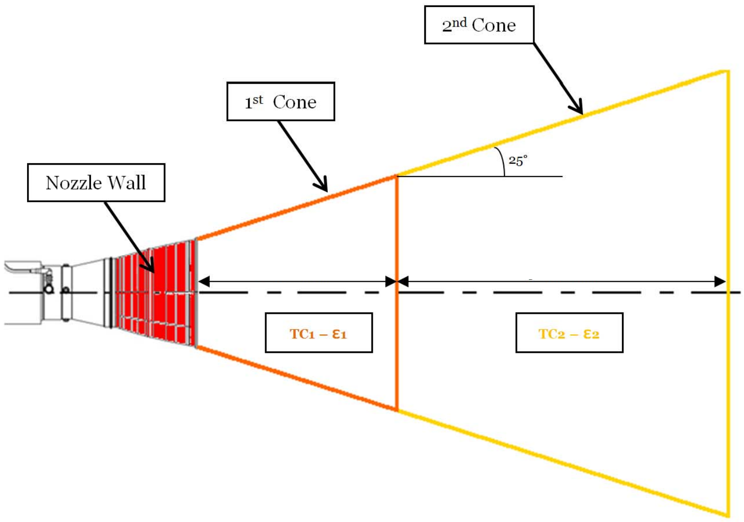

ESA UNCLASSIFIED – For Official Use

ESA Presentation | Hannah Rana & Andrea Passaro | 2016-10-05 | Slide 8

European Space Agency

GMM in ESATAN-TMS

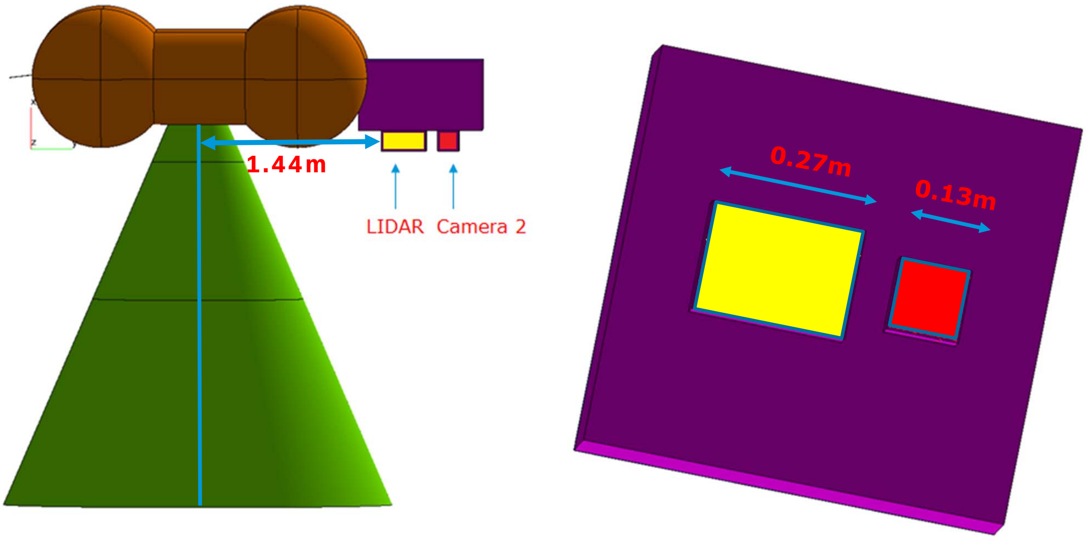

ESA UNCLASSIFIED – For Official Use

ESA Presentation | Hannah Rana & Andrea Passaro | 2016-10-05 | Slide 9

European Space Agency

Impingent Fluxes

Nozzle		**Nozzle**	
Description	**Q (W/m2)**	**Description**	**Q (W/m2)**
Facing nozzle	**779**	Facing nozzle	0
Downwards-facing	29	Downwards-facing	18
Plume cone1		**Plume cone1**	
Description	**Q (W/m2)**	**Description**	**Q (W/m2)**
Facing plume	24	Facing plume	4
Downwards-facing	13	Downwards-facing	8
Plume cone2		**Plume cone2**	
Description	**Q (W/m2)**	**Description**	**Q (W/m2)**
Facing plume	0	Facing plume	0
Downwards-facing	1	Downwards-facing	1
Total			
Facing plume	**803**		

ESA UNCLASSIFIED – For Official Use

ESA Presentation | Hannah Rana & Andrea Passaro | 2016-10-05 | Slide 10

European Space Agency

Sensitivity Analysis

Key parameters impacting radiative fluxes in our case study:

- Distance between nozzle & instrument of interest
- Temperature of the nozzle & plume
- Propellant used

ESA UNCLASSIFIED – For Official Use

ESA Presentation | Hannah Rana & Andrea Passaro | 2016-10-05 | Slide 11

European Space Agency

Nozzle-Instrument Distance

- Doubling distance decreases flux by an order of magnitude

	Distance (m)	Flux (W / m²)
LIDAR	0.86	779
Double distance	1.72	90

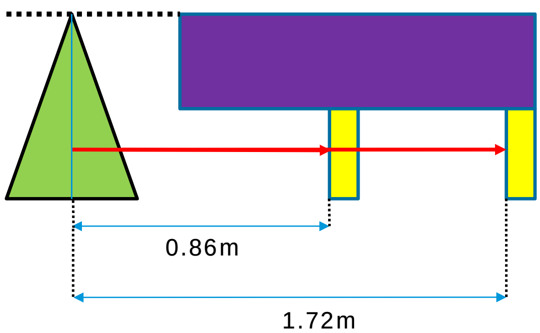

ESA UNCLASSIFIED – For Official Use

ESA Presentation | Hannah Rana & Andrea Passaro | 2016-10-05 | Slide 12

European Space Agency

Propellant Sensitivity

For Plume (Cone1)

- Emissivity for UDMH: 0.018
- Emissivity for H_2 O_2 $_{(aq)}$: 0.215

Propellant	Emissivity	Flux on LIDAR (W / m²)
UDMH	0.018	23.9
H2 O2	0.215	265.5

ESA UNCLASSIFIED – For Official Use

ESA Presentation | Hannah Rana & Andrea Passaro | 2016-10-05 | Slide 13

European Space Agency

Model Limitations

- Collisionless
- Interaction with soil
- Volumetric ray tracing
- Truncating more cones

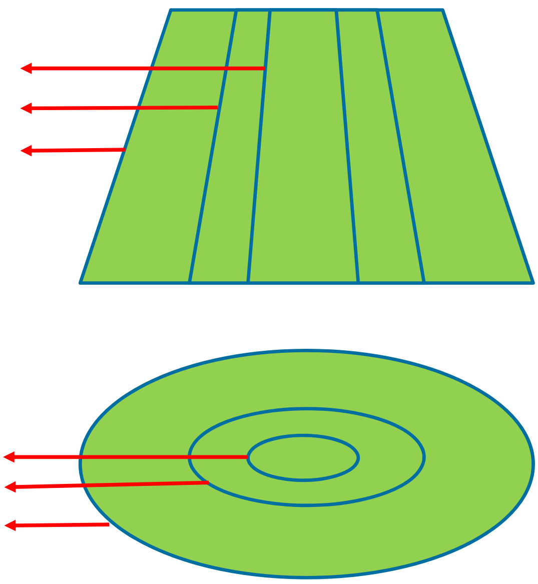

ESA UNCLASSIFIED – For Official Use

ESA Presentation | Hannah Rana & Andrea Passaro | 2016-10-05 | Slide 14

European Space Agency

Concluding Remarks

- Objectives were met in creating methodology for thermally modelling thruster plumes.
- DSMC simulations can provide more detailed plume average temperature & pressure → accounting for collisions.
- Thermally most dominant entity is the thruster nozzle.
- Inputs heavily dependent on propellant, starting nozzle temperature & geometry.

ESA UNCLASSIFIED – For Official Use

ESA Presentation | Hannah Rana & Andrea Passaro | 2016-10-05 | Slide 15

European Space Agency

References

- Cai, C., & Boyd, I. D. (2007). Collisionless gas expanding into vacuum. *Journal of Spacecraft and Rockets*, Vol. 44, No. 6, p1326-1330.
- Howell, J. R., Menguc, M. P., & Siegel, R. (2016). *Thermal radiation heat transfer.* Boca Raton, FL: Sixth Edition: CRC Press.
- HSO-IL. (2015). *Luna resource propulsion system data for the analyses of effects on PILOT units.* ESA-HSO-LEX-MEM-0013.

ESA UNCLASSIFIED – For Official Use

ESA Presentation | Hannah Rana & Andrea Passaro | 2016-10-05 | Slide 16

European Space Agency

Appendix K

Thermal experiments on LISA Pathfinder's Inertial Sensors

Ferran Gibert
(University of Trento, Italy)

Abstract

LISA Pathfinder is an ESA mission with NASA collaboration aimed to test key technologies for a future space-based gravitational wave detector. The main objective of the mission is to demonstrate that two free-falling masses can be controlled inside the satellite with an unprecedented residual relative acceleration of less than 10 fm/s^2/sqrt(Hz) in the band around 1 mHz.
Among other kind of noise sources, temperature fluctuations can potentially play an important role in the experiment, since variations of temperature around the masses produce forces on them via three thermal effects: radiation pressure, outgassing and the radiometric effect. In order to keep these temperature-induced forces monitored, the instrument is equipped with series of high precision temperature sensors and with heaters that allow to inject characterization signals to the system.
Following to its successful launch in December 2015, the satellite started scientific operations in March 2016, and since then different thermal characterization experiments have been performed on the satellite's Inertial Sensors. In this presentation we will describe these experiments and report on the current status of their analysis.

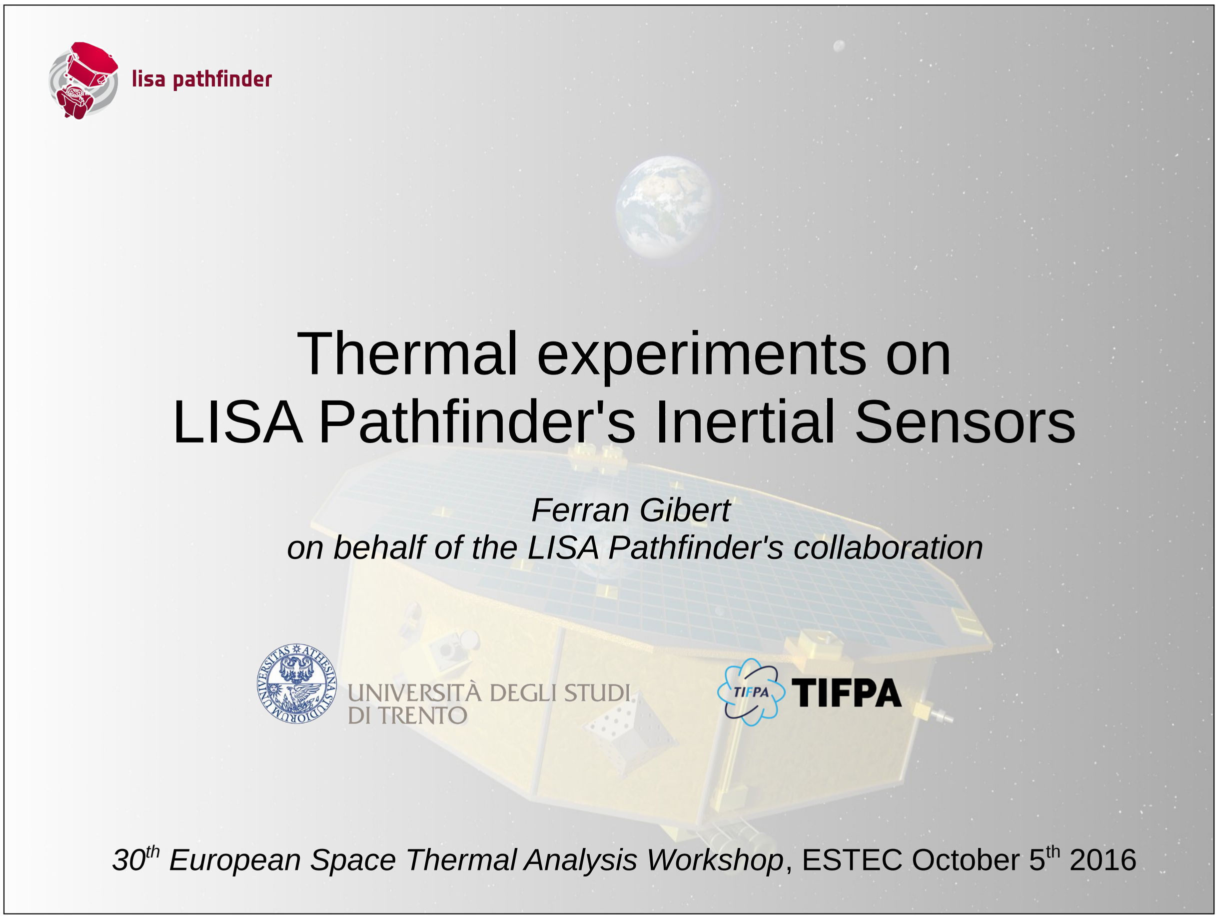
lisa pathfinder
Thermal experiments on
LISA Pathfinder's Inertial Sensors
Ferran Gibert
on behalf of the LISA Pathfinder's collaboration
UNIVERSITÀ DEGLI STUDI
DI TRENTO
TIFPA
30th European Space Thermal Analysis Workshop, ESTEC October 5th 2016

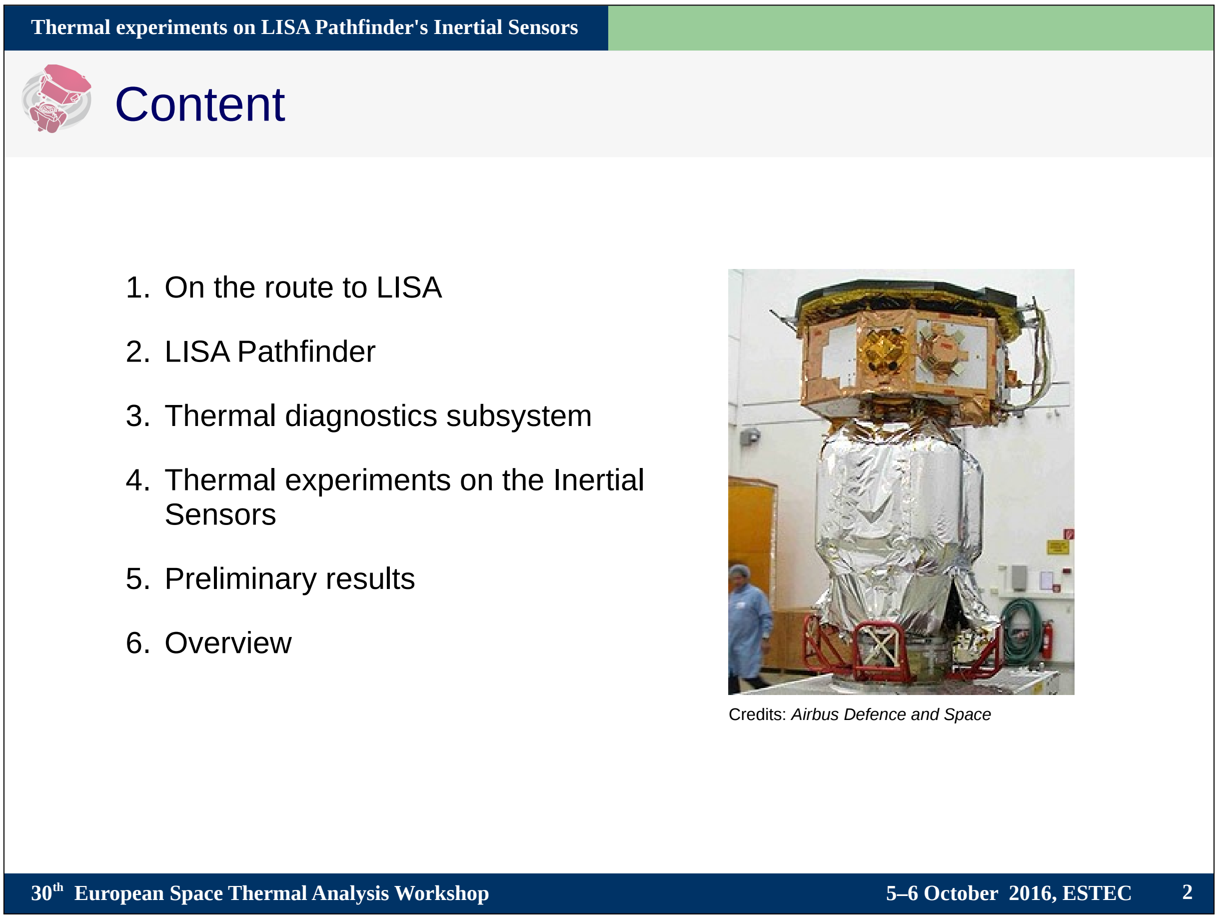
Thermal experiments on LISA Pathfinder's Inertial Sensors
Content
1. On the route to LISA
2. LISA Pathfinder
3. Thermal diagnostics subsystem
4. Thermal experiments on the Inertial Sensors
5. Preliminary results
6. Overview
Credits: Airbus Defence and Space
30th European Space Thermal Analysis Workshop
5–6 October 2016, ESTEC
2

On the route to LISA

- **Gravitational waves** are fluctuations of the space-time caused by accelerated massive bodies or systems of bodies.
- First GW measurement ever done last year (LIGO). Source: merging black holes.
- On-ground observations like LIGO are **limited in frequency to f>1Hz**. Need to go to space to detect low frequency GW.
- **Detection concept** in space: measurement of relative distance variations between separated free-falling bodies.

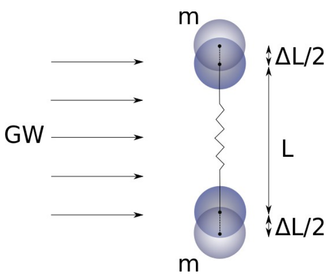

→ Need to measure fluctuations of $h = \Delta L/L \sim [10^{-24}, 10^{-16}]$ m (depending on frequency)

On the route to LISA

- **Classic LISA design** for a future space-based GW detector:
  - 3 spacecrafts separated ~5 Mkm, heliocentric orbit.
  - 2 free-falling masses inside each spacecraft.
  - Interferometry techniques to measure relative displacements (picometer resolution required).
  - Bandwidth of interest: 0.1 to 100mHz.

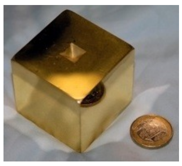

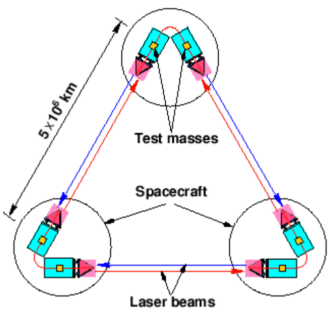

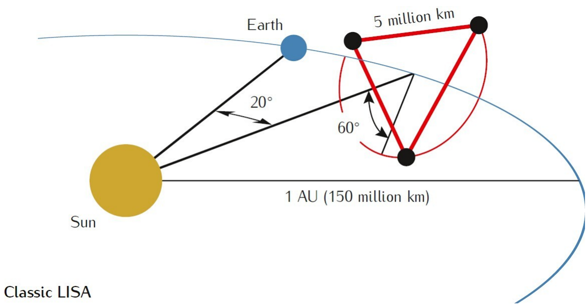

Thermal experiments on LISA Pathfinder's Inertial Sensors

LISA Pathfinder

- A **technology demonstrator** for LISA: LISA Pathfinder
  - ESA mission with NASA collaboration
- **Principle**: squeeze one LISA-arm to ~30cm in a single spacecraft.
- **Objectives:**
  - Demonstrate residual differential acceleration between free falling masses to less than:

$$S^{1/2}_{\Delta a,\mathrm{LPF}}(\omega) \leq 3 \times 10^{-14}\ \mathrm{m\ s^{-2}\ Hz^{-1/2}}$$

    in the band between 1-30mHz
  - Demonstrate feasibility of interferometry in space.
  - Develop a detailed model of main noise sources.

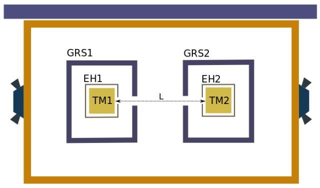

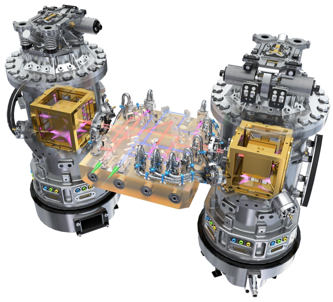

Image credits: *ESA Medialab*

30th European Space Thermal Analysis Workshop 5–6 October 2016, ESTEC 5

Thermal experiments on LISA Pathfinder's Inertial Sensors

LISA Pathfinder

LTP attached to the satellite structure by means of struts

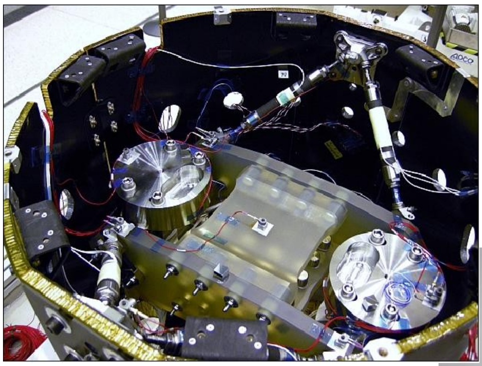

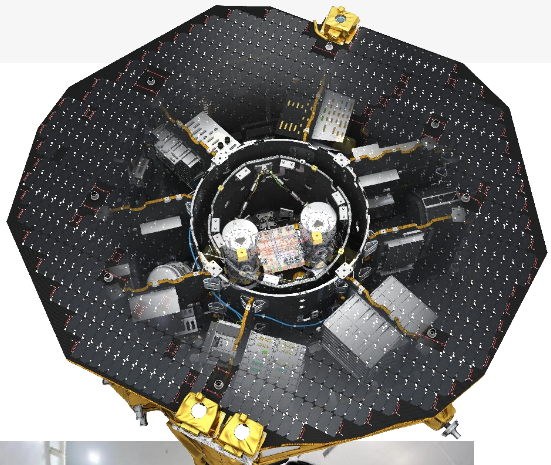

Credits: *Airbus Defence and Space/ESA/ATG medialab.*

30th European Space Thermal Analysis Workshop 5–6 October 2016, ESTEC 6

Thermal experiments on LISA Pathfinder's Inertial Sensors

LISA Pathfinder

- Launched in December 3rd 2015 by means of a VEGA rocket
- Several apogee raising manoeuvres to reach final Lissajous orbit around L1
- Test Masses released between 15–16 February 2016
- Scientific operations started on 1st March (still ongoing)

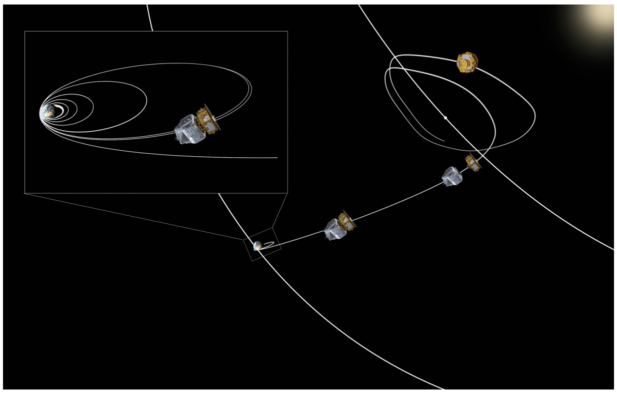

Credits: *ESA–Stephane Corvaja, 2015/ATG medialab.*

30th European Space Thermal Analysis Workshop 5–6 October 2016, ESTEC 7

Thermal experiments on LISA Pathfinder's Inertial Sensors

LISA Pathfinder

- **First results** already published! *PRL 116, 231101 (2016)*

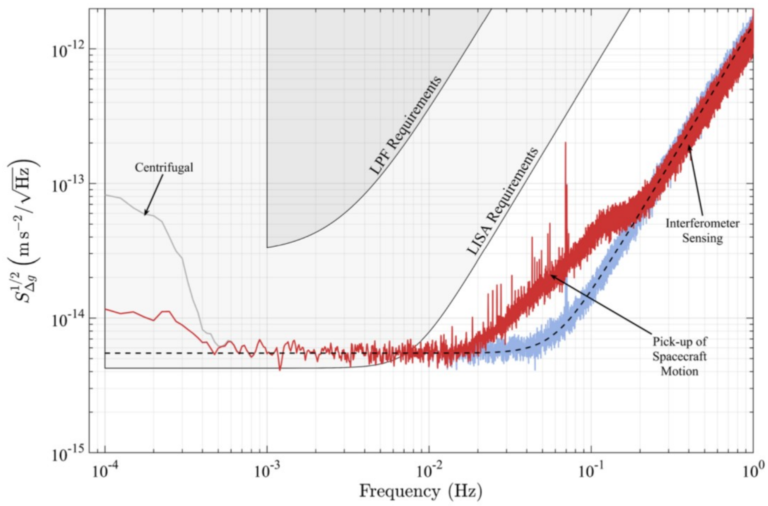

*Main noise contributors:

- Instrumental noise at f higher than ~40mHz
- Brownian motion noise between 1-20mHz (pressure dependent, decreasing with time)

30th European Space Thermal Analysis Workshop 5–6 October 2016, ESTEC 8

Thermal experiments on LISA Pathfinder's Inertial Sensors

Thermal diagnostics subsystem

- Temperature fluctuations potentially affect the LPF performance via:
  - **Temperature-gradient (ΔT) forces** on the Inertial Sensor's masses
  - Thermo-elastic distortion of the structure
  - Thermo-optical disturbance of optical parts.
- Temperature stability requirement: 10^{-4} K/sqrt(Hz)
- A dedicated Thermal diagnostics subsystem:
  - **Temperature sensors**: high precision NTC thermistors with 10^{-5} K/sqrt(Hz) sensitivity in the band of interest
  - **Heaters** able to apply custom signals for characterization purposes

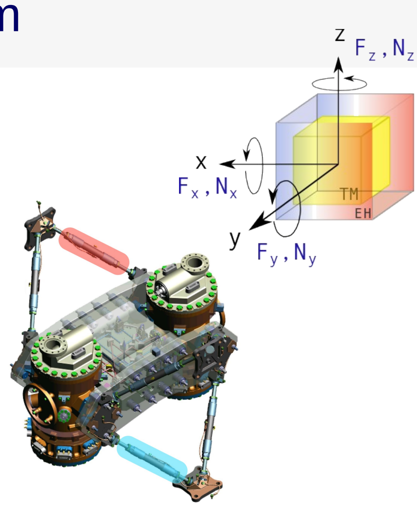

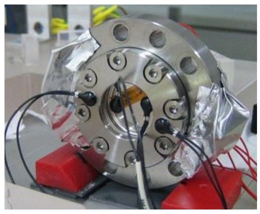

Credits: Institut de Ciències de l'Espai (ICE-CSIC/IEEC) & AEI Hannover

30th European Space Thermal Analysis Workshop 5–6 October 2016, ESTEC 9

Thermal experiments on LISA Pathfinder's Inertial Sensors

Thermal diagnostics subsystem

Max power per heater:

- 2W (OW and Struts)
- 45mW (IS)

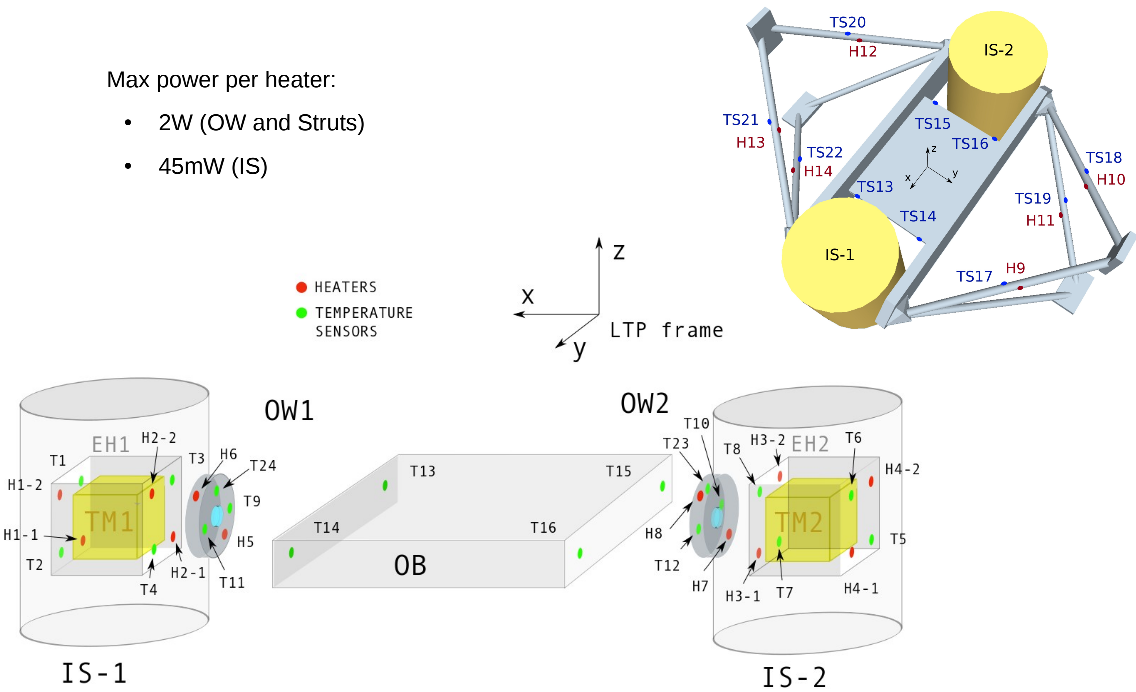

30th European Space Thermal Analysis Workshop 5–6 October 2016, ESTEC 10

Thermal diagnostics subsystem

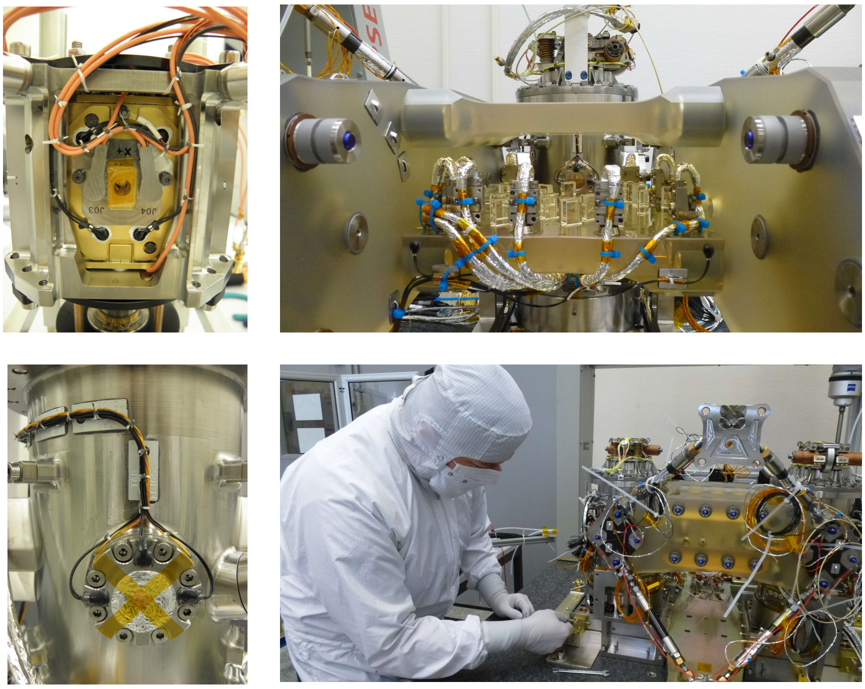

Credits: Compagnia Generale per lo Spazio (CGS SpA,) & Airbus Defence and Space

Thermal experiments on LISA Pathfinder's Inertial Sensors

Thermal experiments on the Inertial Sensors

- Three thermal effects induce forces to the masses in presence of asymmetric temperature distributions (ΔT):
  - **Radiation pressure:** pressure exerted by electromagnetic radiation from the surfaces $F^{RP} = k_{RP} T^3 \Delta T$
  - **Radiometric effect:** significant in rarefied atmospheres where the particle mean free path is longer than the characteristic size of the system, hence particles bounce directly between surfaces $F^{RM} = k_{RM} \frac{p}{T} \Delta T$
  - **Asymmetric outgassing:** forces exerted by the fluxes of particles emitted from the surfaces $F^{OG} = k_{OG} \frac{\Theta_{OG} e^{\frac{-\Theta_{OG}}{T}}}{T^2} \Delta T$
- Expected contributions (via simulations & on-ground tests, Phys. Rev. D 76, 102003)

Radiometer effect | Radiation Pressure | Asymmetric Outgassing

$$F = \left[23\,\frac{\mathrm{pN}}{\mathrm{K}} \left(\frac{P}{10^{-5}\,\mathrm{Pa}}\right) \frac{293\,\mathrm{K}}{T_0} + 9\,\frac{\mathrm{pN}}{\mathrm{K}} \left(\frac{T_0}{293\,\mathrm{K}}\right)^3 + 40\,\frac{\mathrm{pN}}{\mathrm{K}} \left(\frac{Q_0}{1.4\,\mathrm{nJ/s}}\right) \left(\frac{\Theta}{3\times10^4\,\mathrm{K}}\right) \left(\frac{293\,\mathrm{K}}{T_0}\right)^2 \right] \Delta T$$

Thermal experiments on the Inertial Sensors

- **Thermal coefficient** definition:

$$\alpha = \frac{F_{\mathrm{TOTAL}}}{\Delta T}$$

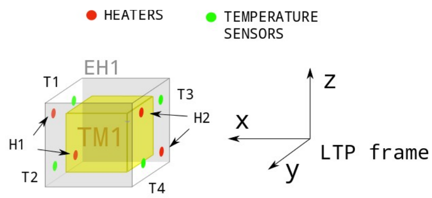

- **Dedicated experiments** performed in order to:
  - Set upper limits of temperature gradient noise contribution to acceleration noise budget

    → Need to measure α
  - Provide an independent tool to estimate pressure (Brownian noise indicator)
    → Need to measure also dα/dT

- **Experiment concept**:
  1. Modulate ΔT by means of heater actuation on +/-x sides to estimate α
  2. Repeat the modulations at different levels of average temperature to estimate dα/dT

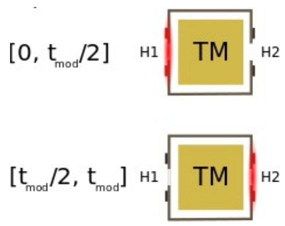

Thermal experiments on LISA Pathfinder's Inertial Sensors

Thermal experiments on the Inertial Sensors

- Example of analysis on simulated data:

H1,H2 heater pattern:

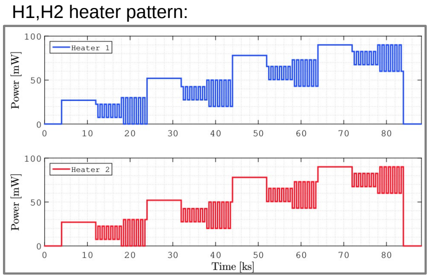

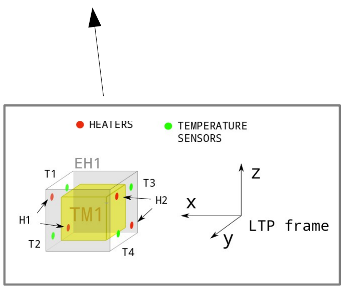

Thermal experiments on LISA Pathfinder's Inertial Sensors

Thermal experiments on the Inertial Sensors

- Example of analysis on simulated data:

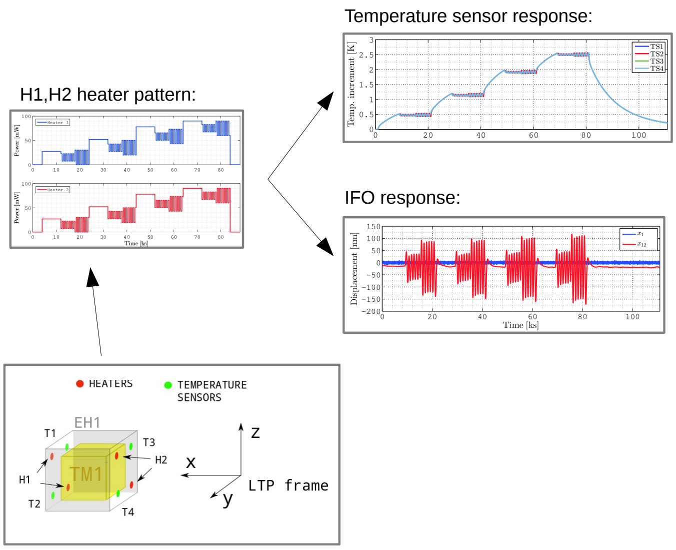

30th European Space Thermal Analysis Workshop 5–6 October 2016, ESTEC 15

Thermal experiments on LISA Pathfinder's Inertial Sensors

Thermal experiments on the Inertial Sensors

- Example of analysis on simulated data:

$$\Delta T_x = \frac{(T_3+T_4)-(T_1+T_2)}{2}$$

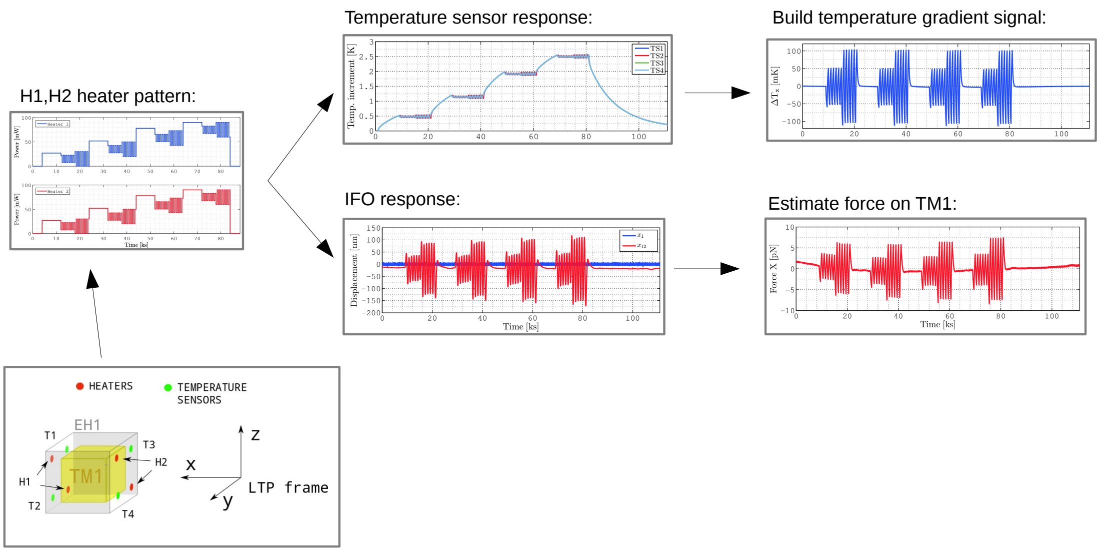

30th European Space Thermal Analysis Workshop 5–6 October 2016, ESTEC 16

Thermal experiments on LISA Pathfinder's Inertial Sensors

Thermal experiments on the Inertial Sensors

- Example of analysis on simulated data:

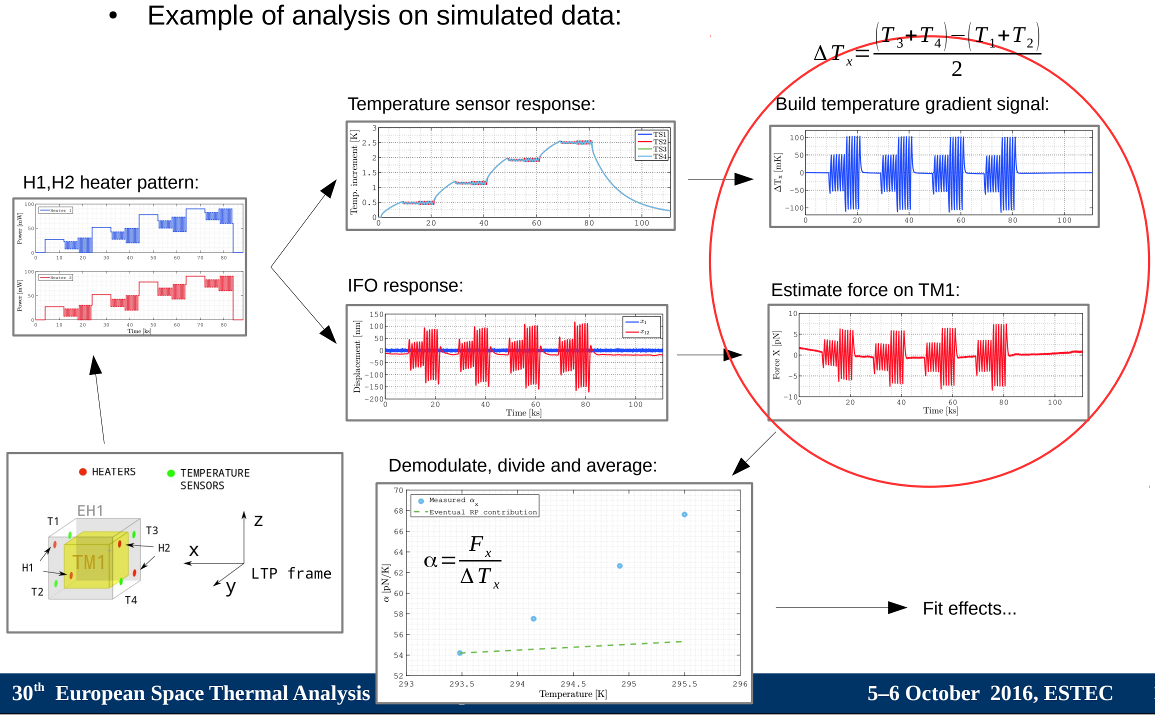

30th European Space Thermal Analysis Workshop 5–6 October 2016, ESTEC 17

Thermal experiments on LISA Pathfinder's Inertial Sensors

[Preliminary] results

- Data analysis tool: a dedicated LTPDA Toolbox developed by the data analysis collaboration to provide a common analysis framework for all the LPF experiments, in MATLAB environment
  - Specific methods for time-domain and frequency-domain objects.
  - Keep history of all actions applied in final products

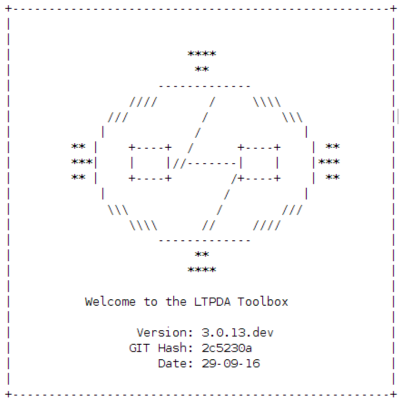

- Analysis pipelines for each experiment based on LTPDA.
- Also used in many labs for data processing and analysis.

Download it in https://www.elisascience.org/ltpda/

30th European Space Thermal Analysis Workshop 5–6 October 2016, ESTEC 18

Thermal experiments on LISA Pathfinder's Inertial Sensors

[Preliminary] results

- Thermal experiments performed between February and May with f_{mod} between 1-7 mHz

Day of Year (DOY)	$\frac{\partial \alpha}{\partial T}$?
60	No
64	No
70	Yes (only TM1)
88	Yes
108	Yes
146	Yes

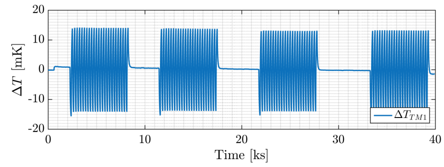

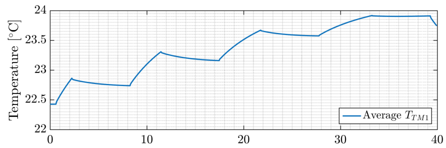

➔ Case of DOY108:

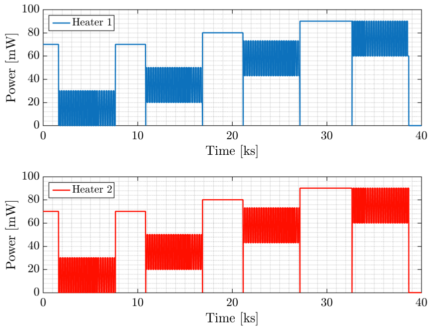

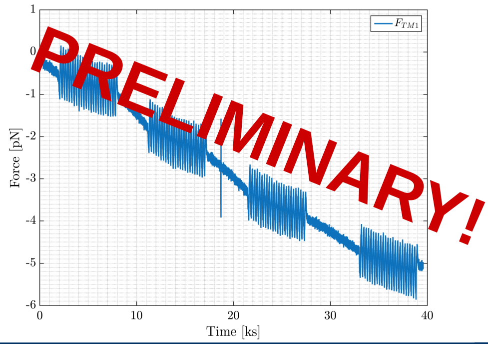

Thermal experiments on LISA Pathfinder's Inertial Sensors

[Preliminary] results

- Measured thermal coefficients:

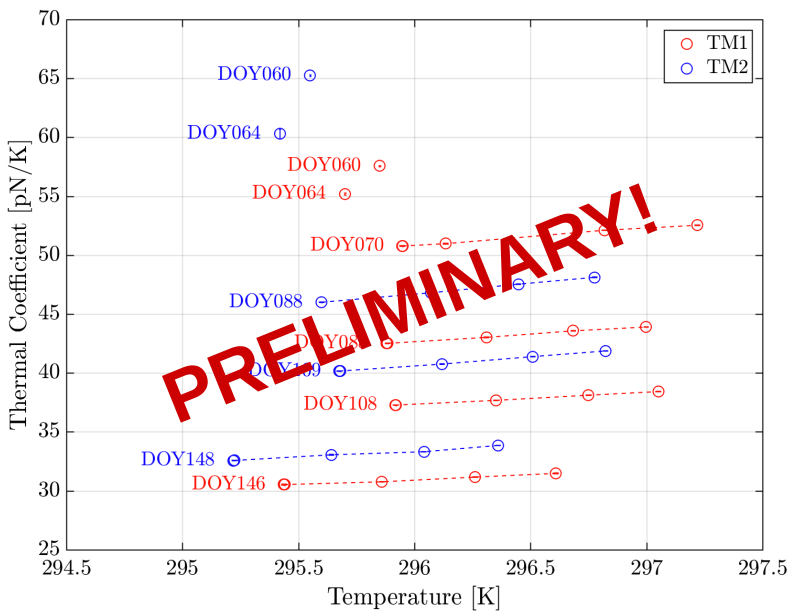

Thermal experiments on LISA Pathfinder's Inertial Sensors

[Preliminary] results

- Thermal coefficients decaying with time
  - Decay consistent with $\alpha(t) = \frac{A}{t-B} + C$ as expected from a vented system (*B* is the venting time, *t* the time after launch)

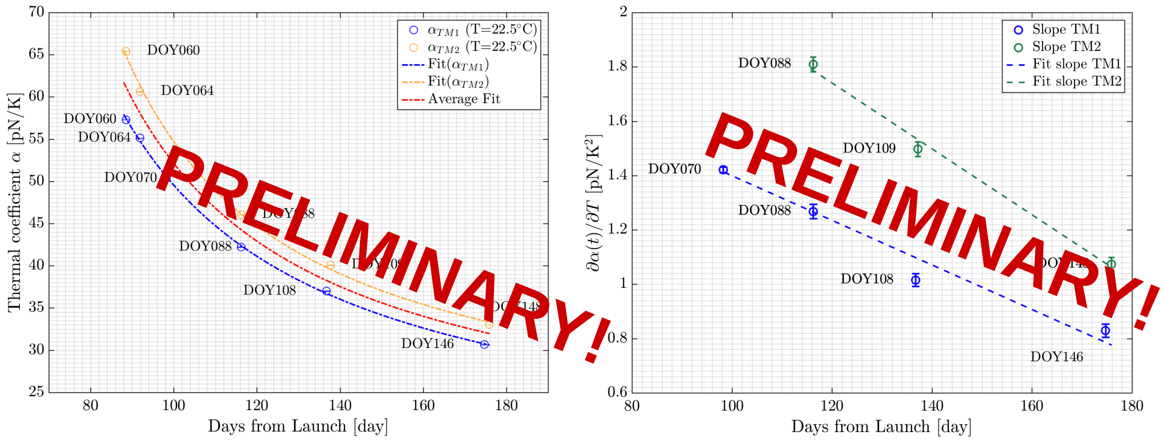

	A [pN day/K]	*B* [day]	*C* [pN/K]
α_{TM1}	2080 ± 740	39 ± 13	15 ± 5
α_{TM2}	1900 ± 1900	48 ± 30	19± 14

30th European Space Thermal Analysis Workshop **5–6 October 2016, ESTEC** 21

Thermal experiments on LISA Pathfinder's Inertial Sensors

[Preliminary] results

- **Temperature stability requirements achieved**: below the sensing noise level!
  - Temperature noise measurement limited by electronic noise
  - ADC non linearities induce low frequency error as a function of temperature drift:
    dT/dt ~ 10nK/s → extra noise at f < 0.2mHz
  - Alternatively, use of *differential* measurements to reduce the impact of this error.

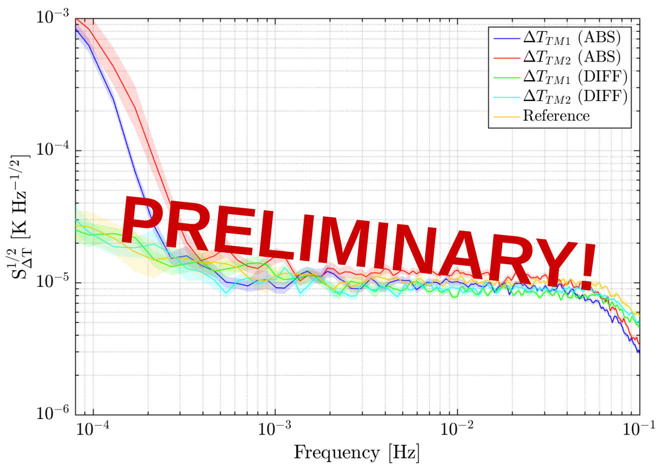

- Working temperature in the LTP ~22ºC
- Static gradients on LTP structure dominated by z axis (sun direction): ΔT~4ºC between upper and lower struts

30th European Space Thermal Analysis Workshop **5–6 October 2016, ESTEC** 22

[Preliminary] results

- Noise projection from temperature gradient noise to acceleration noise:

$$S^{1/2}_{\Delta a,\,\Delta T} = \frac{1}{m}\left(\alpha_{\mathrm{TM1}}\, S^{1/2}_{\Delta T_{\mathrm{TM1}}} + \alpha_{\mathrm{TM2}}\, S^{1/2}_{\Delta T_{\mathrm{TM2}}}\right)$$

- Considering the thermal coefficients from DOY146/148, we obtain the following **upper limits**:

$$S^{1/2}_{\Delta a,\,\Delta T}(f = 0.1\,\mathrm{mHz}) = 3.7\ \mathrm{fm/s^2/sqrt(Hz)}$$
$$S^{1/2}_{\Delta a,\,\Delta T}(f = 1\,\mathrm{mHz}) = 1.3\ \mathrm{fm/s^2/sqrt(Hz)}$$

- Still, the *real* contribution is likely to be well below since the measurement of the *real* temperature gradient noise is actually limited by electronic noise
- Ongoing pressure estimation analysis

Thermal experiments on LISA Pathfinder's Inertial Sensors

Overview

- LISA Pathfinder shows **excellent performance.**
- Temperature stability in the Inertial Sensors well within requirements. Limited by readout noise.
- Measured ΔT coupling to force on the masses initially ~60pN/K and decreasing with time at a rate of 1/t.
- Temperature contributions far from the main noise contributions (actuation noise, sensing noise and Brownian noise)
- Current status: preparing for ESA-lead **mission extension** starting on December.

Thanks for your attention!

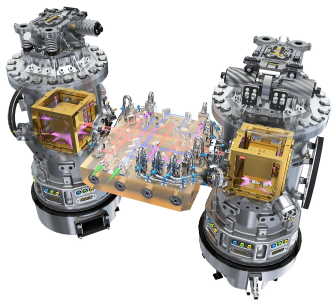

Image credits: *ESA Medialab*

Bibliography

[1] Armano et al., *Sub-Femto-g Free Fall for Space-Based Gravitational Wave Observatories: LISA Pathfinder Results.* Phys. Rev. Lett. **116**, 231101 – Published 7 June 2016. http://journals.aps.org/prl/abstract/10.1103/PhysRevLett.116.231101

[2] L. Carbone et al. *Thermal gradient-induced forces on geodesic reference masses for LISA*. Phys. Rev. D **76**, 102003 – Published 16 November 2007. http://journals.aps.org/prd/abstract/10.1103/PhysRevD.76.102003

Appendix L

Quasi-autonomous spacecraft thermal model reduction

Germán Fernández Rico
(Max Planck Institute for Solar System Research, Germany)

Isabel Pérez Grande   Ignacio Torralbo
(Universidad Politécnica de Madrid, Spain)

Abstract

The lumped parameter method is widely used for thermal analysis of spacecraft. Often, the size of these thermal models needs to be reduced. A new method to reduce automatically the number of nodes has been developed. The reduction algorithm treats a processed conductive couplings matrix as a sparse graph adjacency matrix. Then, in order to identify the strongly connected components that define the condensed nodes, a depth-first search algorithm is used. The resulting restriction matrix serves to reduce the thermal entities, such as the conductive and radiative couplings matrices, thermal loads, etc. The method preserves the physical characteristics of the system (physical conductive paths, couplings matrices symmetry, etc.). The reduction process has been tested with a real thermal model (Solar Orbiter PHI instrument focal plane assembly). The results show a good correlation between the detailed and the reduced model, achieving a reduction in the number of nodes of about 75%. The limitations of the method and next steps are also shown.

QUASI-AUTONOMOUS SPACECRAFT THERMAL MODEL REDUCTION

German Fernández Rico
Max Planck Institute for Solar System Research

Ignacio Torralbo
Isabel Pérez Grande
Universidad Politécnica de Madrid

05 October 2016

MAX PLANCK INSTITUTE FOR SOLAR SYSTEM RESEARCH

Thermal model reduction:

- Time consuming
- Error prone
- Lack of standardization

Goal:

- Develop a tool to reduce (almost) automatically the thermal mathematical models (LP models)

Guidelines:

- Preserve physical interpretation of the model
- Respect the physical characteristics of the model
- Inputs: TMD file from ESATAN

Quasi-autonomous spacecraft thermal model reduction 2

Basics

- GMM: reduced manually, although with input from RTMM
- Results correlation: nodal temperatures and heat fluxes through the model boundaries

How?

- Grouping the nodes, using a search algorithm on a processed conductive coupling matrix, which is treated as a sparse graph adjacency matrix
- The adjacency matrix is obtained according to the way in which they are connected to each other:
  - Strong vs. weak conductive couplings
  - Temperature similarity
  - Model boundaries preserved

Case study – Solar Orbiter PHI FPA

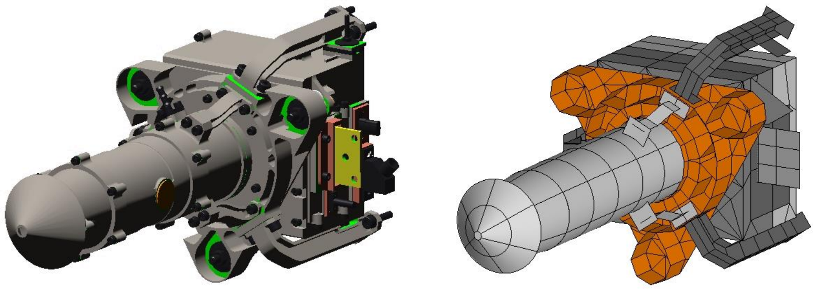

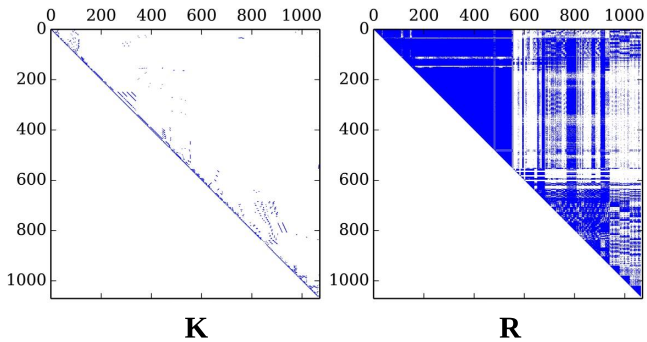

Quasi-autonomous spacecraft thermal model reduction 5

Conductive couplings

- Detailed TMM conductive couplings values can cover a wide range
- Make $\mathbf{K}$ dimensionless with $\mathbf{K}^\mathrm{S}$
- Filter dimensionless $\tilde{\mathbf{K}}$ by a threshold (p_f)

$$\widetilde{K}_{ij} = \begin{cases} 1 & \widetilde{K}_{ij} > p_f \\ 0 & \widetilde{K}_{ij} \leq p_f \end{cases}$$

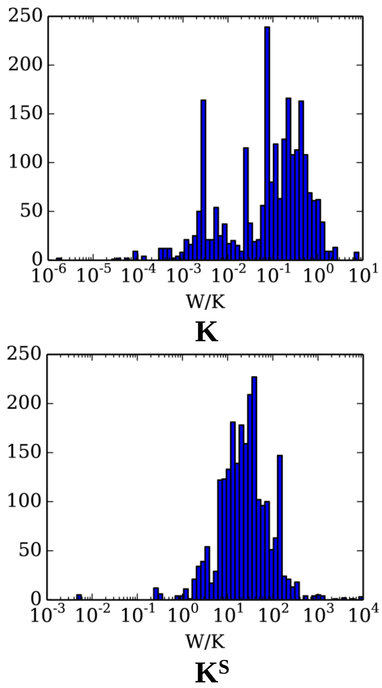

Quasi-autonomous spacecraft thermal model reduction 6

Temperature similarity

- A matrix $\mathbf{\Theta}$ is set up with the temperature difference between every pair of nodes (nodal temperatures are an input for the given thermal case)
- Filter matrix $\mathbf{\Theta}$ by temperature difference threshold ΔT_{max}

$$\Theta_{ij} = \begin{cases} 0 & \Theta_{ij} > \Delta T_{max} \\ 1 & \Theta_{ij} \leq \Delta T_{max} \end{cases}$$

Model boundaries

- To improve the correlation of the results, the boundary nodes are preserved (isolated) in the reduced thermal model
- Also the nodes to which are coupled the boundary nodes are kept independent from the rest of the model

Quasi-autonomous spacecraft thermal model reduction 7

Connected components algorithm

- The algorithm finds the nodes that are connected to each other, and put them into groups
- The relation between the detailed and the reduced thermal model total number of nodes is called reduction ratio, r_r $\left(r_r = 1 - \frac{n_c - n_b}{n_d - n_b}\right)$

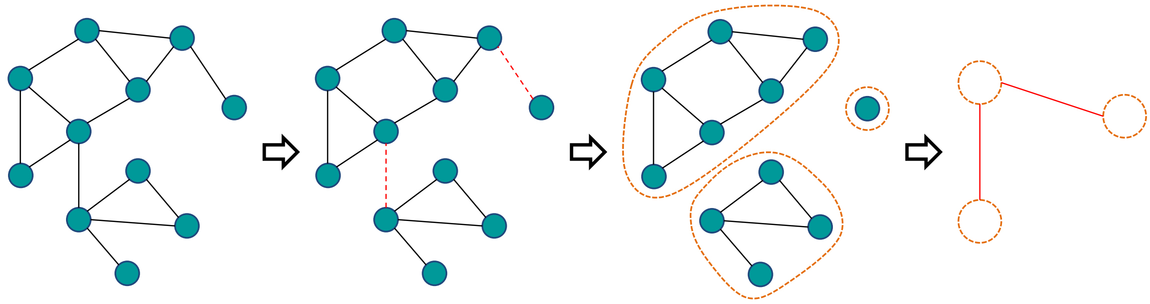

Quasi-autonomous spacecraft thermal model reduction 8

Variation of r_r with p_f and ΔT_{max}

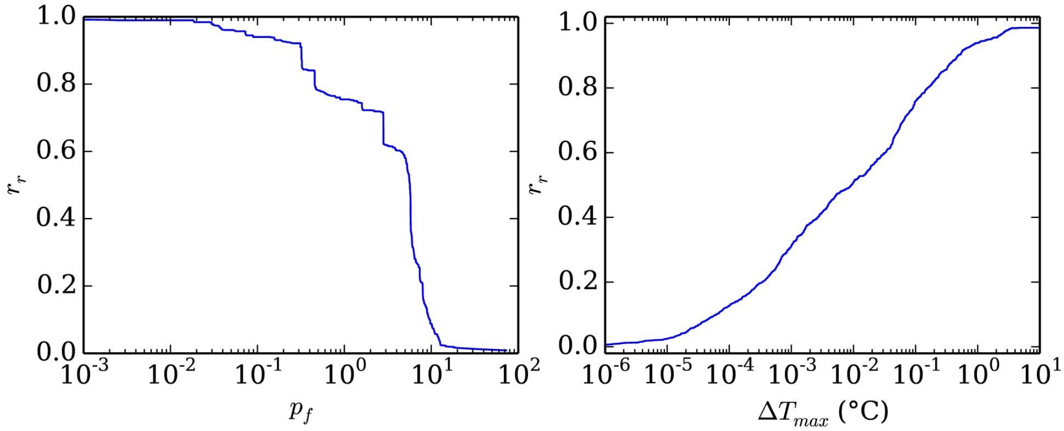

(a) (b)

Quasi-autonomous spacecraft thermal model reduction 9

Model reduction

Reduction of matrices (**K, R**) and vectors (**Q, C, T**)

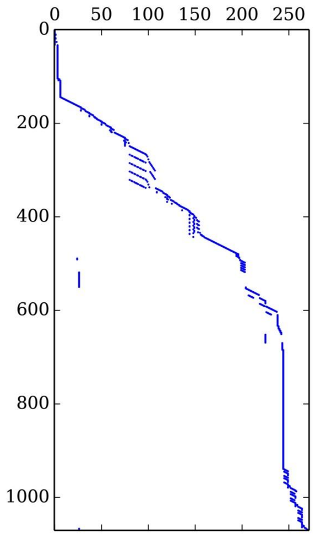

P

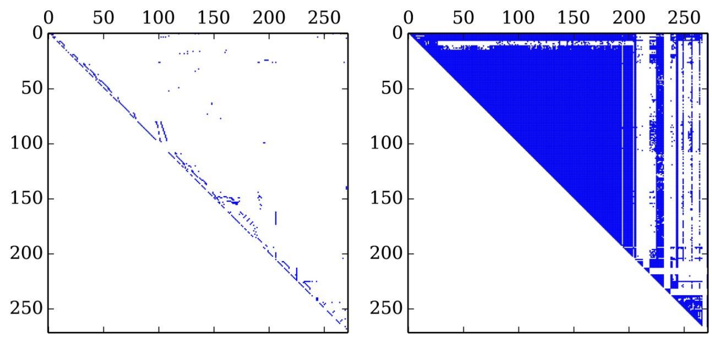

(a) (b)

Quasi-autonomous spacecraft thermal model reduction 10

Contour plot of the function $r_r = f(p_f, \Delta T_{max})$

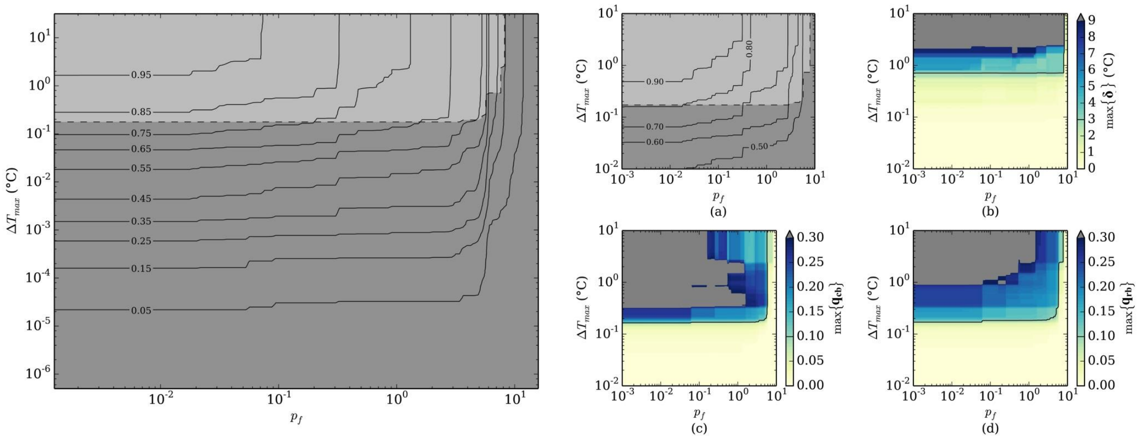

Quasi-autonomous spacecraft thermal model reduction 11

Results

Maximum heat flux difference around 5%

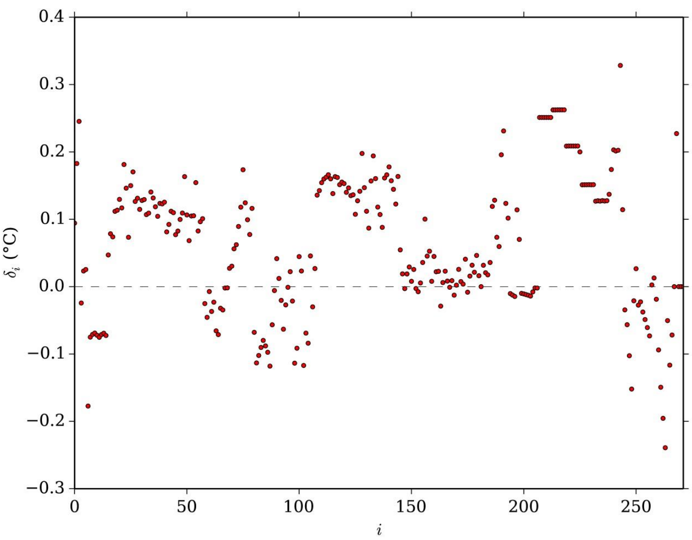

Quasi-autonomous spacecraft thermal model reduction 12

Final remarks

- Focus on internally mounted space scientific instrument thermal models
- Preservation of all the physical characteristics of the detailed model
- Maximum reduction ratio (r_r) ~ 90%
- Only for steady-state conditions
- Correlation only with one thermal case
- GMM reduction

Thanks!

Any questions?

More info: G. Fernández-Rico et al., Quasi-autonomous thermal model reduction for steady-state problems in space systems, Appl. Therm. Eng. (2016), http://dx.doi.org/10.1016/j.applthermaleng.2016.03.017

Contact: fernandez@mps.mpg.de

Appendix M

Space Thermal Analysis through Reduced Finite Element Modelling

Lionel Jacques
(Space Structures and Systems Laboratory, University of Liège   Centre Spatial de Liège, Belgium)

Luc Masset   Gaetan Kerschen
(Space Structures and Systems Laboratory, University of Liège, Belgium)

Abstract

The finite element method (FEM) is widely used in mechanical engineering, especially for space structure design. However, FEM is not yet often used for thermal engineering of space structures where the lumped parameter method (LPM) is still dominant.
LPM offers more accurate surfaces and fewer nodes to generate the radiative links while the FEM has automatic meshing tools and generation of conductive links. Coupled thermo-structural analyses are made straightforward if the same mesh can be used.
The proposed method brings together FEM and LPM by taking advantages on both sides. The structural FE mesh is reduced and the concept of super-node introduced. The reduction provides accurate conductive links and reduces the number of faces to compute the radiative links with Monte Carlo raytracing. The reduced model can integrate user logic in the exact same way a LPM model would do. Once the reduced model is solved using standard techniques, reduction matrices are exploited again to derive the detailed mesh temperatures for thermo-mechanical analyses.
To further reduce the computation time, quasi-Monte Carlo ray-tracing acceleration techniques were presented in the previous editions of the workshop, providing between 50% and one order of magnitude reduction of the number of rays required for a given accuracy. Combined with this acceleration technique, quadric surface fitting of selected regions in the FE mesh is performed to alleviate the FE mesh surface accuracy issue.
This presentation will summarise the research project developments carried out for the last four years. The end-to-end procedure will be detailed with actual space structures.

Université de Liège

SPACE THERMAL ANALYSIS THROUGH REDUCED FINITE ELEMENT MODELLING

Lionel Jacques[1,2], Luc Masset[1], Gaetan Kerschen[1]

[1] Space Structures and Systems Laboratory, University of Liège
[2] Centre Spatial de Liège

30th Space Thermal Analysis Workshop, ESTEC, Oct. 5th, 2016

Finite Element vs. Lumped Parameter

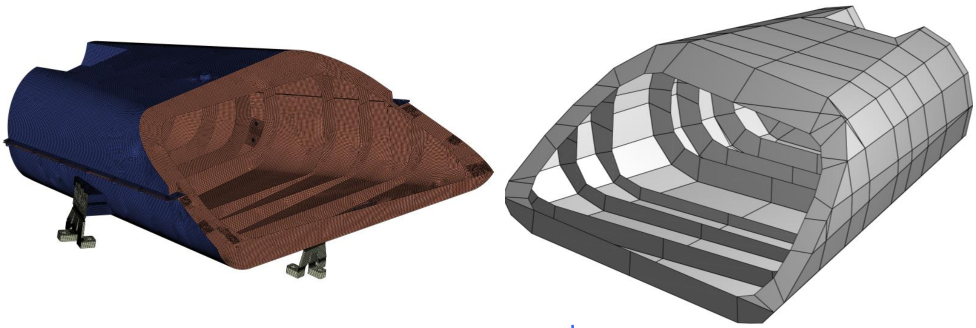

	FEM	LPM
# nodes	10^4 - 10^6	10^1 - 10^3
Conductive links computation	Automatic	Manual, error-prone
Radiative links computation	Prohibitive	Affordable
Surface accuracy for ray-tracing	FE facets	Primitives
User-defined components	Difficult	Easy
Thermo-mech. analysis	Same mesh	Mesh extrapolation

2

Reconciliation through a global approach

Radiative links computation

- Reduce # of rays: quasi-Monte Carlo method (isocell, Halton)
- Reduce # of facets: super-face concept (mesh clustering)

Surface accuracy for ray-tracing

- Quadrics fitting

Conductive links, thermo-mech. analysis and user-defined compts.

- Reduce detailed FE mesh (keep conductive info. of the detailed geometry)
- Able to recover detailed T° from reduced
- Transform reduced FE model to LP model to enable user-defined comp.

3

Outline

Ray-tracing enhancement

FEM clustering & conductive reduction

Super-face ray-tracing

Integrating the developments

Conclusions & perspectives

4

Outline

Ray-tracing enhancement

FEM clustering & conductive reduction

Super-face ray-tracing

Integrating the developments

Conclusions & perspectives

5

Ray-tracing: origin + direction sampling

$$F_{ij}(B_{ij}) = \frac{\text{Number of rays emitted by facet i, directly (finally) hitting j}}{\text{total number of rays emitted by facet i}}$$

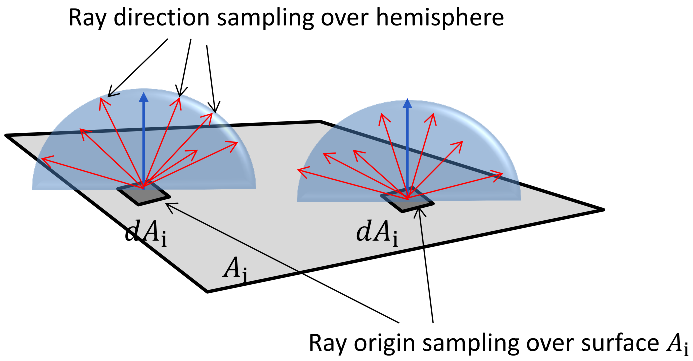

Reference solution: ESATAN-TMS

→ crude Monte Carlo: random direction & origin sampling, 1 ray / origin

$$error \propto \frac{1}{\sqrt{N_{rays}}}$$

6

4-D QUASI-MC SAMPLING: 2 QUADRANGLES

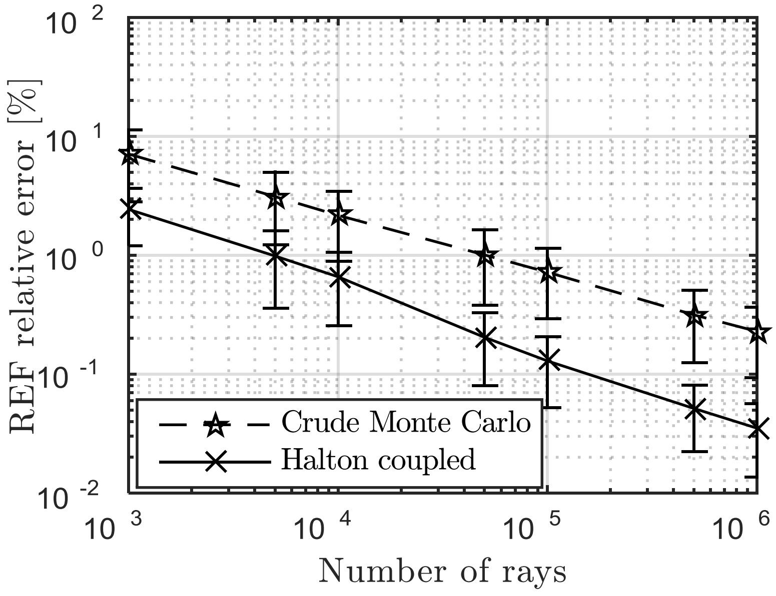

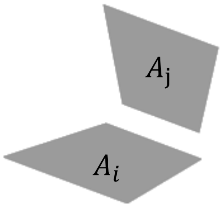

7

4-D QUASI-MC SAMPLING

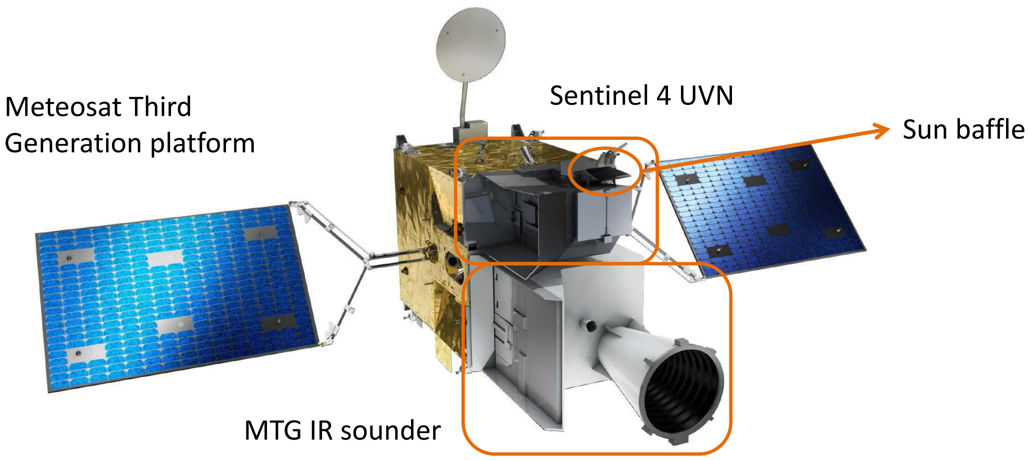

8

4-D QUASI-MC SAMPLING

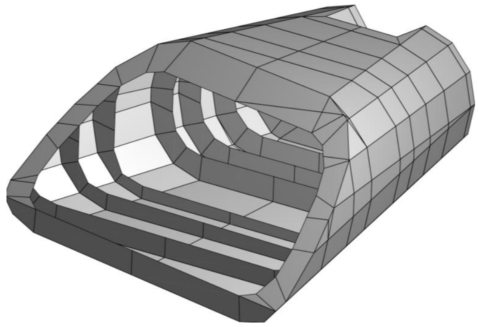

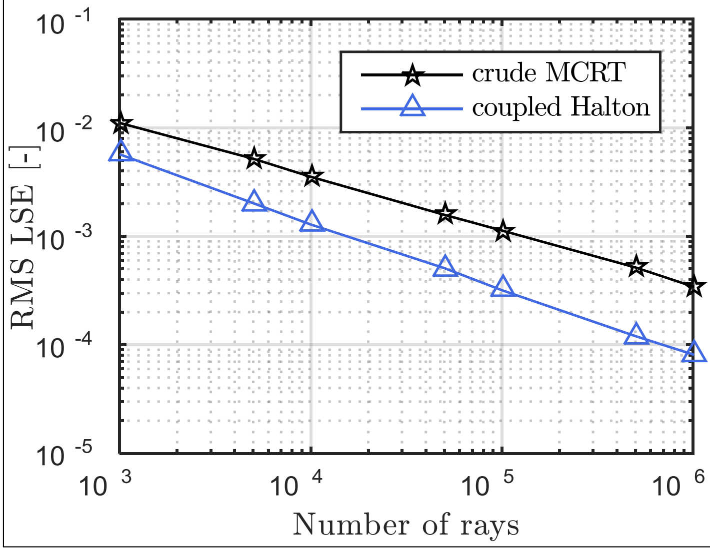

9

APPLIED TO SOLAR HEAT FLUXES

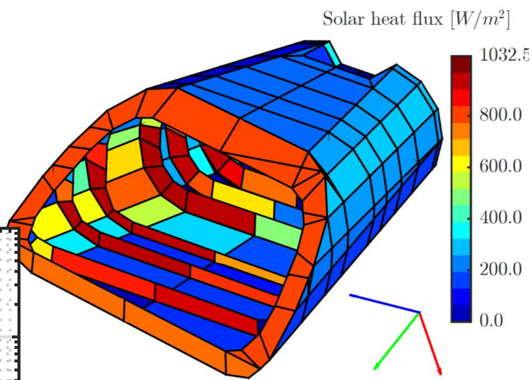

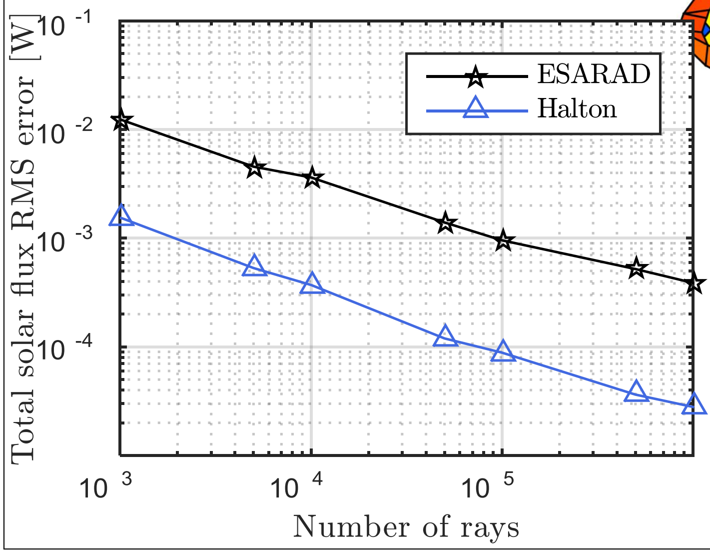

10

Outline

Ray-tracing enhancement

FEM clustering & conductive reduction

Super-face ray-tracing

Integrating the developments

Conclusions & perspectives

11

Philosophy

2D parts: avoid crossing sharp edges

3D parts:

- high k: single super-node for volume and faces
- low k: consider external faces separately

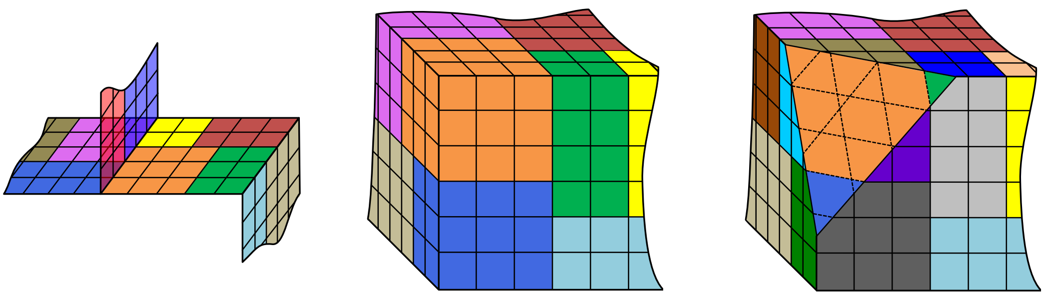

12

K-mean clustering initialization

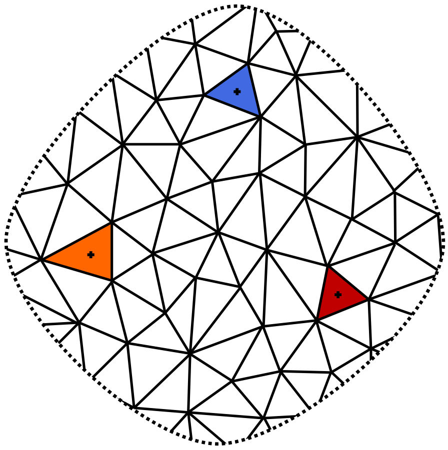

13

Greedy region growing

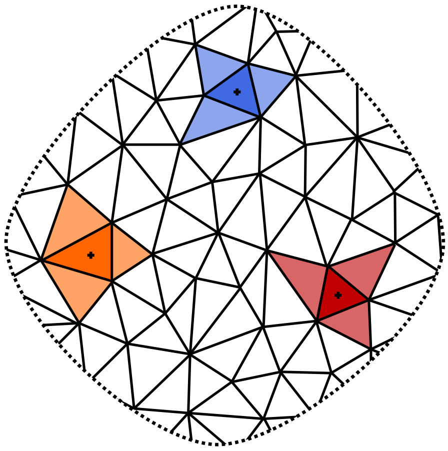

14

Greedy region growing

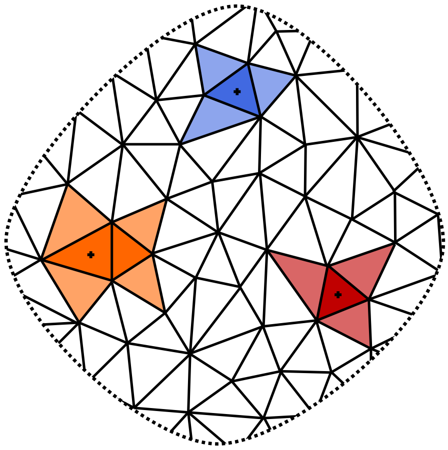

15

Greedy region growing

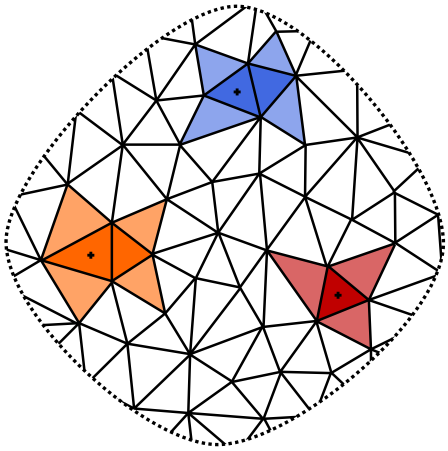

16

Greedy region growing

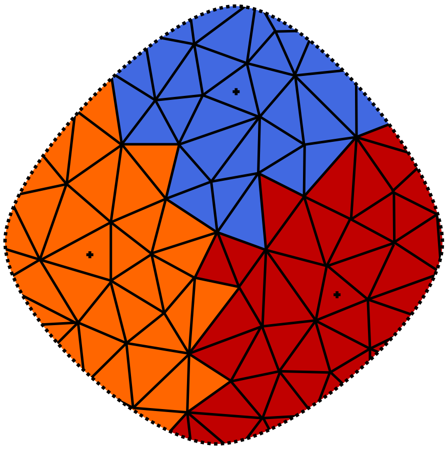

17

Boundary smoothing

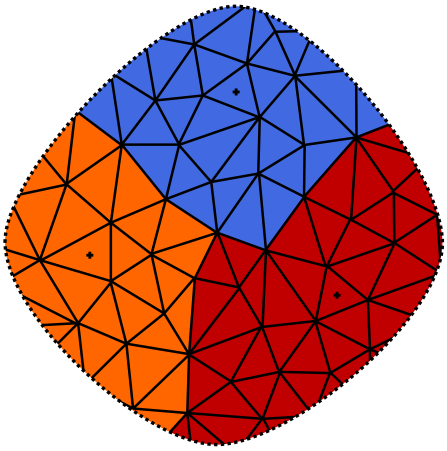

18

Applied to EUI entrance baffle str. mesh

10 super nodes

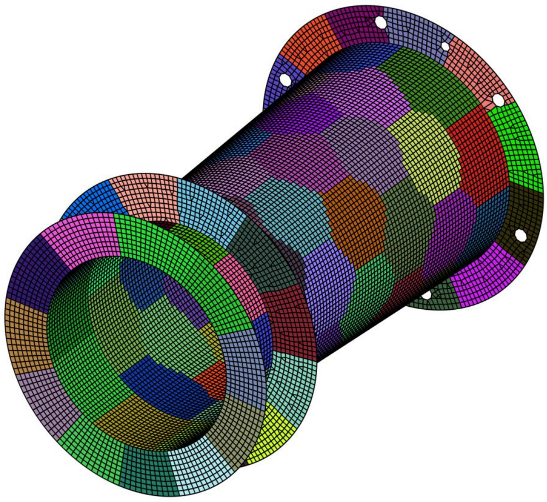

100 super nodes

19

MTG back telescope assembly

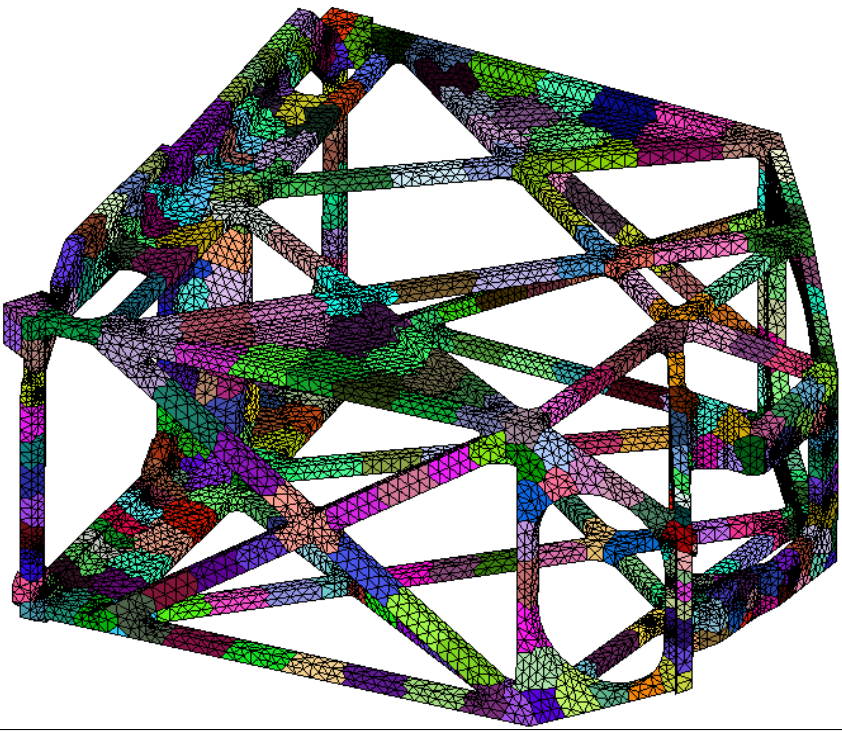

20

Create new “super-nodes” (SINAS)

Not picking a representative node of the cluster but creating new nodes

A super-node = weighted (area, volume) average each node cluster

$$\mathbf{T_{SN}} = \mathbf{AT}$$

$$T_{SN_i} = \sum_{j=1}^{N} A_{ij} T_j \qquad \sum_{j=1}^{N} A_{ij} = 1$$

21

Reduction assumes uniform load

$$\begin{cases} \mathrm{K_L T = Q} \\ \mathrm{T}_{SN} = \mathrm{AT} \end{cases} \Leftrightarrow \begin{bmatrix} K & \mathrm{A^T} \\ \mathrm{A} & 0 \end{bmatrix} \begin{Bmatrix} \mathrm{T} \\ 0 \end{Bmatrix} = \mathrm{M} \begin{Bmatrix} \mathrm{T} \\ 0 \end{Bmatrix} = \begin{Bmatrix} \mathrm{Q} \\ \mathrm{T_{SN}} \end{Bmatrix}$$

$$\begin{Bmatrix} \mathrm{T} \\ 0 \end{Bmatrix} = \mathrm{M}^{-1} \begin{Bmatrix} \mathrm{Q} \\ \mathrm{T_{SN}} \end{Bmatrix} = \begin{bmatrix} \mathrm{X} & \mathrm{Y^T} \\ \mathrm{Y} & \mathrm{Z} \end{bmatrix} \begin{Bmatrix} \mathrm{Q} \\ \mathrm{T_{SN}} \end{Bmatrix}$$

$$\mathrm{YA^T = I = AY^T}$$

$$0 = \mathrm{YQ + ZT_{SN}}$$

If the load is uniform over each super-node ($\mathrm{Q = A^T Q_{SN}}$): $\mathrm{YQ = Q_{SN}}$

$$-\mathrm{ZT_{SN} = Q_{SN}}$$

$$\boxed{\mathrm{K_{SN} = -Z}}$$

And the detailed T° can be recovered:

$$\mathrm{T = XQ + Y^T T_{SN}}$$

22

M is difficult to invert! → Local inversion

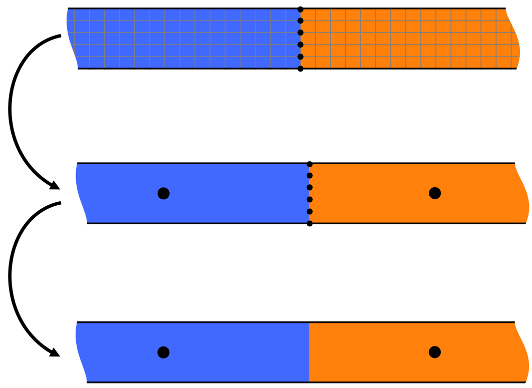

Local inversion of **M** : add super-node & keep all detailed IF nodes

Detailed IF nodes elimination through Guyan condensation

Detailed T° recovery by inverse procedure: no need to store full **X** and **Y**

23

Sources of non-uniformity

Internal radiative heat exchanges

Environmental (solar, albedo, IR) heat loads

Internal dissipations

Internal energy variations (transients)

24

Thermal radiative cantilever beam

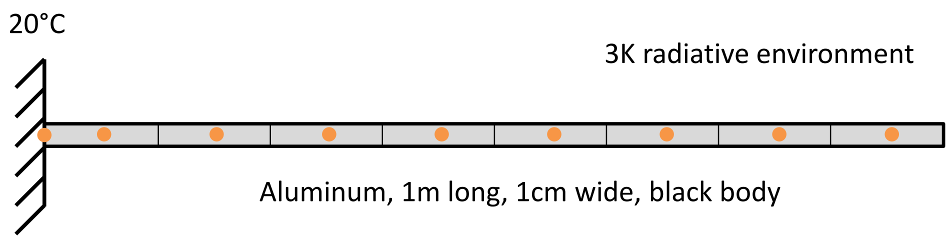

$$K_L T + K_R T^4 + Q_{ext} + C\frac{dT}{dt} = 0$$

25

1 node

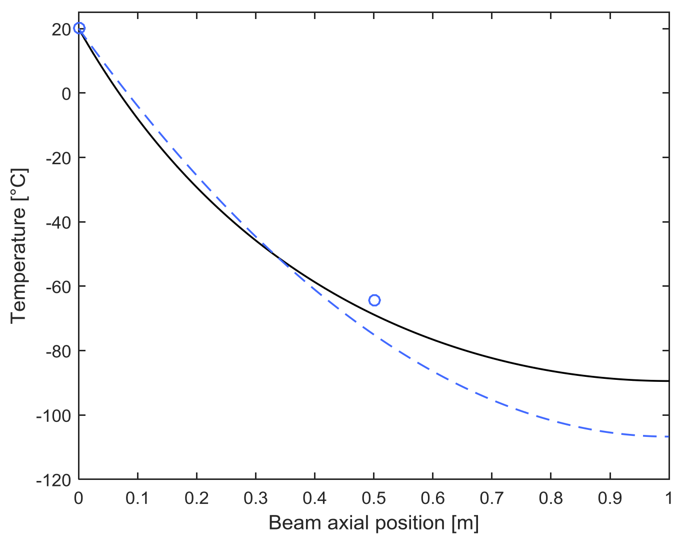

26

2 nodes

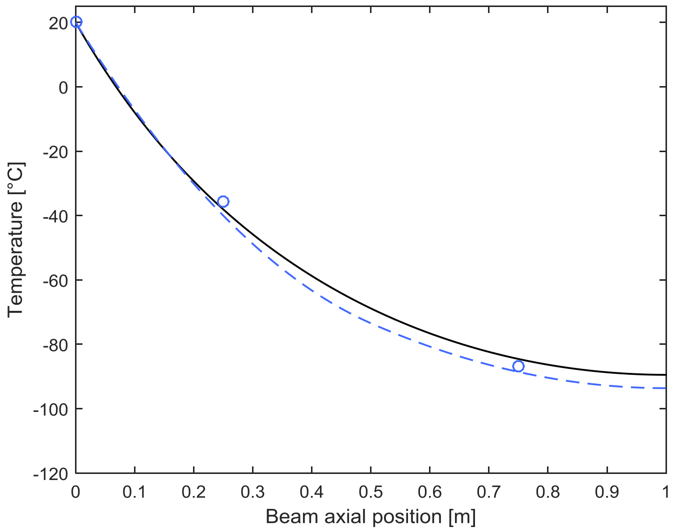

27

Convergence

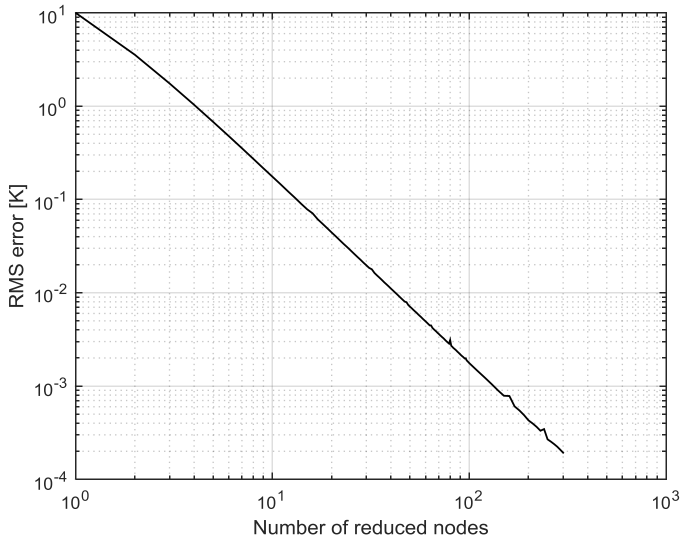

28

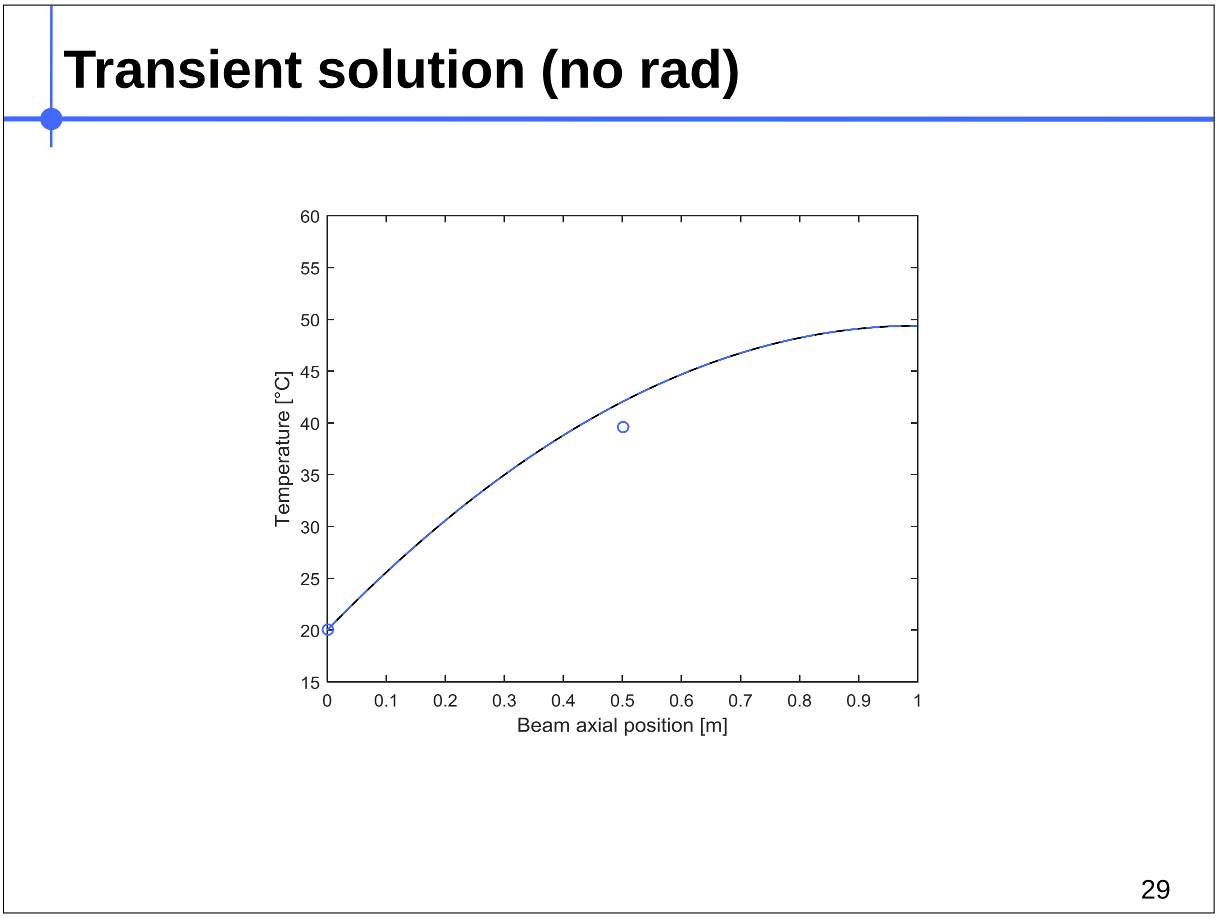

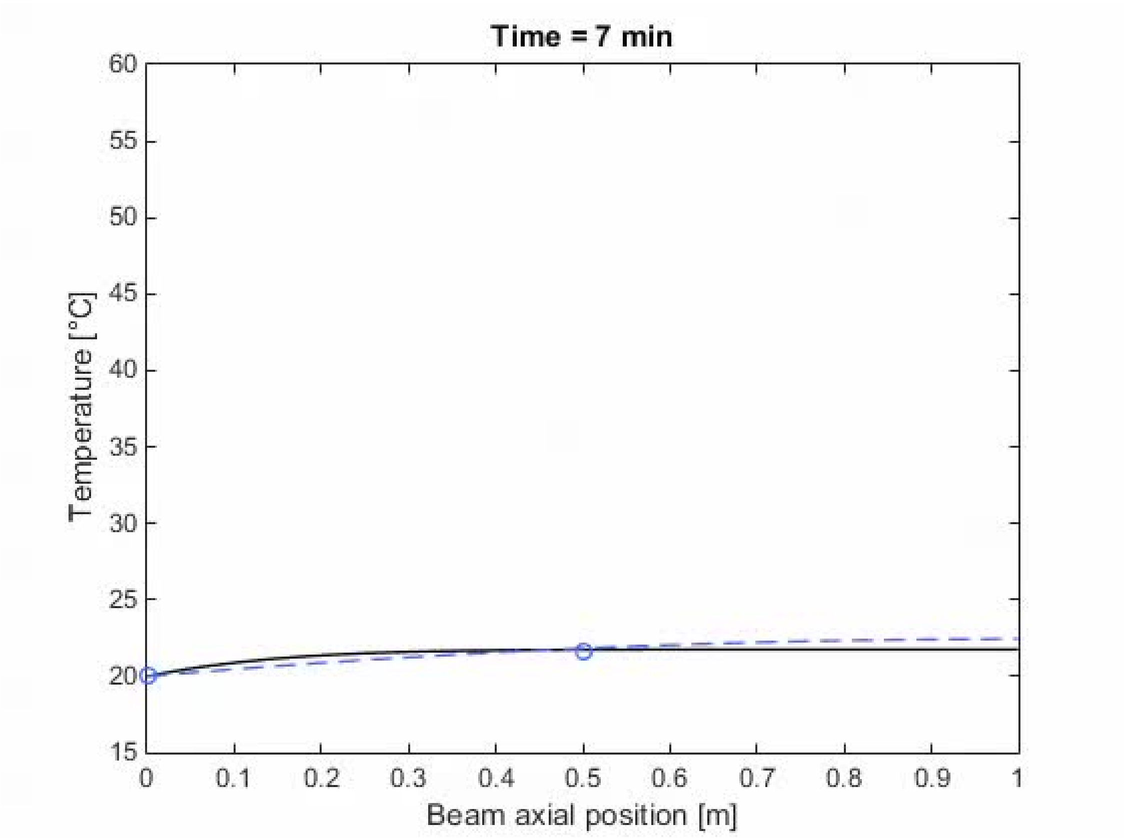

Save the attachment to disk or (double) click on the picture to run the movie.

Outline

Ray-tracing enhancement

FEM clustering & conductive reduction

Super-face ray-tracing

Integrating the developments

Conclusions & perspectives

30

Selective quadric fitting

Automatic quadric mesh fitting of user selected regions (e.g. optics)

$$f(\mathbf{x}) = \mathbf{C}^{\mathrm{T}}\mathbf{F} \qquad \mathbf{F}(\mathbf{x}) = [1, x, y, z, xy, xz, yz, x^2, y^2, z^2]^{\mathrm{T}}$$

$$\mathbf{C} = [c_0, \dots, c_9]^{\mathrm{T}}$$

$$error \approx \sum_{S_i \in R} \int_{S_i} \frac{f(\mathbf{x})^2}{|\nabla f(\mathbf{x})|^2} d\sigma \approx \frac{\mathbf{C}_0^{\mathrm{T}} M \mathbf{C}_0^{\mathrm{T}}}{\mathbf{C}_0^{\mathrm{T}} N \mathbf{C}_0^{\mathrm{T}}}$$

With $\mathbf{M} = \frac{1}{n} \sum_{\substack{i=1, \\ \mathbf{x}_i \in R}}^{n} \mathbf{F}(\mathbf{x}_i)\mathbf{F}(\mathbf{x}_i)^{\mathrm{T}}$ $\qquad \mathbf{N} = \frac{1}{n} \sum_{\substack{i=1, \\ \mathbf{x}_i \in R}}^{n} \nabla\mathbf{F}(\mathbf{x}_i)\nabla\mathbf{F}(\mathbf{x}_i)^{\mathrm{T}}$

$\mathbf{C}$ is the eigen vector associated with minimum eigen value of

$$\mathbf{M} - \lambda\mathbf{N}$$

31

Ray-tracing with quadrics

Use directly the quadric for the intersection computation

→ avoid lost grazing rays

→ better shadow

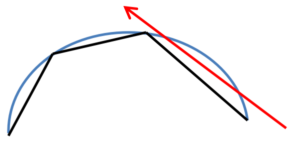

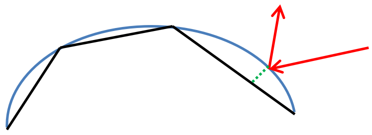

Project normally to the quadric to determine which super-face

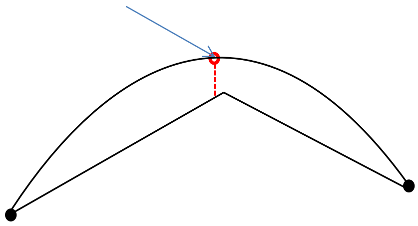

32

Fitted cylinder vs. ESARAD cylinder

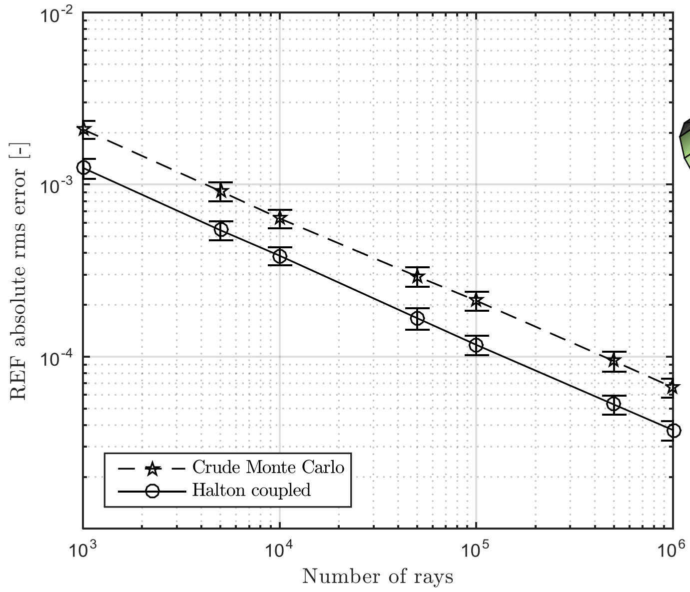

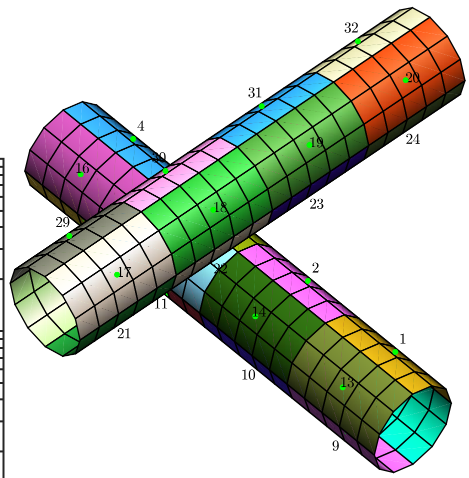

33

Outline

Ray-tracing enhancement

FEM clustering & conductive reduction

Super-face ray-tracing

Integrating the developments

Conclusions & perspectives

34

Putting the building blocks together

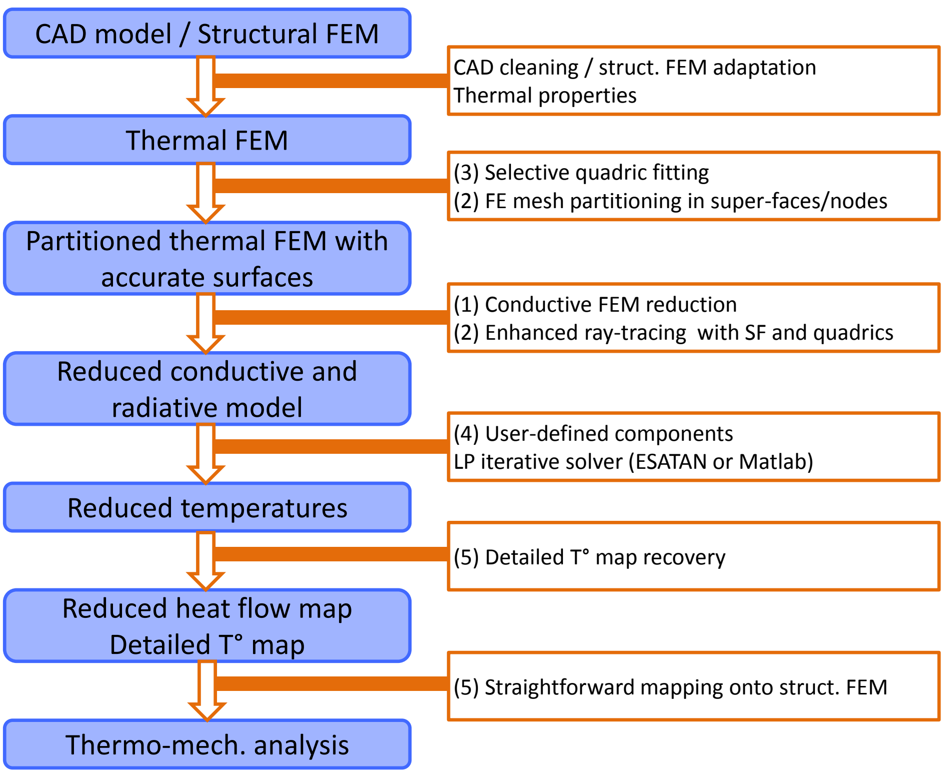

35

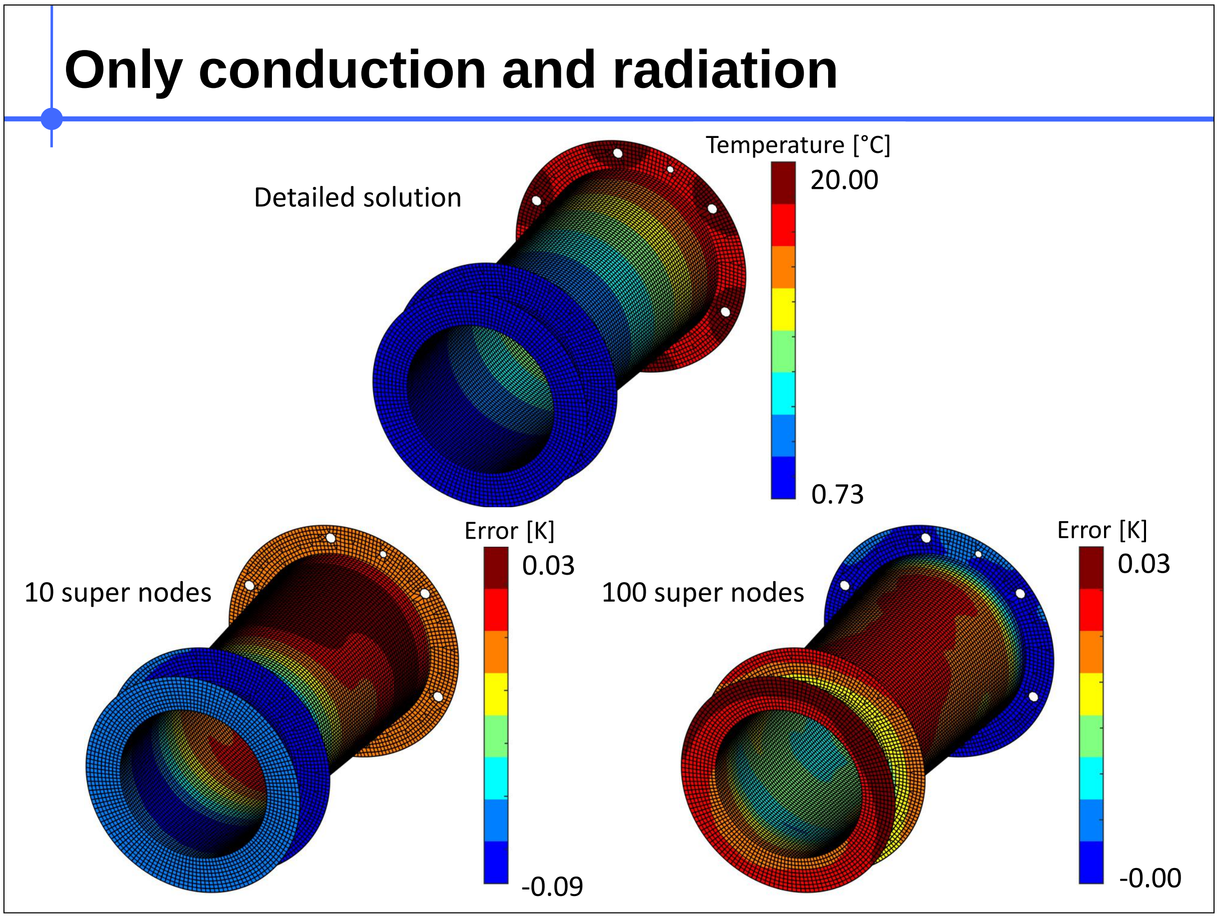
Only conduction and radiation
Detailed solution
Temperature [°C]
20.00
0.73
10 super nodes
Error [K]
0.03
-0.09
100 super nodes
Error [K]
0.03
-0.00

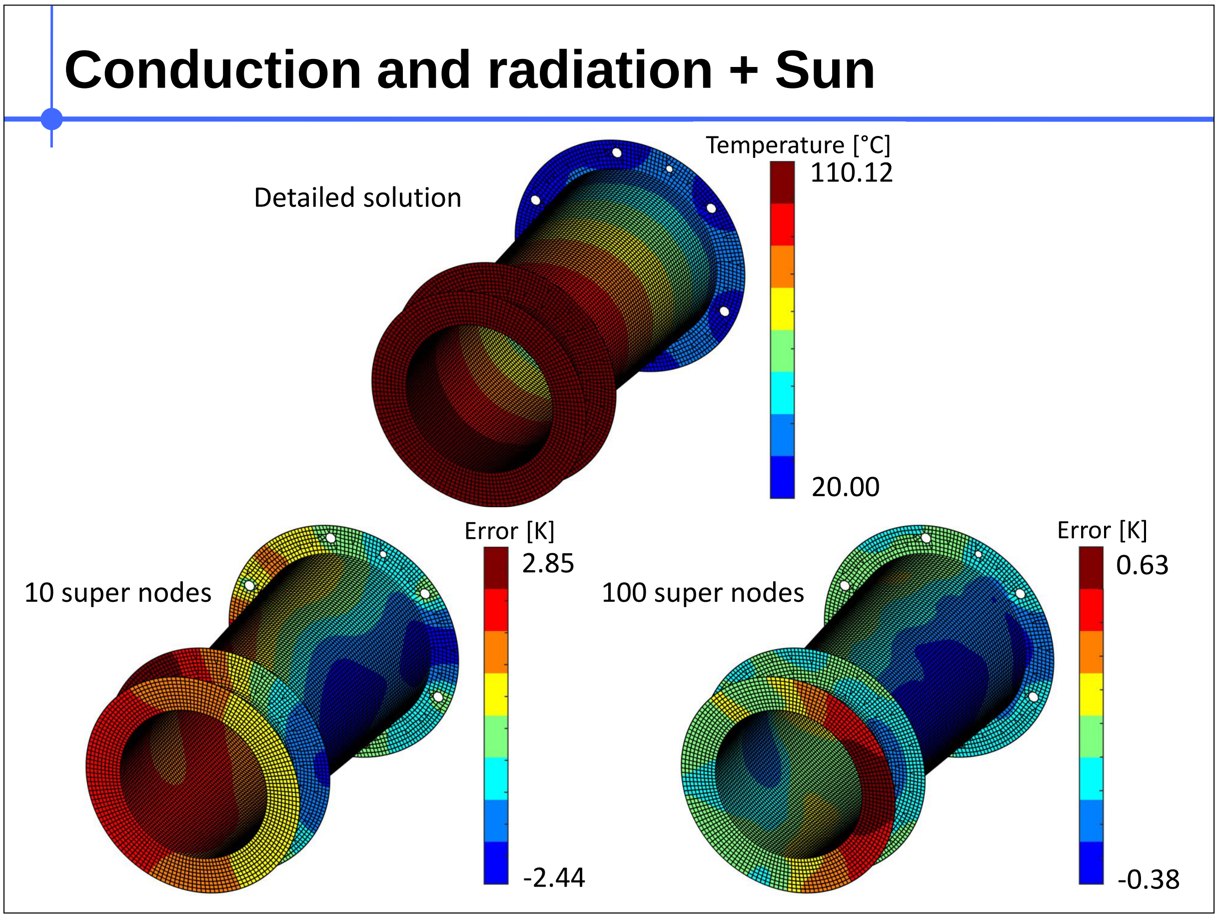
Conduction and radiation + Sun
Detailed solution
Temperature [°C]
110.12
20.00
10 super nodes
Error [K]
2.85
-2.44
100 super nodes
Error [K]
0.63
-0.38

Conclusions & perspectives

Integrated approach for detailed analysis of complex structures

No GMM needed, no T° mapping → time and costs saving!

Takes advantages of both lumped parameter and finite element methods:

- More accurate conductive links
- Accurate shape recognition used for ray-tracing
- Reduce the gap between thermal and structural analyses

Perspectives:

- Iterative process with automatic refinement in high ΔT regions
- Quadric fitting → opto-thermo-structural analyses

38

Thank you for your attention…

Any question?

39

CONTACT

Lionel Jacques, ljacques@ulg.ac.be
Thermal Engineer & PhD student

- University of Liège
  Space Structures and Systems Lab
  1, Chemin des Chevreuils (B52/3)
  Liege, B-4000, Belgium
  http://www.ltas-s3l.ulg.ac.be/

- Centre Spatial de Liège
  Liège Science Park
  Avenue Pré-Aily
  B-4031 Angleur Belgium
  http://www.csl.ulg.ac.be

40

Appendix N

VEGA Launch Vehicle
Improved Fluidic Thermal Prediction Model

P. Perugini David Moroni Matteo Tirelli
(Avio S.p.A., Italy)

Abstract

The VEGA Launch Vehicle Thermal Prediction Model is introduced and its latest improvements described. With increased availability of sensor data from successfully performed flights it was possible to highlight the need for higher predictive accuracy, both in temperature trends and values, in some specific but crucial elements, in particular the 4^{th} stage liquid propulsion system main engine. It is in fact one of the most critical component due to the long mission requirements with respect to other stages engines, with complex attitude profiles in space environment and multiple re-ignitions.

In an upper Stage Assy, as the VEGA LV A4, the major concern is the propellant temperature, especially in the moments just before engine start-up, being related with combustion instabilities and performances. For this reason, ESATAN FHTS library capabilities were studied and fluidic network representing the engine feeding lines introduced in the Thermal Model.

Propellants properties are taken from available literature and dedicated libraries are developed to fit ESATAN required format.

Thrust Chamber cooling system is also included and complex heat exchanges between hot gases and engine structure accounted. Simulations temperature trends are compared with flight sensor data for previous flights resulting in a very good correlation.

The whole model is finally optimized in order to minimize impacts on runtime due to the new solution loop. Further improvements are foreseen both in fluid properties and model details.

VEGA LAUNCH VEHICLE:
Improved fluidic thermal prediction model

Noordwijk, October 2016

Introduction

Scope of this work is to present the latest improvements introduced in the VEGA **T**hermal **M**athematical **M**odel (**TMM**) concerning the 4th stage **L**iquid **P**ropulsion **S**ystem (**LPS**). The content of the presentation is:

- Thermal activities performed by AVIO
- Objectives of the improvements and background in the **L**aunch **V**ehicle (**LV**) **TMM**
- New Geometrical Mathematical Model of the **LPS** feeding lines (4th stage)
- Improvements in the **LPS** Thrust Chamber nodal definition
- Our experience with *ESATAN-TMS* fluidic networks capabilities
- Application to the VEGA **LV** 4th Stage **LPS** Assy
- Correlation with respect to reference documentation
- Model verification with respect to flight data
- New information available from the improved model

Produced by AVIO SP/PRC department 1

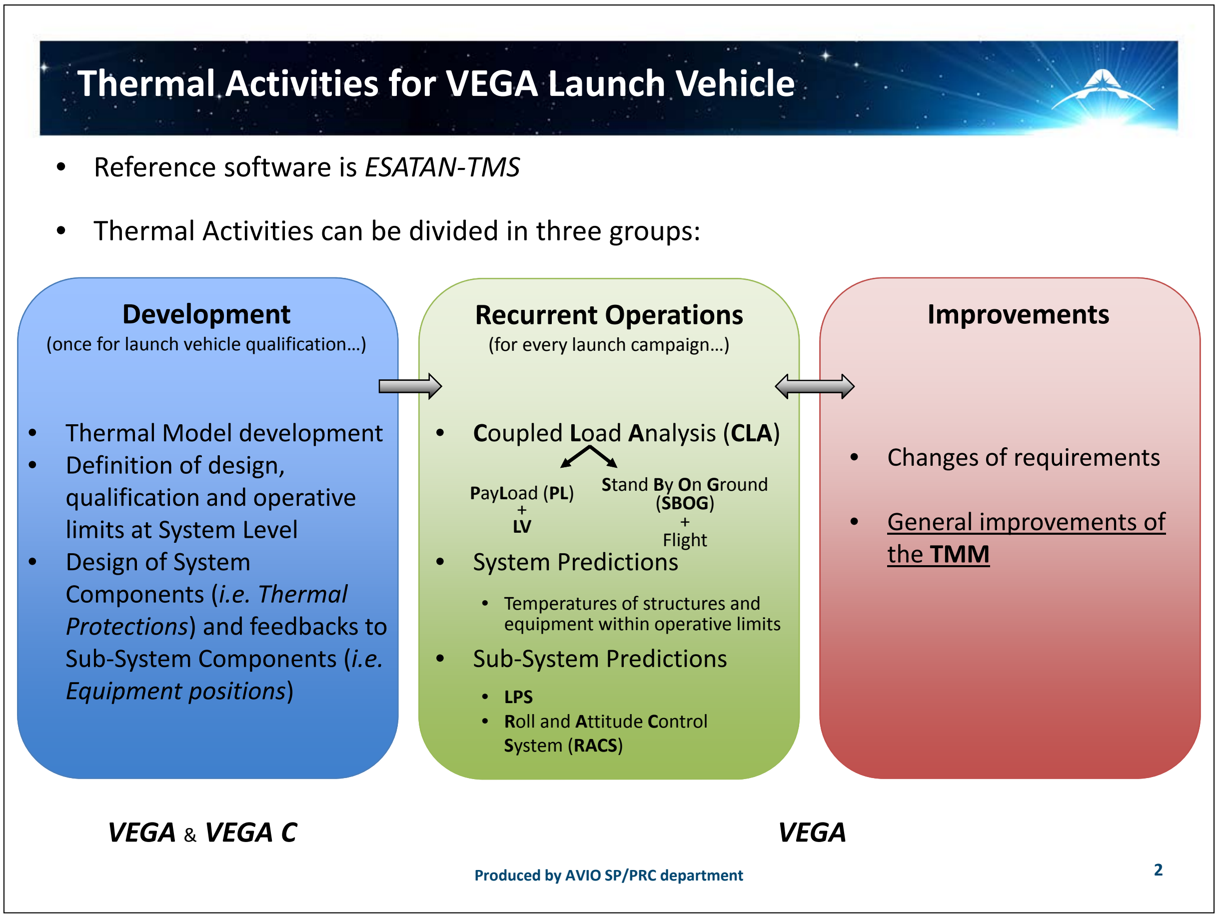
Thermal Activities for VEGA Launch Vehicle
Reference software is ESATAN-TMS
Thermal Activities can be divided in three groups:
Development
(once for launch vehicle qualification…)
Thermal Model development
Definition of design, qualification and operative limits at System Level
Design of System Components (i.e. Thermal Protections) and feedbacks to Sub-System Components (i.e. Equipment positions)
Recurrent Operations
(for every launch campaign…)
Coupled Load Analysis (CLA)
PayLoad (PL) + LV
Stand By On Ground (SBOG) + Flight
System Predictions
Temperatures of structures and equipment within operative limits
Sub-System Predictions
LPS
Roll and Attitude Control System (RACS)
Improvements
Changes of requirements
General improvements of the TMM
VEGA & VEGA C
VEGA
Produced by AVIO SP/PRC department
2

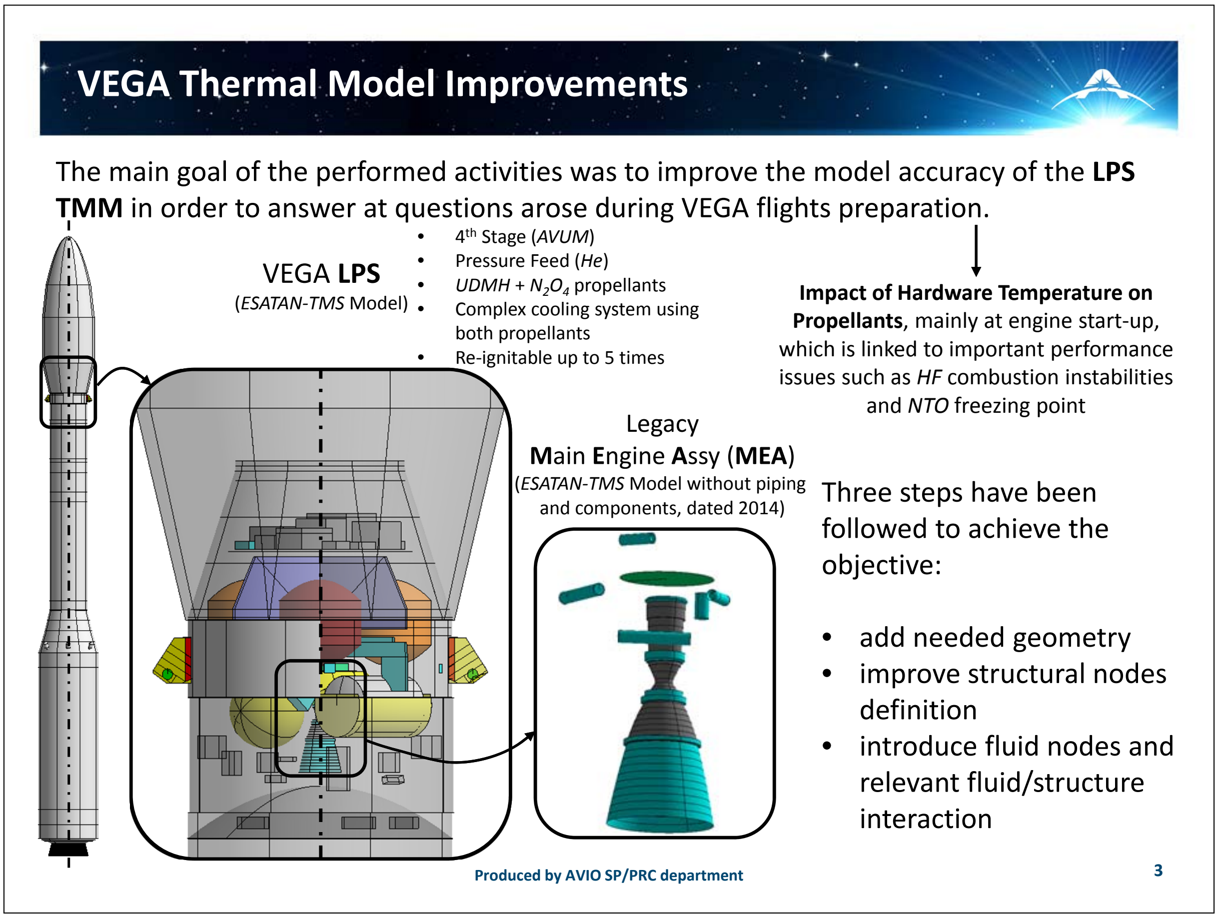
VEGA Thermal Model Improvements
The main goal of the performed activities was to improve the model accuracy of the LPS TMM in order to answer at questions arose during VEGA flights preparation.
VEGA LPS
(ESATAN-TMS Model)
4th Stage (AVUM)
Pressure Feed (He)
UDMH + N_2O_4 propellants
Complex cooling system using both propellants
Re-ignitable up to 5 times
Impact of Hardware Temperature on Propellants, mainly at engine start-up, which is linked to important performance issues such as HF combustion instabilities and NTO freezing point
Legacy
Main Engine Assy (MEA)
(ESATAN-TMS Model without piping and components, dated 2014)
Three steps have been followed to achieve the objective:
add needed geometry
improve structural nodes definition
introduce fluid nodes and relevant fluid/structure interaction
Produced by AVIO SP/PRC department
3

New geometry included in the Thermal Model

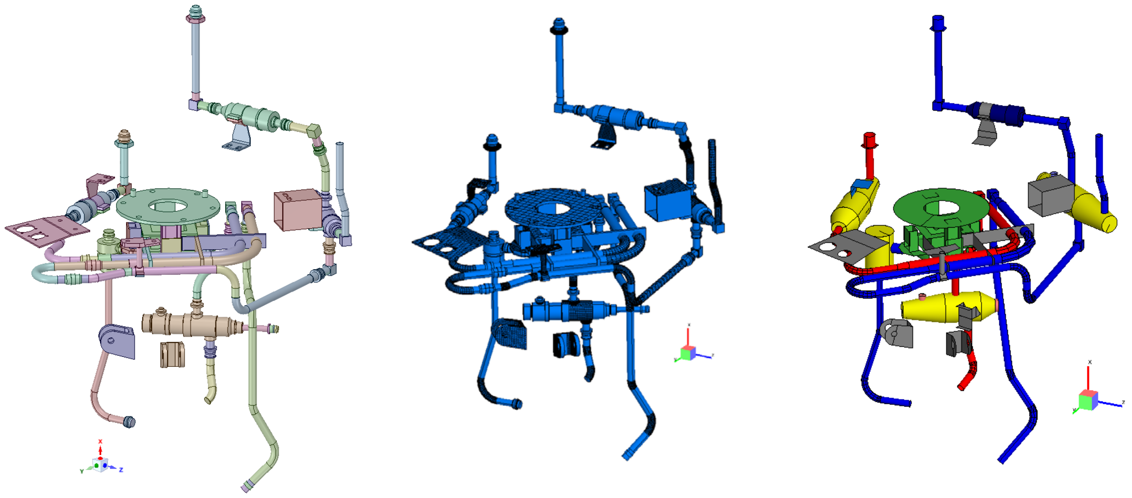

Relevant geometry imported from .step to *CADBench* → Conversion to *ESATAN-TMS* .erg geometry format → Geometry simplification and improvements in *ESATAN-TMS*

- The simplification process reduced the overall number of faces from 113396 to 1228 resulting in low expected impact on radiative cases computation times (comparable to average **PL**).
- Attention to small size faces…

Produced by AVIO SP/PRC department

4

Geometry comparison with real hardware (1)

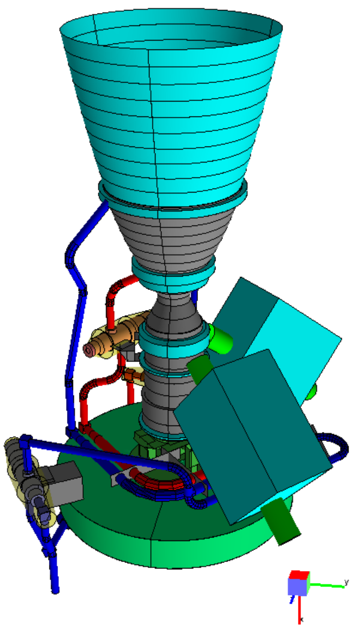

Produced by AVIO SP/PRC department

5

Geometry comparison with real hardware (2)

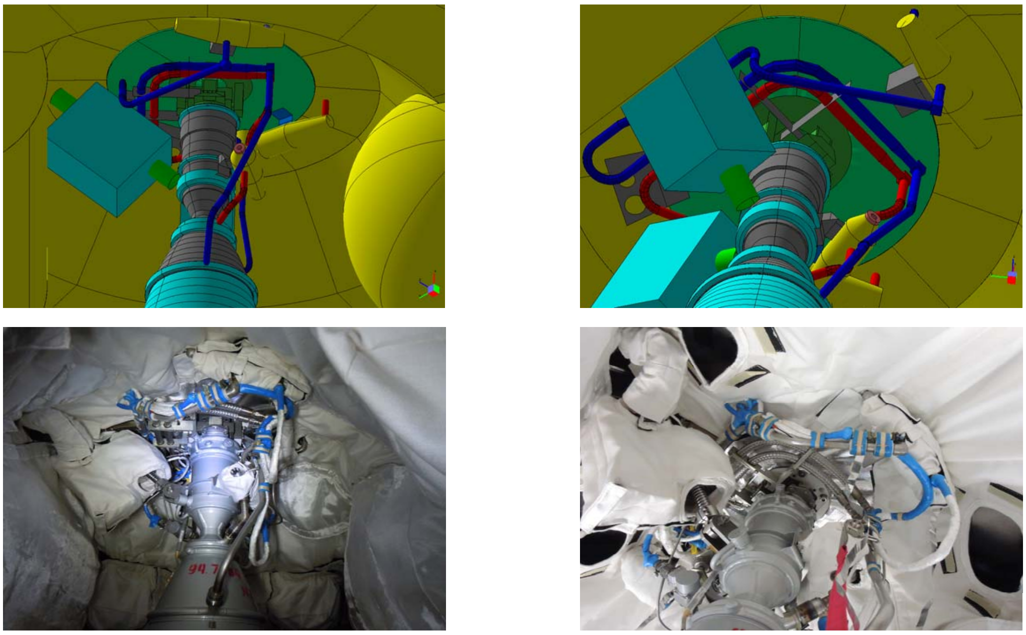

Produced by AVIO SP/PRC department

6

Structural Nodes overview

Detailed thickness discretization of the **T**hrust **C**hamber (**TC**) was needed to properly reproduce steep temperature gradients across engine walls and interaction with cooling propellants

Radial Direction	**Longitudinal Direction**	**Circumferential Direction**
(thickness)	(**LV** axis)	
4+1 nodes	*33 nodes*	*3 nodes (@120°)*

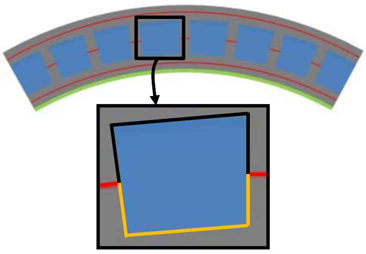

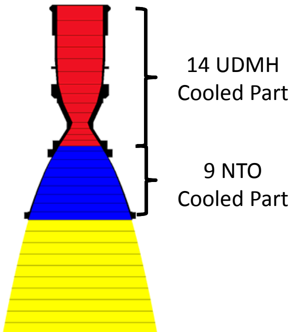

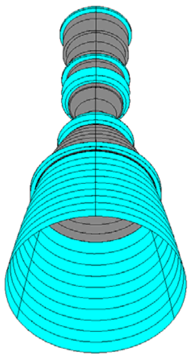

Nodes interfaces
Coating material node (only for NTO cooled)
Fluid node
Structural node

External node/fluid contact area
Internal node/fluid contact area

The two areas are approximately equals
(this allows to use * option for GLs…)

Produced by AVIO SP/PRC department

7

Structural Nodes properties calculation

A total of *363* nodes are used for the **TC** with ≈1000 *GLs*

Nodes and *GLs* have different averaged properties for each **TC** longitudinal section and for each radial position, depending on:

MATLAB is used to generate definitions in ESATAN-TMS format

- longitudinal position
- radius
- walls thicknesses
- cooling channels heights, widths, number, *swirling angle*

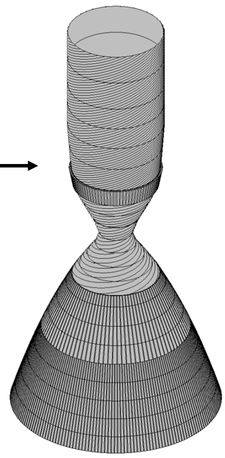

The total mass of computed nodes is compared with the expected engine mass resulting in an error of ≈ $\mathbf{0.05\ kg}$

In this phase also the properties of fluidic nodes for cooling channels are computed (hydraulic diameters, flow areas, lengths, heat exchange areas)

→ 1 fluidic node for each longitudinal node

Produced by AVIO SP/PRC department 8

ESATAN-TMS Fluid Networks overview

ESATAN-TMS allows to model fluidic networks interacting with solid nodes (FHTS)

- 1D Fluid models
- steady/transient
- single/two phases

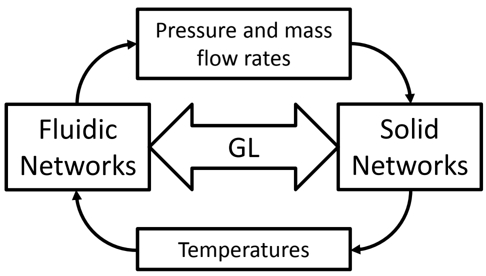

The overall complexity of a thermal model coupled with a fluidic model is higher both in number of required inputs and solution time

- Fluid definition
- Network definition
- Coupling definition

Two solutions routines requiring two different coupled convergences

Produced by AVIO SP/PRC department 9

Fluid Definition overview

- Default fluids source codes in *ESATAN-TMS* are stored in ***"flpDefs"*** folder as *.flp* ASCII files (***Fl***uid ***P***roperties)
- Before being used, any fluid must to be precompiled to a Fortran library .a through dedicated *ESATAN-TMS* procedure
- The library must to be included in Analysis Case definition in order to be linked by *ESATAN-TMS* during preprocessing to the solution *.exe*
- The default fluid library is distributed with *ESATAN-TMS* in the ***"bin"*** folder named as *flpobj.a* and it is automatically linked to any model with fluid networks if no other is specified
- A single library can contain more fluids which may or may not be used in the studied model: the default library include **AIR**, **AIRW**, **AMMONIA**, **R11**, **R12**, **R21**, **R22**, **R114**, **R502** and **WATER**

Produced by AVIO SP/PRC department 10

Fluid Definition properties

- A fluid properties file defines the thermodynamic and transport properties for the fluid:

• Density	`$RHO`	kg/m^3
• Specific heat (at constant pressure)	`$CP`	J/kgK
• Thermal conductivity	`$COND`	W/mK
• Dynamic viscosity	`$VISC`	kg/ms
• Surface tension	`$SIG`	N/m
• Specific enthalpy	`$ENTH`	J/kg
• Temperature	`$TEMP`	$°C$
• Pressure	`$PRES`	Pa
• Joule-Thompson coefficient	`$JT`	K/Pa
• Isothermal compressibility	`$KT`	$1/Pa$

- For each property values have to be provided in different states:

• Liquid	`$LIQUID`	
• Saturated liquid	`$SAT_LIQ`	
• Two-phase	`$TWO_PHASE`	→ `$SAT`
• Saturated vapor	`$SAT_VAP`	
• Vapor	`$VAPOUR`	

Produced by AVIO SP/PRC department 11

Fluidic Network overview

- *ESATAN-TMS* fluid model are best suited to simulate closed-loop circuits such as satellites thermal control systems (it is not possible to "deactivate" a fluidic node to account, in example, for the emptying of a pipe)
- Fluid nodes are defined by the letter **F**
- Open-loops can be simulated by imposing two boundaries at the inlet and outlet:
  - Pressure-Pressure
  - Pressure-Mass Flow
- Boundary types are:
  - **J** user prescribed pressure
  - **K** user prescribed temperature
  - **R** user prescribed pressure and temperature
  - **H** arithmetic node

Produced by AVIO SP/PRC department 12

Fluidic Network nodal properties

- *ESATAN-TMS* fluid nodes have the following main properties:
  - **A** heat transfer area m^2
  - **FD** hydraulic diameter m
  - **FL** length m
  - **P** static pressure Pa
  - **T** temperature °C
  - **FF** wall surface roughness m
  - **FQ** internal heat source W
  - **FM** mass source rate kg/s
  - **FT** fluid type
  - **VQ** vapor quality
  - **FLA** flow area m^2

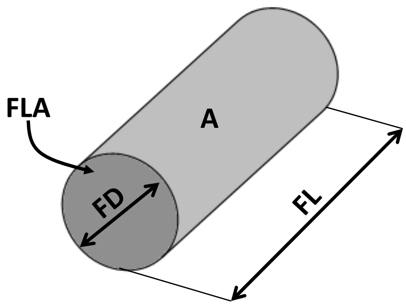

- **P** and **T** have to be specified only on boundary nodes, for fluid nodes they are used as initial condition

Produced by AVIO SP/PRC department 13

Fluidic Network nodes connections

- The network topography is defined by Mass-Flow links (type **M**)
- The value is computed automatically by *ESATAN-TMS* during solution time as result of the pressure drops balance in the network and fluid properties: the initial value is useful only to reach quickly the first convergence to numerical solution value of Mass-Flow.
- For each **M** link, a **GP** link is automatically created representing the conductance between the linked nodes.

$$GP = \frac{\rho u^2}{2\Delta p} = \frac{\dot{m}^2}{2\rho A^2 \Delta p}$$

- A dedicate function is created to handle conductance links:

$$\texttt{CORRGP(NODE, MASS FLOW, }\underbrace{\texttt{PRESSURE DROP}}_{bar}\texttt{);}$$

Produced by AVIO SP/PRC department 14

Fluid-Solid Coupling Definition

- *ESATAN-TMS* allows an automatic calculation of Heat Exchange coefficient (HTC) for a Fluid Node interacting with a Solid Node

```
GL(FLUID, SOLID) = *;
```

- The reference parameter *ESATAN-TMS* uses for calculation is the Hydraulic Diameter
- Natural and forced convection are accounted (for natural convection, horizontal pipes are the reference)
- Single Phase and Two Phase (boiling or condensing fluid) are taken into account with relevant equations (*Re*, *Pr*, *Gr*, *Nu*)

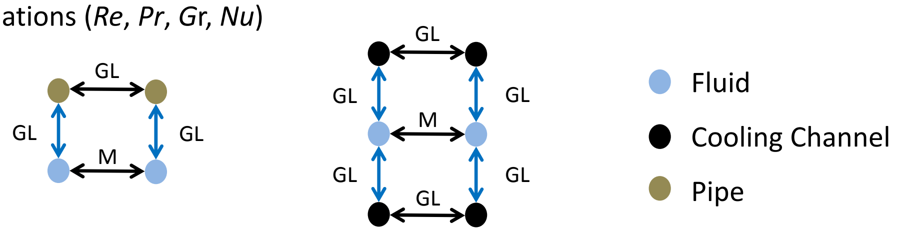

- Detailed explanation in *ESATAN-TMS* User Manual Appendix K

Produced by AVIO SP/PRC department 15

Fluidic Nodes properties check

Computed fluidic properties such as Hydraulic Diameter and Flow Area are verified with respect to reference documentation.

- Documentation values are in ***RED*** for UDMH and ***BLUE*** for NTO
- *ESATAN-TMS* model is in ***BLACK***
- Dots are nodes positions

Hydraulic Diameter

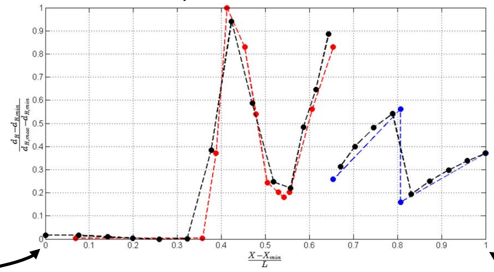

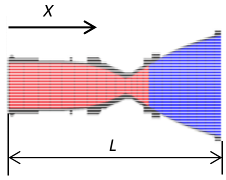

End of UDMH cooled part of ***TC***

Start of NTO cooled part of ***TC***

Flow Area

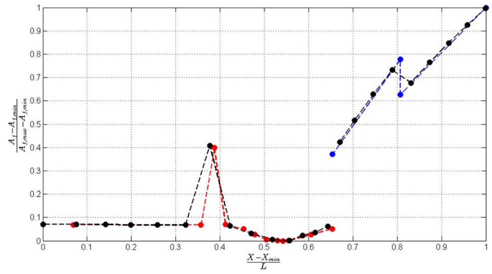

To be noted that position of documentation nodes may differ from position of *ESATAN-TMS* nodes explaining the difference in punctual values

Produced by AVIO SP/PRC department

16

Fluid properties and Fluidic Network application

Propellant libraries in *ESATAN-TMS* formats are created from available literature

Feeding lines are implemented with fluidic nodes linked through *Ms*, *GPs* and *GLs*

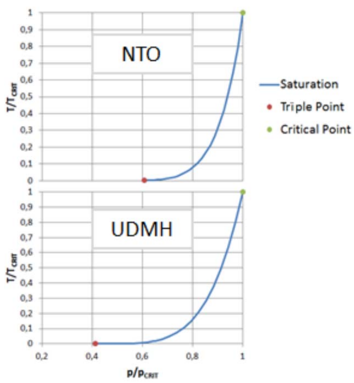

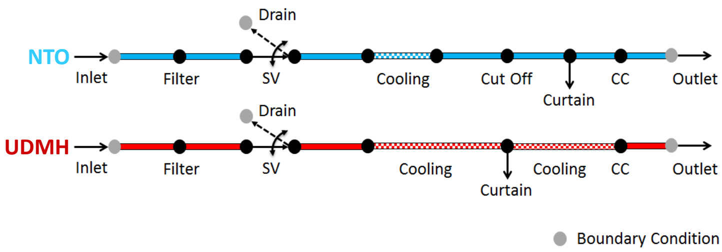

- Boundary conditions *R* and *J* to simulate open circuit
- Pressure drops from hydraulic tests
- Curtain coolant mass flow extracted through negative *FM*

Several custom outputs are implemented such as density, mass, Prandtl, Reynolds and velocity to crosscheck against reference documentations

To correctly model cooling system, heat flux is applied as boundary to ***TC*** hot gas side

Produced by AVIO SP/PRC department

17

Fluidic Network Properties Check

Comparison of Fluidic Network properties with respect to reference documentation at engine nominal operative condition and steady state

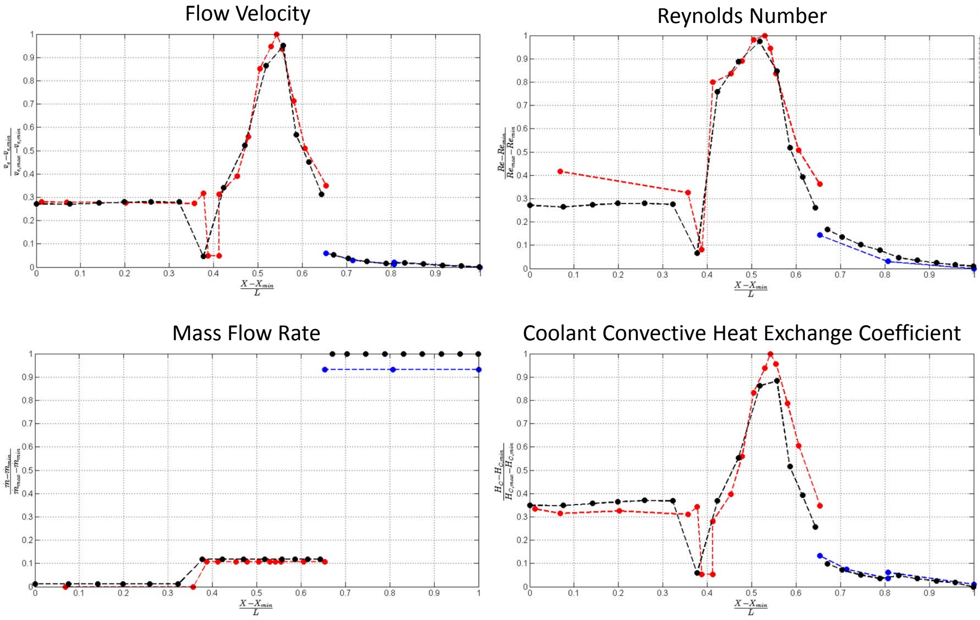

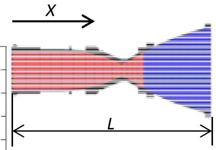

- Documentation values are in ***RED*** for UDMH and ***BLUE*** for NTO
- Documentation values are verified through test campaign during **TC** design
- *ESATAN-TMS* model is in ***BLACK***
- Dots are nodes positions

Produced by AVIO SP/PRC department 18

Flight verification of model improvements

The model was verified with flight data from VV04, VV05 and VV06 missions revealing a good agreement between sensor data and predictions. The improved model has been used also for VV07 mission (sensor data currently under exploitation)

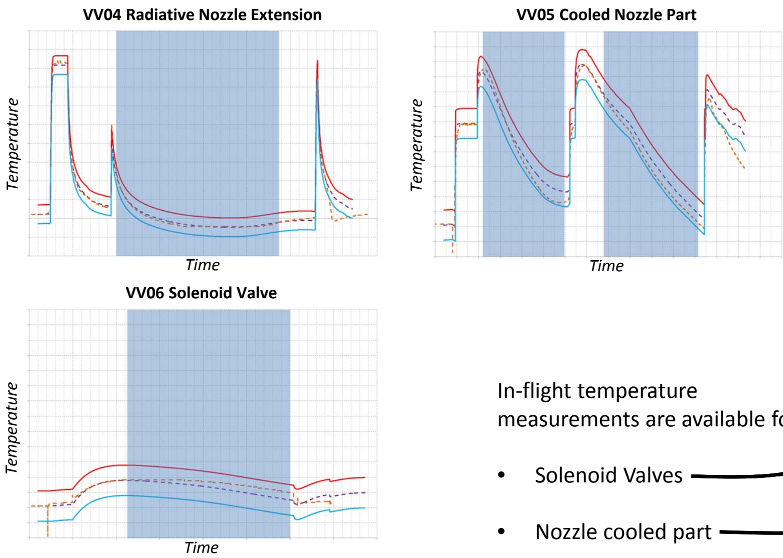

Best accuracy where the trajectory data were fully available

In-flight temperature measurements are available for:

- Solenoid Valves
- Nozzle cooled part
- Nozzle radiative extension

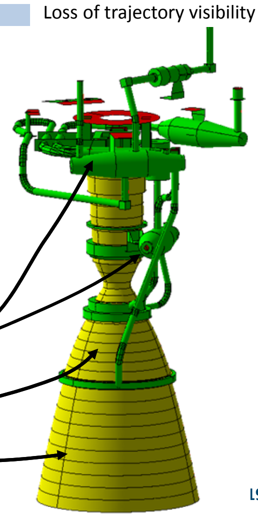

Produced by AVIO SP/PRC department 19

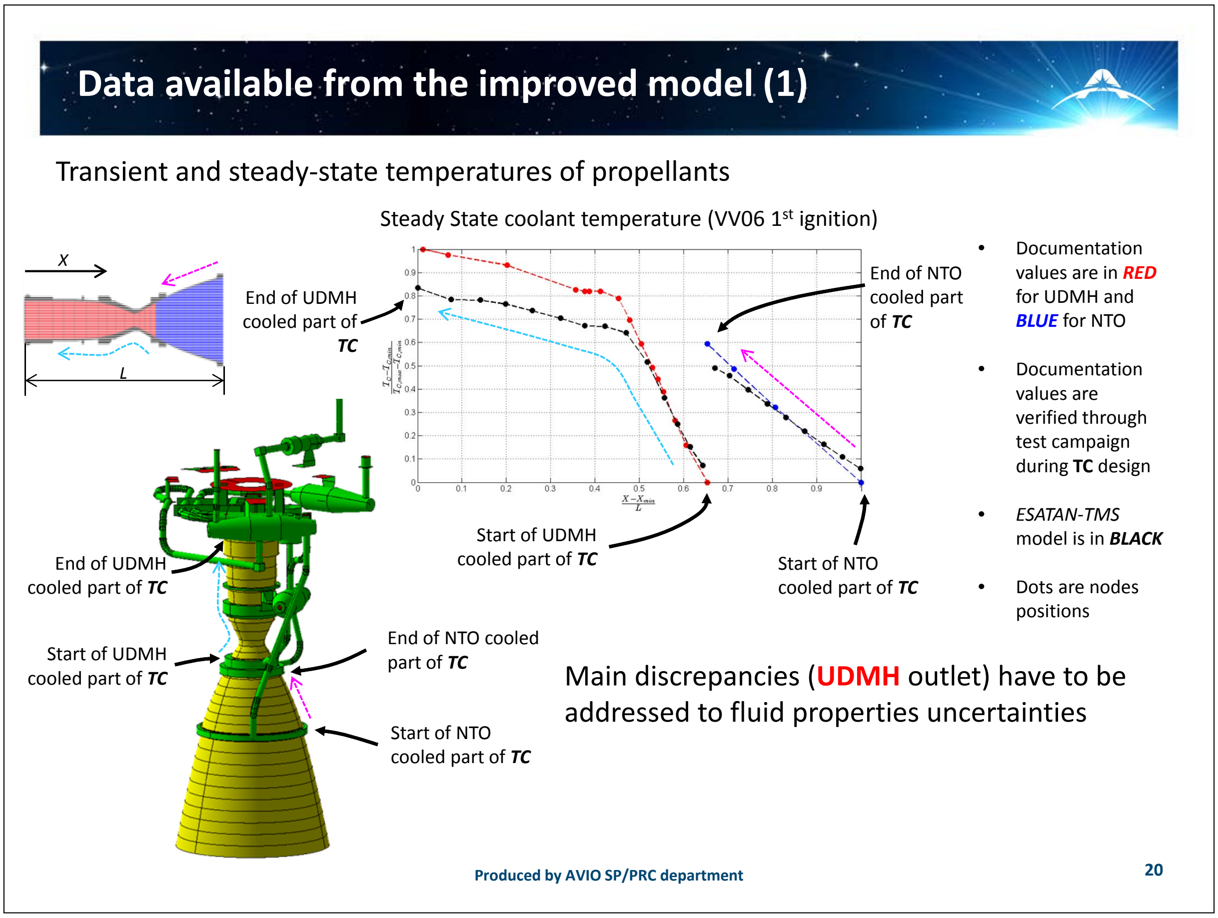
Data available from the improved model (1)
Transient and steady-state temperatures of propellants
Steady State coolant temperature (VV06 1st ignition)
X
L
End of UDMH cooled part of TC
End of NTO cooled part of TC
Start of UDMH cooled part of TC
Start of NTO cooled part of TC
End of UDMH cooled part of TC
Start of UDMH cooled part of TC
End of NTO cooled part of TC
Start of NTO cooled part of TC
Documentation values are in RED for UDMH and BLUE for NTO
Documentation values are verified through test campaign during TC design
ESATAN-TMS model is in BLACK
Dots are nodes positions
Main discrepancies (UDMH outlet) have to be addressed to fluid properties uncertainties
Produced by AVIO SP/PRC department
20

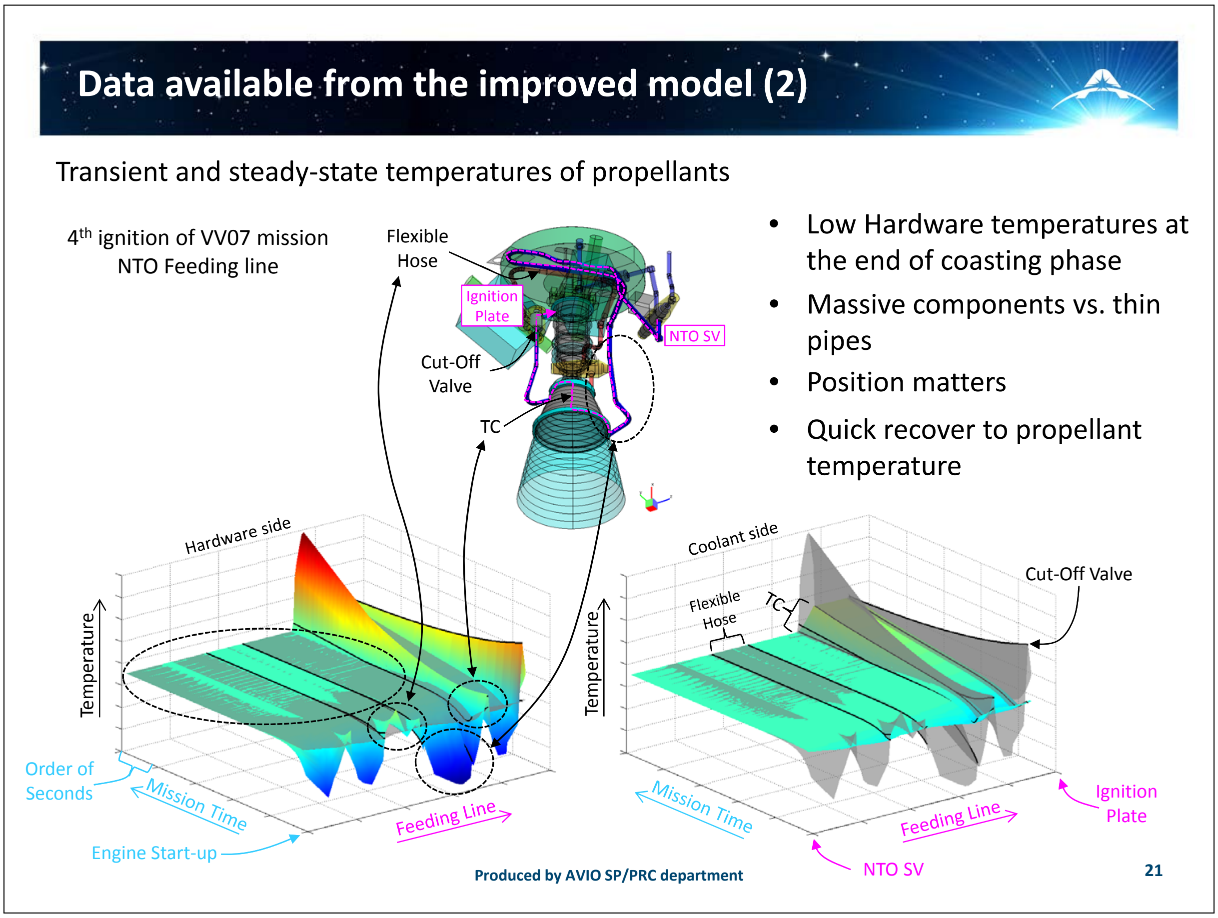
Data available from the improved model (2)
Transient and steady-state temperatures of propellants
4th ignition of VV07 mission
NTO Feeding line
Flexible Hose
Ignition Plate
NTO SV
Cut-Off Valve
TC
Low Hardware temperatures at the end of coasting phase
Massive components vs. thin pipes
Position matters
Quick recover to propellant temperature
Hardware side
Temperature
Order of Seconds
Mission Time
Feeding Line
Engine Start-up
Coolant side
Flexible Hose
TC
Cut-Off Valve
Temperature
Mission Time
Feeding Line
Ignition Plate
NTO SV
Produced by AVIO SP/PRC department
21

Data available from the improved model (3)

Hardware temperature maps

2nd ignition of VV05 mission

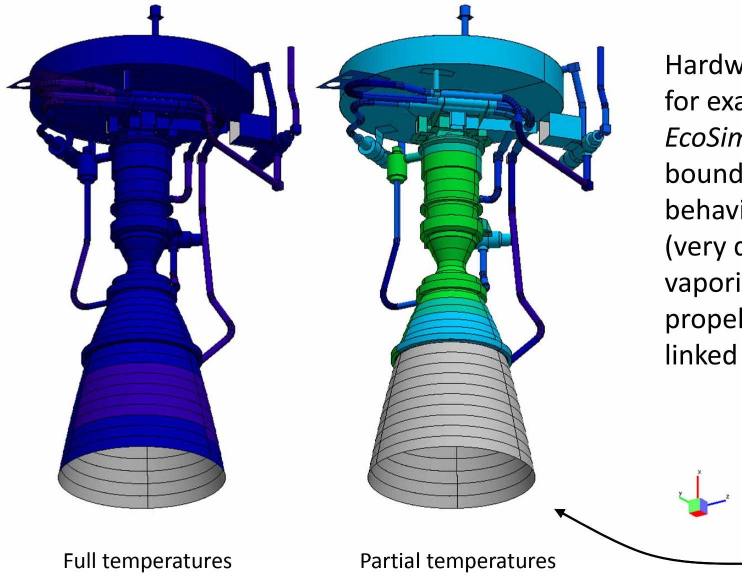

Hardware temperatures are used for example in a dedicated *EcoSimPRO* model as thermal boundary condition to simulate NTO behavior across engine start-up (very quick transient with partial vaporization of propellant) to asses propellant temperature at ignition, linked with *HF* instabilities

Full temperatures range

Partial temperatures range

Each frame is 10s simulation time for and overall duration of 200s

Produced by AVIO SP/PRC department

22

Resume

- The VEGA launch vehicle Thermal Model has been improved for what concern the **LPS**, introducing propellant feeding lines.
- Detailed geometry of piping, gimbaling, supports and valves have been included.
- Thermal properties for each new component have been defined and relevant nodes linked to the rest of the **LV TMM**.
- New discretization of **TC** has been introduced to better reproduce temperature gradients in the walls and correctly interact with cooling fluids.
- *ESATAN-TMS* FHTS capabilities have been investigated and a brief overview of main characteristics presented.
- *ESATAN-TMS* fluid libraries have been created for used propellants.
- Application of fluidic network has been implemented to simulate nominal operative condition of VEGA **LPS**.

Produced by AVIO SP/PRC department

23

Conclusions

- Hydraulic and Heat Exchange parameters have been compared with reference data and documentation (experimental data), resulting in a good correlation between model and expected values.
- The improved model has been verified with respect to previous VEGA flights VV04, VV05 and VV06 sensor measurements, again resulting in a very good correlation both for transient and stationary phenomena.
- Thanks to the Improved **TMM**, new reliable data are now available during VEGA **LV** launch preparation phases.

Produced by AVIO SP/PRC department

24

Thanks

Contacts:

Avio SpA – Via Ariana, km 5.2
00034 Colleferro (RM), Italy

P. Perugini	pierluigi.perugini@avio.com	
	+39 06 972 85804	
M. Moroni	david.moroni@avio.com	
	+39 06 972 85684	
M. Tirelli	matteo.tirelli@avio.com	

25

Appendix O

SYSTEMA — THERMICA

Timothée Soriano Antoine Caugant
(Airbus Defense and Space SAS, France)

Abstract

Systema version 4.8.0 includes many improvements and corrections. Especially, the material database now handles different phases so to be able to set not only beginning-of-life and end-of-life properties but also for any customizable condition.
Moreover, a new ray-tracing algorithm based on a quasi-random approach has been developed and shown a very significant improvement in the accuracy of radiative couplings and external fluxes evaluations.
The python interface keeps being improved with more and more features and there are available scripts to export/import models in ASCII format or to help in the setting of parametric analysis.
Besides, the current developments are focusing on several new features. Some have already well progressed like the integration of Systema in test facilities or the management of convection so to ease the correlation with ambient testing. A particular attention is also given to the Step-Tas interface. The 4.8.0 version stabilizes a lot the export of Systema and Thermisol models (GMM and TMM). In the next 4.8.1 version, the import should also be improved thanks to an improved management of the cutters.


Systema
Systema - Thermica
30th European Space Thermical Analysis Workshop
Timothée Soriano – Antoine Caugant
05-06 October 2016
AIRBUS
DEFENCE & SPACE

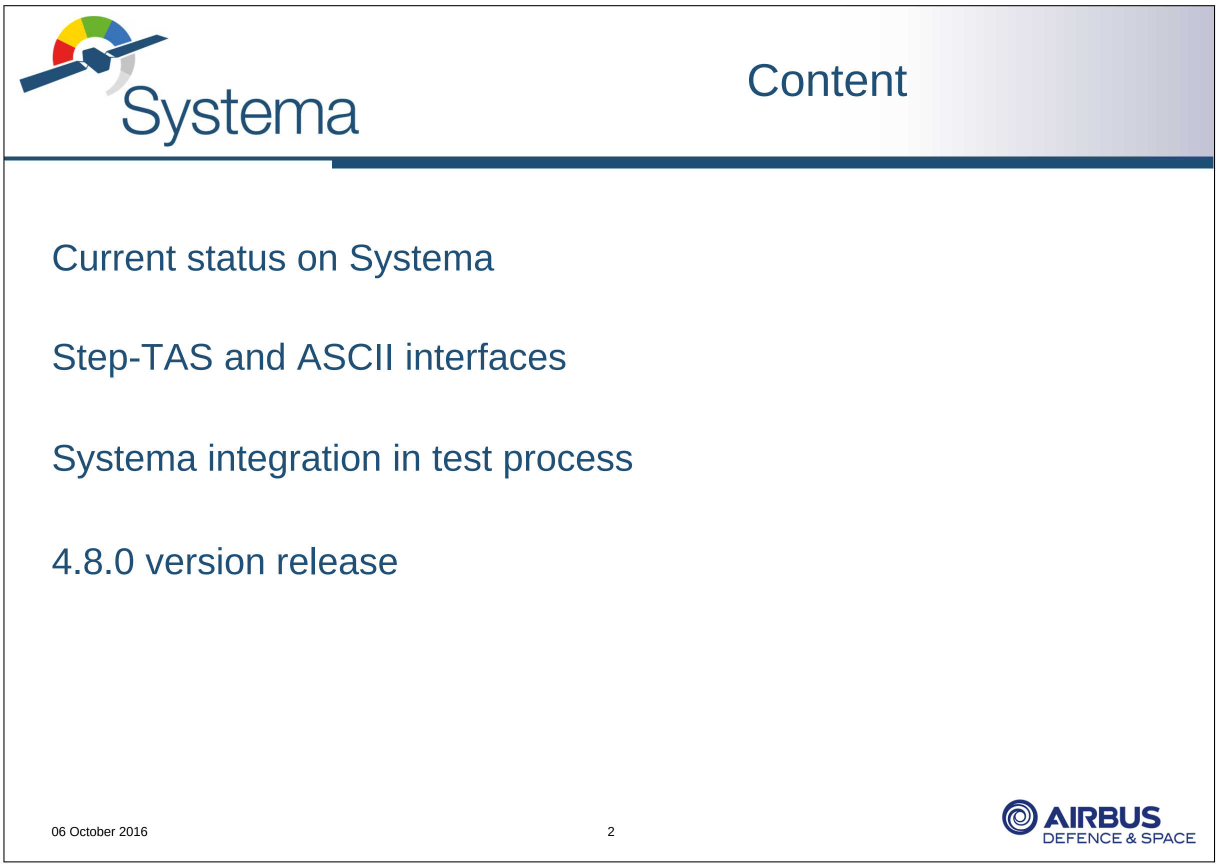
Systema
Content
Current status on Systema
Step-TAS and ASCII interfaces
Systema integration in test process
4.8.0 version release
06 October 2016
2
AIRBUS
DEFENCE & SPACE

Systema

Current status

Long Term Support current version: v4.5.3 (08/2013)

Short Term Support release: v4.8.0 (07/2016)

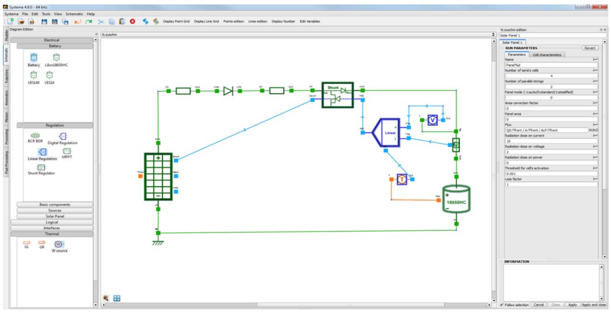

Demonstration video: https://www.youtube.com/watch?v=oT8ZIjX7nV0

06 October 2016 3

AIRBUS DEFENCE & SPACE

Systema

Systema interfaces

- Step-TAS and ASCII

AIRBUS DEFENCE & SPACE

Systema

Step-TAS interface

Having a more complete and robust Step-TAS interface is one of the main objectives of current developments. The version 4.8.0 stabilizes many features and 2017 developments will also increase the robustness of import / export functionalities.

A guideline is available for Step-TAS / Systema import export

4.8.0 corrections

- Thermo-optical properties are correctly exported (imported) even with transparency
- Truncated Disc / Cylinder / Cone with swapped angles corrected
- Boxes are split into rectangles
- Polygon cutters may be split into extruded triangle cutters

06 October 2016 5

AIRBUS DEFENCE & SPACE

Systema

Step-TAS interface

2017 developments

- **Better support of cutters**
  - Half-space cutter implementation
  - Inside / Outside cutting
  - Finite / Infinite cutters
  - Transformations

- **Corrections**
  - Automatization of polygon splitting on shapes and cutters on export
  - Other fixes (sides numbering on reversed shapes, …)

06 October 2016 6

AIRBUS DEFENCE & SPACE

Systema

ASCII format

Why needing an ASCII interface (other than Step-TAS)

- To be able to read / write easily a meshed model
- To ease copy / paste and model assembly using a simple text file
- To interface with other tools (mainly in-house tools)
- To be able to interface with Excel for geometrical definitions
- … *Because many people asked for it !*

Which ASCII format

Different purpose, different needs, different formats…

- CSV-like: Interface with Excel
- Yaml: Simple indented format easy to read and write (available standard libraries)
- …

06 October 2016 7

AIRBUS DEFENCE & SPACE

Systema

ASCII format

ASCII interfaces: technical choice – Python script

It exists a Python library able to read/write Systema geometrical models

- The library may be used as it is (no Python knowledge required)
- It may be modified independently of Systema (no need to wait for a new release of Systema for updating or correcting a Import/Export)
- It is based on a structure allowing the definition of new format definitions

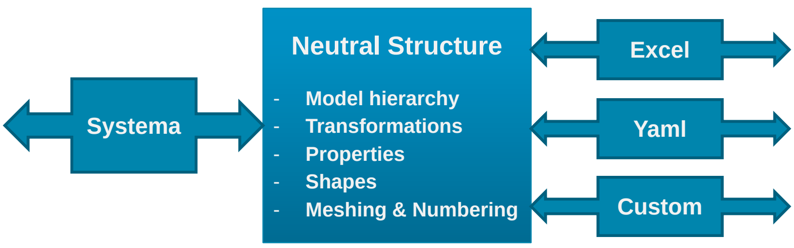

06 October 2016 8

AIRBUS DEFENCE & SPACE

Systema

ASCII format

Customize your export

Possibilities to (implemented in the existing library but not exhaustive):

- Define bijective export / import (model1 > export > import > model2 = model1)
- Extend properties (no inheritance)
- Remove transformations (all data in main frame)
- Explicit numbering (no numbering rules)
- Use only triangles and quadrangles (split of curved shapes)

06 October 2016 9

AIRBUS DEFENCE & SPACE

Systema

ASCII format

Example of Yaml

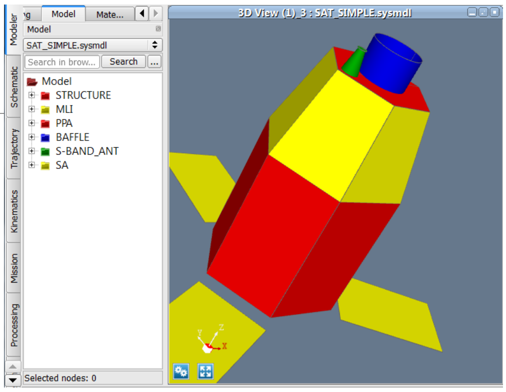


```yaml
Model :
  Name: SAT_Simple
  Meshing:
    Subdivision: {a: 1, b: 1, c: 1}
    Numbering: {start: 100, inc: 100}
    Method: Generic
    MeshInc: 1
    Order: '1st dir / 2nd dir'
  Objects:
    - STRUCTURE:
        Color: [255, 0, 0]
        CoatActivity: 'Only positive'
        Coatings:
          Emission: ['Normal', 'Normal']
          Material: ['SM_Ext_MatF', 'SM_Ext_MatF']
        BulkActivity: 'Both sides'
        Bulk:
          Thickness: 0.001
          Material: 'DEF_MAT'
        Shapes:
          - New Quadrangle:
              Geometry:
                Type: Quadrangle
                Points: {P1: (-0.5 0.8 0.06), P2: (0.5 0.8 0.06), P3: (0.5 0.8 1.86), P4: (-0.5 0.8 1.86)}
          - New Quadrangle (1):
              Geometry:
                Type: Quadrangle
                Points: {P1: (-0.5 0.8 1.86), P2: (-0.5 0.8 0.06), P3: (-1 0 0.06), P4: (-1 0 1.86)}
          - New Quadrangle (2):
              Geometry:
```


06 October 2016 10

AIRBUS DEFENCE & SPACE

Systema

Systema integration in test process

• DySCO synergy and convection

AIRBUS DEFENCE & SPACE

Systema

DySCO synergy

DySCO – *Dynaworks-Systema Collaboration*

Objectives

- Allow a smooth thermal process from simulation to tests
- Get rid of manual operations
- Shorten test campaigns

Systema - *simulation*

- Generates mathematical models from digital mock-ups
- Produces prediction data (ex: temperatures)

Dynaworks - *testing*

- Support test campaigns
- Process and store sensors data

06 October 2016 12

AIRBUS DEFENCE & SPACE

Systema

DynaWorks

DynaWorks

- Integrated solution for data management, visualization, processing and reporting

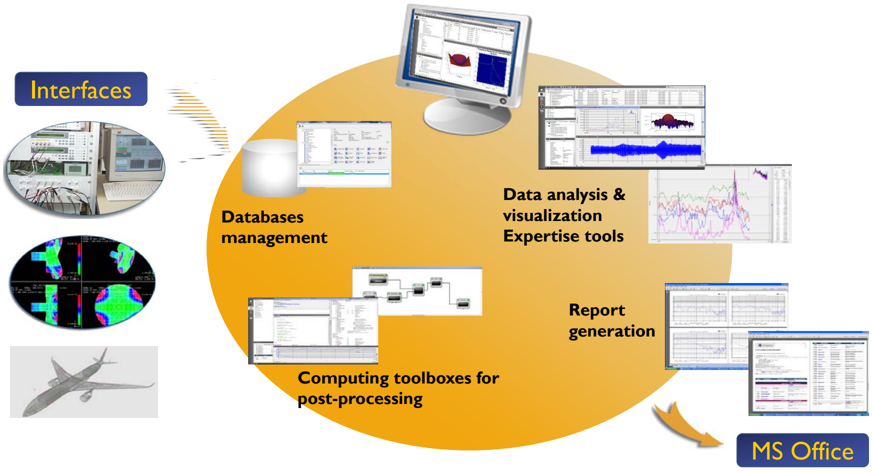

06 October 2016 DynaWorks® 7 13 intespace AIRBUS DEFENCE & SPACE

Systema

DynaWorks

DynaWorks

- Integrated solution for data management, visualization, processing and reporting

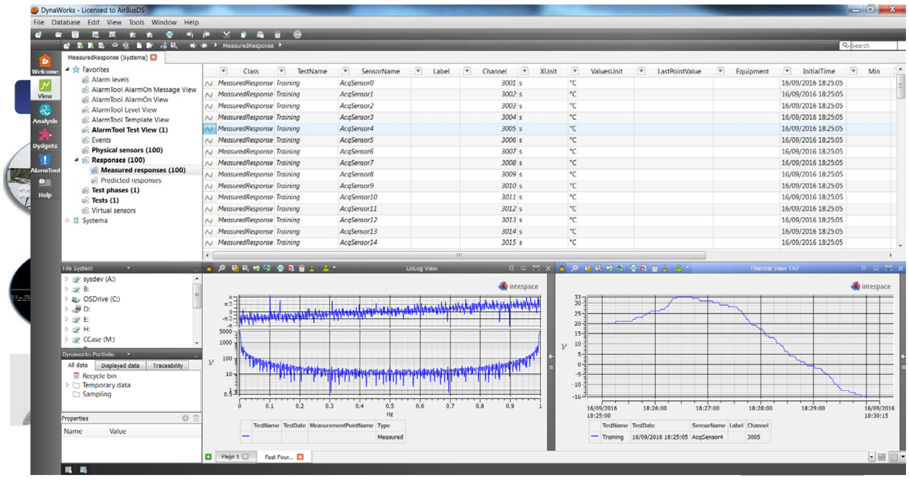

06 October 2016 DynaWorks® 7 14 intespace AIRBUS DEFENCE & SPACE

Systema

Current activities

Automatic import of simulation data in Dynaworks data-base

- Systema GMM (material, model and meshing) and Step-TAS formats
- Temperature data for every thermal nodes (Thermisol output)
- Thermal node / sensor pairing

Integrated 3D display in Dynaworks

- Large model management and display
- Real-time data over thermal models
- Comparison simulation / tests
- Replay of data sequences

06 October 2016 15 AIRBUS DEFENCE & SPACE

Systema

Upcoming activities

2017 activities

- Sensor management including invalidation
- Test results exploitation on thermal model
- Test prediction
- Advanced data import

Perspectives

- Integration of Post-prediction: launch of Thermica from Dynaworks

06 October 2016 16 AIRBUS DEFENCE & SPACE

Systema

Convection

A new Thermica module

- **Setting the convection**

More and more, it is required to take into account in the thermal analysis the contribution of natural and/or forced convection, i.e. the thermal exchange due to the contact of the model surfaces with a fluid (usually called "air nodes" in the TMM).

- **Convection in TMM vs CFD analysis**

The integration of the convection in TMMs requires a simplification of this physical phenomena, not as accurate as a CFD analysis, but allows combining it with radiative and conductive effects within a complete mathematical model.

06 October 2016 17

AIRBUS DEFENCE & SPACE

Systema

Convection

Convective exchanges

- **Surface / Air nodes conducto-convective couplings**

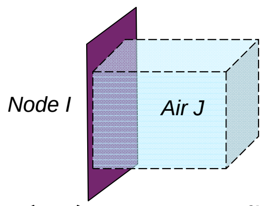

$$GL(I,J) = k.S.\Delta T^{\alpha}$$

The conducto-convective coupling between the surface and the air node depends on the surface *S* of the contact and two coefficients *k* and α that can be set constant by cavity (usually scaled by comparison with CFD analysis or test), or according to the Mac Adams formulae.

- **Air / Air nodes other couplings**

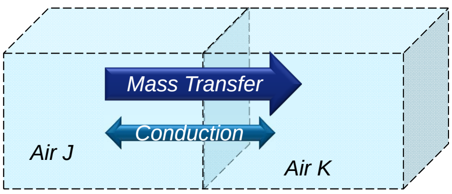

06 October 2016 18

AIRBUS DEFENCE & SPACE

Systema

Convection

Cavity identification

This is the major task of this module:

- Identifies and set cavities
- Computes area of nodes belonging to cavities

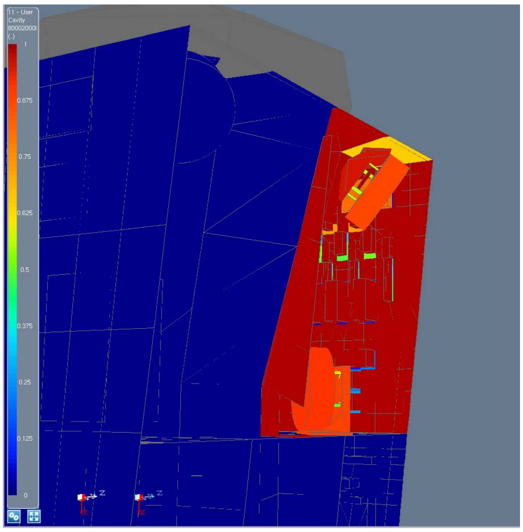

06 October 2016 19

AIRBUS DEFENCE & SPACE

Systema

Convection

Export of couplings

Surfaces – Air couplings automatically set by cavities using different formula choices written with parametric formulations so to ease the correlations. Couplings are generally written in the form of

$k.S.\Delta T^{\alpha}$

```
#   Convective Couplings
#   --------------------
#
#   File : SAT_A_int_conv.gf.nwk
#   Version : Thermica  V.4.8.1dev1 released on August 2016
#   Executed on : Wed Aug 29 19:49:04 1923
#   Input files :
#      - Sysset : SAT_A_int_conv.sysset


$LOCALS
   K_External = 3.0;
   Alpha_External = 0.25;
   K_Cavity1 = 3.0;
   Alpha_Cavity1 = 0.25;
   K_Cavity2 = 3.0;
   Alpha_Cavity2 = 0.25;
   ...
   ...

$NODES
   # Cavity nodes
   B 8000000 = 'External cavity', T = 0;
   B 80001000 = 'Cavity 1', T = 0;
   B 80002000 = 'Cavity 2', T = 0;
   B 80003000 = 'Cavity 3', T = 0;
   B 80004000 = 'Cavity 4', T = 0;

$CONDUCTORS
   # Conducto-Convective Couplings in Cavity 8000000
      GL( 8000000 , 210000 )  =  K_External * (1.302902E-02 * 5.370652E-02) * (ABS(T:8000000 - T:210000))**Alpha_External;
      GL( 8000000 , 210001 )  =  K_External * (1.082140E-02 * 6.018357E-02) * (ABS(T:8000000 - T:210001))**Alpha_External;
      GL( 8000000 , 210002 )  =  K_External * (6.120670E-03 * 6.666063E-02) * (ABS(T:8000000 - T:210002))**Alpha_External;
      GL( 8000000 , 210003 )  =  K_External * (1.012743E-03 * 7.313768E-02) * (ABS(T:8000000 - T:210003))**Alpha_External;
      GL( 8000000 , 210500 )  =  K_External * (2.071565E-02 * 5.370652E-02) * (ABS(T:8000000 - T:210500))**Alpha_External;
      GL( 8000000 , 210501 )  =  K_External * (1.197503E-02 * 6.018357E-02) * (ABS(T:8000000 - T:210501))**Alpha_External;
      GL( 8000000 , 210502 )  =  K_External * (4.917708E-03 * 6.666063E-02) * (ABS(T:8000000 - T:210502))**Alpha_External;
      ...
      ...
   # Conducto-Convective Couplings in Cavity 80004000
      GL( 80004000 , 13450 )  =  K_Cavity1 * (8.635908E-01 * 5.194920E-01) * (ABS(T:80004000 - T:13450))**Alpha_Cavity1;
      GL( 80004000 , 18302 )  =  K_Cavity1 * (9.939398E-01 * 2.360051E-02) * (ABS(T:80004000 - T:18302))**Alpha_Cavity1;
      GL( 80004000 , 18303 )  =  K_Cavity1 * (6.312625E-01 * 5.120003E-03) * (ABS(T:80004000 - T:18303))**Alpha_Cavity1;
      GL( 80004000 , 18304 )  =  K_Cavity1 * (5.681363E-01 * 5.119996E-03) * (ABS(T:80004000 - T:18304))**Alpha_Cavity1;
      GL( 80004000 , 18305 )  =  K_Cavity1 * (5.571142E-01 * 5.120004E-03) * (ABS(T:80004000 - T:18305))**Alpha_Cavity1;
      GL( 80004000 , 18306 )  =  K_Cavity1 * (6.202405E-01 * 5.119997E-03) * (ABS(T:80004000 - T:18306))**Alpha_Cavity1;
      ...
      ...
   # Conducto-Convective Couplings in Cavity 80003000
      GL( 80003000 , 16500 )  =  K_Cavity2 * (1.000000E+00 * 3.954220E-01) * (ABS(T:80003000 - T:16500))**Alpha_Cavity2;
      GL( 80003000 , 18402 )  =  K_Cavity2 * (1.000000E+00 * 2.360050E-02) * (ABS(T:80003000 - T:18402))**Alpha_Cavity2;
      GL( 80003000 , 18403 )  =  K_Cavity2 * (7.034068E-01 * 5.120000E-03) * (ABS(T:80003000 - T:18403))**Alpha_Cavity2;
      GL( 80003000 , 18404 )  =  K_Cavity2 * (7.034068E-01 * 5.120002E-03) * (ABS(T:80003000 - T:18404))**Alpha_Cavity2;
      GL( 80003000 , 18405 )  =  K_Cavity2 * (7.034068E-01 * 5.120001E-03) * (ABS(T:80003000 - T:18405))**Alpha_Cavity2;
      GL( 80003000 , 18406 )  =  K_Cavity2 * (7.034068E-01 * 5.120000E-03) * (ABS(T:80003000 - T:18406))**Alpha_Cavity2;
      GL( 80003000 , 18407 )  =  K_Cavity2 * (9.195491E-01 * 1.631379E-01) * (ABS(T:80003000 - T:18407))**Alpha_Cavity2;
      GL( 80003000 , 18411 )  =  K_Cavity2 * (9.219219E-01 * 3.420595E-01) * (ABS(T:80003000 - T:18411))**Alpha_Cavity2;
      GL( 80003000 , 40001 )  =  K_Cavity2 * (1.000000E+00 * 2.343217E-02) * (ABS(T:80003000 - T:40001))**Alpha_Cavity2;
```

06 October 2016 20

AIRBUS DEFENCE & SPACE

Systema

Convection

Further improvements

- **Cavity stratification**

The stratification of cavities will allow defining several layer of air nodes within a cavity and getting their properties. This will help the user setting convective couplings.

- **Use of Mac Adams formulas**

As an option, conducto-convective couplings will be written using Mac Adams formulas which take into account the orientation of the shapes (vertical, horizontal upper, horizontal lower surfaces…) and the flow type (laminar or turbulent) according to the value of the Prandtl and Grashof numbers product.

06 October 2016 21 AIRBUS DEFENCE & SPACE

Systema

IR Camera

Another new Thermica module

- **What for ?**

The IR camera simulator is a tool designed to reproduce the behavior of a camera in a test facility. It produces a map of pixels with incoming IR fluxes.
It is then also possible to isolate the reflection of the environment onto the model.

- **Camera modelling**

The camera is modeled taking into account the localization of the instrument and its aperture angle.

06 October 2016 22 AIRBUS DEFENCE & SPACE

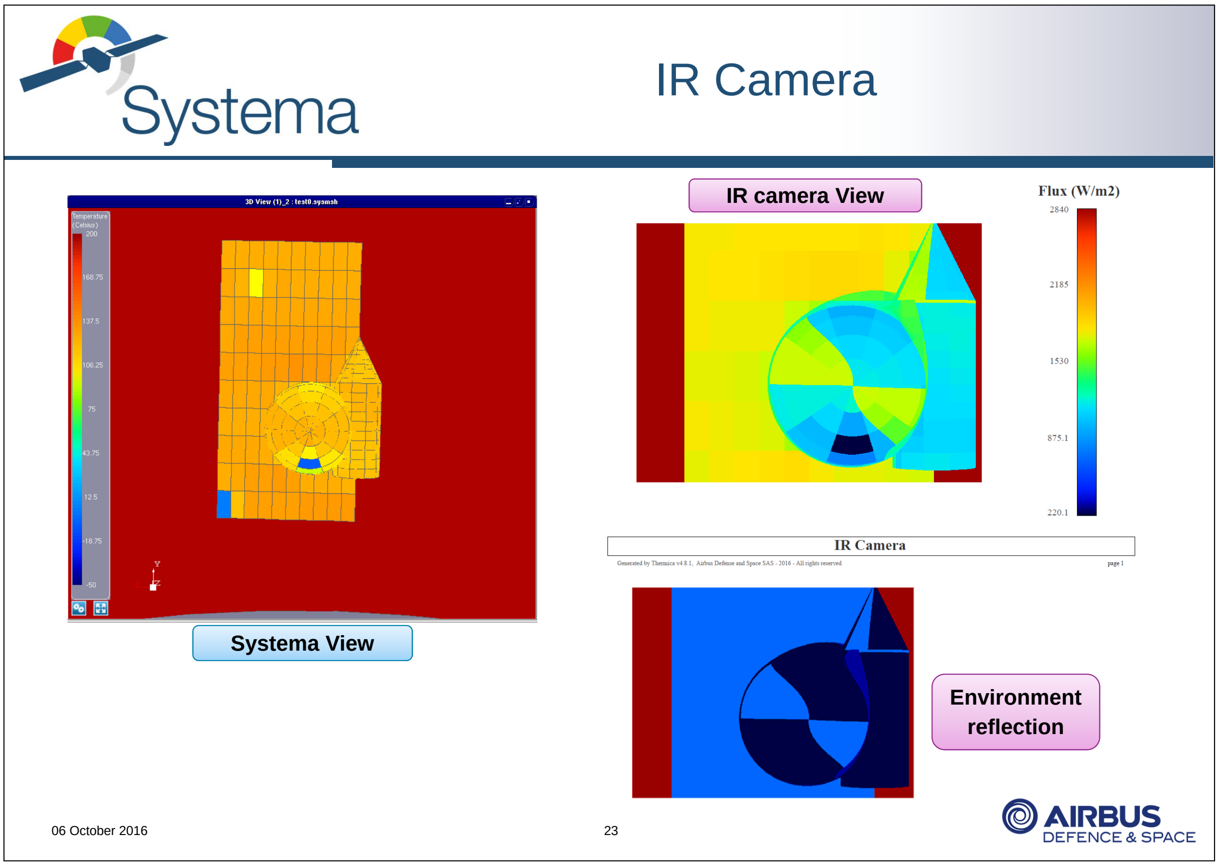
Systema
IR Camera
IR camera View
Flux (W/m2)
2840
2185
1530
875.1
220.1
IR Camera
Systema View
Environment reflection
06 October 2016
23
AIRBUS
DEFENCE & SPACE

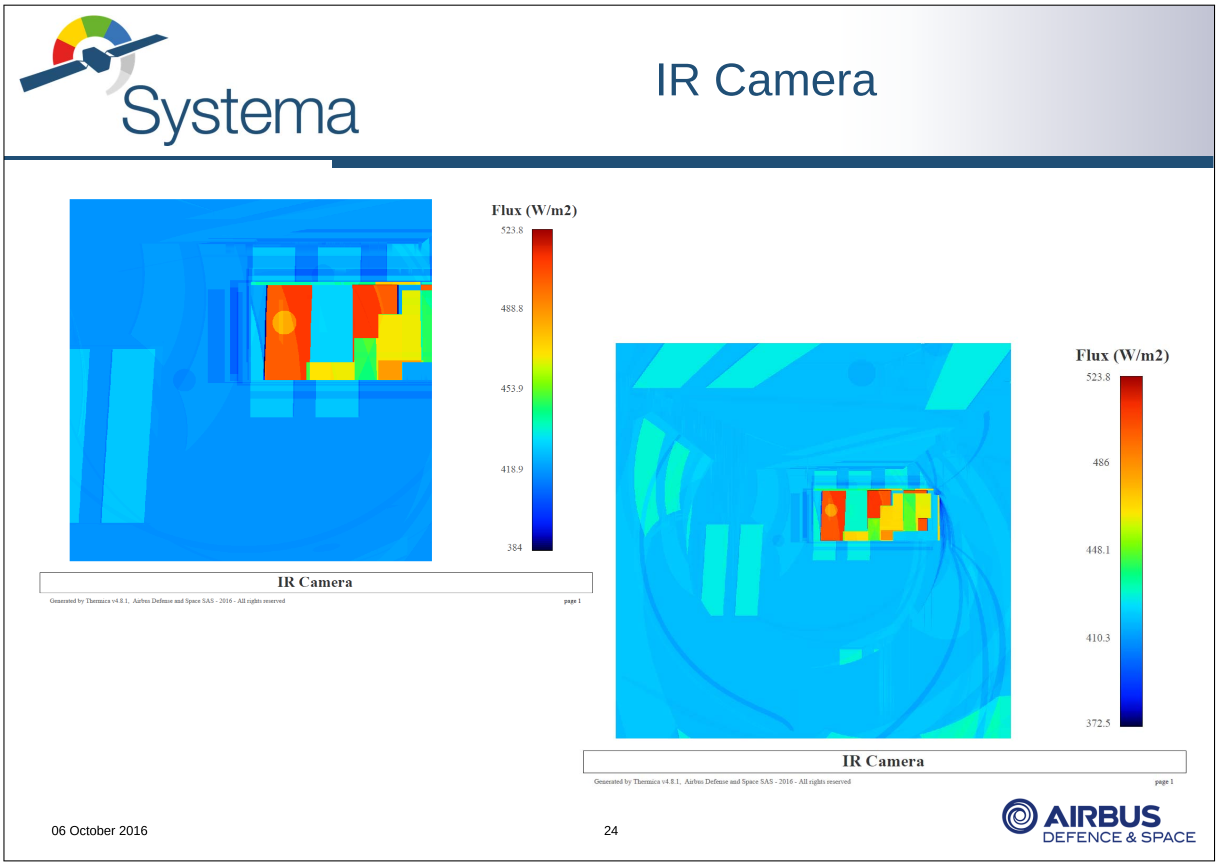
Systema
IR Camera
Flux (W/m2)
523.8
488.8
453.9
418.9
384
IR Camera
Flux (W/m2)
523.8
486
448.1
410.3
372.5
IR Camera
06 October 2016
24
AIRBUS
DEFENCE & SPACE

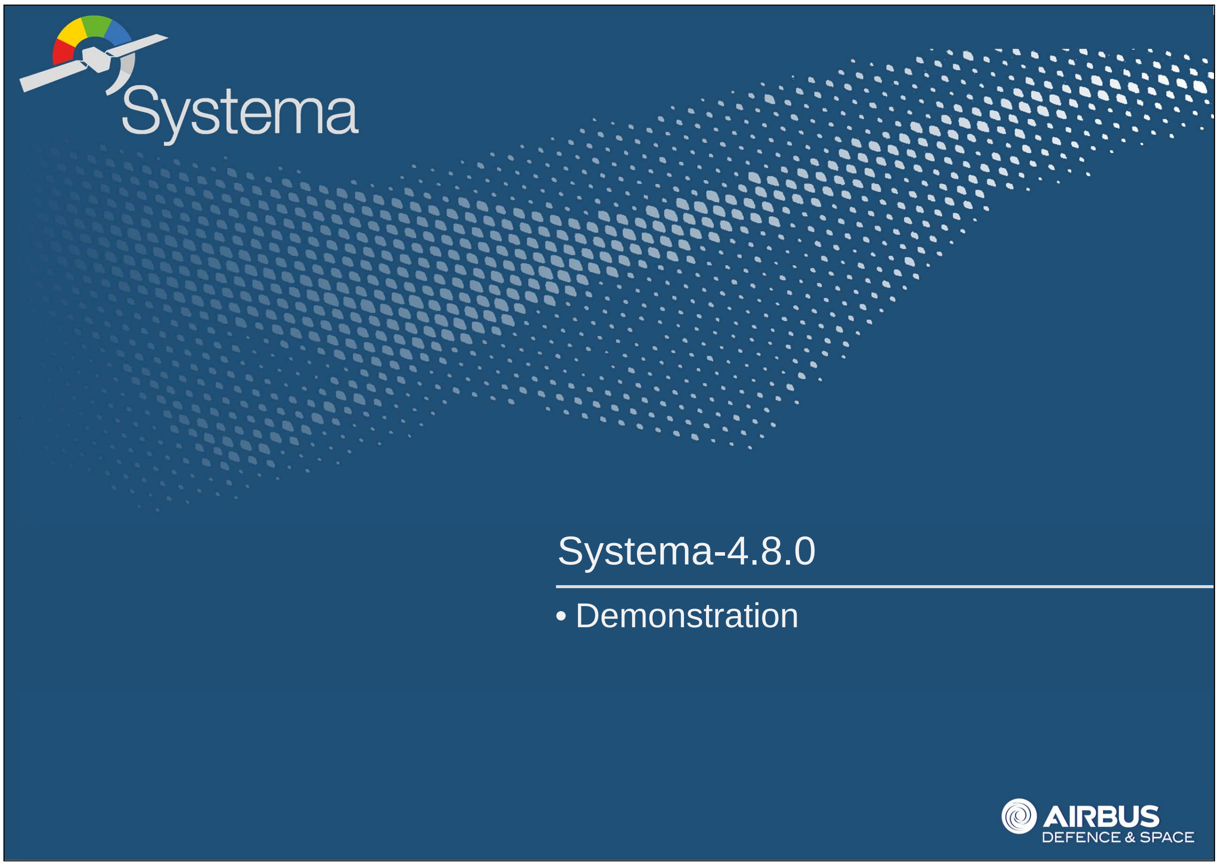
Systema
Systema-4.8.0
• Demonstration
AIRBUS
DEFENCE & SPACE

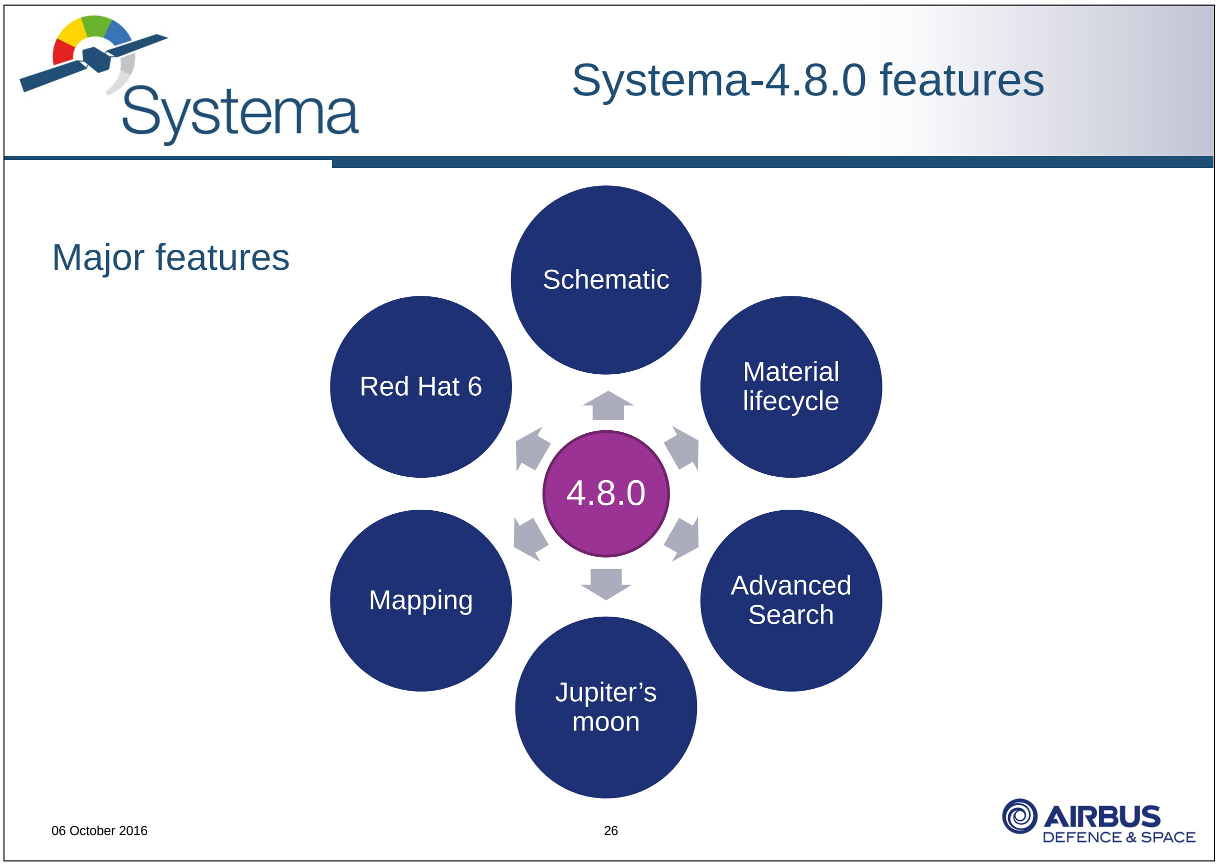
Systema
Systema-4.8.0 features
Major features
Schematic
Red Hat 6
Material lifecycle
4.8.0
Mapping
Advanced Search
Jupiter's moon
06 October 2016
26
AIRBUS
DEFENCE & SPACE

Systema

Quasi Monte-Carlo

Improvement of Ray-Tracing accuracy

- **Classical Monte-Carlo**
  - Uses independent random numbers between 0 and 1 for each parameter

  (*4 parameters are required for the ray emission; 2 for emission point / 2 for direction)*

- **Quasi Monte-Carlo approach**
  - Minimize the discrepancy of parameters

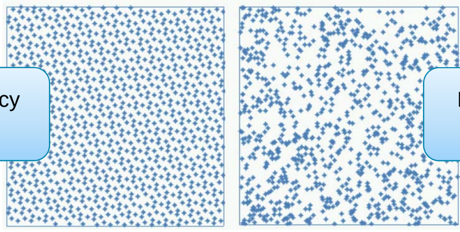

Low discrepancy method

Pseudo random method

06 October 2016 27

AIRBUS DEFENCE & SPACE

Systema

Quasi Monte-Carlo

Improvement of Ray-Tracing accuracy

- **Evaluation of the View Factor convergence between two squares**

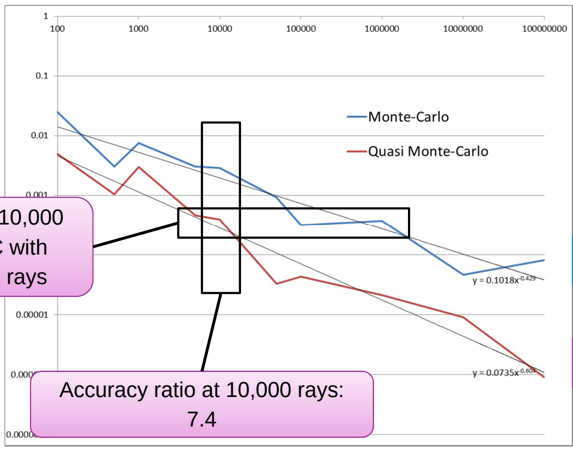

Accuracy of QMC with 10,000 rays equivalent to MC with 100,000 or 1,000,000 rays

Convergence rate 0.429

Convergence rate 0.604

Accuracy ratio at 10,000 rays: 7.4

06 October 2016 28

AIRBUS DEFENCE & SPACE

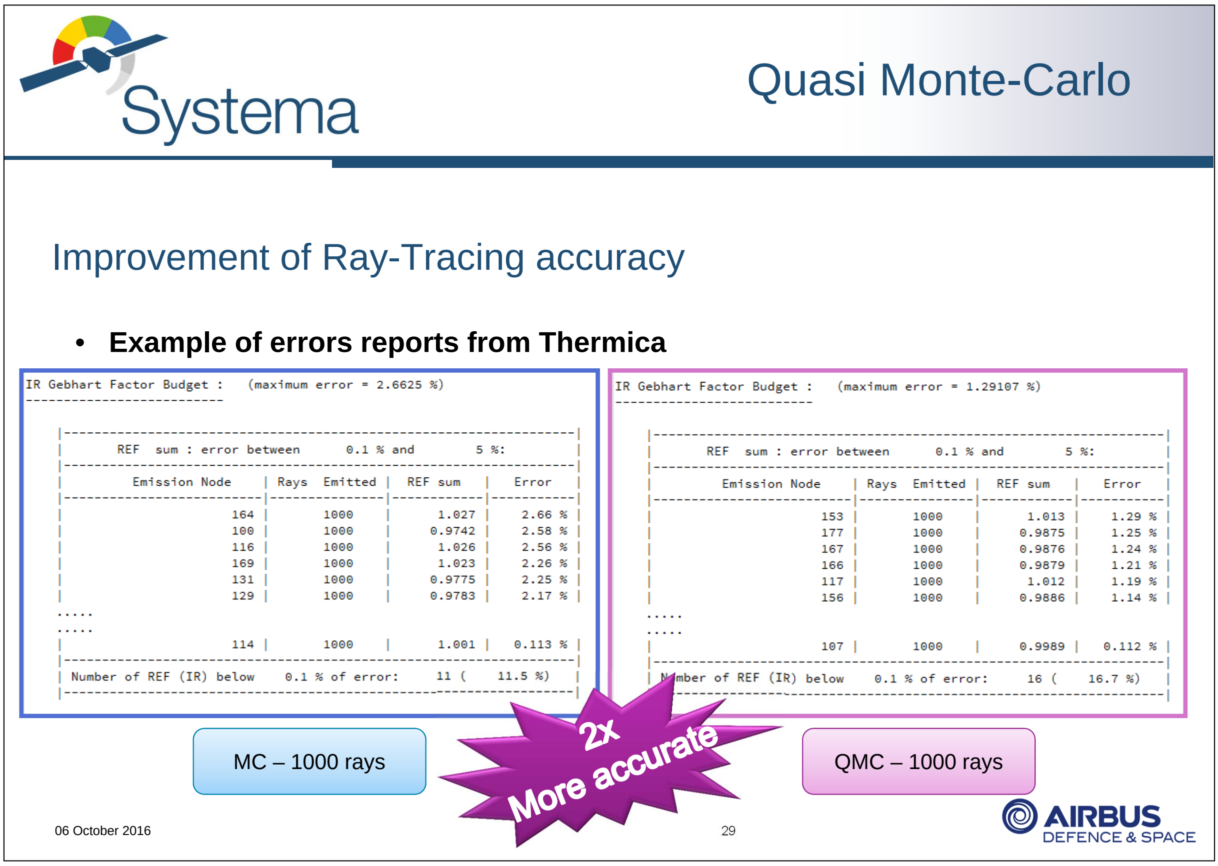
Systema
Quasi Monte-Carlo
Improvement of Ray-Tracing accuracy
• Example of errors reports from Thermica
IR Gebhart Factor Budget : (maximum error = 2.6625 %)
REF sum : error between 0.1 % and 5 %:
Emission Node | Rays Emitted | REF sum | Error
164 | 1000 | 1.027 | 2.66 %
100 | 1000 | 0.9742 | 2.58 %
116 | 1000 | 1.026 | 2.56 %
169 | 1000 | 1.023 | 2.26 %
131 | 1000 | 0.9775 | 2.25 %
129 | 1000 | 0.9783 | 2.17 %
.....
.....
114 | 1000 | 1.001 | 0.113 %
Number of REF (IR) below 0.1 % of error: 11 (11.5 %)
IR Gebhart Factor Budget : (maximum error = 1.29107 %)
REF sum : error between 0.1 % and 5 %:
Emission Node | Rays Emitted | REF sum | Error
153 | 1000 | 1.013 | 1.29 %
177 | 1000 | 0.9875 | 1.25 %
167 | 1000 | 0.9876 | 1.24 %
166 | 1000 | 0.9879 | 1.21 %
117 | 1000 | 1.012 | 1.19 %
156 | 1000 | 0.9886 | 1.14 %
.....
.....
107 | 1000 | 0.9989 | 0.112 %
mber of REF (IR) below 0.1 % of error: 16 (16.7 %)
MC – 1000 rays
2x
More accurate
QMC – 1000 rays
06 October 2016
29
AIRBUS
DEFENCE & SPACE

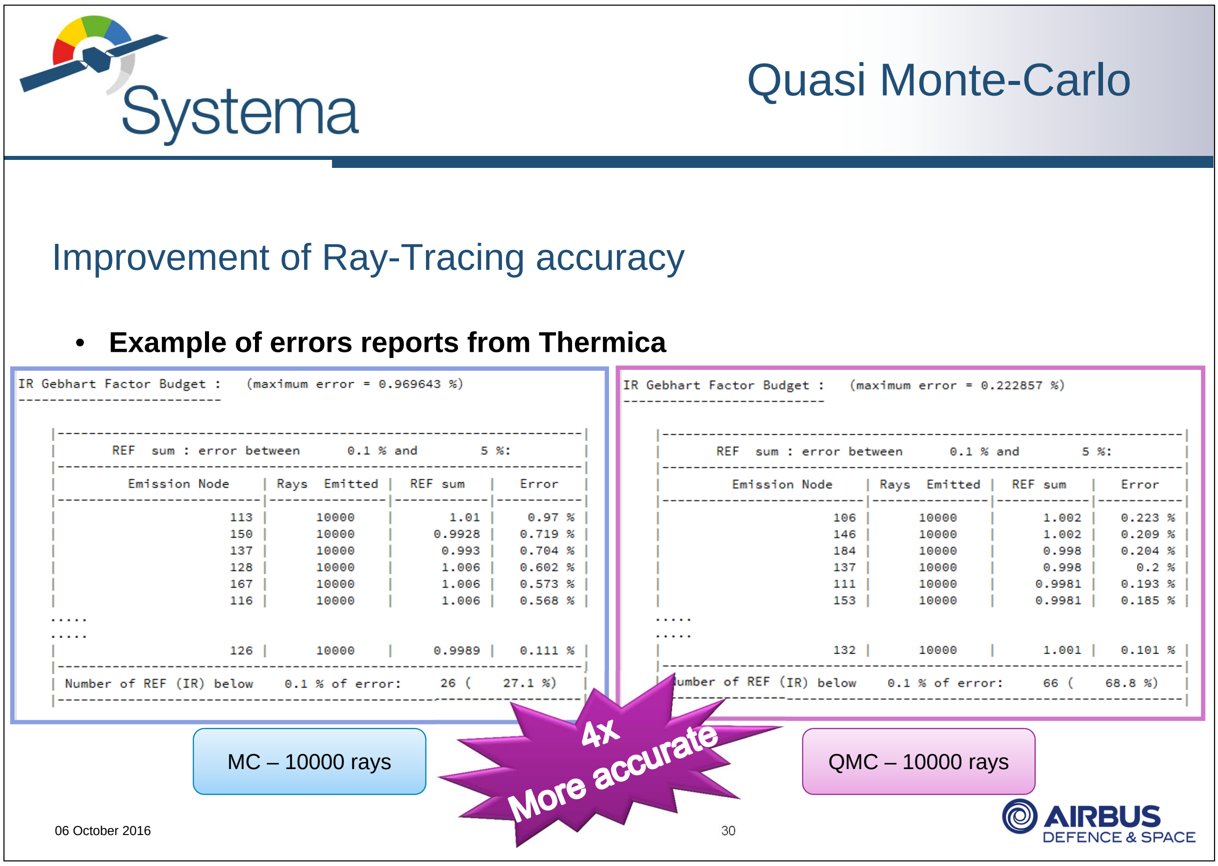
Systema
Quasi Monte-Carlo
Improvement of Ray-Tracing accuracy
• Example of errors reports from Thermica
IR Gebhart Factor Budget : (maximum error = 0.969643 %)
REF sum : error between 0.1 % and 5 %:
Emission Node | Rays Emitted | REF sum | Error
113 | 10000 | 1.01 | 0.97 %
150 | 10000 | 0.9928 | 0.719 %
137 | 10000 | 0.993 | 0.704 %
128 | 10000 | 1.006 | 0.602 %
167 | 10000 | 1.006 | 0.573 %
116 | 10000 | 1.006 | 0.568 %
.....
.....
126 | 10000 | 0.9989 | 0.111 %
Number of REF (IR) below 0.1 % of error: 26 (27.1 %)
IR Gebhart Factor Budget : (maximum error = 0.222857 %)
REF sum : error between 0.1 % and 5 %:
Emission Node | Rays Emitted | REF sum | Error
106 | 10000 | 1.002 | 0.223 %
146 | 10000 | 1.002 | 0.209 %
184 | 10000 | 0.998 | 0.204 %
137 | 10000 | 0.998 | 0.2 %
111 | 10000 | 0.9981 | 0.193 %
153 | 10000 | 0.9981 | 0.185 %
.....
.....
132 | 10000 | 1.001 | 0.101 %
umber of REF (IR) below 0.1 % of error: 66 (68.8 %)
MC – 10000 rays
4x
More accurate
QMC – 10000 rays
06 October 2016
30
AIRBUS
DEFENCE & SPACE

Systema

Quasi Monte-Carlo

Conclusion

- **Get better accuracy**
  For the same computational effort, the ray-tracing process is much more accurate
  Usually, The computation is about 4 times more accurate with 10,000 rays

- **Save computation time**
  For reaching a certain level of accuracy, the QMC approach will require about 10 times less rays than the classical Monte-Carlo approach, leading to a great computation time reduction
  Especially in the 4.8.0 in which it is possible to automatize the re-run of the Monte-Carlo so to reach a specified level of accuracy

06 October 2016 31 AIRBUS DEFENCE & SPACE

Systema

Conclusion

The 4.8.0 version

- **New features**
  The current version brings many improvements and new features such as
  - The Quasi Monte-Carlo ray-tracing
  - The materials lifecycle management
  - The advanced search
  - Schematic module for thermo-electrical analysis
  - Mapping module
  - Step-TAS export corrections
  - …

06 October 2016 32 AIRBUS DEFENCE & SPACE

Systema

Conclusion

2017 developments

- **More to come…**

  Next year developments will add and stabilize even more new features
  - The convective module
  - The IR camera simulator
  - Extended cutters definitions
  - Step-TAS improvements
  - The DySCO plugins for Dynaworks
  - …

See you next year to know more about other new developments

06 October 2016 33

AIRBUS DEFENCE & SPACE

Systema

SYSTEMA

THERMICA

THERMISOL

Visit our web site :

www.systema.airbusdefenceandspace.com

Contact:
timothee.soriano@airbus.com
antoine.caugant@airbus.com
engineering.software@airbus.com

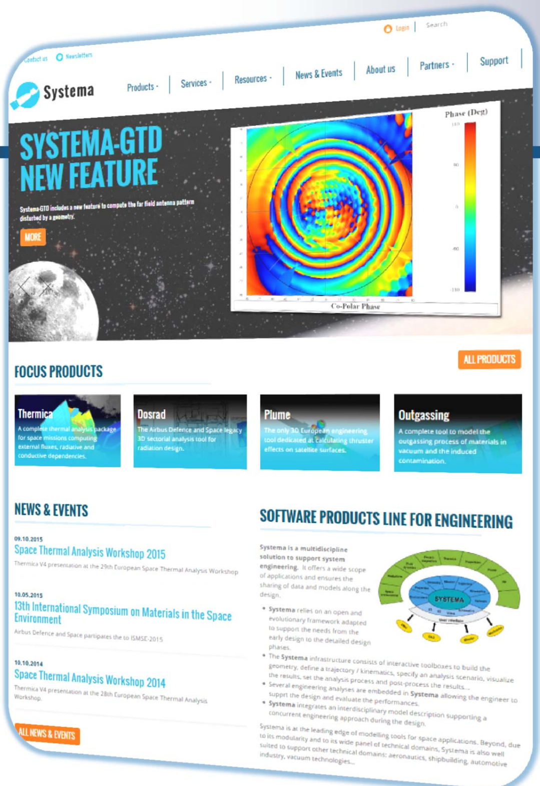

06 October 2016 34

AIRBUS DEFENCE & SPACE

Appendix P

Gas conduction and convection modelling techniques for the ExoMars Rover

Joshua Katzenberg
(Airbus Defence and Space, United Kingdom)

Abstract

The operation of the ExoMars rover in the gaseous atmosphere at Mars's surface has led to several challenges in the thermal analysis. Many parameters not normally encountered in spacecraft thermal analysis - such as wind speed - have been considered. To simulate the heat transfer to the environment, the external nodes couple to a single node via a convection modelling subroutine - switching between natural and forced convection depending on the wind-speed. Due to the complex geometry inside the rover, the approach for the internal model has been to use multiple gas nodes coupled to the geometry either via conduction or convection. ESATAN-TMS tools such as; non-geometric gas nodes for visualisation, contact zones for calculating gas node coupling areas and switching flags for heat transfer method have also been used to aid analysis tasks. Modelling techniques and the choice of thermal heat transfer approach based on the geometry are discussed in this presentation.

Gas conduction and convection modelling techniques for the ExoMars Rover

30th European space thermal analysis workshop

Joshua Katzenberg
5-6th October 2016

AIRBUS DEFENCE & SPACE

Gas conduction and convection modelling for the ExoMars rover

The ExoMars Rover

The ExoMars Programme comprises of two missions and is conducted with the broad cooperation of Roscosmos. TAS-I is the prime contractor for the Rover Module and Airbus Defence & Space is developing the Rover Vehicle.

- The 2016 mission consists of a Trace Gas Orbiter and an EDL Demonstrator Module
- The 2020 mission consists of a Carrier Module and a Descent Module with a Rover and a stationary Landing Platform
- The programme is a large International Cooperation with Roscosmos and some contributions from NASA

04 October 2016 2 AIRBUS DEFENCE & SPACE

Overview

- Convection theory overview
- Gas convection modelling for the ExoMars external model
- Gas modelling for the ExoMars internal model
- Automatic generation of gas conductive coupling areas
- Cruise cases

Gas conduction and convection modelling for the ExoMars rover

Convection theory overview

- The convective coupling is based on constants, correction factors and empirical formulae.
- This in turn is based on the geometry.

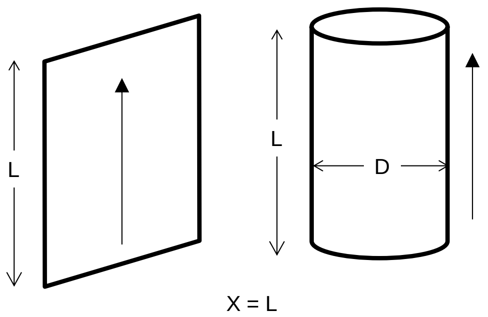

- L (or X) is the characteristic length
  - This can be the length of the flat plate (node) or the diameter of a cylinder
- Only flat plates and cylinders have been considered in the ExoMars model

- The constants are based on the orientation of the geometry:
  - Vertical plates/cylinders with large diameters
  - Horizontal plate facing upwards
  - Horizontal plate facing downwards

Convection theory overview

- Convection increases the heat transfer from a surface to its environment
- Two types of convection modelled – natural and forced (laminar)
- The basic formulation of the convective coupling subroutine is shown below

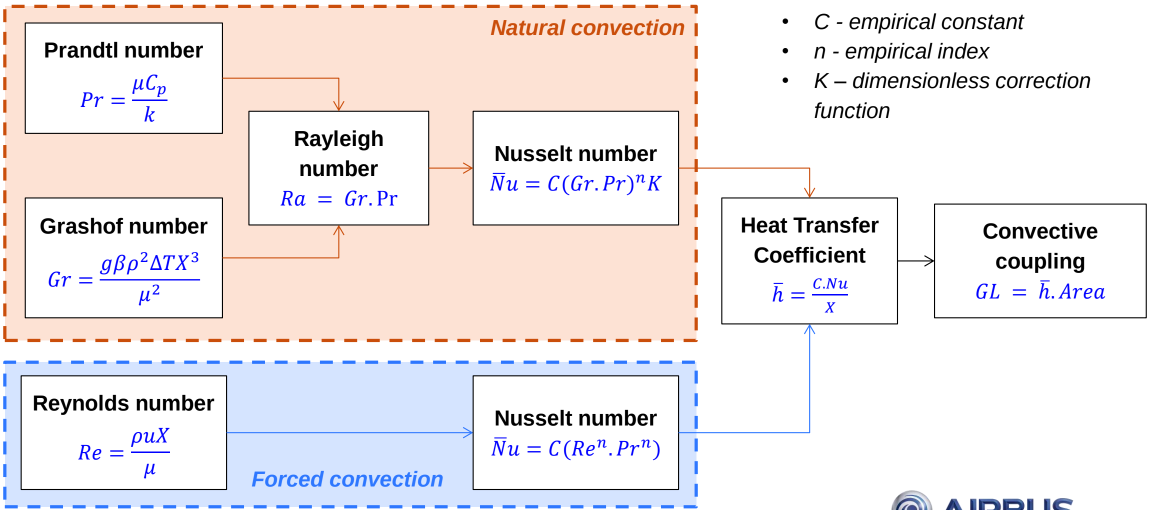

04 October 2016 5 AIRBUS DEFENCE & SPACE

Gas conduction and convection modelling for the ExoMars rover

Gas convection modelling for the ExoMars external model

- The external model uses only convective couplings.
- Wind in the Martian environment determines if natural or forced convection is used.
  - Forced convection adds a Reynolds number term to the Nusselt number
- Each external node is coupled to a single environment boundary node.
- Each coupling assumes the full wind speed in the worst case direction – pessimistic approach for cold cases

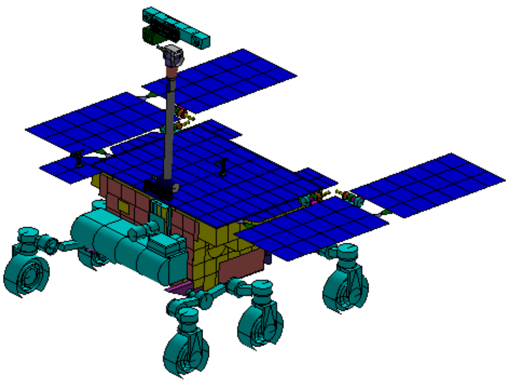

Two convective cases:

- Wind speed = 0m/s
- Hot case – natural convection

- Wind speed = 30m/s
- Cold case – forced convection

04 October 2016 6 AIRBUS DEFENCE & SPACE

Gas convection modelling for the ExoMars external model

- The area of each node is generated via the GMM and used in the coupling calculation by the subroutine.

```
D1502 = 'ROVER_VEHICLE', T = 0.0,
A = 0.002348, ALP = 0.368000, EPS = 0.150000,
        FX = -0.444568, FY = 0.372371, FZ = 0.133114;
```

```
GL(10000,92000) = CONVEZ(10000,92000, 1, 7.000E-2 , 3 , 12 );
```

CONVEZ(convN, convM, Intext, Xcha,inatu,iforce)

```
# Input description
# convN - INTEGER - Node number to be coupled to gas
# convM - INTEGER - Gas node number
# Intext - INTEGER - Internal or external gas flag, 0 = Internal, 1 = External
# Xcha - REAL - Characteristic length
# inatu - INTEGER - Integer corresponding to the natural convection equation for a specific geometry, can take values of 1 to 4
# iforce - INTEGER - Integer corresponding to the forced convection equation for a specific geometry, can take values of 11 to 13
```


Gas convection area method for the ExoMars external model

- Convection area code example:

```
GL(DMA:2500110,92000) = CONVEZ_AREA(INTNOD(DMA,2500110),
INTNOD(CURRENT,92000),3.941E-4,  1 , 1.120E-2 , 1 , 12) * CRUISE_CASE;
```

CONVEZ_AREA(convN, convM, Narea, Intext, Xcha,inatu,iforce)

```
# Input description
# convN - INTEGER - Node number to be coupled to gas (internal node number, obtained using INTNOD function)
# convM - INTEGER - Gas node number(internal node number, obtained using INTNOD function)
# Narea – REAL – Node area
# Intext - INTEGER - Internal or external gas flag, 0 = Internal, 1 = External
# Xcha - REAL - Characteristic length
# inatu - INTEGER - Integer corresponding to the natural convection equation for a specific geometry, can take values of 1 to 4
# iforce - INTEGER - Integer corresponding to the forced convection equation for a specific geometry, can take values of 11 to 13
```

- Cannot parse submodel name as string into the subroutine if the GL is calculated at a lower level in the model tree.
- INTNOD returns the internal node number from submodel name.
- Internal model calculated via same method when area considered.

Gas conduction and convection modelling for the ExoMars rover

Gas modelling for the ExoMars internal model

- The internal model can use conduction or convection
- It has been broken down into multiple gas nodes
  - This allows gradients to be observed

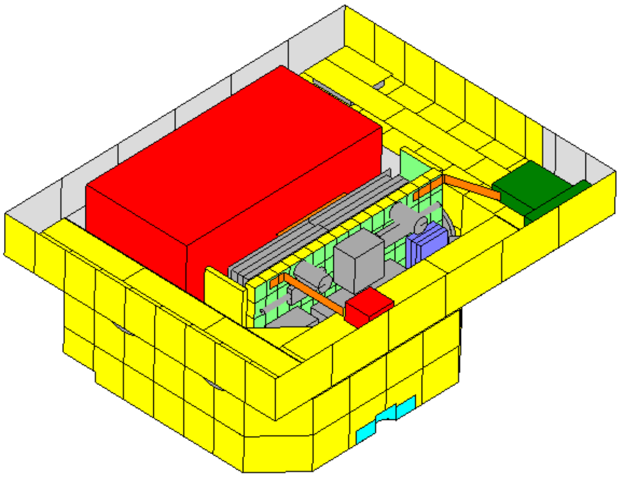

04 October 2016 9

Gas conduction and convection modelling for the ExoMars rover

Non-geometric nodes for the ExoMars internal model

- To act as a visual aid, non-geometric nodes have been added to the GMM
- Helps determine couplings for the TMM

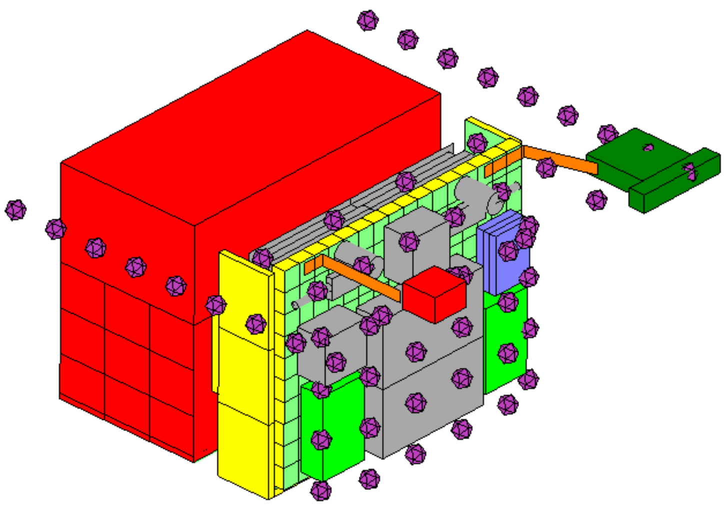

04 October 2016 10

Gas convection method for the ExoMars internal model

- Only natural convection is considered in the internal model
- Convection will only occur in gaps greater than ~30mm
- Manual checks on gap sizes - Conduction used if gap less than ~30mm

- Certain nodes will be double-sided or cover multiple gas nodes
- The convection subroutine is updated here to scale the coupling based on area (CONVEZ_AREA method)

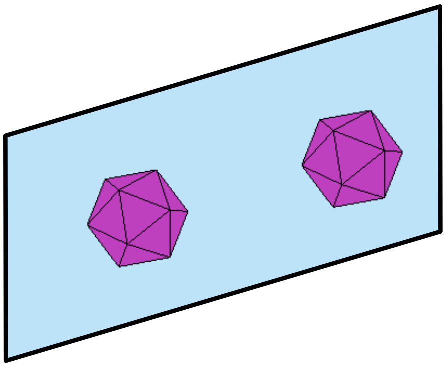

Single node to multiple gas nodes

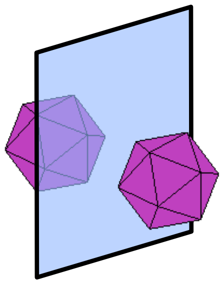

Double-sided node to multiple gas nodes

Gas conduction and convection modelling for the ExoMars rover

Gas conduction for the ExoMars internal model - Large gaps

- For gas conduction couplings with large gaps i.e. to gas nodes:

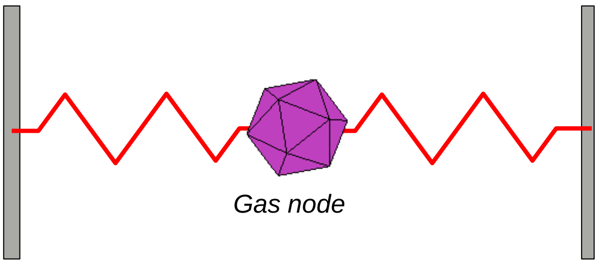

- Acts as a traditional conductive through coupling (kA/x)
- Conductivity of the carbon dioxide is interpolated between the gas and geometry node temperatures
- Area for the coupling is determined as the area facing the gas node

```
GL(21150,41004) = CNDFNC(1, CO2_K1, 1) * 0.002475 / 3.829E-2 *CRUISE_CASE;
```

```
GL(58002,21678) = INTRP1(T21678, CO2_K1, 1) * A58002 / 8.187E-2 *CRUISE_CASE ;
```

- CNDFNC: Average temperature of gas and structure (Tn1+Tn2)/2 – small gaps
- INTRP1: Just gas node temperature – larger volume gas nodes where effect of structure node is, relatively, reduced.

Gas conduction and convection modelling for the ExoMars rover

Gas conduction for the ExoMars internal model - Large gaps

- The area and path length for gas conduction couplings can become difficult to determine as the internal geometry becomes more complex. It is particularly prominent for:
  - Edges of panels and units
  - Where a gas node only partially encompasses a geometry node

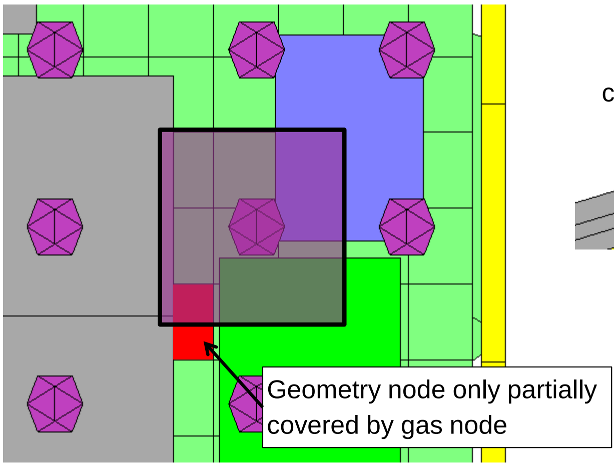

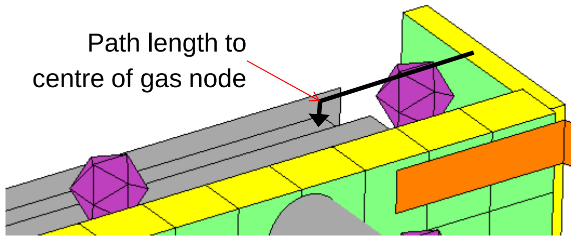

- Scaling factors and meticulous manual path length calculations are required via referencing 3D CAD models or CAD drawings.

04 October 2016 13

AIRBUS DEFENCE & SPACE

Gas conduction and convection modelling for the ExoMars rover

Gas conduction for the ExoMars internal model - Small gaps

- There are several sites in the internal model where the gap size is small and no gas node is present
- As the conductive coupling through the gas must still be considered, a different approach is used for surface-surface couplings for small gap sizes
- The coupling needs to reflect each node's area facing its opposite node and the gas between the nodes:

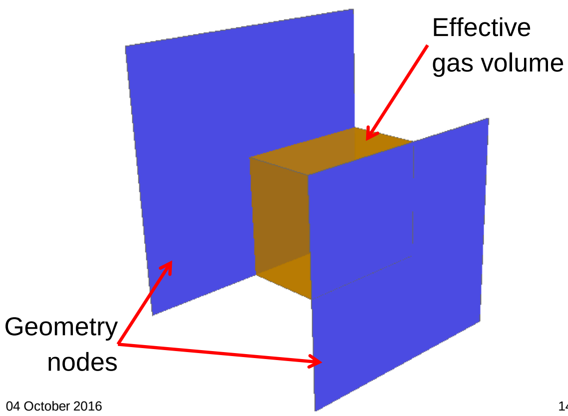

- As the model becomes more detailed, this task becomes more complex and time consuming
- A way to automate this process was used

04 October 2016 14

AIRBUS DEFENCE & SPACE

Gas conduction for the ExoMars internal model - ESATAN auto-coupling generator

- A contact zone between two groups of faces/surfaces can be defined in ESATAN-TMS:
  - For coupling units → panels over small gaps.
- This works by firing rays from a source to a sink
- For each source node, the area that directly faces a sink node will be calculated and can be output as a text file.

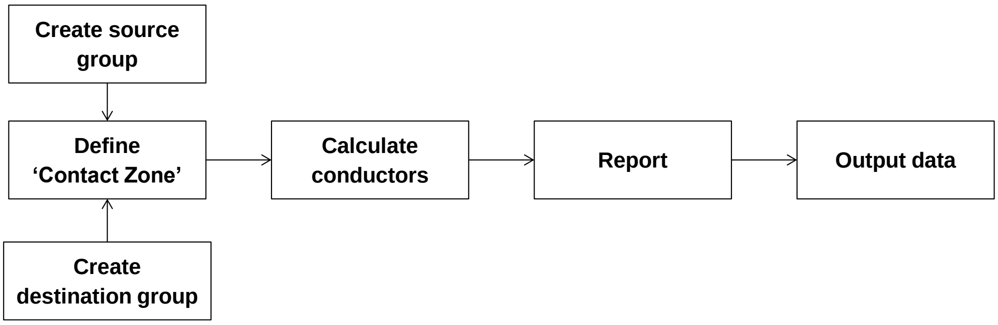

AIRBUS DEFENCE & SPACE

Gas conduction for the ExoMars internal model - ESATAN auto-coupling generator

- Visualisation of setup

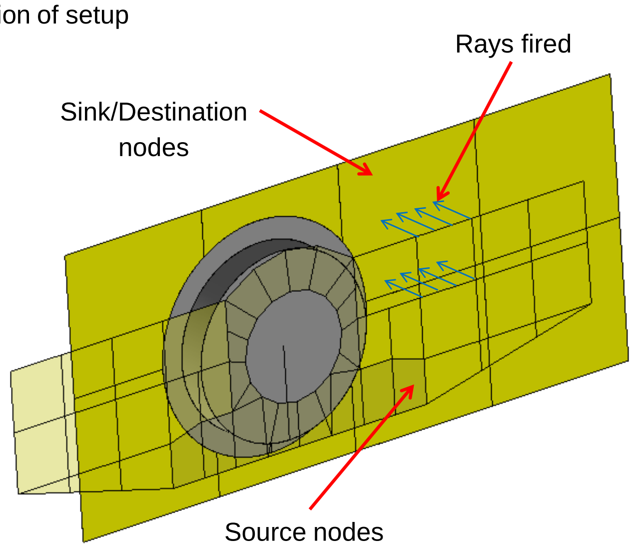

- Rays are fired normal to surface unlike when generating GRs.

AIRBUS DEFENCE & SPACE

Gas conduction and convection modelling for the ExoMars rover

Gas conduction for the ExoMars internal model - ESATAN auto-coupling generator

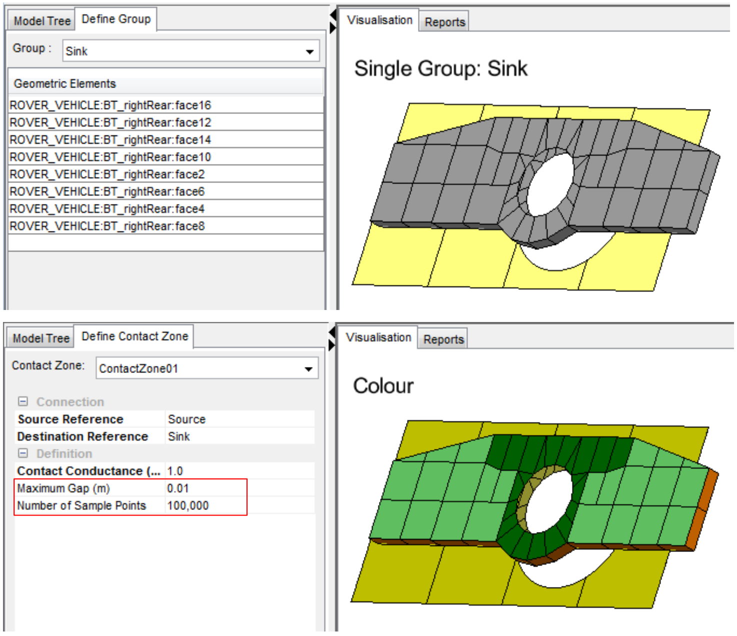

- Defining source and sink groups
- Defining contact zone
  - Gap distance and sample points critical

04 October 2016 17

AIRBUS DEFENCE & SPACE

Gas conduction and convection modelling for the ExoMars rover

Gas conduction for the ExoMars internal model - ESATAN auto-coupling generator

- After 'calculating conductors', a report can be produced from the contact zone:
- This output can be saved as a text file

Visualisation Reports

```
Contact Zone                      ContactZone01
Source Type                       GROUP
Source Reference                  Sink
Destination Type                  GROUP
Destination Reference             Source
Contact Conductance (W/m2K)       1.
Maximum Gap (m)                   0.1
Number of Sample Points           100000

Node Pair Areas (m2)
(ROVER_VEHICLE:11119, ROVER_VEHICLE:51149)    0.001312
(ROVER_VEHICLE:11119, ROVER_VEHICLE:51150)    0.0007043
(ROVER_VEHICLE:11119, ROVER_VEHICLE:51153)    0.001437
(ROVER_VEHICLE:11119, ROVER_VEHICLE:51155)    0.0003586
(ROVER_VEHICLE:11119, ROVER_VEHICLE:51158)    0.001057
(ROVER_VEHICLE:11119, ROVER_VEHICLE:51159)    0.0001985
(ROVER_VEHICLE:11123, ROVER_VEHICLE:51150)    0.0001346
(ROVER_VEHICLE:11123, ROVER_VEHICLE:51151)    0.001118
(ROVER_VEHICLE:11123, ROVER_VEHICLE:51152)    0.001687
(ROVER_VEHICLE:11123, ROVER_VEHICLE:51153)    0.0002578
(ROVER_VEHICLE:11123, ROVER_VEHICLE:51154)    0.0004311
(ROVER_VEHICLE:11123, ROVER_VEHICLE:51155)    6.301e-005

Total Contact Area (m2)   0.008759
```

- Comparing to hand-calculations and depending on the number of nodes/geometry, approximately 100,000 rays are required.
- A test between 10,000 and 100,000 rays, the area output generated:
  - At 10k rays = +16%
  - At 100k rays = -0.2%
- Works with cuts.
- Some areas may appear with magnitudes 10^{-6}. These can be safely excluded.

04 October 2016 18

AIRBUS DEFENCE & SPACE

Cruise cases

- During cruise, no gas will be present
- To save from having to duplicate coupling include files, a ‘CRUISE’ flag was added.
- When the cruise case is run, this flag is set to zero, negating all gas couplings.

```
GL(21150,41004) = CNDFNC(1, CO2_K1, 1) * 0.002475 / 3.829E-2 * CRUISE_CASE;
```


Thank you

Any questions?

Gas conduction and convection modelling for the ExoMars rover

Convection theory notations

Prandtl number

- μ – Viscosity of fluid (kg/ms)
- C_p - Specific heat (J/kg.K)
- k – Conductivity (W/m.K)

Grashof number

- g – Gravitational acceleration (m/s^2)
- β – Coefficient of volumetric thermal expansion ≈ 1/T_f for gases (K^{-1})
- ρ – Density (kg/m^3)
- T – Temperature (K)
- X – Characteristic length (m)

- C – Empirical constant
- n – Empirical index
- K – Dimensionless correction function

04 October 2016 21 AIRBUS DEFENCE & SPACE

Appendix Q

Modelling of complex satellite manoeuvres with ESATAN-TMS

Nicolas Bures
(ITP Engines UK Ltd, United Kingdom)

Abstract

Requirements from the Space industry demand performing radiative and thermal analysis combined with more complex spacecraft manoeuvres and attitudes; for example the MetOp-SG project has multiple rotating and spinning components which can prove challenging to model.
This presentation focuses on how ESATAN-TMS eases the process of defining and visualising complex kinematics as well as performing radiative simulation.


ESATAN-TMS
thermal modelling suite
Modelling of complex
Satellite manoeuvres with
ESATAN-TMS
Nicolas Bures
30th European Thermal & ECLS Software Workshop
5 – 6 October 2016, ESA/Estec, Noordwijk, The Netherlands

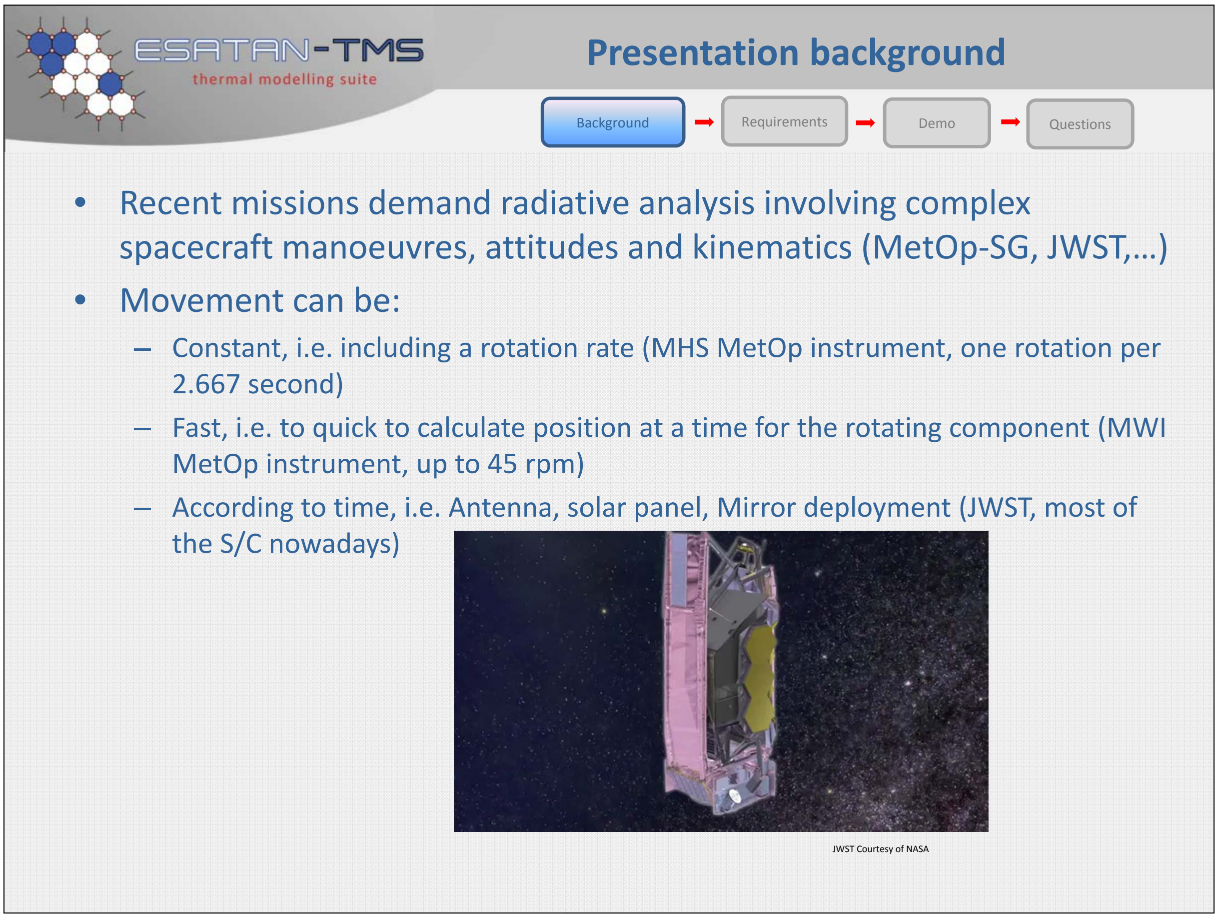
ESATAN-TMS
thermal modelling suite
Presentation background
Background
Requirements
Demo
Questions
• Recent missions demand radiative analysis involving complex spacecraft manoeuvres, attitudes and kinematics (MetOp-SG, JWST,…)
• Movement can be:
– Constant, i.e. including a rotation rate (MHS MetOp instrument, one rotation per 2.667 second)
– Fast, i.e. to quick to calculate position at a time for the rotating component (MWI MetOp instrument, up to 45 rpm)
– According to time, i.e. Antenna, solar panel, Mirror deployment (JWST, most of the S/C nowadays)
JWST Courtesy of NASA

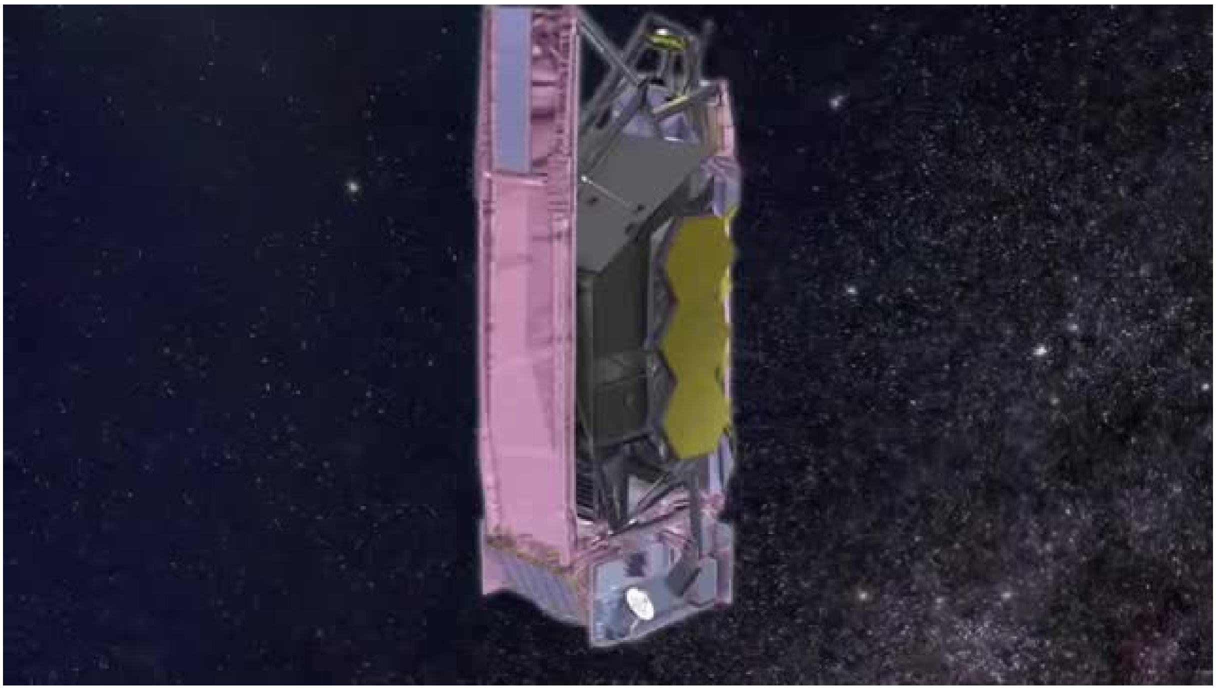

Save the attachment to disk or (double) click on the picture to run the movie.

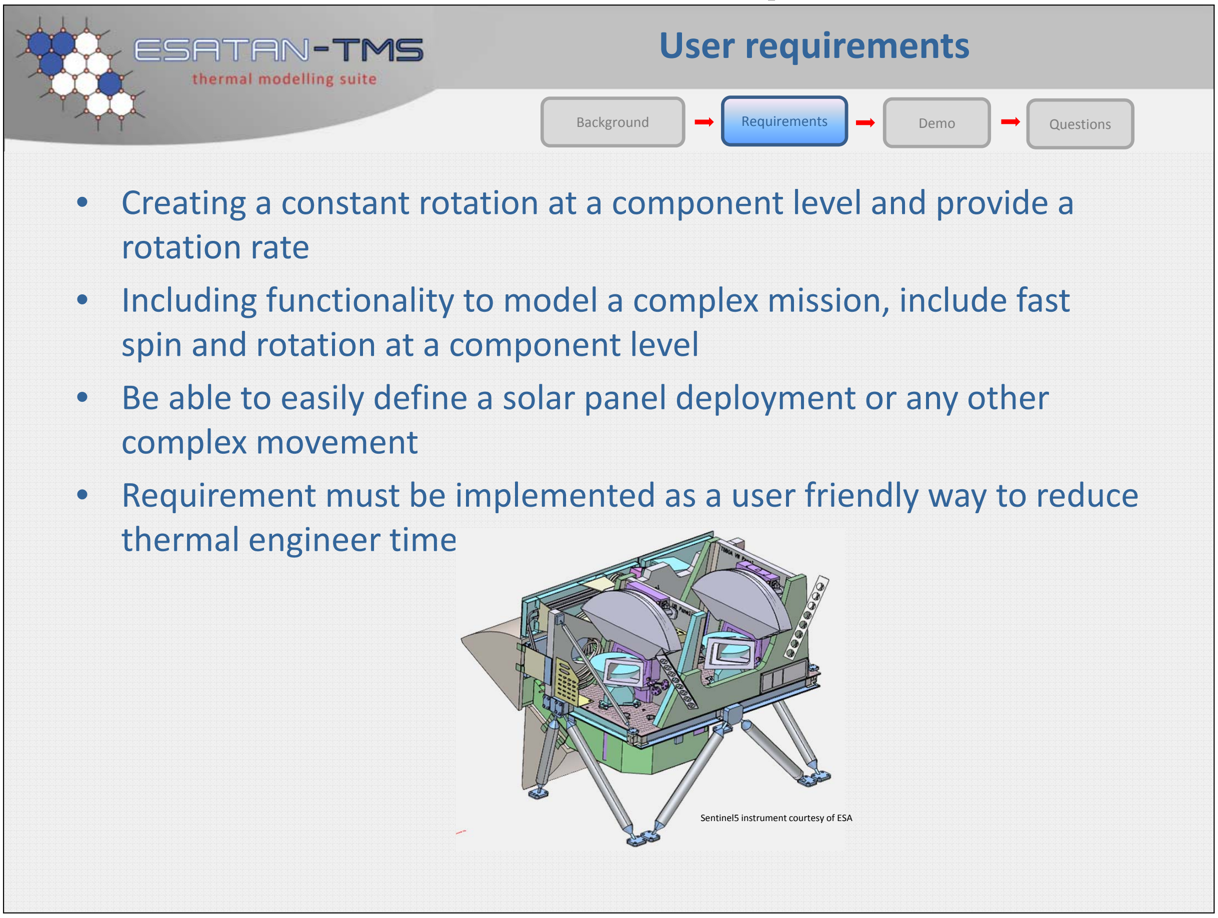

ESATAN-TMS thermal modelling suite

Example use-case

Background ➡ Requirements ➡ Demo ➡ Questions

- Demonstrate a use-case showing complex kinematics
- Radiative calculations needs to be calculated during the deployment
  - 4s, 8s, 12s, 16s, 20s
- Validation of kinematics
- Post-process radiative results

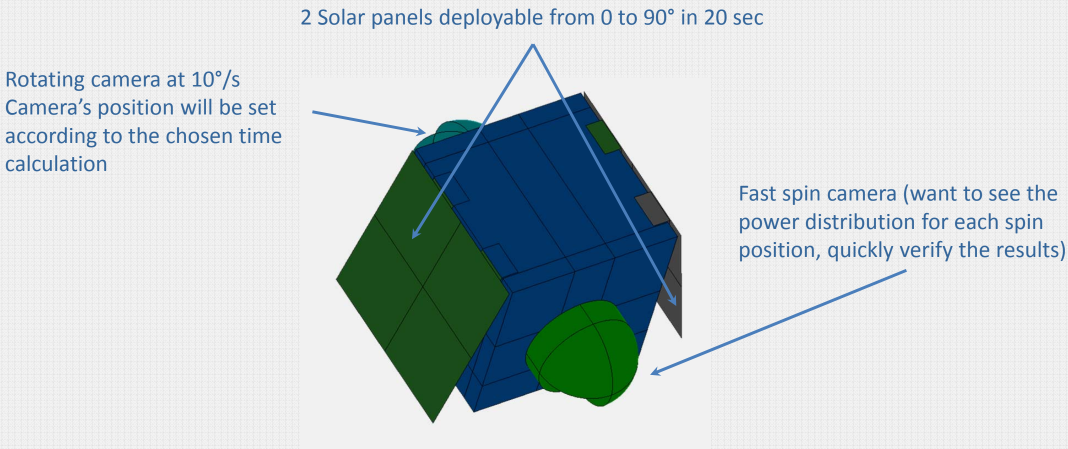

ESATAN-TMS thermal modelling suite

Demo

Background ➡ Requirements ➡ Demo ➡ Questions

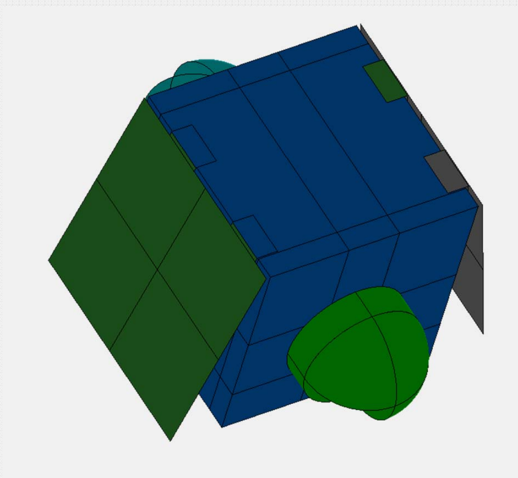

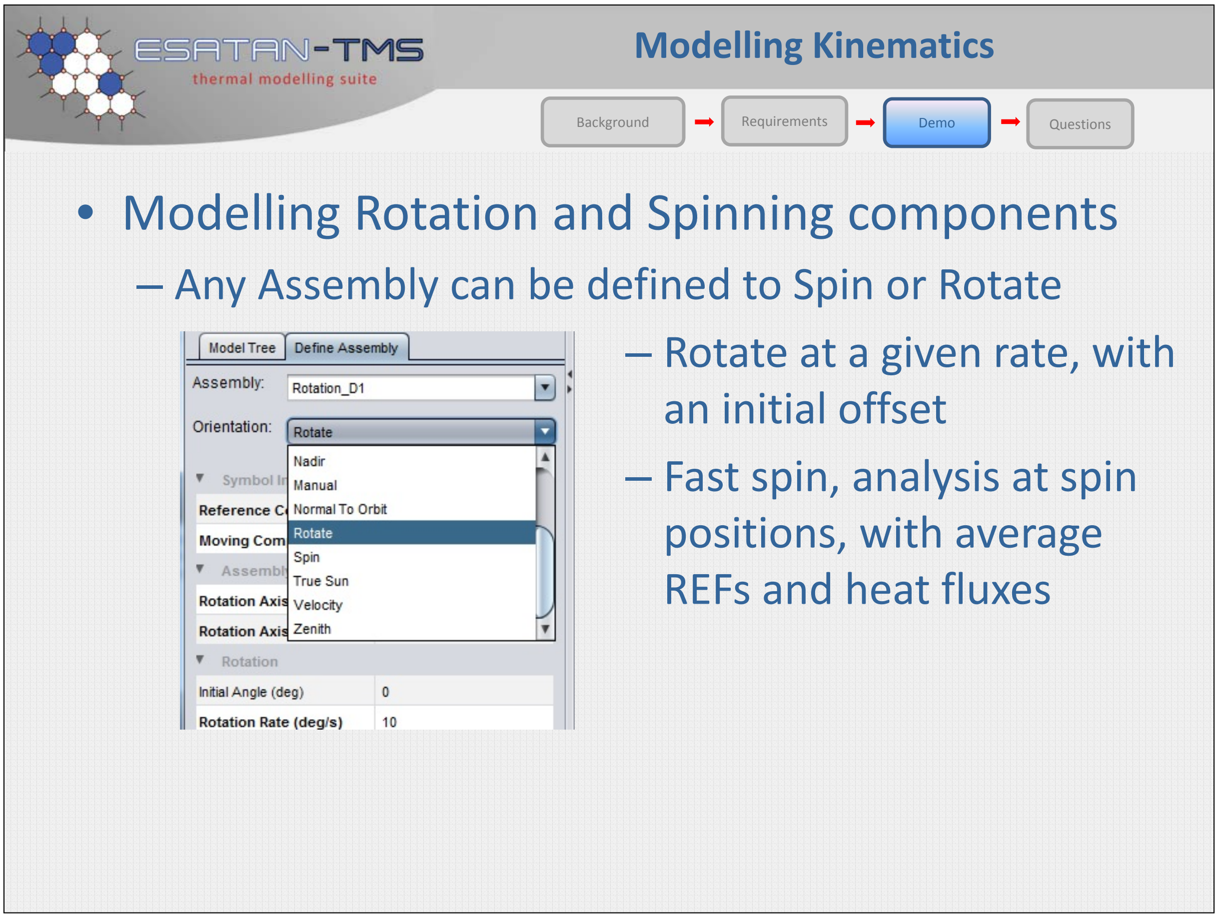
ESATAN-TMS
thermal modelling suite
Modelling Kinematics
Background
Requirements
Demo
Questions
• Modelling Rotation and Spinning components
– Any Assembly can be defined to Spin or Rotate
Model Tree
Define Assembly
Assembly:
Rotation_D1
Orientation:
Rotate
Nadir
Manual
Normal To Orbit
Rotate
Spin
True Sun
Velocity
Zenith
Rotation
Initial Angle (deg)
0
Rotation Rate (deg/s)
10
– Rotate at a given rate, with an initial offset
– Fast spin, analysis at spin positions, with average REFs and heat fluxes

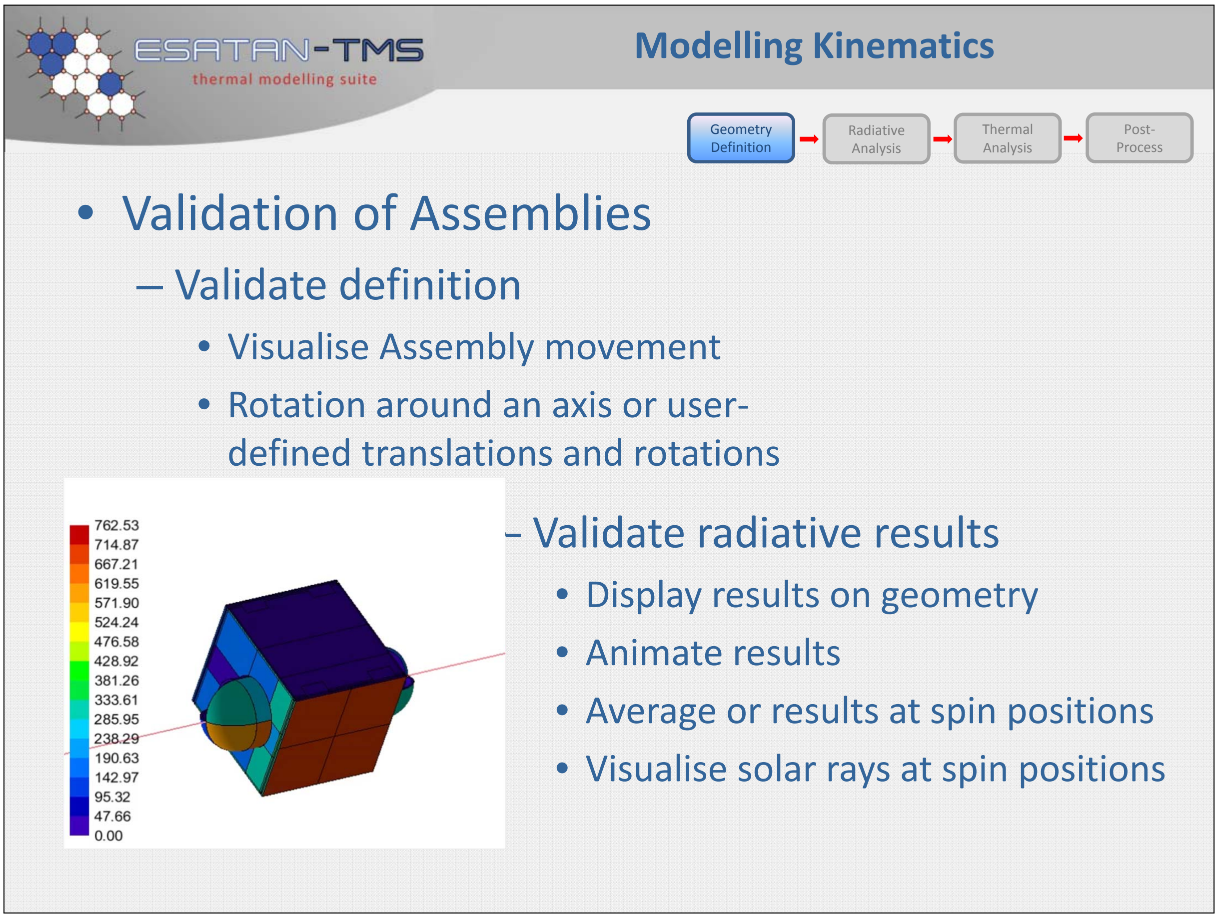
ESATAN-TMS
thermal modelling suite
Modelling Kinematics
Geometry Definition
Radiative Analysis
Thermal Analysis
Post-Process
• Validation of Assemblies
– Validate definition
• Visualise Assembly movement
• Rotation around an axis or user-defined translations and rotations
762.53
714.87
667.21
619.55
571.90
524.24
476.58
428.92
381.26
333.61
285.95
238.29
190.63
142.97
95.32
47.66
0.00
– Validate radiative results
• Display results on geometry
• Animate results
• Average or results at spin positions
• Visualise solar rays at spin positions

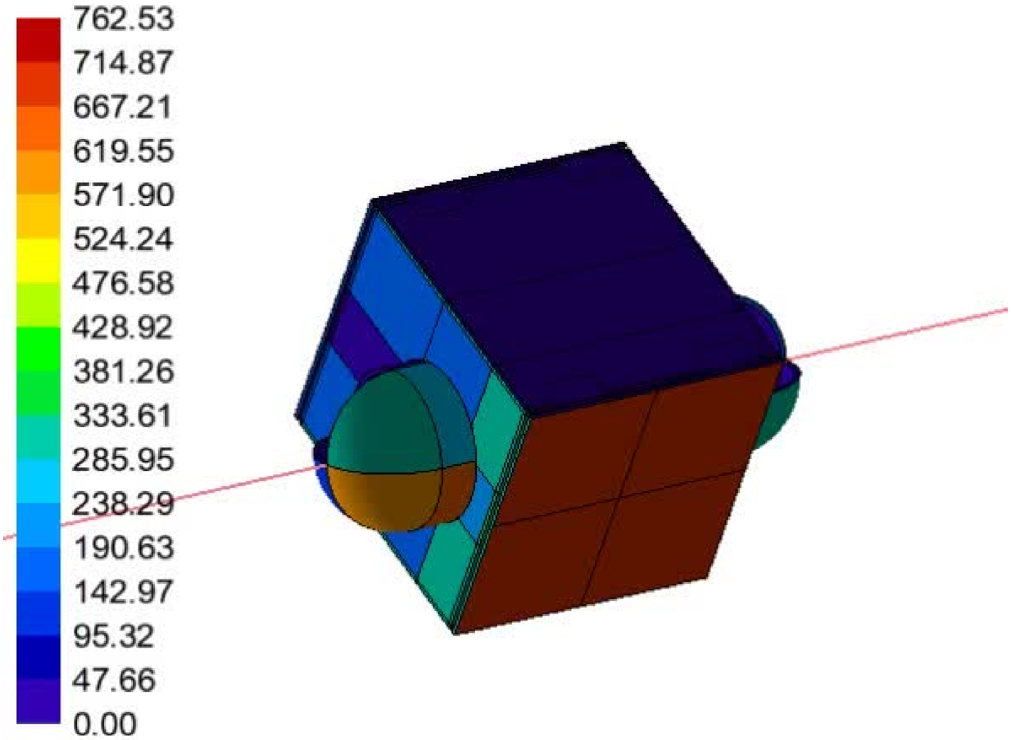

Save the attachment to disk or (double) click on the picture to run the movie.

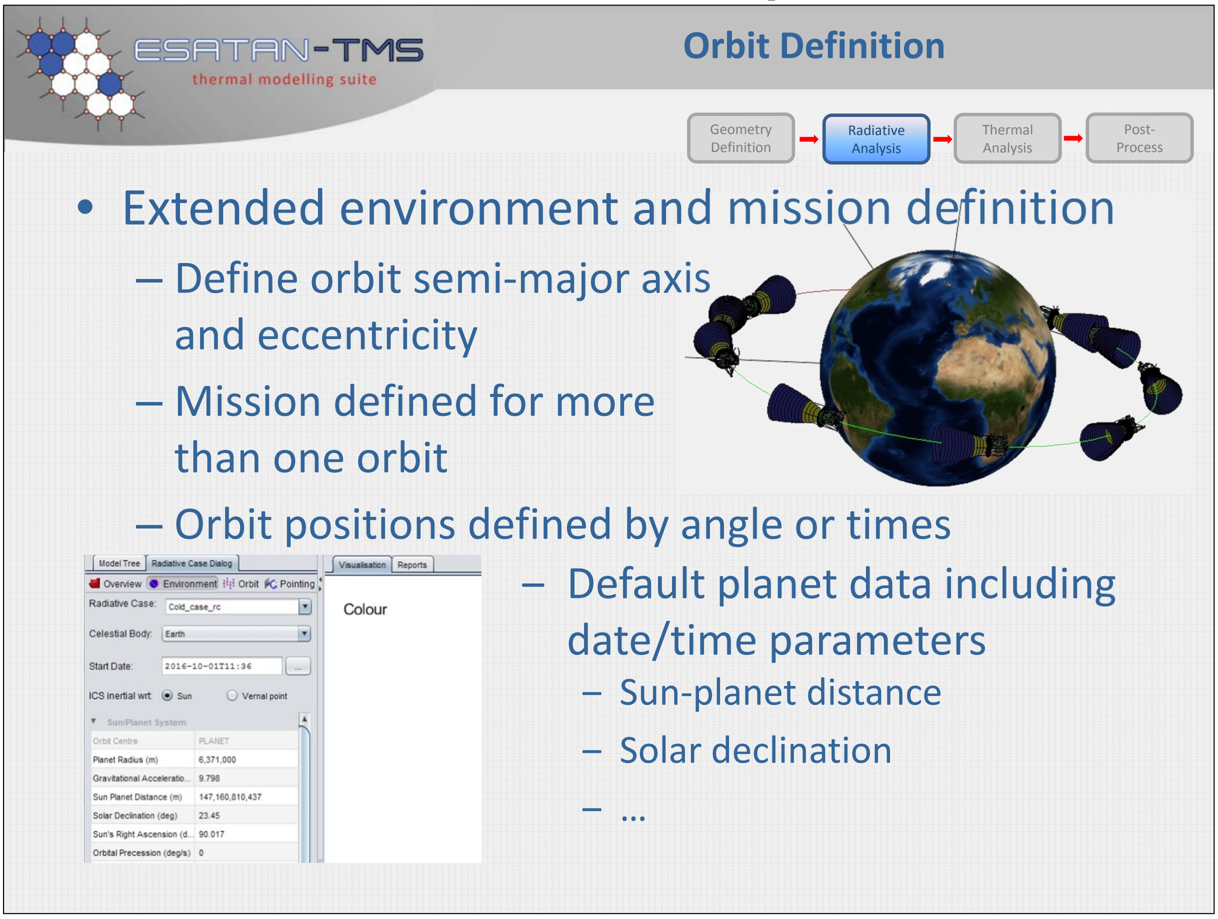

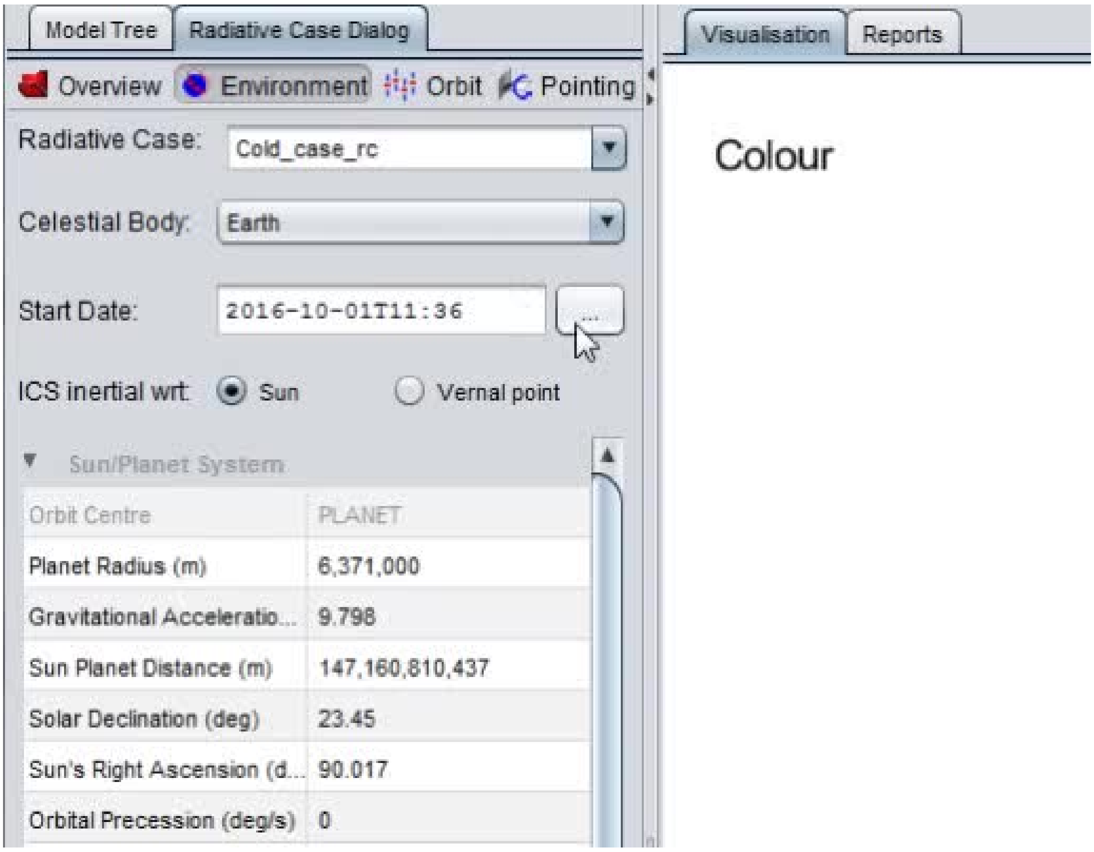

Save the attachment to disk or (double) click on the picture to run the movie.

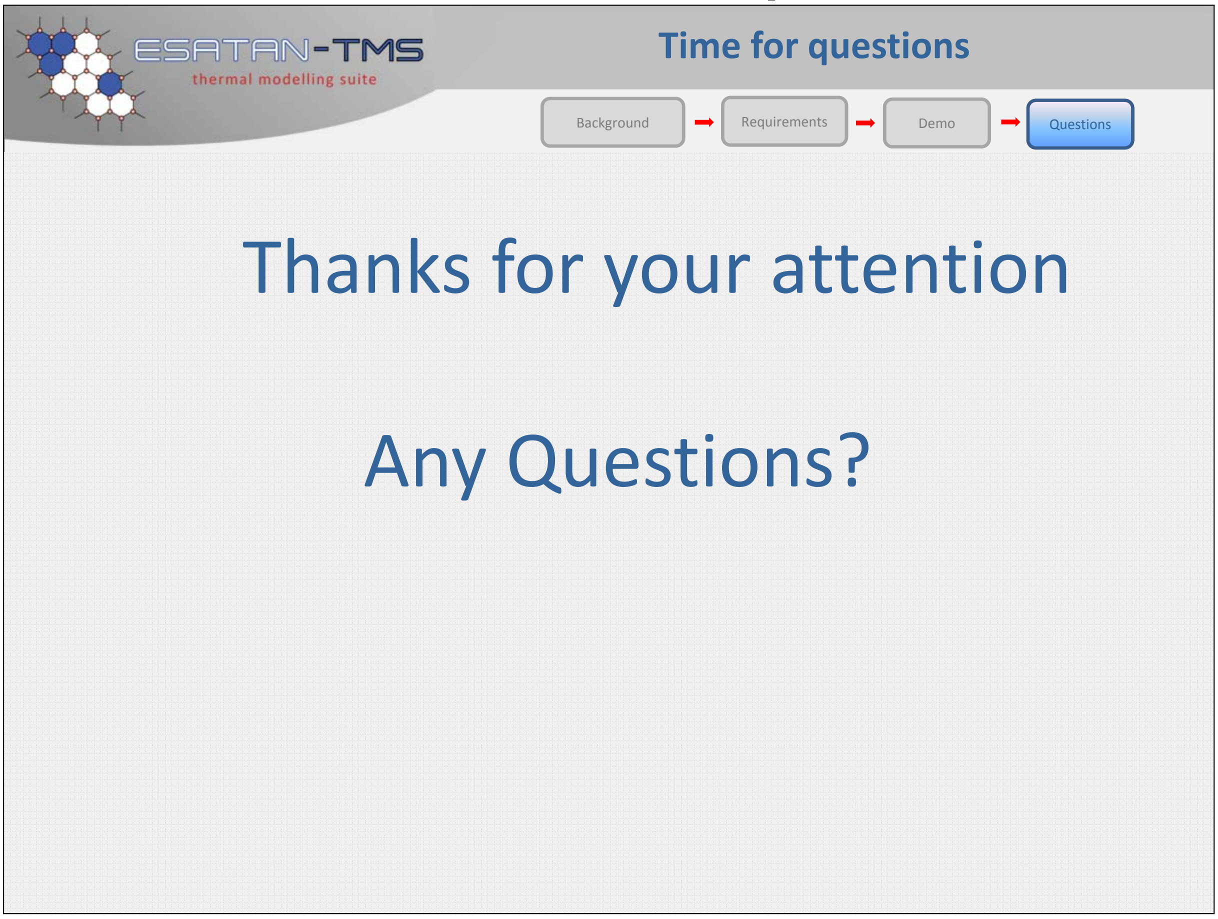

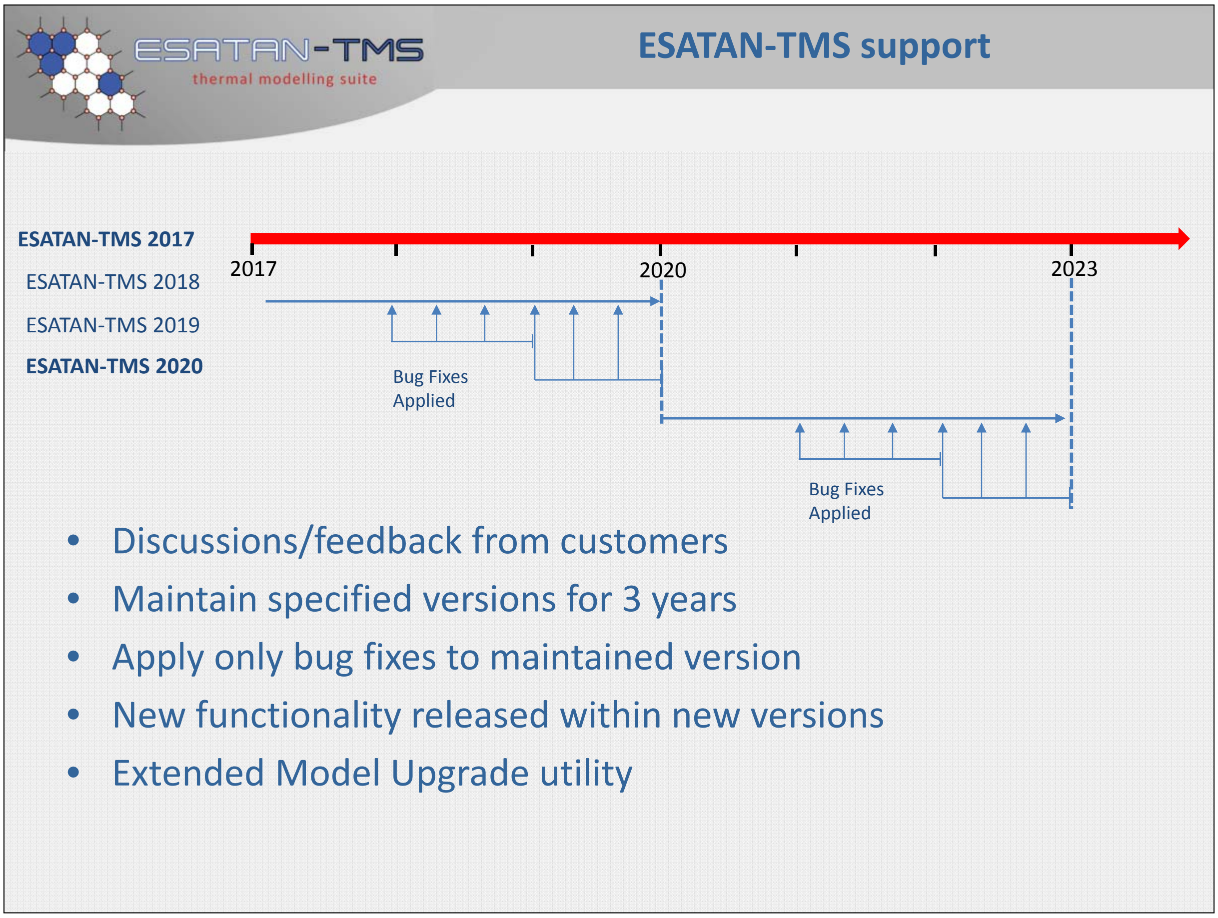
ESATAN-TMS
thermal modelling suite
ESATAN-TMS support
ESATAN-TMS 2017
ESATAN-TMS 2018
ESATAN-TMS 2019
ESATAN-TMS 2020
2017
2020
2023
Bug Fixes Applied
Bug Fixes Applied
• Discussions/feedback from customers
• Maintain specified versions for 3 years
• Apply only bug fixes to maintained version
• New functionality released within new versions
• Extended Model Upgrade utility


ESATAN-TMS
thermal modelling suite
www.esatan-tms.com

Appendix R

pyTCDT (TCDT 2.0)
A flexible and scriptable toolbox for thermal analyses.

Marco Giardino Andrea Tosetto
(Blue Engineering, Italy)

James Etchells Harrie Rooijackers
(ESA/ESTEC, The Netherlands)

Abstract

The tool provide users an integrated environment with analytical functions, ARTIFS and TOPIC integration, array function execution, editors, plotting and scripts management. As the name suggest it is implemented in Python so it will be available for different platforms and its distribution will be simplified wrt version 1.X.

Thermal Concept Design Tool (pyTCDT)

Andrea Tosetto
Marco Giardino
Blue Engineering, Torino, Italy
James Etchells
Harrie Rooijackers
European Space Agency, Noordwijk, The Netherlands

30th European Space Thermal Analysis Workshop
5-6 October 2016, ESA/ESTEC
Sheet 1

Overview

- **Why a New Tool**
- **Version 2.0: pyTCDT**
- **Simple example**
- **Future Developments**
- **Video Examples**

30th European Space Thermal Analysis Workshop
5-6 October 2016, ESA/ESTEC
Sheet 2

Version 2.0:
Why a New Tool

Keywords:

Stand Alone	Multiplatform	Maintainable
Parametric	Scriptable	Pythonic

- **Useful features from old version**
  - THECAL functions.
  - User extendibility.
  - ARTIFIS/TOPIC integration.
- **Upgraded features**
  - Simplified distribution & installation.
  - Simplified maintenance.
- **New features**
  - Unit of measure management.
  - Automatic function iterations.
  - Fluids Properties library.

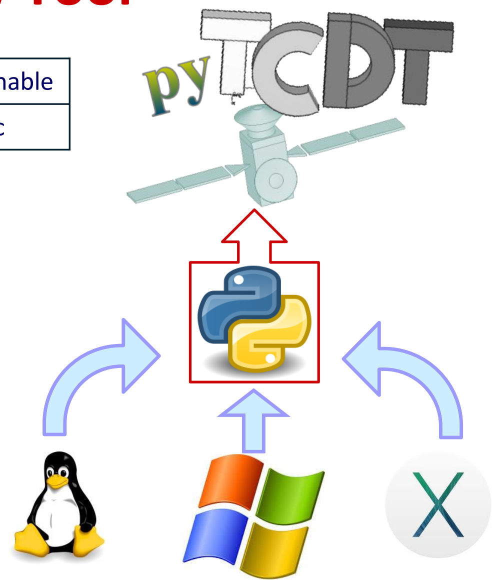

30th European Space Thermal Analysis Workshop
5-6 October 2016, ESA/ESTEC
Sheet 3

Version 2.0:
pyTCDT (1)

- Useful thermal design and analysis functions are included into a stand alone computing environment.
- Operated by using GUI or by command line in the embedded console.
- Complex problems can be solved combining THECAL functions in user scripts.

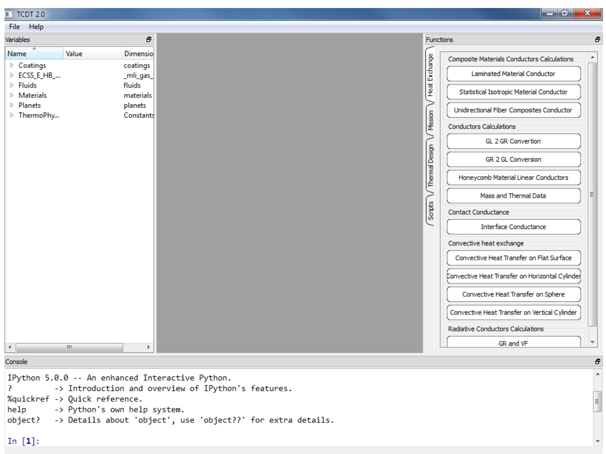

30th European Space Thermal Analysis Workshop
5-6 October 2016, ESA/ESTEC
Sheet 4

Version 2.0: pyTCDT (2)

- TCDT Parameters are quantities, they may contains unit of measure information (dimension).
- Parameters values can be converted in any compatible unit of measure included in the toolbox.
- Parameters can contains single or multiple values, of the same unit.
- Operators can be applied to parameter in the usual way, the unit of measure of the result will be generated according the operation (*e.g. 1 joule / 2 seconds = 0.5 watt*).

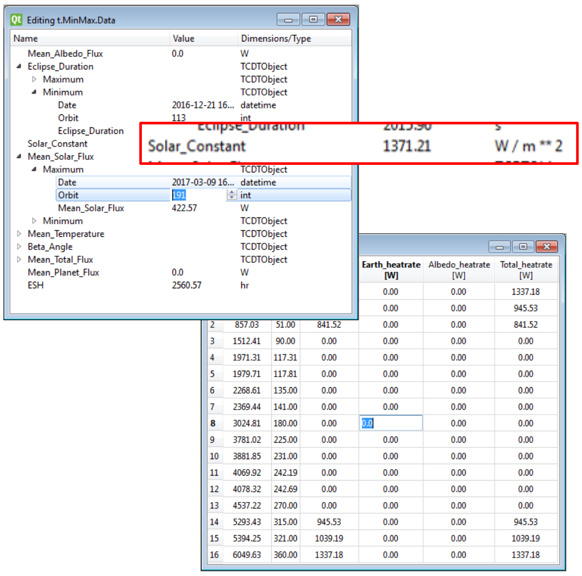

30th European Space Thermal Analysis Workshop
5-6 October 2016, ESA/ESTEC
Sheet 5

Version 2.0: pyTCDT (3)

- Pure Fluids objects derives their properties directly using Coolprop library, included in the distribution

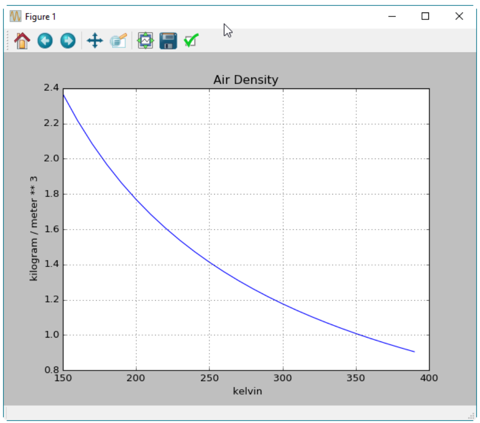

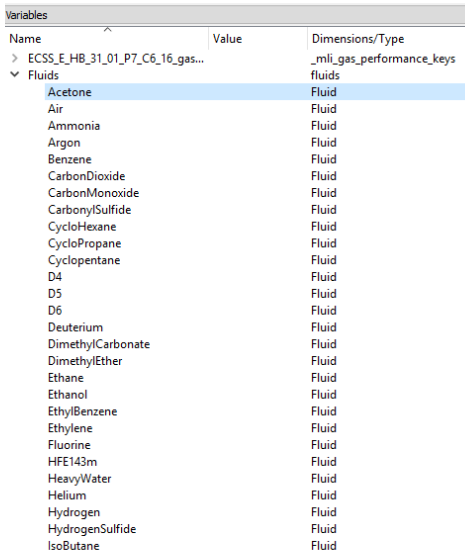

30th European Space Thermal Analysis Workshop
5-6 October 2016, ESA/ESTEC
Sheet 6

Version 2.0: pyTCDT (4)

- Functions user interface can accept single values or arrays.
- Unit of measure conversions can be performed within the GUI.
- Function widgets contains graphical aids to help user to input correct data.
- Each input parameter can be evaluated by a formula typed directly in the input textbox.
- Widgets shown the function call command line, completed with all required input parameters.

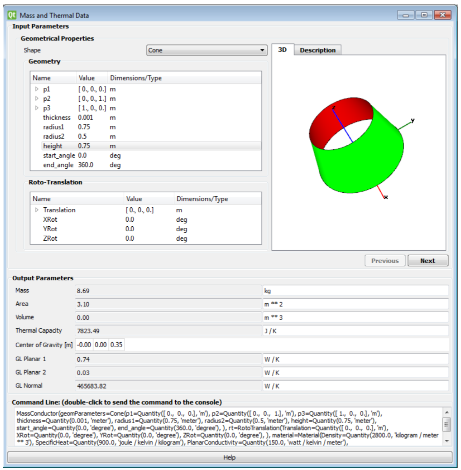

30th European Space Thermal Analysis Workshop
5-6 October 2016, ESA/ESTEC
Sheet 7

Version 2.0: pyTCDT (5)

- Data can be shown in 2D/3D plots or 3D views.

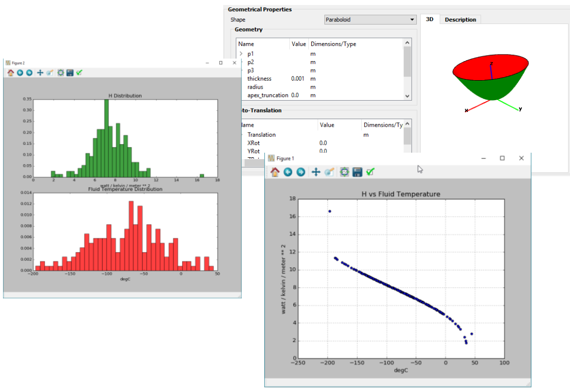

- Functions can be used in stochastic and sensitivity analyses.

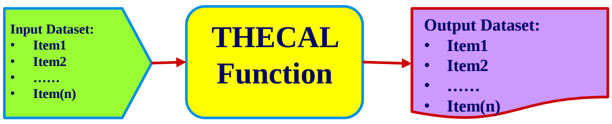

30th European Space Thermal Analysis Workshop
5-6 October 2016, ESA/ESTEC
Sheet 8

New User Interface

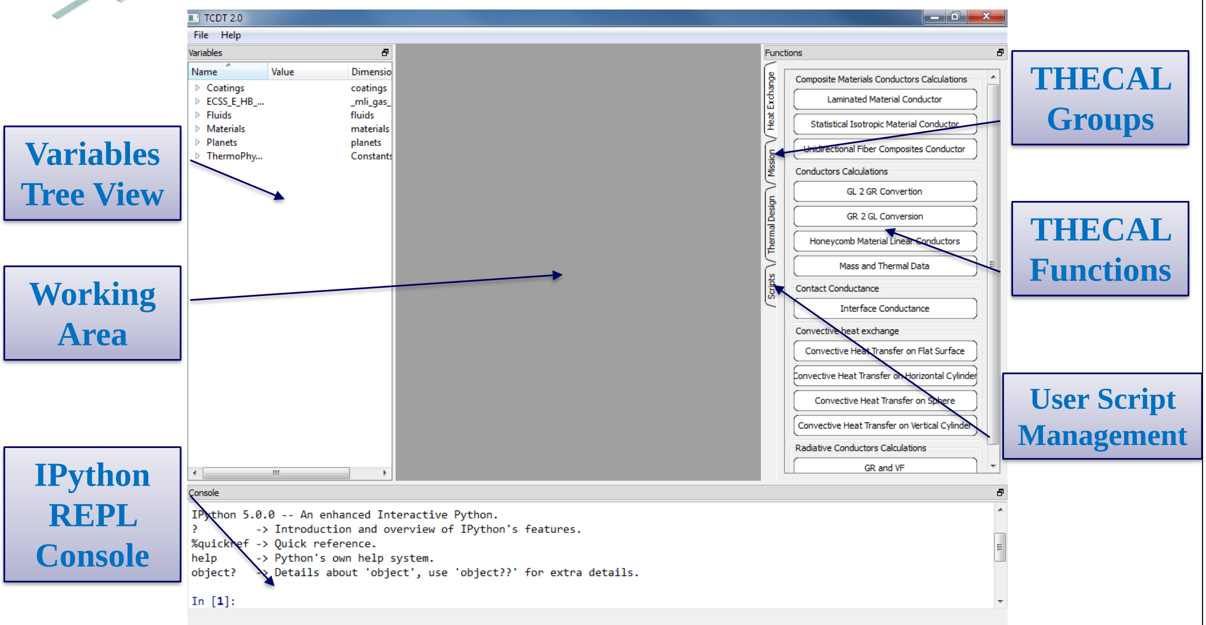

30th European Space Thermal Analysis Workshop
5-6 October 2016, ESA/ESTEC
Sheet 9

Thermal Analysis Calculator Functions List

- Mission related calculations:
  - Eclipse Calculator
  - ARTIFS manager
  - TOPIC manager
- Linear Conductor calculations:
  - Laminated Material GL
  - Isotropic Material
  - Unidirectional Fiber Composites
  - Honeycomb Material **(with thermal network generation)**
  - Bulk Material
- Radiative Conductance
  - GR and VF
- Contact Conductance
  - Bolt
  - Interface
- **Convective Heat Exchange**
  - **General Inclined Flat Surface**
  - **Horizontal Cylinder**
  - **Vertical Cylinder**
  - **Sphere**
- Thermal Design
  - Define Battery
  - Solar Array Power
  - Solar Array Size
  - MLI Performance
  - **MLI ECSS Gas Performance**

30th European Space Thermal Analysis Workshop
5-6 October 2016, ESA/ESTEC
Sheet 10

Example (1) Problem definition

Find the best honeycomb thickness (*tk*) of a panel of 0.2X0.2 m^2:

- painted with a external coating (ε = 0.9).
- exposed to Space (T_{space} = 3 K).
- internal temperature of T_{req} = 20 °C.

Requiring:

- A maximum heater power of 13.7 W on internal plate.
- A maximum panel weight of 0.35 Kg.
- Honeycomb thickness shall be between 15 and 150 mm.

30th European Space Thermal Analysis Workshop
5-6 October 2016, ESA/ESTEC
Sheet 11

Example (2) Mathematical Model

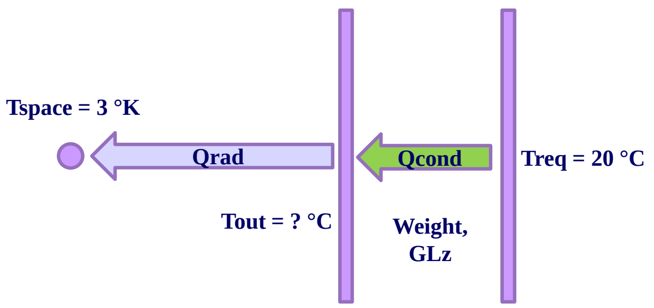

Heat Balance:

$$Qrad = Qcond$$

So:

$$\sigma \varepsilon A(Tout^4 - Tspace^4) = GLz(Treq - Tout)$$

Where *GLz* is evaluated by THECAL HoneyComb function according *tk*

Choose *tk* → Evaluate *GLz* and Weigth → Compute *Tout* → Evaluate *Qcond*

30th European Space Thermal Analysis Workshop
5-6 October 2016, ESA/ESTEC
Sheet 12

Example (3)
Solution with pyTCDT

Create a script with 2 functions:

- *HCData(Epsilon, Tspace, Treq, Tk, L, W)*: Solve the mathematical problem and return HC weight and flux
- *OptimHC(testThicknessArray, maxweight, maxheat)*: find the optimal value, thickness range where the requirements match and generate reporting plots.

Launch Script in pyTCDT Console

Console

```
In [3]: Optimization.OptimHC([x/10 for x in range(150,1500,1)],0.35, 13.7)
Out[3]:
BestT = Quantity(73.2, 'millimeter')
MaxTk = Quantity(85.7, 'millimeter')
MinTk = Quantity(60.7, 'millimeter')

In [4]:
```

30th European Space Thermal Analysis Workshop
5-6 October 2016, ESA/ESTEC
Sheet 13

Example (4)
Results

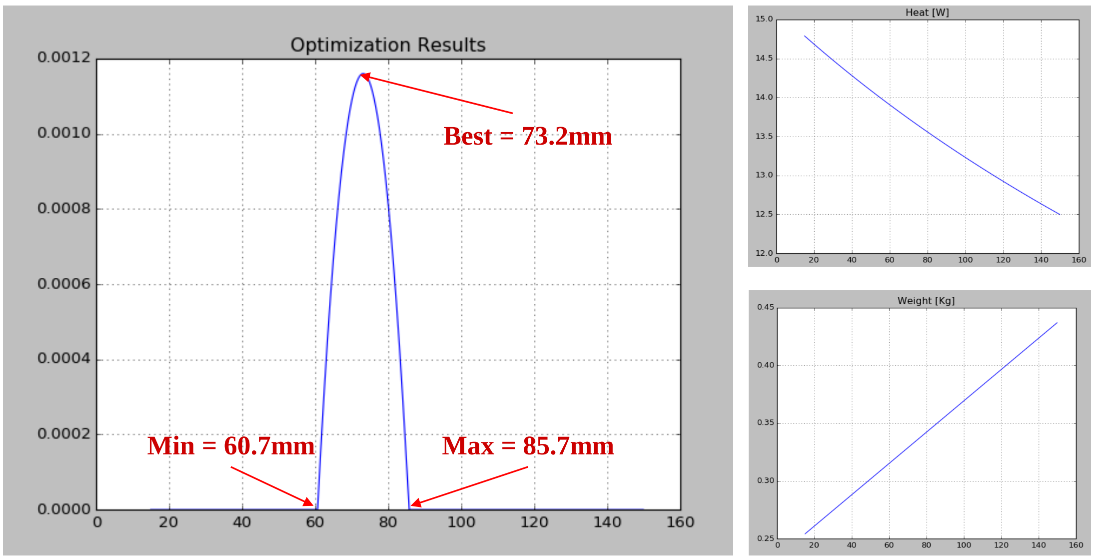

30th European Space Thermal Analysis Workshop
5-6 October 2016, ESA/ESTEC
Sheet 14

Road Map

- pyTCDT will be released to ESA before the end of October 2016.
- TCDT web site will be updated with new user agreement and new download link.
- pyTCDT will be release to the community after ESA approval, TCDT users that have an account will be notified with an email.

30th European Space Thermal Analysis Workshop
5-6 October 2016, ESA/ESTEC
Sheet 15

Possible Future Developments

- New THECAL Functions
  - Forced convection heat exchange.
  - Heat fluxes computation for complex shapes.
  - GUI Auto generation for user defined functions.
- Management of a thermal model
  - Build and edit a model.
  - Import/export in ESATAN TMS format (including GMM).
  - Simplified solver for thermal network.
- Optimization features
  - Latin hypercube matrix generation.
  - Stochastic optimization engine.
  - Allow numpy tensors

30th European Space Thermal Analysis Workshop
5-6 October 2016, ESA/ESTEC
Sheet 16

Video example

- Using TCDT Function GUIs
- Using the TreeView and the Console
- Settings and Scripting
- Vectorial Functions
- TCDT Data Structures

30th European Space Thermal Analysis Workshop
5-6 October 2016, ESA/ESTEC
Sheet 17

Save the attachment to disk or (double) click on the picture to run the movie.

TCDT Team

DISTRIBUTION & MAINTENANCE

BLUE ENGINEERING S.R.L.	ESA - ESTEC
Marco Giardino - Software Development *m.giardino@blue-group.it* **Andrea Tosetto** – Project Manager *a.tosetto@blue-group.it* **Support** *tcdtsw@blue-group.it* Blue Engineering - Engineering & Design WEB: *http://www.blue-group.it*	**Benoit Laine** - Head of Thermal Analysis and Verification Section *Benoit.Laine@esa.int* **Dr. Harrie Rooijackers** - Technical Support *Harrie.Rooijackers@esa.int* **James Etchells** - Project Manager *James.Etchells@esa.int* ESTEC-D/TEC-MTV WEB: *http://www.esa.int*

WEB: www.blue-group.it/TCDT

30th European Space Thermal Analysis Workshop
5-6 October 2016, ESA/ESTEC
Sheet 18

Appendix S

A comprehensive integration methodology based on cosimulation

Integration of thermal management in early phases of an electronic / electrical design

Benoit Triquigneaux M.Bareille Julien Pouzin Laurent Labracherie
J.Vidal
(ALTRAN Technologies, France)

Abstract

Thermal management is becoming a critical issue in electronic systems design due to the high dissipated power in electrical architectures and to the environment to which they are submitted.
Multi-physics simulation is an efficient way to solve some of the raised problems at various development steps. It helps designers in their choices by giving them more realistic predictions from the earliest stage of their development process.
The objective of this presentation is to demonstrate the benefits of thermal integration at the predesign stage of an electrical system. This integration is performed through a cosimulation technique which couples two dedicated simulation tools:

- SABER (SYNOPSYS®) for electrical / electronic modelling,
- IDEAS NX (SIEMENS®) for 3D thermal studies.

Coupled by a communication bus (COSIMATE, CHIASTEK®), they improve significantly the understanding of the system. Cosimulation becomes then a differentiating practice during the development phase.
This approach will be applied here to the predesign of an autonomous water search drilling system embarked on a spatial probe for MARS exploration. The objective is to develop a multi-physic Virtual Test Rig in order to validate technological choices and anticipate integration issues in the probe working environment (MARS atmosphere).
The methodology tested during this test case is generic and can be successfully applied to any system design for which the account of heat dissipation is mandatory.
The conclusion of this work is that, if it is generalized at various stages of the system development V-cycle, the "bus" cosimulation technique represents an efficient way to increase the designer confidence in his architecture. It provides a realistic virtual test rig gathering all the most important thermal phenomena influencing its piece of equipment functioning so that an early design error or integration issue can be anticipated in a cost effective way.

ESTEC/TEC-MTV

Thermal Division

30th European Space Thermal Analysis Workshop - 2016

A COMPREHENSIVE INTEGRATION METHODOLOGY BASED ON MULTI-PHYSICS COSIMULATION - CASE STUDY: ELECTRO-THERMAL SIMULATION OF A DRILLING SYSTEM IN A HARSH ENVIRONMENT

ALTRAN : Julien POUZIN, Benoit TRIQUIGNEAUX
in partnership with CHIASTEK : Pierre BOULON

30th European Space Thermal Analysis Workshop - 2016

ALTRAN in few words

ALTRAN Expertise Center
Fluids & Thermal Engineering
Simulations & testing

Our Competencies

Structural & Systems Thermal Engineering
> Thermal analysis, analysis and mitigation of thermal risks
> Energy balances, thermal testing and qualification

Fluid Mechanics & complex flows
> Internal and external flow analysis (Aero & Hydro dynamics)
> De-icing, multiphase flows, Combustion

Heating, Ventilation & Air Conditioning (HVAC)
> Modeling & simulations
> Thermal comfort studies
> Smoke & fire detection and simulation

Energy
> Thermal machines, Energy recuperation & conversion
> Renewable energies

Electronic Packaging & Power cabinets
> Thermal analysis of casings, cards & electrical components
> Ventilation studies for power cabinets

Turbomachinary, engines & rotating machinery
> Aerothermal studies for turbomachinary
> Engine performance, blade design, motor integration
> Electric engine & rotating machinery studies

1

Methods & Tools

- A design office comprising 120 qualified engineers, with offshoring capability
- We are familiar with the following methods and commercial software: Fluent, StarCCM+, I-deas TMG, Flotherm, Catia, Nx Thermal/Flow, Cedre, Ansys, Systema, ESATAN, Matlab, AMESim…

Key Figures

10 M€ Turnover
120 Consultants
> 30 Active clients
> 60 Projects
4 Research Projects

30th European Space Thermal Analysis Workshop

ALTRAN in few words

Space Thermal Engineering Offers

Team : 30 engineers in space activities

Skills and know-how

- Space systems/sub systems/units thermal modelling
- Flight and test prediction or rebuilding
- Thermal vacuum tests specification, follow-up and correlation
- Thermal architecture
  - Platform, payload, propulsion, antenna
- Design and qualification of systems
  - Optronics, electronics, RF
- Thermal tools development and maintenance

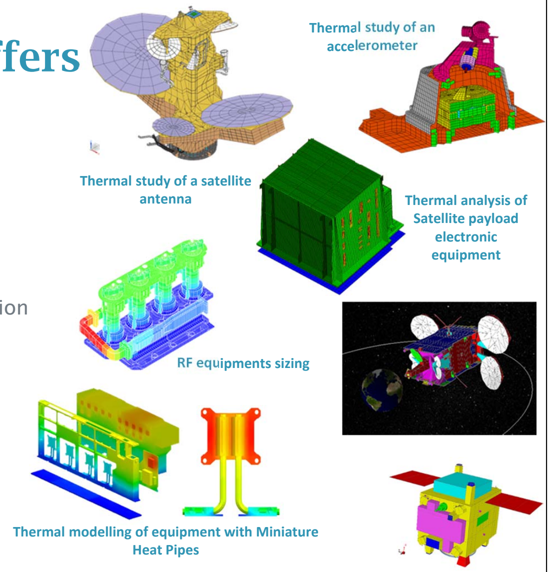

Thermal environment caracterisation, orthography, thermal control, tests, instrumentation, thermoelastic analysis, round the clock team shifts …

Customers

uropean Space The kshop

OUTLINE

1. Introduction
2. Co-simulation in design
3. Electrical model
4. Thermal model
5. Coupling method
6. Cosimulation Analysis
7. Added values
8. Conclusions

30th European Space Thermal Analysis Workshop

OUTLINE

1. Introduction
2. Co-simulation in design
3. Electrical model
4. Thermal model
5. Coupling method
6. Cosimulation Analysis
7. Added values
8. Conclusions

30th European Space Thermal Analysis Workshop

Tested cosimulation method : “cosimulation bus”

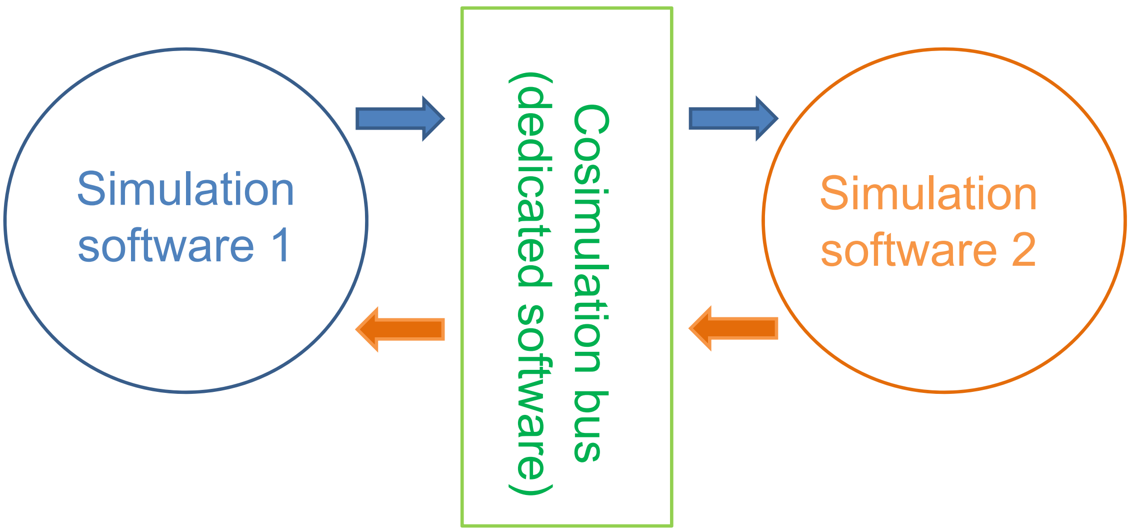

30th European Space Thermal Analysis Workshop

INTRODUCTION
Presentation context

- **Objectives**
  - Demonstrate the benefits of a genuine multi-physics approach based on “bus” cosimulation (time saving, accuracy, representativeness)
  - Demonstrate how co-engineering is enhanced by the use of cosimulation
- **Test case**
  - Pre-design stage of a drilling system on a Martian Probe
  - System integration in a realistic harsh environment
  - Electrical / Thermal cosimulation coupled by a dedicated communication bus

30th European Space Thermal Analysis Workshop

INTRODUCTION
Test case presentation

- Mars Probe with drilling system for water search
- Integration of electrical and thermal models
  - SABER (SYNOPSYS®) for electro-mechanics and control laws.
  - NX-TMG (SIEMENS®) for 3D thermal studies.
- Coupled together by the COSIMATE, CHIASTEK® communication bus

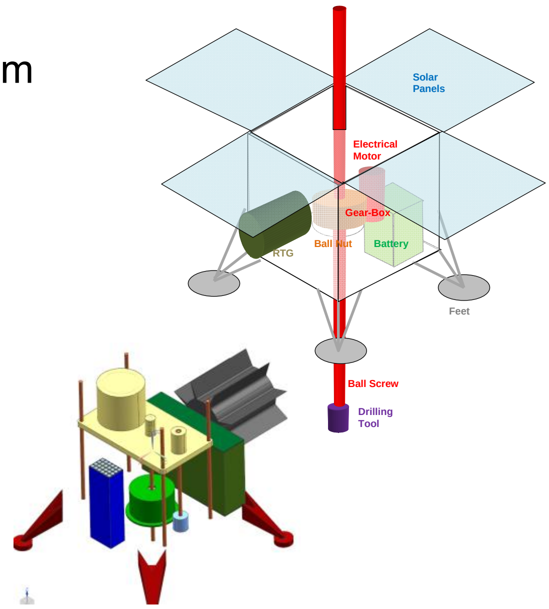

30th European Space Thermal Analysis Workshop

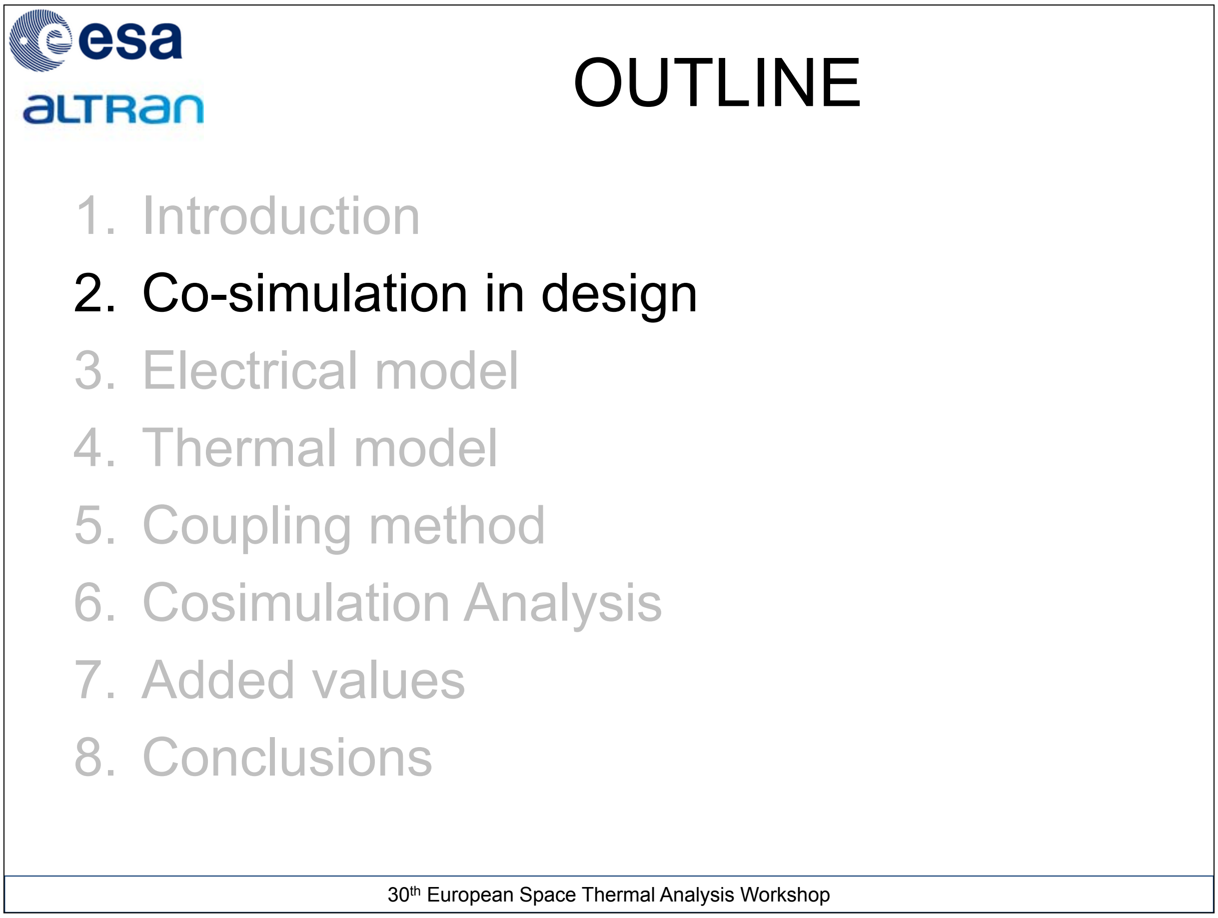
esa
altran
OUTLINE
1. Introduction
2. Co-simulation in design
3. Electrical model
4. Thermal model
5. Coupling method
6. Cosimulation Analysis
7. Added values
8. Conclusions
30th European Space Thermal Analysis Workshop

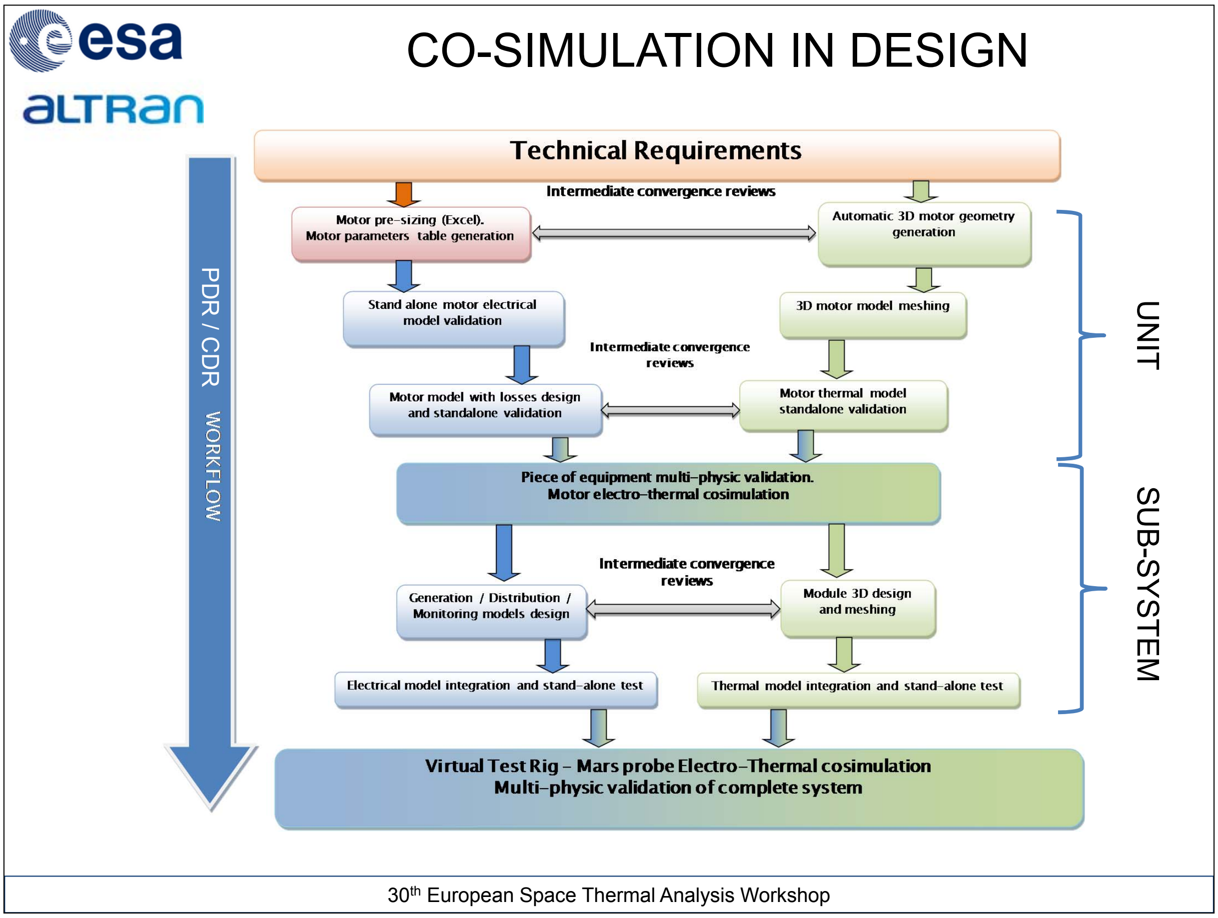
esa
altran
CO-SIMULATION IN DESIGN
Technical Requirements
Intermediate convergence reviews
Motor pre-sizing (Excel). Motor parameters table generation
Automatic 3D motor geometry generation
Stand alone motor electrical model validation
3D motor model meshing
Intermediate convergence reviews
Motor model with losses design and standalone validation
Motor thermal model standalone validation
Piece of equipment multi-physic validation. Motor electro-thermal cosimulation
Intermediate convergence reviews
Generation / Distribution / Monitoring models design
Module 3D design and meshing
Electrical model integration and stand-alone test
Thermal model integration and stand-alone test
Virtual Test Rig – Mars probe Electro-Thermal cosimulation
Multi-physic validation of complete system
PDR / CDR WORKFLOW
UNIT
SUB-SYSTEM
30th European Space Thermal Analysis Workshop

esa

altran

OUTLINE

1. Introduction
2. Co-simulation in design
3. Electrical model
4. Thermal model
5. Coupling method
6. Cosimulation Analysis
7. Added values
8. Conclusions

30th European Space Thermal Analysis Workshop

esa

altran

ELECTRICAL MODEL

Proposed electrical architecture

- Functional modeling approach in order to adapt to the thermal model time constant

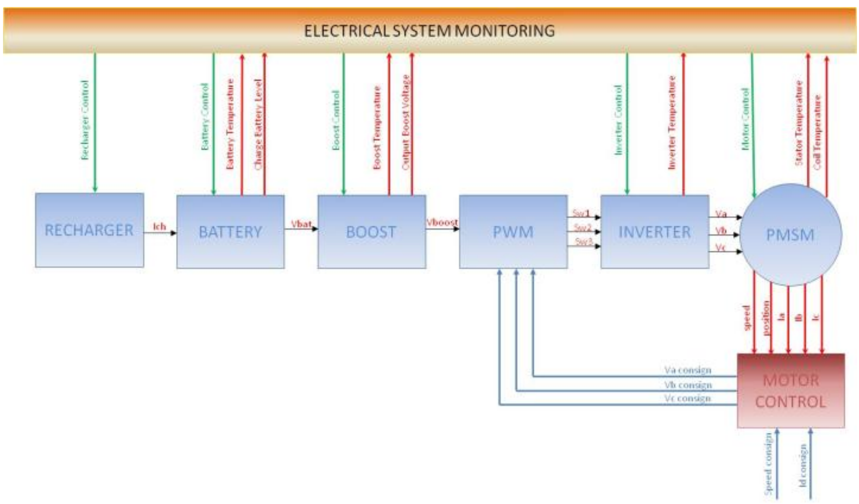

30th European Space Thermal Analysis Workshop

ELECTRICAL MODEL

Electrical system

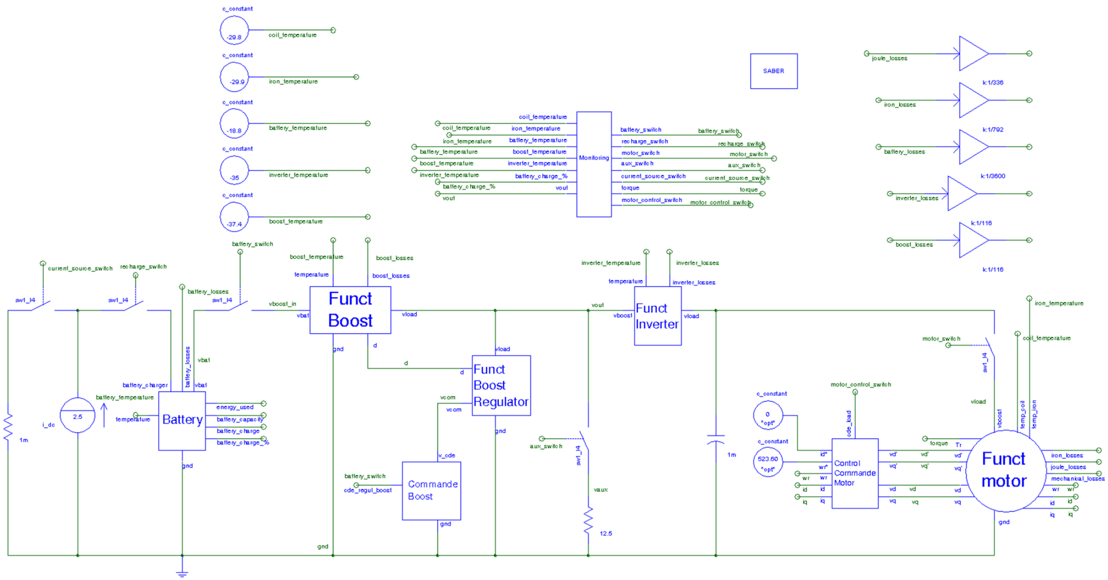

13

30th European Space Thermal Analysis Workshop

OUTLINE

1. Introduction
2. Co-simulation in design
3. Electrical model
4. Thermal model
5. Coupling method
6. Cosimulation Analysis
7. Added values
8. Conclusions

30th European Space Thermal Analysis Workshop

THERMAL MODEL

Environmental conditions

- Simulation cases
  - Initial case: electrical system off except RTG
  - Hot case
  - Cold case
- Boundary conditions
  - External convection (pressure=600 Pa)
  - Radiation
  - Solar heating (580 W*m²)
  - Convection into motor (usual correlation)
- Thermal management of the probe
  - External Radiator and MLI
  - Heat-Pipe
  - RTG

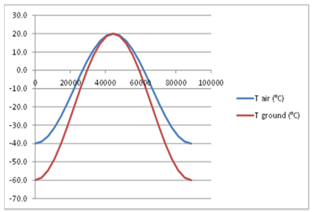

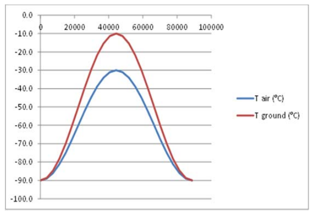

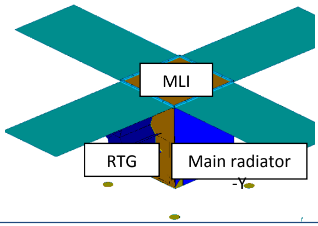

30th European Space Thermal Analysis Workshop

THERMAL MODEL

Mars probe thermal model

- The Martian probe is mainly composed of
  - a probe box and its feet
  - four solar arrays
  - a RTG = an autonomous power supply generator (uranium fuel)
  - a drilling system including
    - a electrical motor
    - an upper panel
    - four guide rods
    - some gearings
    - a drilling screw
    - a secondary screw
    - a drilling screws charging box
  - an electronic power equipment
  - a battery

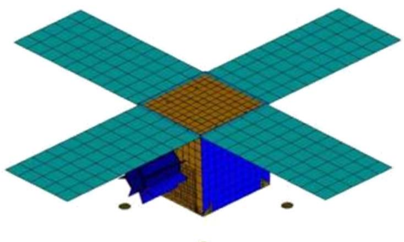

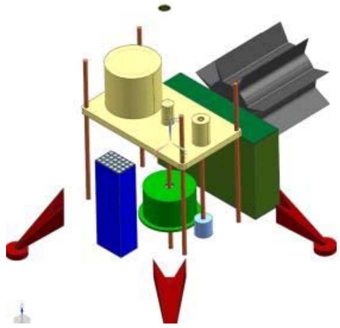

30th European Space Thermal Analysis Workshop

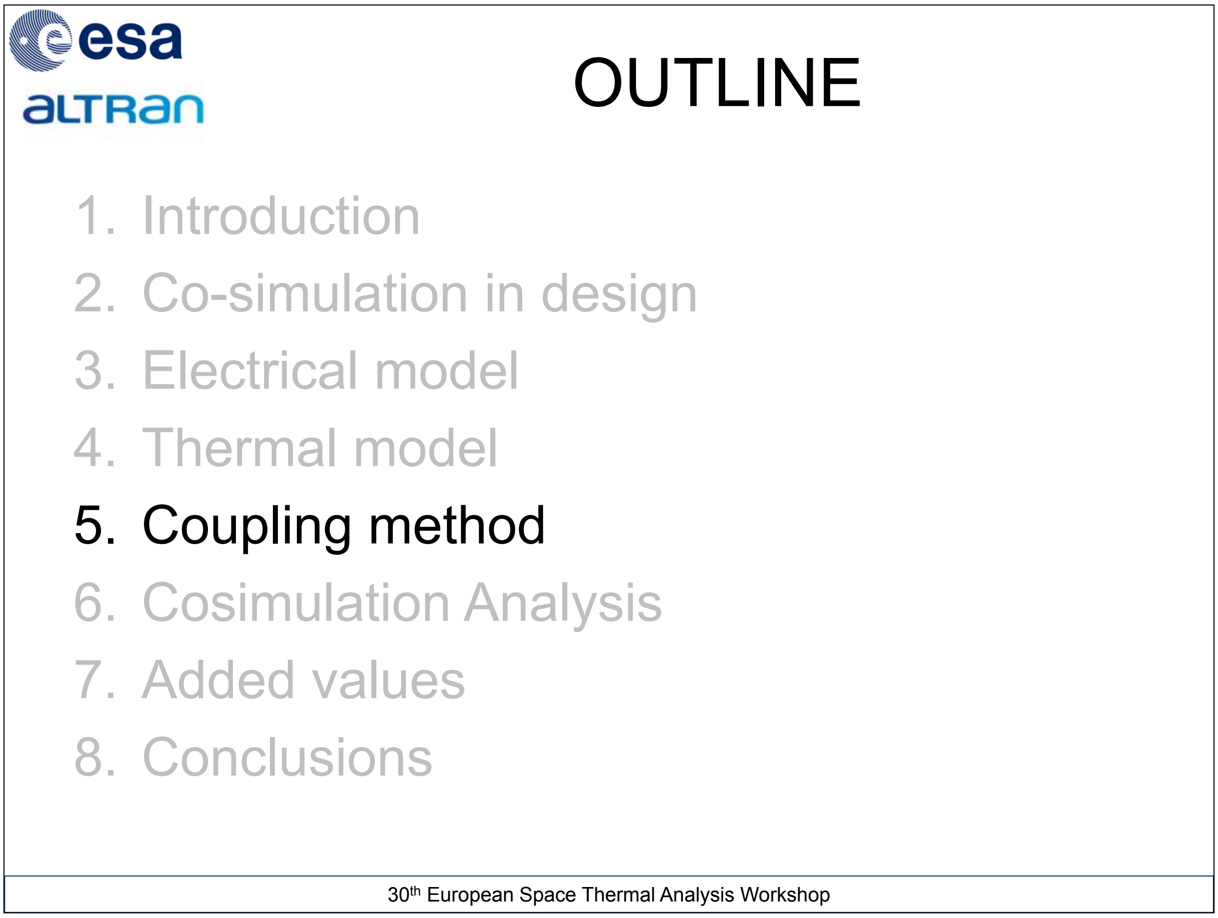
esa
altran
OUTLINE
1. Introduction
2. Co-simulation in design
3. Electrical model
4. Thermal model
5. Coupling method
6. Cosimulation Analysis
7. Added values
8. Conclusions
30th European Space Thermal Analysis Workshop

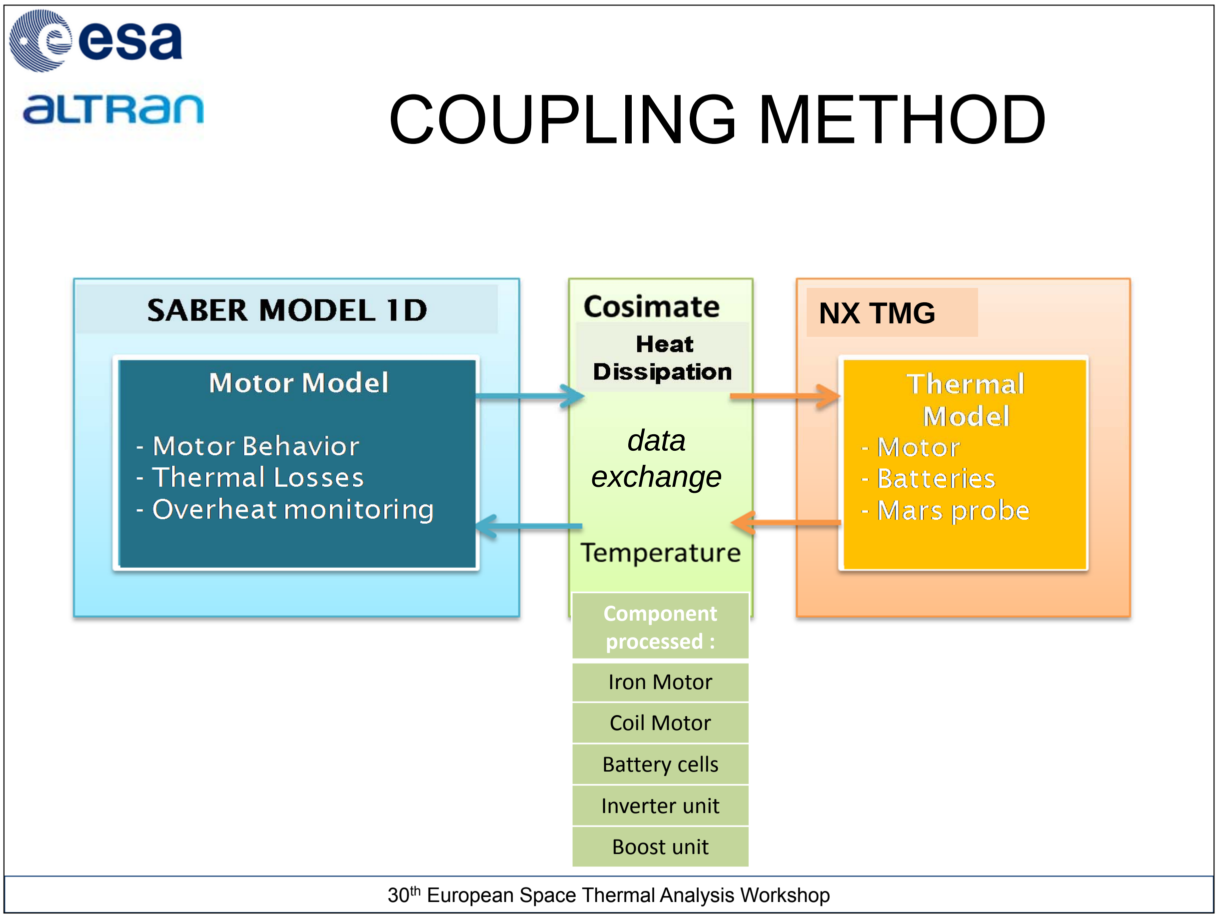
esa
altran
COUPLING METHOD
SABER MODEL 1D
Motor Model
- Motor Behavior
- Thermal Losses
- Overheat monitoring
Cosimate
Heat Dissipation
data exchange
Temperature
Component processed :
Iron Motor
Coil Motor
Battery cells
Inverter unit
Boost unit
NX TMG
Thermal Model
- Motor
- Batteries
- Mars probe
30th European Space Thermal Analysis Workshop

COUPLING METHOD

- Cosimulation type : softwares in // with a dedicated protocol cosimulation
- Approach in parallel : Both SABER and NX-TMG perform calculation based on previous time step results

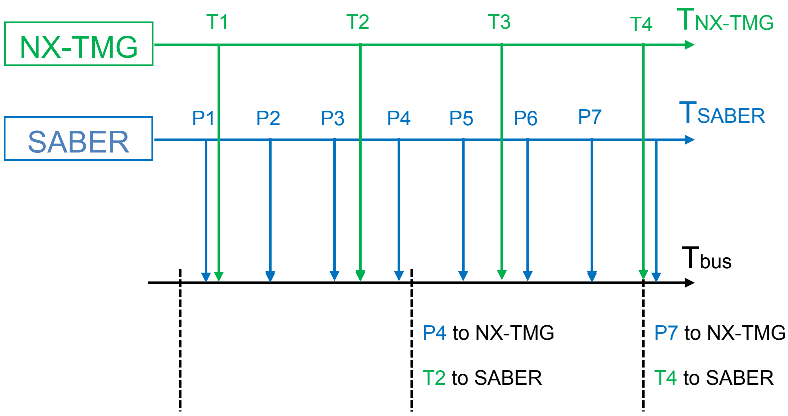

30th European Space Thermal Analysis Workshop

OUTLINE

1. Introduction
2. Co-simulation in design
3. Electrical model
4. Thermal model
5. Coupling method
6. Cosimulation Analysis
7. Added values
8. Conclusions

30th European Space Thermal Analysis Workshop

ANALYSIS
Normal operating Hot-case

- Evolution of losses, temperature and battery charge level

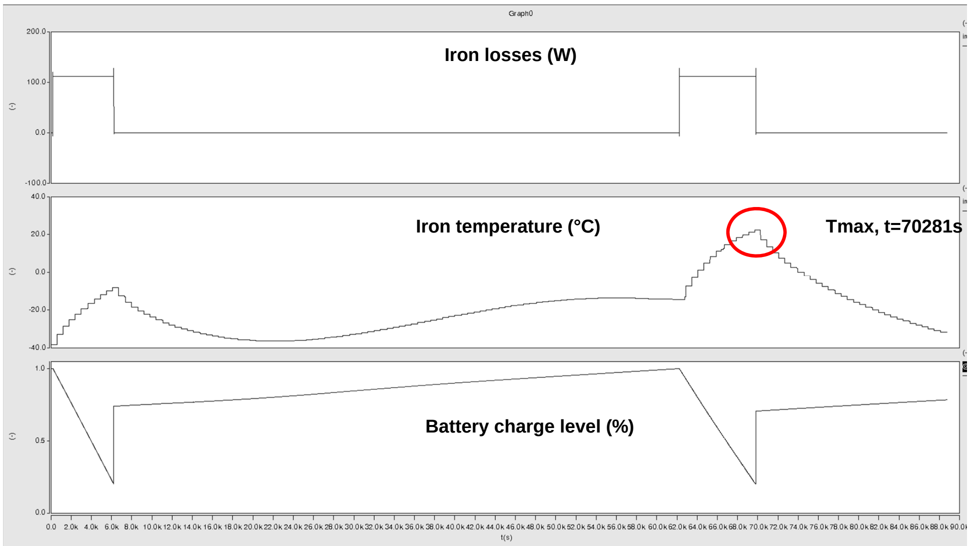

30th European Space Thermal Analysis Workshop

ANALYSIS
Normal operating Hot-case

- Probe and motor thermograph - t=70281s

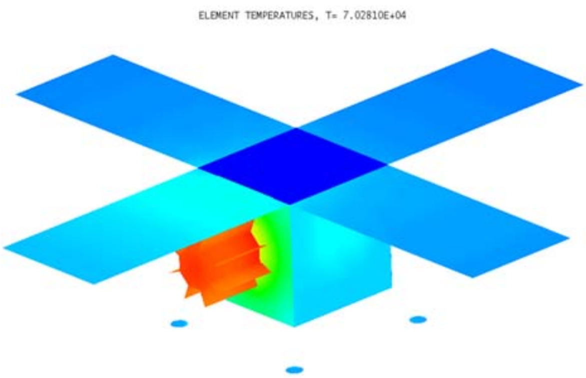

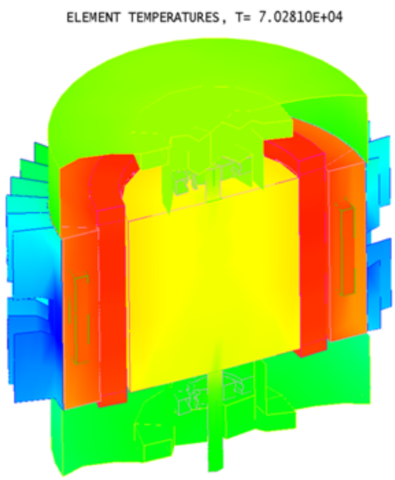

30th European Space Thermal Analysis Workshop

ANALYSIS

Failure case: motor over-heating

- Controlling rules test (motor temperature): System off when Tmotor > 100°C

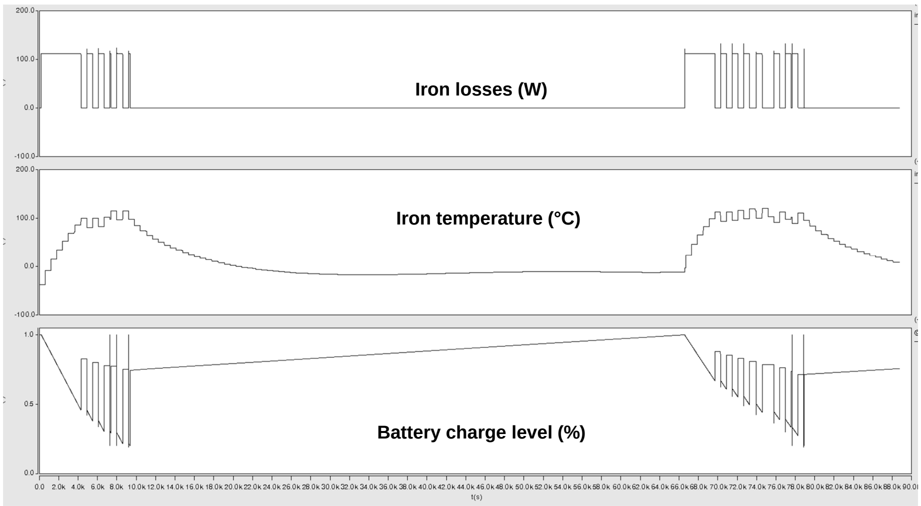

30th European Space Thermal Analysis Workshop

OUTLINE

1. Introduction
2. Co-simulation in design
3. Electrical model
4. Thermal model
5. Coupling method
6. Cosimulation Analysis
7. Added values
8. Conclusions

30th European Space Thermal Analysis Workshop

esa
altran

ADDED VALUES
Coupling vs not coupling

- Better accuracy
  - dissipations,
  - thermo-dependent quantity,
  - battery charge,
  - temperatures
- Better representativeness
- Re-use of existing models
- Low training necessary

30th European Space Thermal Analysis Workshop

esa
altran

ADDED VALUES
Coupling vs not coupling

- Possibility to simulate more complex management (failure…)
- Remote co-simulation possible
- Possibility > 2 coupled softwares (thermal, electrical, mechanical…)

⇒
- Less margin
- Less mass
- Time saving
- Cost reduction

30th European Space Thermal Analysis Workshop

esa
altran

OUTLINE

1. Introduction
2. Co-simulation in design
3. Electrical model
4. Thermal model
5. Coupling method
6. Cosimulation Analysis
7. Added values
8. Conclusions

30th European Space Thermal Analysis Workshop

esa
altran

CONCLUSIONS

- Simulation challenge : having data that makes sense
- Design challenge : reduction of cost & developpement cycle duration

→ Co-engineering / multi-physics approach in one peforming answer

- Co-simulation in one solution
  - enhances the data quality,
  - avoids worst case assumptions,
  - works without models change
- With our test case,
  - feasibility method (co-simulation bus) is shown
  - demonstration of advantages is highlighted

30th European Space Thermal Analysis Workshop

CONCLUSIONS

- Other co-simulation architectures exist (same software, API…)

Way forwards in space application

- Electronic units (co-sim thermal-electrical)
- Sensitive optical instruments (co-sim thermal-mechanical)
- Power supply management of battery, solar arrays… (co-sim thermal-electrical)
- On orbit Loop heat pipes performances (co-sim CFD-thermal)

30th European Space Thermal Analysis Workshop

THANK YOU FOR YOUR ATTENTION

30th European Space Thermal Analysis Workshop

APPENDIXES

30th European Space Thermal Analysis Workshop

INTEGRATION IN COSIMULATION PLATFORM

Complete integration

- Communication ports

Name	Ports	Physical quantity	Component
COSIMATEINPUT1	Input	Power Dissipation	Iron Motor
COSIMATEINPUT2	Input	Power Dissipation	Coil Motor
COSIMATEINPUT3	Input	Power Dissipation	Battery cells
COSIMATEINPUT4	Input	Power Dissipation	Inverter unit
COSIMATEINPUT5	Input	Power Dissipation	Boost unit
COSIMATEOUTPUT1	Output	Average Temperature	Iron Motor
COSIMATEOUTPUT2	Output	Average Temperature	Coil Motor
COSIMATEOUTPUT3	Output	Average Temperature	Battery cells
COSIMATEOUTPUT4	Output	Average Temperature	Inverter unit
COSIMATEOUTPUT5	Output	Average Temperature	Boost unit

30th European Space Thermal Analysis Workshop

INTRODUCTION

Cosimulation approaches

- **« Bridge » approach**
  - Point to point communication
  - Notion of Master/Slave => more difficult to control the cosimulation
  - Developed by different companies => more difficult to setup the platform
  - Difficult to instantiate more than 1 instance

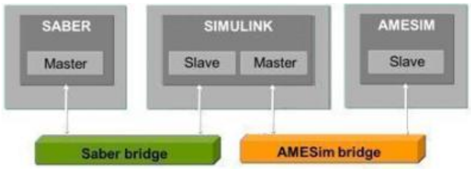

- **« Bus » approach**
  - Cosimulation bus
  - Acts as a unique communication controller => easier to control
  - No notion of Master/Slave => each solver launched separately
  - Multiple instances and multiple versions of a same simulator

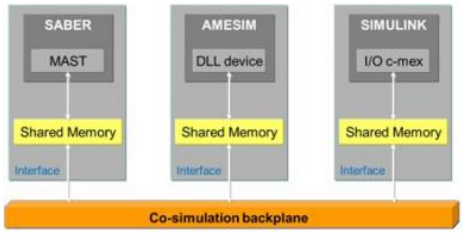

30th European Space Thermal Analysis Workshop

ELECTRICAL MODEL

Electrical pre-sizing

- Pre-sizing of the electrical pieces of equipment with Excel tables + analytical equations
  - Motor => PMSM (800 W, η=80%)
  - Battery => 144 cells (12x12, 1.8A/3.6V)
  - Boost => Input 48V/Output 100 V (η=95%)
  - Inverter DC/AC => Input 100VDC/Output 50V 3ϕ AC (η=94%)
- Automatic generation of the CATIA Motor model

Reference-PN	Ref-Rint	Ref-Rext	Ref-L	Ref-F-Ep	Ref-F-nbr	Ref-E-instance	Ref-E-longueur	Ref-E-largeur	Ref-gap
moteur1	54,5mm	95,5mm	120mm	2mm	60	12	72mm	10mm	0,8mm
	diamètre entrefer	diamètre moteur	longueur de l'entrefer	épaisseur des tôles du feuilletage	à calculer : F= D/E nbr feuilletage	nbr encoches	taille encoches C > H > B	largeur encoches	jeu moteur

Reference-PN	f-B-jeu	Ref-B-Ep	Ref-axeL	Ref-axeD	Ref-R-Dext	Ref-R-Dint	Ref-R-Ep	Ref-R-Dbille	Ref-R-jeu	Ref-A-Ep	Ref-A-L
moteur1	mm	10mm	50mm	10mm	50mm	10mm	10mm	6mm	0,2mm	15mm	35mm
	bine	hauteur chignon	longueur axe	diametre axe	D extérieur roulement	D intérieur roulement	Largeur roulement	D des billes	jeu fonctionnel	épaisseur aimant	longueur aimant

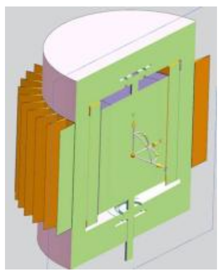

34

30th European Space Thermal Analysis Workshop

Appendix T

THERM3D / e-Therm GMM (conductive) and TMM generation of thermo-mechanical antenna support designed for ALM

Patrick Connil Jean Paul Dudon Thierry Basset Patrick Hugonnot
(TAS, France)

François Brunetti
(DOREA, France)

Abstract

Additive Layer Manufacturing (ALM) becomes more and more in the wave of spacecraft pieces manufacturing (i.e. antenna support). Experiences in aeronautics and medical implants bring opportunities for innovation, lower costs and make ALM a modern fabrication process.
However, 3D printing needs 3D models that fit mechanical and thermal constraints. The main objective is to converge to a single model iterating through CAD, mechanical and thermal expertises. CAD constraints evolved from classical manufacturing to ALM by increasing the complexity of CAD model, not in the size but by the use of a complex mix of shapes largely depending on B-Spline surfaces, extrusions and cuts.
For the thermal point of view, and as the 3D conduction optimisation always depends on material characteristics, fluxes direction, shape optimisation, the thermal expert is still needed for such calculation and a push-button CAD software is not sufficient.
For these reasons, THALES ALENIA SPACE (TAS) decided to improve the actual existing 3D conductive session within e-Therm in order to provide CAD import, meshing facilities, automated nodal breakdown that fit ALM constraints. In this presentation we would discuss about TAS needs and progress on ALM design for thermal analysis, the actual THERM3D research and development that has been integrated into e-Them since 2007, but also how DOREA solved major technical issues on importing raw CAD models for meshing to finally conductivity calculation and temperatures cartography. We will show in this presentation an example on an antenna support but is also used for heat-pipe 3D section modelling.

THALES

THERM3D / e-Therm GMM (conductive) and TMM generation of thermo-mechanical antenna support designed for ALM

F. BRUNETTI (DOREA) / P. CONNIL – P. HUGONNOT – T. BASSET (THALES ALENIA SPACE – FRANCE)

www.thalesgroup.com

Content

2

THALES

Introduction - Context

- Additive Layer Manufacturing (ALM) becomes more and more in the wave of spacecraft pieces manufacturing
- 3D printing needs 3D models that fit mechanical and thermal constraints
- TAS decided to improve the actual existing 3D conductive session within e-Therm , in order to provide CAD import, meshing facilities (both surfacic and volumic), automated nodes split that fit ALM constraints
- DOREA solved major technical issues on importing raw CAD models for meshing to finally conductivity calculation and temperatures cartography
- Presentation will focus on application requirement (ALM antenna support), technical issues to solve, THERM3D improvement, application process

3

THALES

E-Therm 2.0 – New Functionalities

- Data Base : Information on nodes, on exchanges and on heater lines

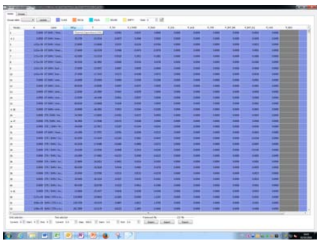

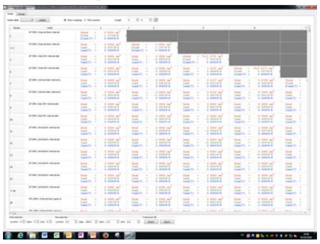

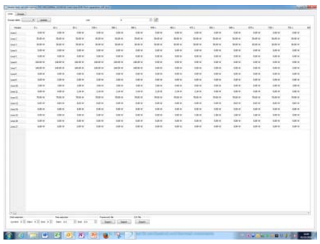

- Graphical Post Processing

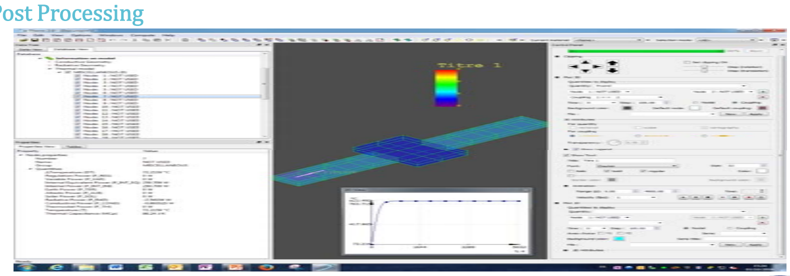

4

THALES

E-Therm 2.0 – New Functionalities

- Porting e-Therm to 64 bits platform :upgrade of all open-source libraries
- 3D Conductive Session :
  - Import CAD model (STEP AP203/214)
  - Automated Surfacic and Volumic meshing : NetGen or GMSH (open source meshers) Automated 3D Nodal Breakdown
  - Facilities to affect thermo physical and optical properties : Affectation of material files directly on the CAD shape
  - Results :
    - Cartography of temperatures
    - Determination of equivalent conductive exchanges on kept nodes (elimination of other nodes and vertices temperatures recovery using FEM algorithm)

5 THALES

Application requirement (GMM and TMM generation of thermo-mechanical antenna support designed for ALM)

- ALM Techniques for Space Items
  - Possible complex geometries : from simple geometric volumes to "organic" shapes
  - Optimized shape for performance purpose : mechanical, thermal, mass, manufacturing process…. and cost
- eTherm development for Thermal performance characterization/validation
  - CAD model import in the Thermal suite Interface and surfacic / volumic Thermal Meshing
  - Reduced Nodal distribution mapping and materials selection
  - Conductor matrix calculation (TAS heritage Equivale method : Therm3D)
  - Temperature resolution, cartography analysis
- Use Case: an antenna support
  - Selected for amazing geometry
  - Designed mainly for mechanical purpose
  - No link to external environment, internal Radiation neglected, may produce low equivalent conductive coupling… but not too much

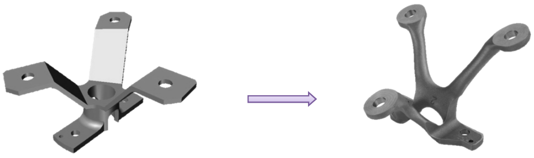

6 THALES

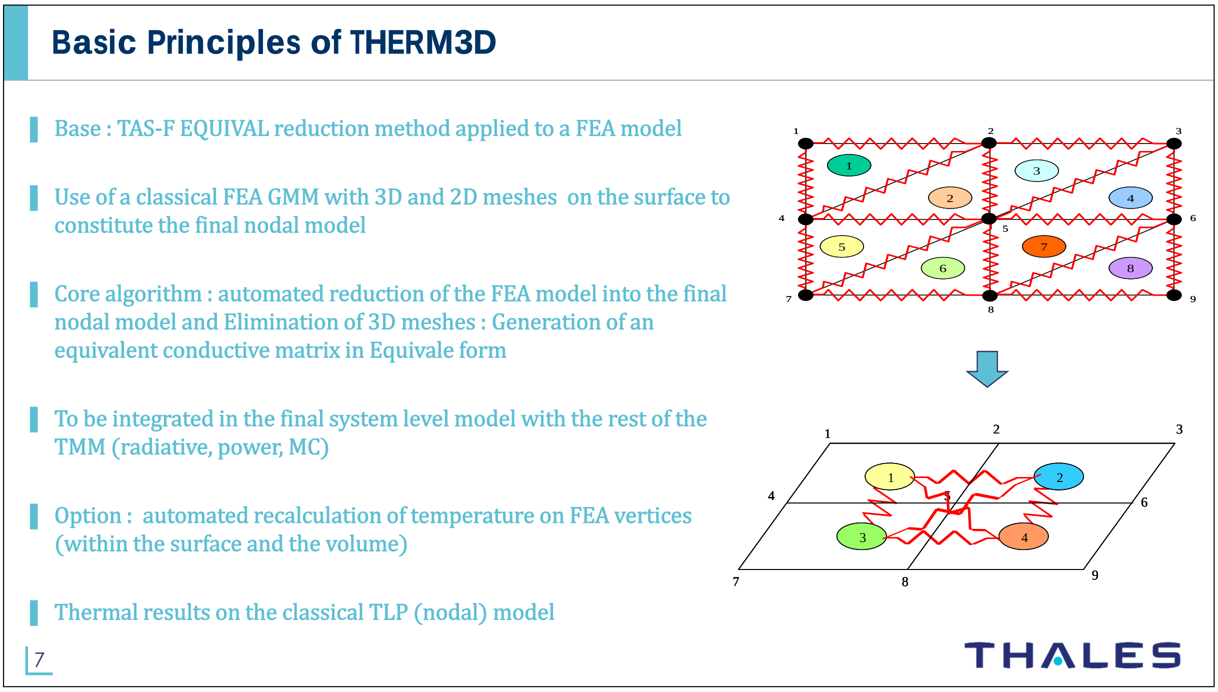

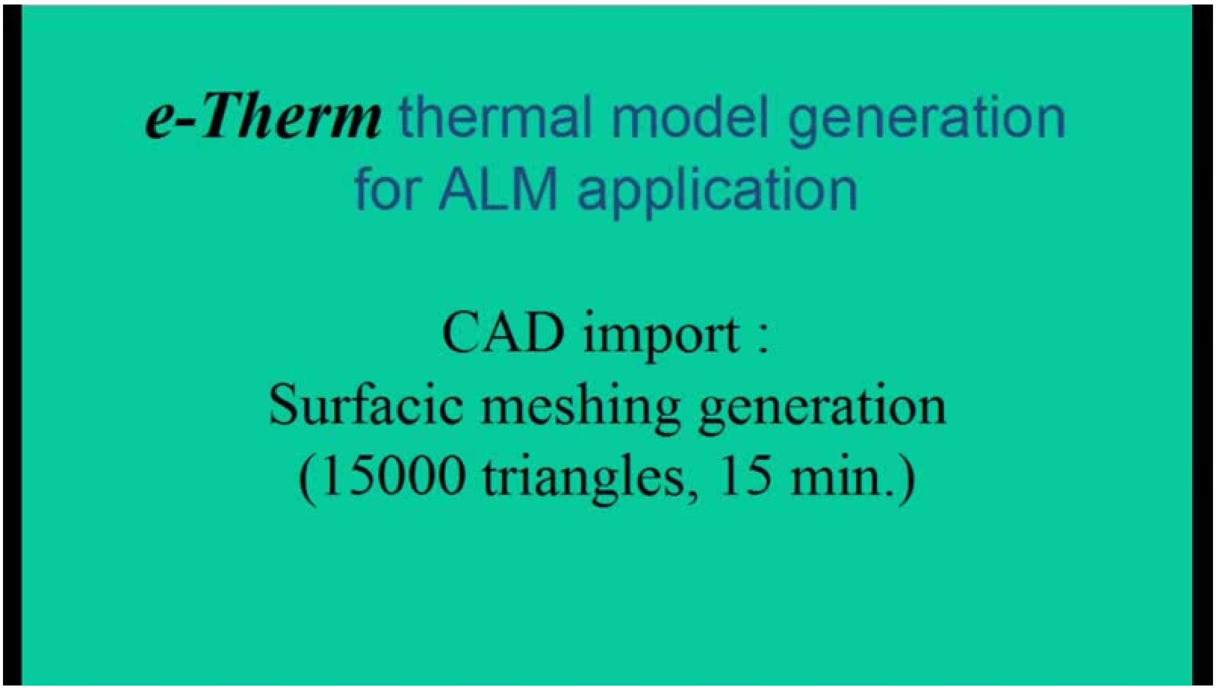

Save the attachment to disk or (double) click on the picture to run the movie.

Conclusion - Perspectives

Conclusion :

- Major issues due to complex CAD geometry have been solved in this first step
  - Ability to create semi-automatic nodal breakdown directly from CAD model
  - The full process duration is optimized and process is used within industrial program in TAS Cannes
- Other application : study of the heat pipe profile for the characterization of the conductance between fluid and sole
  - Function able to calculate surface of contact between fluid and grooves for example

Perspectives :

- A major improvement is to implement the radiative geometry model reduction for TMM integration, derived from the CAD model (reduced from 15000 faces to 150 faces)
- Development of post processing module able to compare automatically RTMM results with initial FEM temperatures calculation at vertices for nodal breakdown validation
- Due to the good performances, e-Therm / THERM3D can be envisaged for ALM shapes topologic mechanical / thermal optimization

8

THALES

Appendix U

Development towards 3D thermography

Gianluca Casarosa
(ESA/ESTEC, The Netherlands)

Abstract

The presentation reports on an activity aimed at solving the biggest issue of existing IR camera thermography, i.e. the temperature measurement of objects with significant 3D surface variability (wrinkles and folds). Such variations can alter the interpretation of images where the surfaces have significant directional emissivity variations and hot sources are brought in the field of view of the test surfaces. The latter is especially critical when measuring cold objects.
The activity covered the development of a method using IR cameras for 3D geometrical mapping of the test specimen and IR flux measurement. Correction of measured apparent temperature is based on a ray tracing approach. The method developed was validated by test.

Non-contact temperature measurement for thermal vacuum testing

Dr Rob Simpson
Senior Research Scientist, Thermal imaging

D. Robinson (Psi-tran Ltd), J. A. Parian (Photocore AG), A Whittam (NPL), T Fletcher (NPL)
A. Cozzani, G. Casarosa, S. Sablerolle, H. Ertel, M. Appolloni (ESTEC)

e: rob.simpson@npl.co.uk
t: +44 (0) 208 943 6438
w: www.npl.co.uk/temperature-humidity/research/thermal-imaging-metrology-research

Non-contact temperature measurement for thermal (vacuum) testing

- Introduction
- Background
- Concept
- Development and validation
- Testing at ESTEC
- Conclusions

2

NPL - Commercial

Introduction

All space-craft need a validated thermal model – tested in a TVC

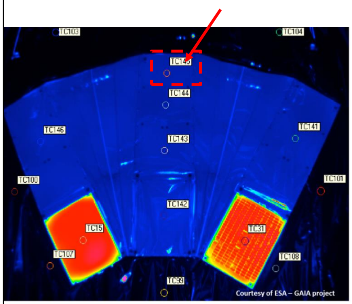

Contact sensor (*limitations*)

- single point; spatially limited
- slow response time (vs camera)
- thermally disruptive (adds to thermal leakage)
- requires all sensors to be perfectly matched (and calibrated) when used in multiples
- visualisation not automatic

Non-contact sensor (*advantages)*

- visualisation available live - detect areas “missed” by contact sensors
- rapid response time (vs. contact sensors)
- non-contact i.e. no thermal disruption, no contamination, or potential for physical damage
- can read true surface temperatures (except if not corrected for ambient/material)

Objective: from captured *apparent* temperature thermal images recover *true* surface temperature

3

Background – Thermal imaging challenges

- Emissivity: varies with temperature, wavelength, surface angle (material structure)
- TVAC: wide temperature range (including sub ambient)
- Background radiation: external (environment & ‘hotspots’) AND local radiant sources can be reflected from the surface of interest
- Robust thermal imaging temperature measurement traceability (temperature calibration)
- Robust thermal / dimensional spatial registration (geometrical calibration)

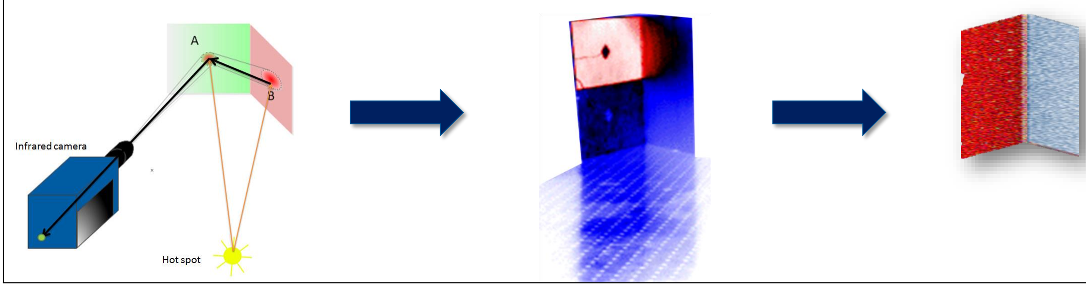

4

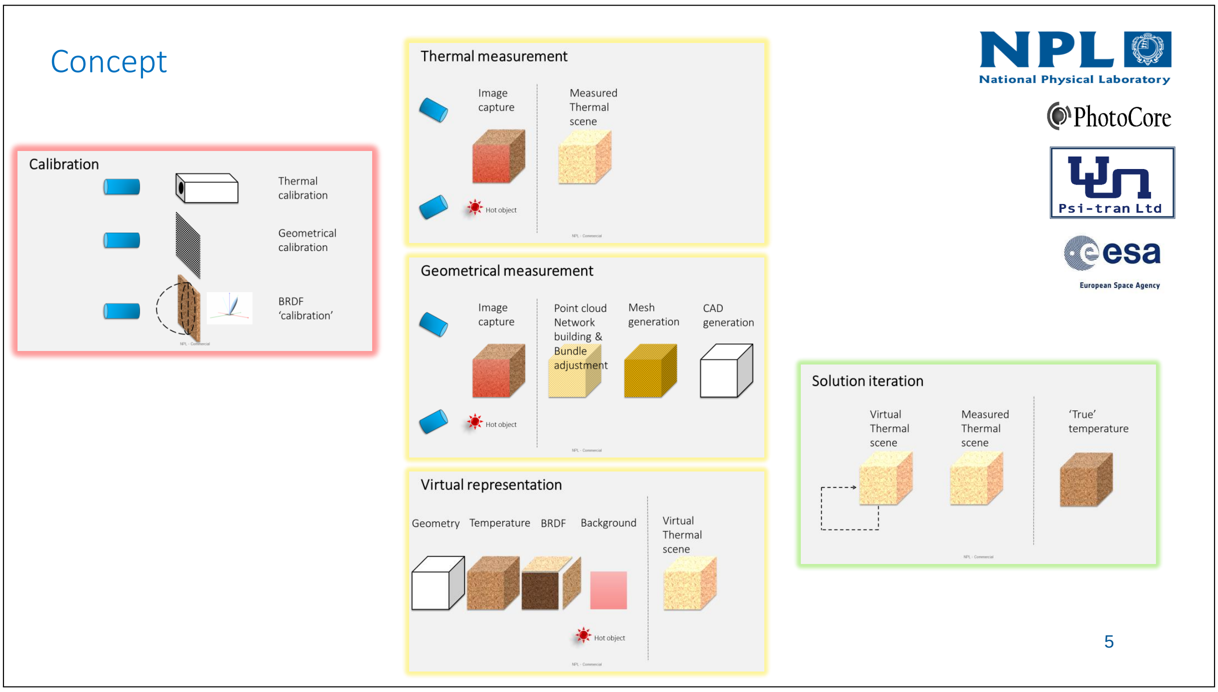
Concept
Calibration
Thermal calibration
Geometrical calibration
BRDF 'calibration'
Thermal measurement
Image capture
Measured Thermal scene
Hot object
Geometrical measurement
Image capture
Point cloud Network building & Bundle adjustment
Mesh generation
CAD generation
Hot object
Virtual representation
Geometry
Temperature
BRDF
Background
Virtual Thermal scene
Hot object
Solution iteration
Virtual Thermal scene
Measured Thermal scene
'True' temperature
NPL
National Physical Laboratory
PhotoCore
Psi-tran Ltd
esa
European Space Agency
5

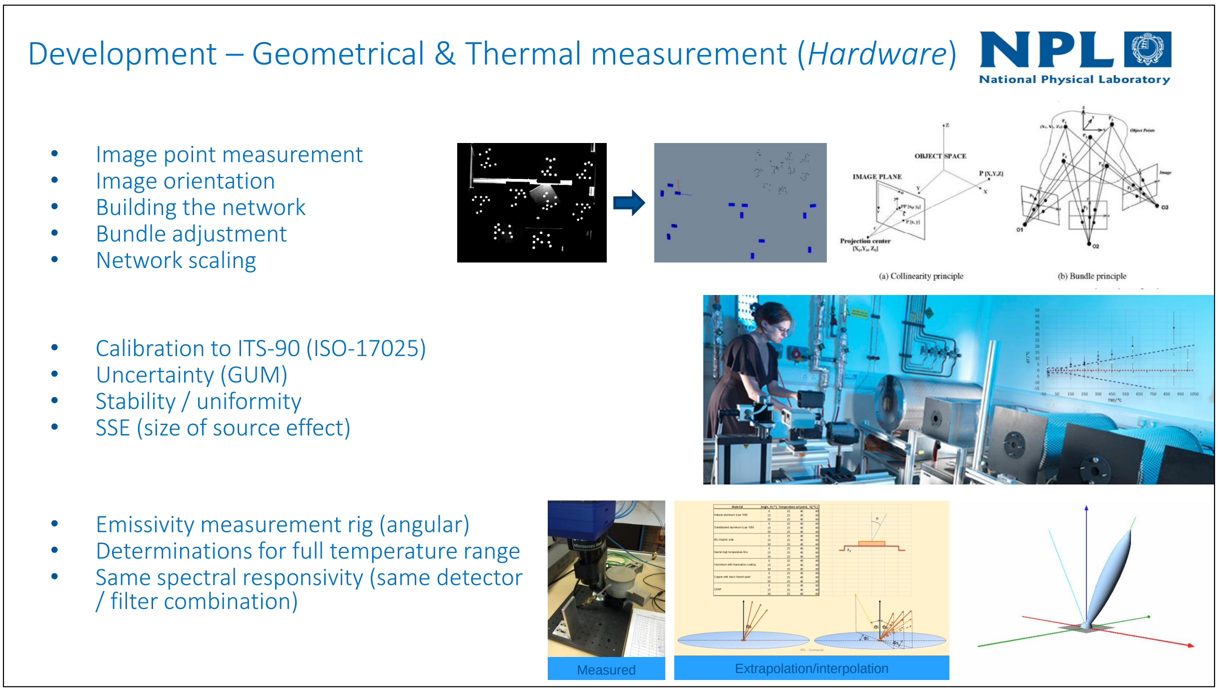
Development – Geometrical & Thermal measurement (Hardware)
NPL
National Physical Laboratory
• Image point measurement
• Image orientation
• Building the network
• Bundle adjustment
• Network scaling
OBJECT SPACE
IMAGE PLANE
Projection center
(a) Collinearity principle
(b) Bundle principle
• Calibration to ITS-90 (ISO-17025)
• Uncertainty (GUM)
• Stability / uniformity
• SSE (size of source effect)
• Emissivity measurement rig (angular)
• Determinations for full temperature range
• Same spectral responsivity (same detector / filter combination)
Measured
Extrapolation/interpolation

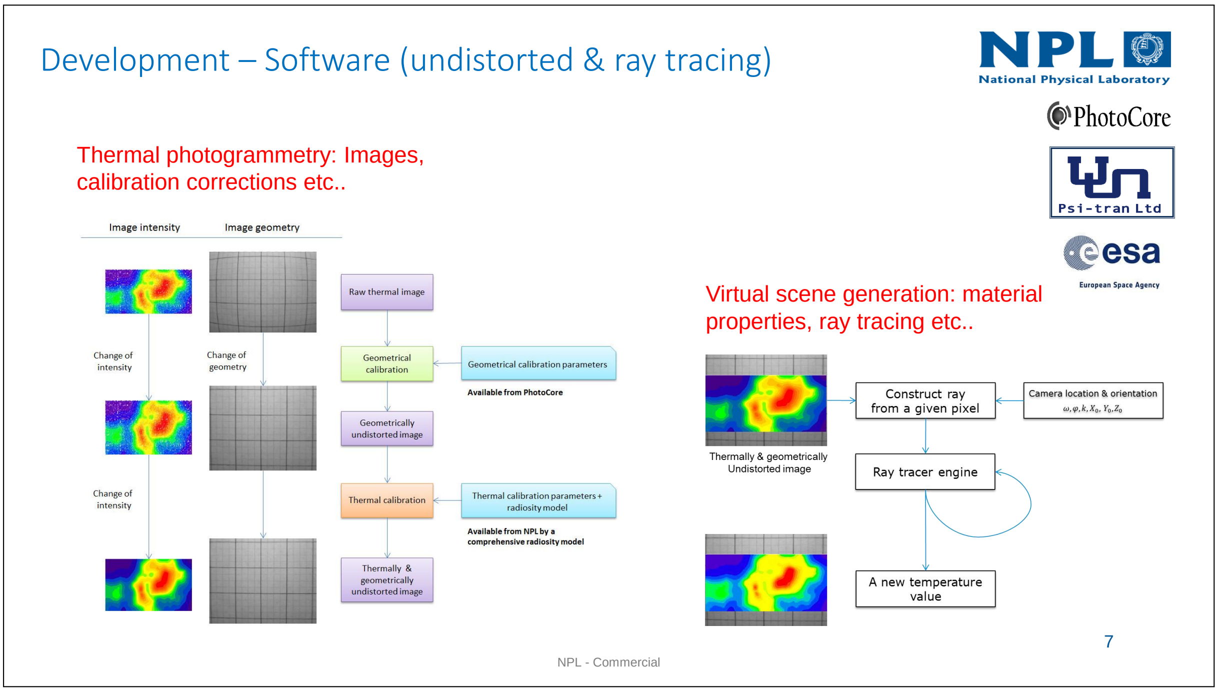
Development – Software (undistorted & ray tracing)
NPL National Physical Laboratory
PhotoCore
Psi-tran Ltd
esa European Space Agency
Thermal photogrammetry: Images, calibration corrections etc..
Image intensity
Image geometry
Change of intensity
Change of geometry
Change of intensity
Raw thermal image
Geometrical calibration
Geometrical calibration parameters
Available from PhotoCore
Geometrically undistorted image
Thermal calibration
Thermal calibration parameters + radiosity model
Available from NPL by a comprehensive radiosity model
Thermally & geometrically undistorted image
Virtual scene generation: material properties, ray tracing etc..
Construct ray from a given pixel
Camera location & orientation
Thermally & geometrically Undistorted image
Ray tracer engine
A new temperature value
7
NPL - Commercial

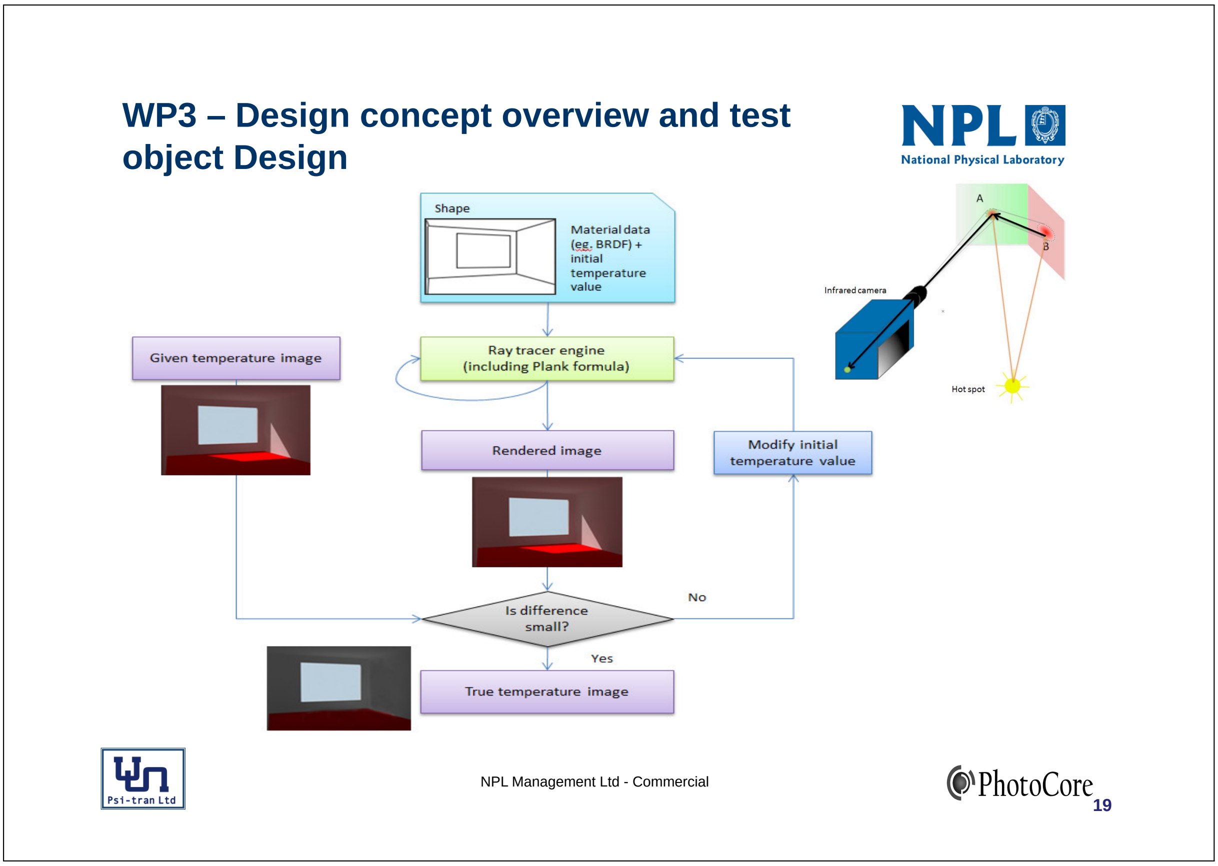
WP3 – Design concept overview and test object Design
NPL National Physical Laboratory
Shape
Material data (eg. BRDF) + initial temperature value
Given temperature image
Ray tracer engine (including Plank formula)
Rendered image
Modify initial temperature value
Infrared camera
Hot spot
A
B
Is difference small?
No
Yes
True temperature image
Psi-tran Ltd
NPL Management Ltd - Commercial
PhotoCore
19

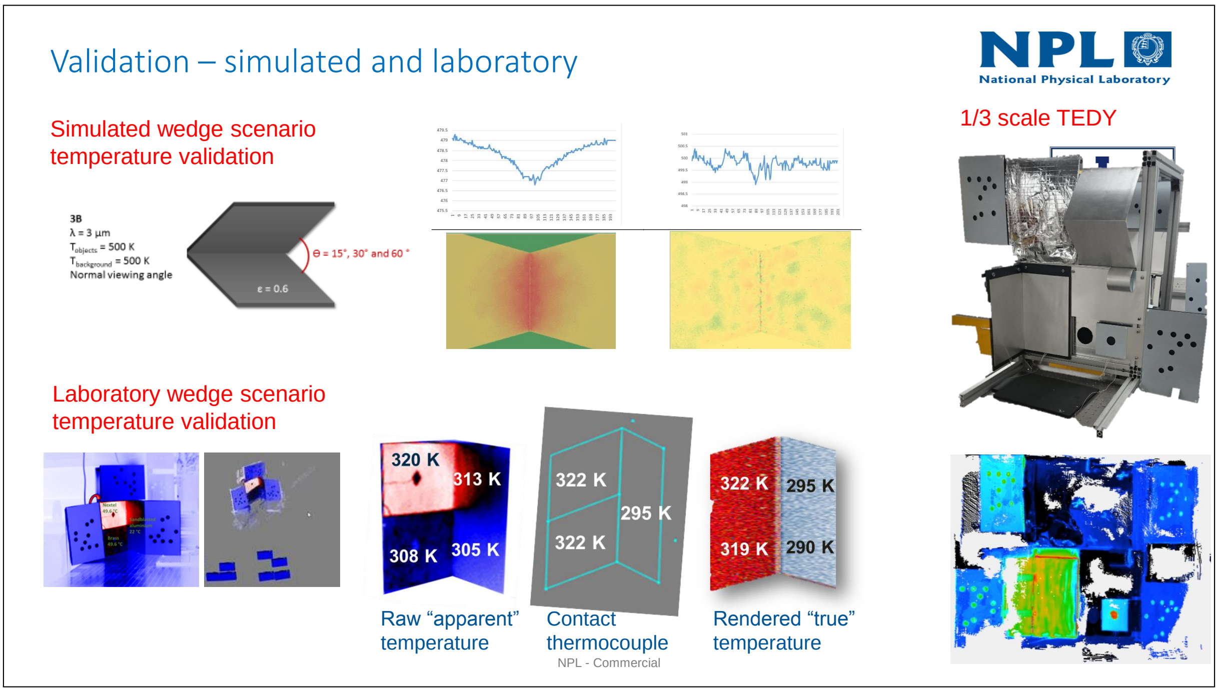

Validation – ESTEC

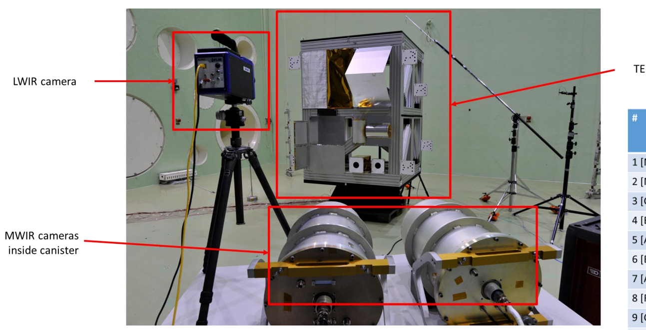

#	E1 20 °C	E2 30 °C	E3 30 °C rpt	E4 50 °C	E5 50 °C +1kW	E6 50 °C rpt	E7 50 °C +2kw	E8 70 °C	E9 70 °C + hotspot
1 [Nextel]	**None**	None	None	None	None	**None**	None	**None**	None
2 [MLI]	**20.5**	-	20.9	20.8	21.2	**21.6**	22.0	**22.4**	21.6
3 [CFRP]	**20.5**	-	20.6	20.9	22.0	**20.9**	22.7	**21.2**	21.3
4 [B1]	**20.7**	-	31.7	51.1	51.5	**51.7**	51.6	**72.3**	73.0
5 [A1]	**20.4**	-	20.6	20.9	21.3	**20.9**	21.1	**21.3**	21.4
6 [B2]	**20.7**	-	31.3	50.3	50.6	**51.2**	50.9	**71.7**	71.8
7 [A2]	**20.4**	-	20.6	20.8	21.2	**20.8**	21.2	**21.1**	21.2
8 [Roof]	**20.5**								
9 [CylHrz]	**20.9**								
10 [CylVrt]	**20.8**								
11 [BB]	**20.8**								

#	E10 50 °C rpt	E11 50 °C set up	E12 50 °C 12.5kW	E13 50 °C 25kW	E14 50 °C Cool down	E15 50 °C 25kW	E16 50 °C Cool down
1 [Nextel]	None	None	None	None	**None**	None	None
2 [MLI]	21.3	21.4	24.0	27.1	**24.5**	27.7	28.5
3 [CFRP]	21.0	21.1	25.6	34.6	**30.9**	32.2	36.3
4 [B1]	50.1	52.9	53.1	53.1	**53.4**	53.8	54.1
5 [A1]	20.8	21.1	21.3	22.9	**22.9**	22.7	23.8
6 [B2]	49.6	51.9	51.8	52.2	**52.2**	52.3	52.6
7 [A2]	20.7	21.0	21.2	22.8	**22.7**	22.4	23.5
8 [Roof]	23.0	23.3	24.0	25.9	**25.9**	25.8	27.3
9 [CylnH]	48.7	49.6	49.9	52.6	**52.6**	52.3	54.0
10 [CylnV]	48.5	49.4	49.9	52.5	**52.2**	52.2	53.9
11 [BB]	48.4	54.8	54.8	55.0	**55.0**	55.1	55.2

NPL - Commercial

8b. WP5 -Pre-test at NPL and ESA pre test and full test at ESTEC – data collection

NPL National Physical Laboratory

- Software validation trials at ESTEC
  - A pre-test was done to check operation of the TEDY and cameras and to trial process some data – this was successful producing similar results to the NPL test.
  - Then - ESTEC TEDY (full test) was done with project team collecting data and pre-evaluation results.
  - TEDY shown in ambient conditions and with 25kw "sun"

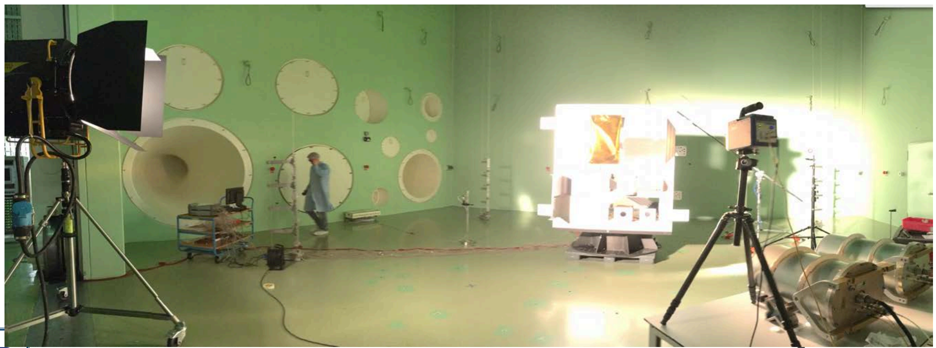

Psi-tran Ltd

NPL Management Ltd - Commercial

PhotoCore 31

8c. WP5 -Pre-test at NPL and ESA pre test and full test at ESTEC – data collection

NPL National Physical Laboratory

- Example test data collected – thermocouple data and example IR image from one MW camera
- 16 data sets in all collected with 2 MW and 1 LW – temperatures of heated zones from 20-70°C

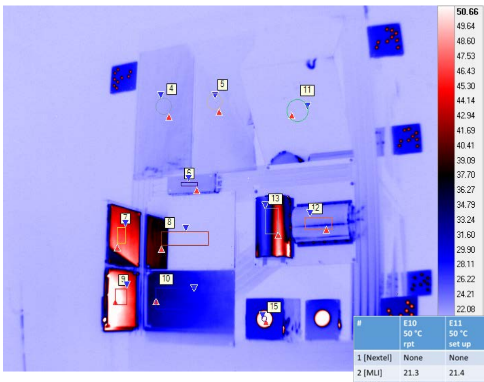

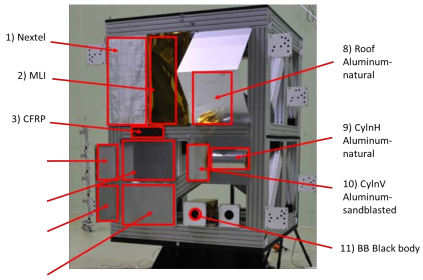

#	E1 20 °C	E2 30 °C	E3 30 °C rpt	E4 50 °C	E5 50 °C +1kW	E6 50 °C rpt	E7 50 °C +2kw	E8 70 °C	E9 70 °C + hotspot
1 [Nextel]	None	None	None	None	None	None	None	None	None
2 [MLI]	20.5	-	20.9	20.8	21.2	21.6	22.0	22.4	21.6
3 [CFRP]	20.5	-	20.6	20.9	22.0	20.9	22.7	21.2	21.3
4 [B1]	20.7	-	31.7	51.1	51.5	51.7	51.6	72.3	73.0
5 [A1]	20.4	-	20.6	20.9	21.3	20.9	21.1	21.3	21.4
6 [B2]	20.7	-	31.3	50.3	50.6	51.2	50.9	71.7	71.8
[illegible]	[illegible]	[illegible]	[illegible]	20.8	21.2	20.8	21.2	21.1	21.2
[illegible]	[illegible]	[illegible]	[illegible]	22.9	23.1	23.2	23.4	25.2	25.1
[illegible]	[illegible]	[illegible]	[illegible]	50.3	50.4	50.4	50.3	70.0	70.0
[illegible]	[illegible]	[illegible]	[illegible]	49.9	50.3	49.9	49.8	69.3	69.2
[illegible]	[illegible]	[illegible]	[illegible]	53.4	54.3	53.4	53.8	70.3	70.6

#	E10 50 °C rpt	E11 50 °C set up	E12 50 °C 12.5kW	E13 50 °C 25kW	E14 50 °C Cool down	E15 50 °C 25kW	E16 50 °C Cool down
1 [Nextel]	None	None	None	None	None	None	None
2 [MLI]	21.3	21.4	24.0	27.1	24.5	27.7	28.5
3 [CFRP]	21.0	21.1	25.6	34.6	30.9	32.2	36.3
4 [B1]	50.1	52.9	53.1	53.1	53.4	53.8	54.1
5 [A1]	20.8	21.1	21.3	22.9	22.9	22.7	23.8
6 [B2]	49.6	51.9	51.8	52.2	52.2	52.3	52.6
7 [A2]	20.7	21.0	21.2	22.8	22.7	22.4	23.5
8 [Roof]	23.0	23.3	24.0	25.9	25.9	25.8	27.3
9 [CylnH]	48.7	49.6	49.9	52.6	52.6	52.3	54.0
10 [CylnV]	48.5	49.4	49.9	52.5	52.2	52.2	53.9
11 [BB]	48.4	54.8	54.8	55.0	55.0	55.1	55.2

Psi-tran Ltd

PhotoCore 32

9b. WP6 – Overview of Test data analysis, performance assessment, conclusions, recommendations and forward outlook

NPL National Physical Laboratory

- Effect of reflections and external hot spots reproduced in the ray traced simulations of the IR temperature field.
- Ray-traced/rendered corrected temperature of all regions agrees to thermocouple almost within uncertainties at k=2 (95%confidence)

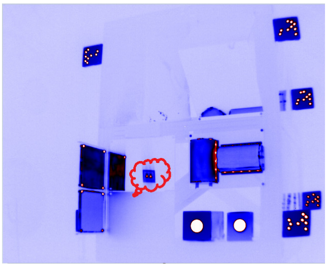

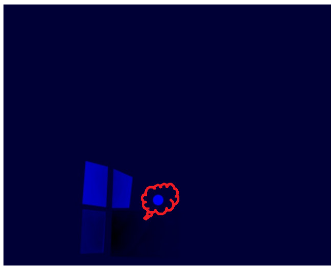

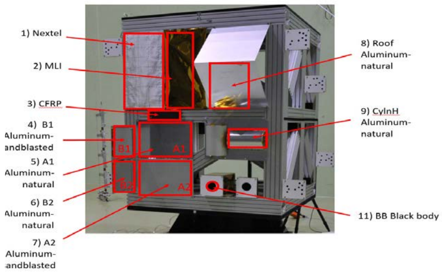

Table 1. Epoch 14 – 50d – after 25kw cool down.

Material and pbrt internal BDRF function	Apparent temperature	Thermocouple temperature	True temperature	Difference temperature
Nextel (0.8, matte)	300	N	301	N
MLI (0.7, mirror)	299	297	302	+5
CFRP (0.9 matte)	306	304	304	0
B1 (0.3, matte)	305	327	330	+3
A1 (0.1, mirror)	306, 297	295	300	+5
B2 (0.1, mirror)	300	325	330	+5
A2 (0.3, matte)	298	295	305	+10
Roof (0.1, mirror)	298	297	302	+5
CylinH (0.1, mirror)	300	326	336	+10
Black body (0.99, matte)	327	328	328	0

Psi-tran Ltd

nercial

PhotoCore

36

Validation – ESTEC: 50 °C (no illumination)

NPL National Physical Laboratory

PhotoCore

Psi-tran Ltd

esa European Space Agency

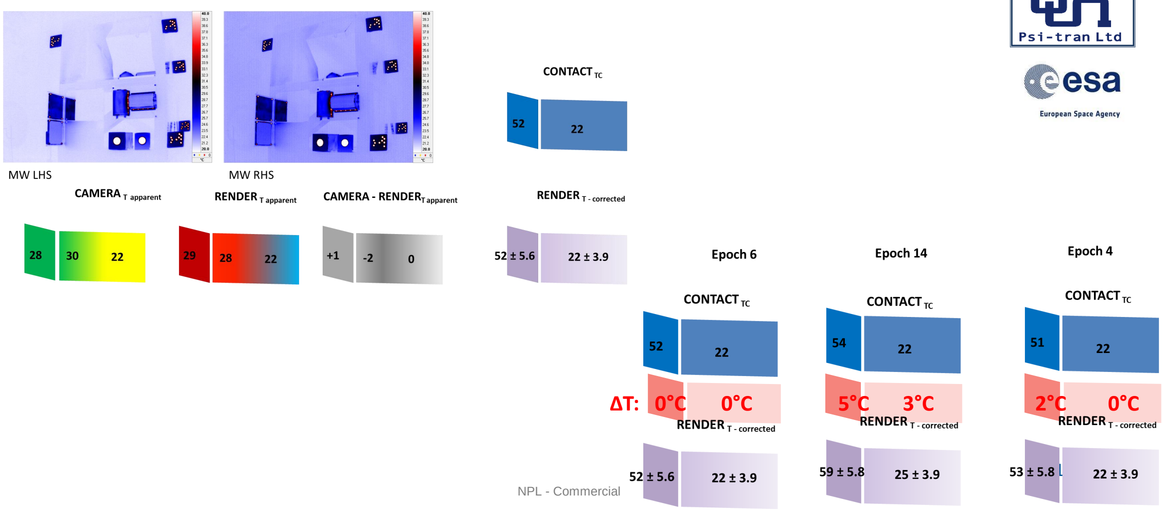

NPL - Commercial

Validation – Uncertainty model

First model uncertainty

Measurement temperarure (IR) =	326	K
Background temperature =	295	K
Surface emissivity =	0.3	
Wavelength =	4.00E-06	µm
c2/lamba Tapparent-1	1.61E-05	
c2/lamba Tsurroundings-1	5.06E-06	
L(TI)+U(emiss) =	-11.54	
L(TI)-U(emiss) =	-11.86	

Symbol	Source of Uncertainty	Value ± std unit	Type	Divisor	Conversion std/°C	Ui
U1	Camera calibration	2.00	B (normal)	1	1	2.0
U2	SSE	0.05	B (normal)	1.73205	0.99999	0.0
U3	Image non-uniformity	5.00	B (rectangular)	1.73205	1	2.9
U4	Distance effect	0.06	B (rectangular)	1.73205	0.88786	0.0
U5	Digitalisation of signal	0.01	B (rectangular)	1.73205	1	0.0
U6	Camera responsivity	0.03	A (normal)	1.00000	1	0.0
U7	T determination of hot objects	2.00	B (rectangular)	1.73205	1	1.2
U8	T determination of background	2.00	B (rectangular)	1.73205	1	1.2
U9	Emissivity of material	0.12	B (normal)	2.00000	70.01	4.2
U10	Camera location	0.06	B (rectangular)	1.73205	1	0.0
U11	Software processing	0.35	A (normal)	1.73205	1	0.2
U12	Ray tracing (BRDF)	1.06	A (normal)	1.73205	1	0.6
				k = 1	U combined	5.8
				k = 2	U combined	11.5

T1	T2
K	K
324	322
330	324

U1	Camera calibration	Value used from manufacturers calibraiton uncertainty and assumed to be k
U2	SSE	Value taken from recent assessment of size of source effect, NPL LW calibra
U3	Image non-uniformity	Value taken from recent calibration assessment of LW IR camera for this ten
U4	Distance effect	Value taken from recent NPL LW IR camera assessment for this temperature
U5	Digitalisation of signal	Estimate from NPL MW IR camera for this temperature set point
U6	Camera responsivity	Estimate from NPL MW IR camera for this temperature set point
U7	T determination of hot objects	Estimate of tempeature determination assuming type T thermocouple used
U8	T determination of background	Estimate of tempeature determination assuming type T thermocouple used
U9	Emissivity of material	Unknown, however estimate taken from recent emissivity investigation with ESTEC and adjusted for this temperature
U10	Camera location	Unknown, likely small effect alignment error from recent NPL LW IR calibration used
U11	Software processing	Multiple runs of software to determine statistical uncertainty
U12	Ray tracing (BRDF)	Multiple runs of software using different BRDF fitted data

Symbol	Source of Uncertainty	Value ± std unit	Type	Divisor	Conversion std/°C	Ui
U1	Camera calibration	1.00	B (normal)	1	1	1.0
U2	SSE	0.05	B (normal)	1.73205	0.99999	0.0
U3	Image non-uniformity	1.00	B (rectangular)	1.73205	1	0.6
U4	Distance effect	0.06	B (rectangular)	1.73205	0.88786	0.0
U5	Digitalisation of signal	0.01	B (rectangular)	1.73205	1	0.0
U6	Camera responsivity	0.03	A (normal)	1.00000	1	0.0
U7	T determination of hot objects	1.00	B (rectangular)	1.73205	1	0.6
U8	T determination of background	1.00	B (rectangular)	1.73205	1	0.6
U9	Emissivity of material	0.05	B (normal)	2.00000	69.64	1.7
U10	Camera location	0.06	B (rectangular)	1.73205	1	0.0
U11	Software processing	0.18	A (normal)	1.73205	1	0.1
U12	Ray tracing (BRDF)	0.64	A (normal)	1.73205	1	0.4
				k = 1	U combined	2.3
				k = 2	U combined	4.6

European Space Agency

11

9f. WP6 – main conclusions

National Physical Laboratory

- The 3-D thermography system can detect most surfaces and reconstruct the surface angles successfully where there is thermal contrast / texture in the image, or where external patterning is “achieved” on mirror surfaces – to better than 1mm at 3m standoff.
- The ray tracing process for correcting temperatures compares well to thermocouple data within the combined standard uncertainty of the system based on a GUM assessment / estimate.
- The system can correct apparent T(IR) temperatures for internal reflections within the structure and external hot sources (where the hot source is correctly modelled or imported into pbrt).
- The system has illustrated how correcting T(IR) temperatures can improve on poorly located thermocouples or where heating is dynamic.
- Uncertainties are on average +/-5°C at 68% confidence with the largest sources of uncertainty being the image non-uniformity and the hemispherical emissivity measurement.
- Uncertainties can be reduced by full traceable calibration of the instruments.

NPL Management Ltd - Commercial

40

Conclusions

- A non-contact temperature measurement solution (hardware + software) is fully operational for testing (in ambient scenario)
- Validation tests proved the uncertainty of the true temperature for the mean case to be within the anticipated range, but can be improved as we see the largest sources of uncertainty can be readily reduced
- The method gives confidence in situations where thermocouples are erroneous (placement / malfunction / transient heating)
- A robust metrological approach (calibration, traceability, uncertainty mapping and standardised procedure) ensuring confidence in the geometrical and thermal outputs

12

NPL - Commercial

Applications:

- In general where:
  - Non-contact thermometry is beneficial or necessary
  - Higher thermal nodes (measurement points) are of benefit / required
  - Additional measurement (e.g. geometric / dynamic) information is required
  - Thermocouples are missed or read wrong due to their location or local transient heating

Future development:

- In situ thermal and geometrical calibration of sensors
- Use of higher resolution IR cameras
- Combining the visible and IR images
- Improving the true temperature estimation
- Speed-up of the computation

13

NPL - Commercial

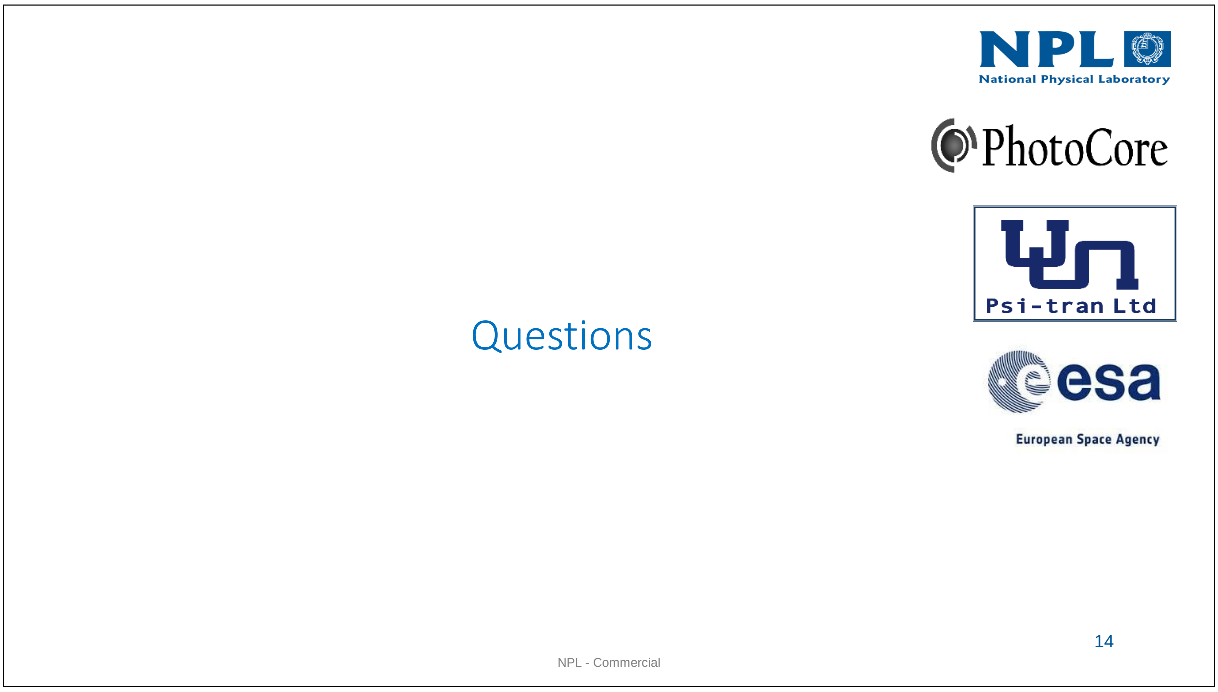
NPL
National Physical Laboratory
PhotoCore
Psi-tran Ltd
esa
European Space Agency
Questions
14
NPL - Commercial

Appendix V

Data exchange for thermal analysis
a status update

James Etchells Duncan Gibson Harrie Rooijackers Matthew Vaughan
(ESA/ESTEC, The Netherlands)

Abstract

This short presentation will give a factual overview of the current status for thermal analysis data exchange. A summary of current known issues and lessons learned will be presented at a practical level. Additionally the status with STEP-TAS and interfaces inside the thermal tools will be covered. Finally the STEP-TAS based TMM converter "TMMverter" will be introduced along with some usage examples.

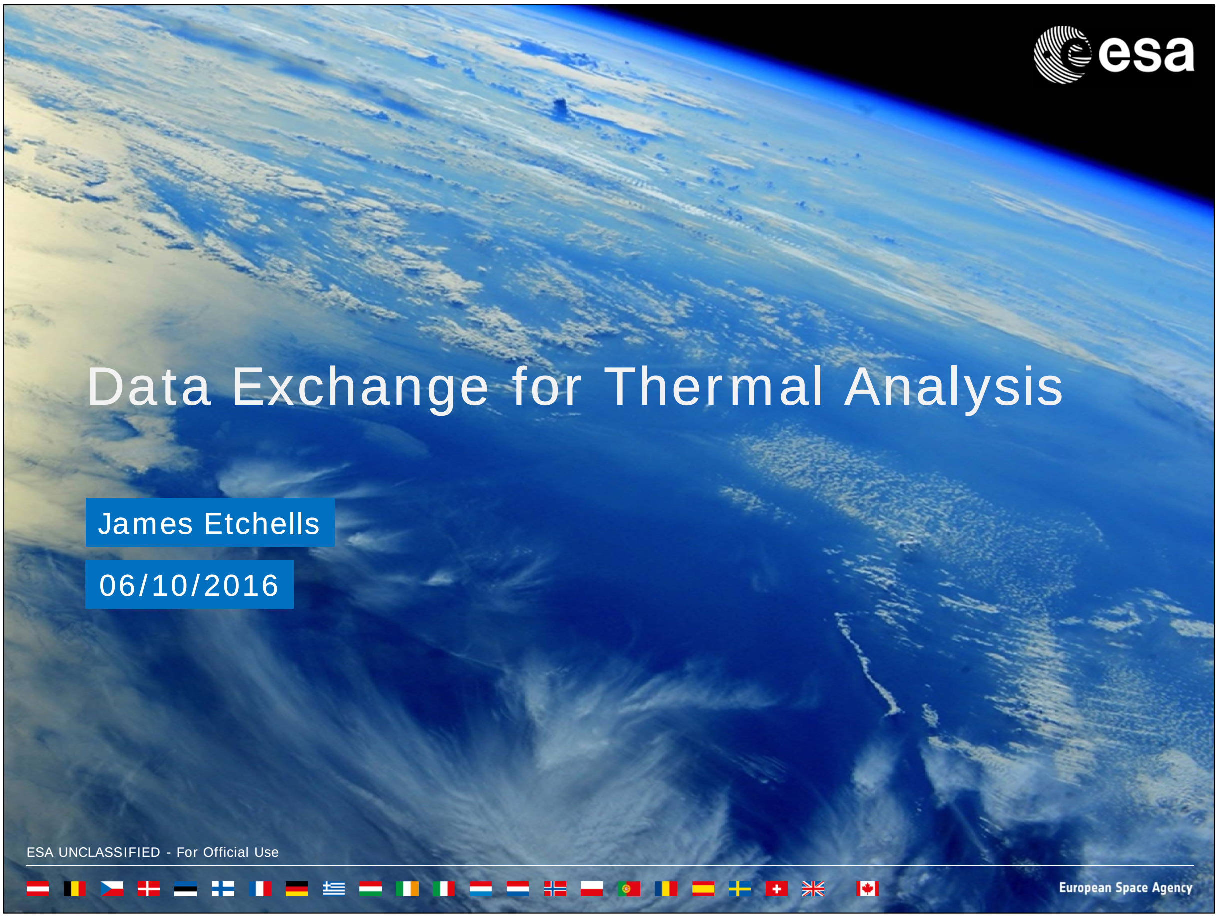
esa
Data Exchange for Thermal Analysis
James Etchells
06/10/2016
ESA UNCLASSIFIED - For Official Use
European Space Agency

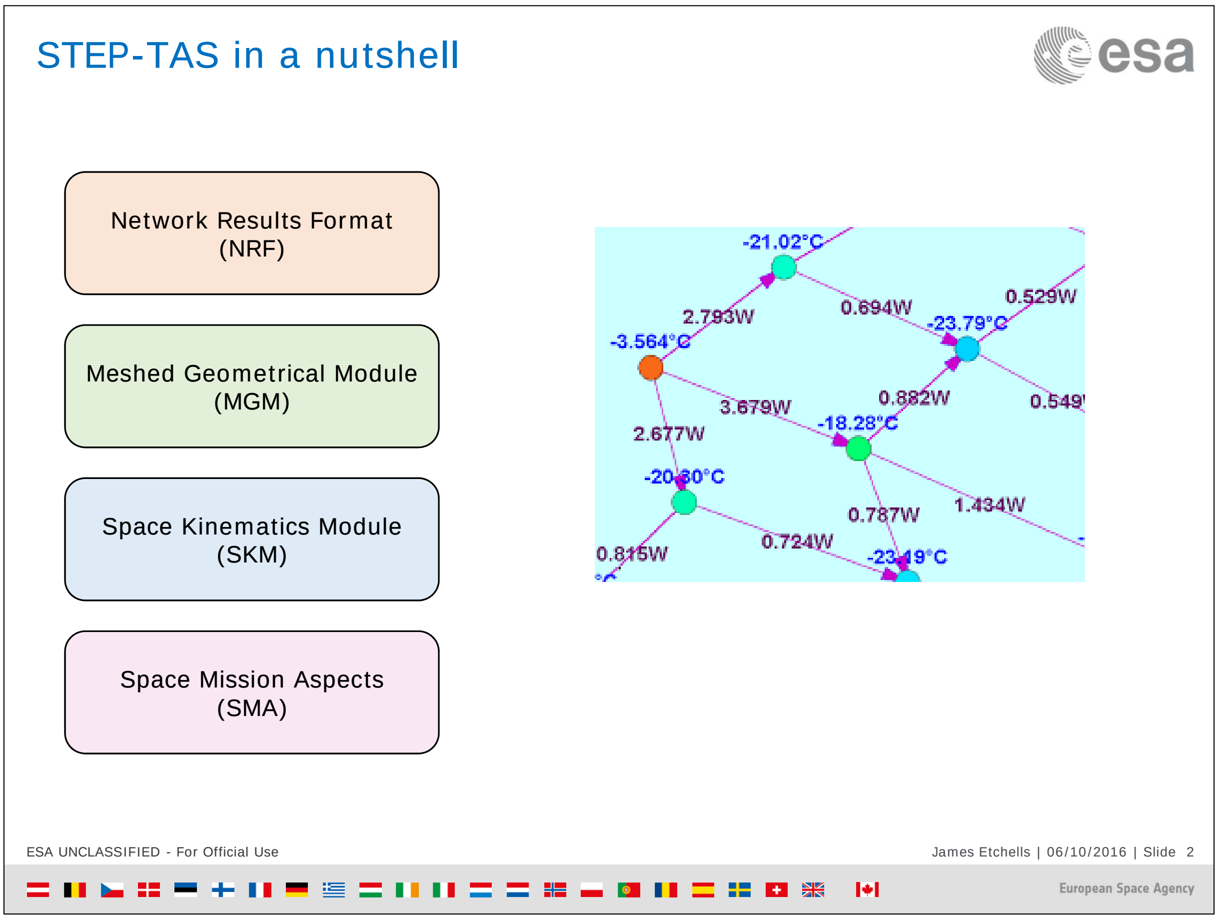
STEP-TAS in a nutshell
esa
Network Results Format (NRF)
Meshed Geometrical Module (MGM)
Space Kinematics Module (SKM)
Space Mission Aspects (SMA)
-21.02°C
2.793W
0.694W
0.529W
-23.79°C
-3.564°C
3.679W
0.882W
-18.28°C
2.677W
-20.30°C
0.787W
1.434W
0.724W
0.815W
-23.49°C
ESA UNCLASSIFIED - For Official Use
James Etchells | 06/10/2016 | Slide 2
European Space Agency

STEP-TAS in a nutshell

Network Results Format (NRF)

Meshed Geometrical Module (MGM)

Space Kinematics Module (SKM)

Space Mission Aspects (SMA)

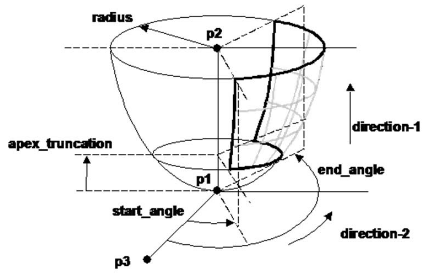

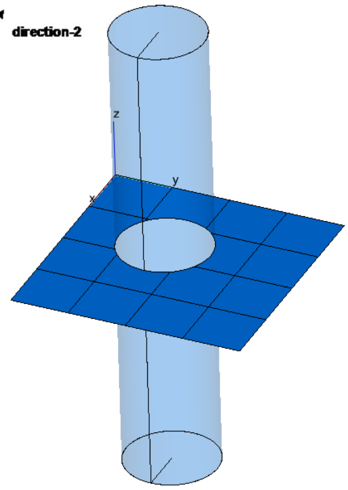

ESA UNCLASSIFIED - For Official Use

James Etchells | 06/10/2016 | Slide 3

European Space Agency

STEP-TAS in a nutshell

Network Results Format (NRF)

Meshed Geometrical Module (MGM)

Space Kinematics Module (SKM)

Space Mission Aspects (SMA)

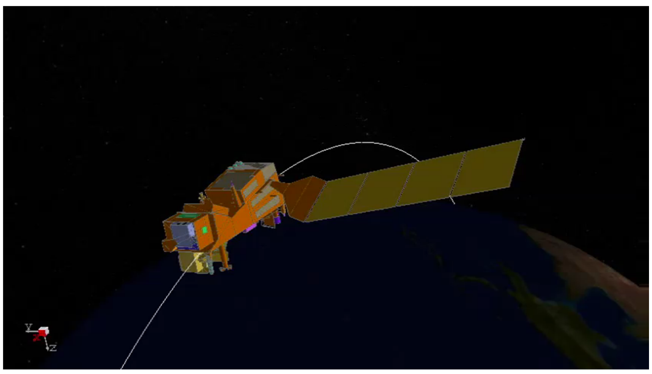

ESA UNCLASSIFIED - For Official Use

James Etchells | 06/10/2016 | Slide 4

European Space Agency

CURRENT STATUS
GEOMETRY

ESA UNCLASSIFIED - For Official Use

James Etchells | 06/10/2016 | Slide 5

European Space Agency

SYSTEMA <-> ESATAN-TMS

- Many conversion have been requested this year
- Native STEP-TAS interfaces working pretty well, several issues resolved
- Boolean cutting is (relatively) new in THERMICA and uses a slightly different approach to ESATAN-TMS
- Things to be aware of: **cutting**, **recursive / heirachical attributes**, **bulks / thicknesses**, **double sides inactivity**

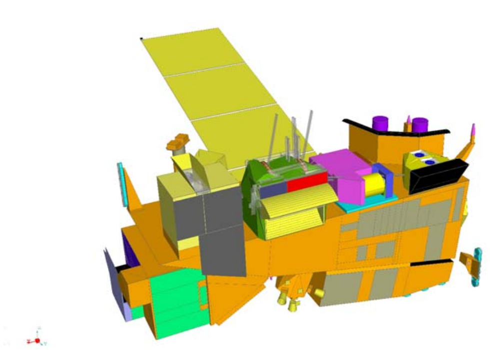

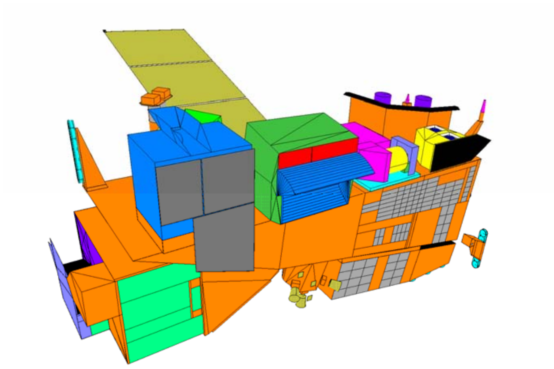

ESA UNCLASSIFIED - For Official Use

James Etchells | 06/10/2016 | Slide 6

European Space Agency

Thermal Desktop + NX Space Systems Thermal

- STEP-TAS 5.2 interfaces were reinstated in recent version
    - up/down converter to version 6.0 can be made available on request
- C&R express some interest in updating to a v6.0 interface and are in communication with ESA – **no funding source, no clear commitment**
- Best approach is currently TRASYS and TASverter to STEP-TAS 6.0 (used frequently in ESA)
- For **NX** an interface does exist, but challenges more fundamental but dialog is open with MAYA to see what we can improve

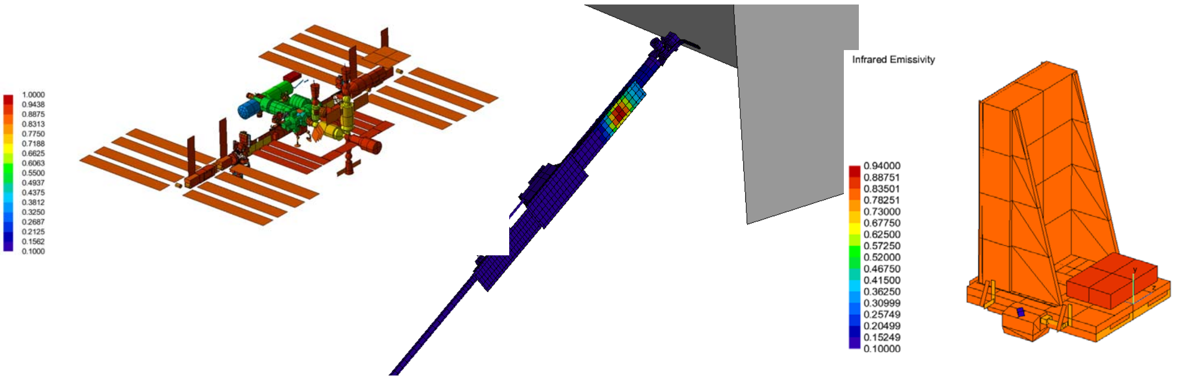

ESA UNCLASSIFIED - For Official Use James Etchells | 06/10/2016 | Slide 7

European Space Agency

Viewer

- Long term request to replace BAGHERA view STEP-TAS viewer

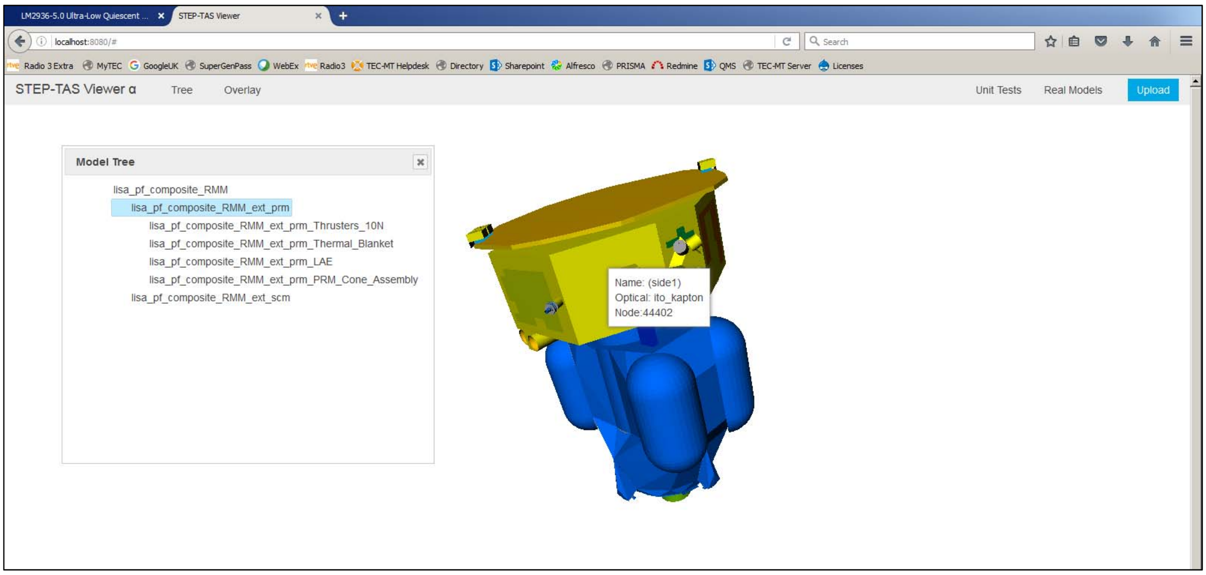

ESA UNCLASSIFIED - For Official Use James Etchells | 06/10/2016 | Slide 8

European Space Agency

CURRENT STATUS
NETWORK MODELS

ESA UNCLASSIFIED - For Official Use | James Etchells | 06/10/2016 | Slide 9

European Space Agency

TMMverter

What is TMMverter?

- Converter of TMMs using STEP-TAS as a neutral format

Features

- Bidirectional conversion between ESATAN and SINDA
- Supports most features of DATA blocks
    - a few rarely used SINDA macros are not implemented
- Most OPERATION block syntax is supported
    - plain MORTRAN/FORTRAN syntax is supported
    - a limited number of tool subroutines are supported (e.g. thermostats, interpolations, etc.) plus user defined mapping file
- Fluid analysis modules (FHTS and FLUINT) and not supported

Validation status

- Currently in a beta status
- Used on a number of real conversions in ESTEC
- Performance is OK
    - Large sets of radiative couplings will slow the tool down

ESA UNCLASSIFIED - For Official Use | James Etchells | 06/10/2016 | Slide 10

European Space Agency

TMMverter: Tips for use

Preparation

- Strip all unnecessary features from the TMM
- In particular remove superfluous user logic for results, reporting etc.

Conversion

- Generally works, but if problems...
- Adopt a step by step approach:
    - First remove all logic and attempt conversion with only DATA blocks
    - Add in part of model step

Verification

- It is essential to carry out a verification of the conversion
- Compare results from native and destination tools and assess the
- Arthimtic nodes,
    - Same (reduced) time step
    - Convergece

ESA UNCLASSIFIED - For Official Use

James Etchells | 06/10/2016 | Slide 11

European Space Agency

CURRENT STATUS

WRAP UP + LINKS

ESA UNCLASSIFIED - For Official Use

James Etchells | 06/10/2016 | Slide 12

European Space Agency

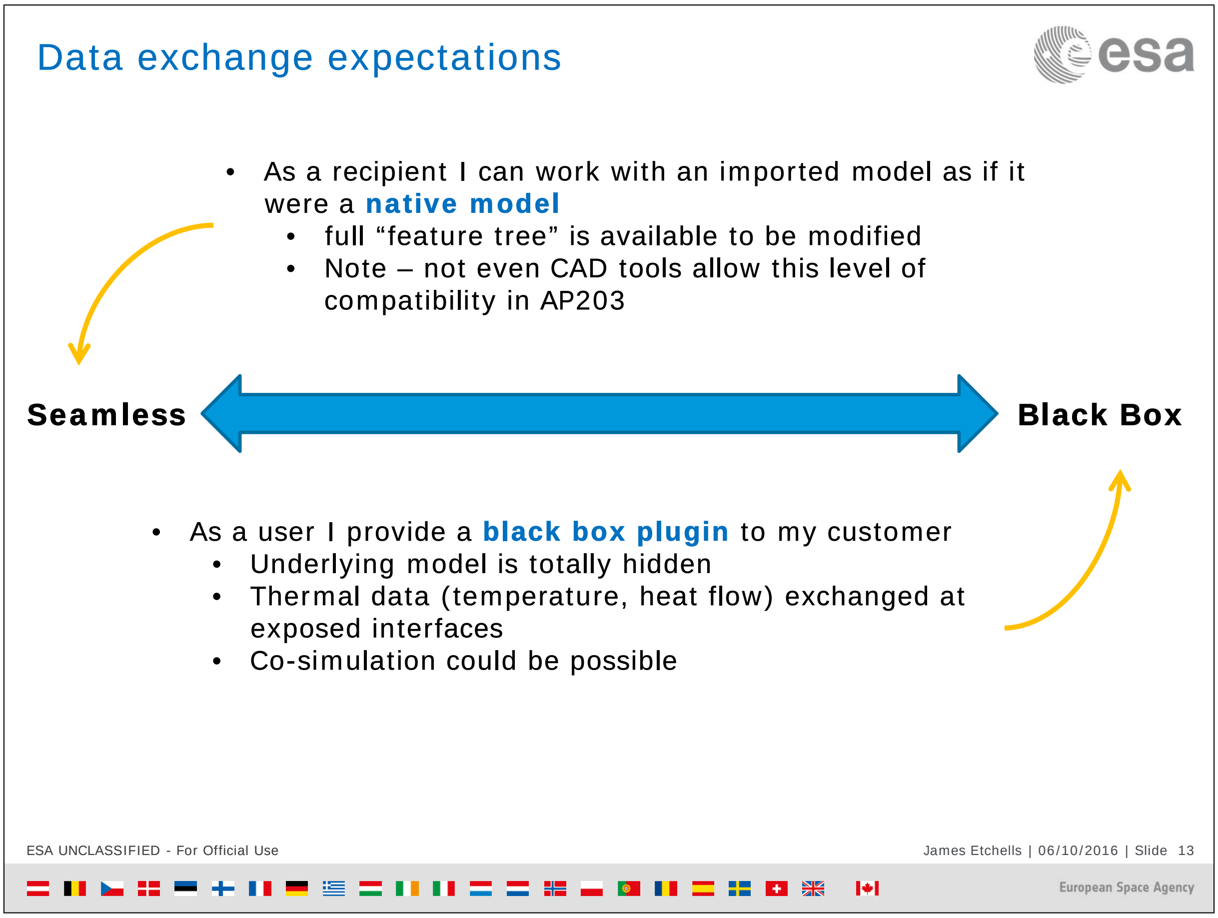
Data exchange expectations
esa
As a recipient I can work with an imported model as if it were a native model
full "feature tree" is available to be modified
Note – not even CAD tools allow this level of compatibility in AP203
Seamless
Black Box
As a user I provide a black box plugin to my customer
Underlying model is totally hidden
Thermal data (temperature, heat flow) exchanged at exposed interfaces
Co-simulation could be possible
ESA UNCLASSIFIED - For Official Use
James Etchells | 06/10/2016 | Slide 13
European Space Agency

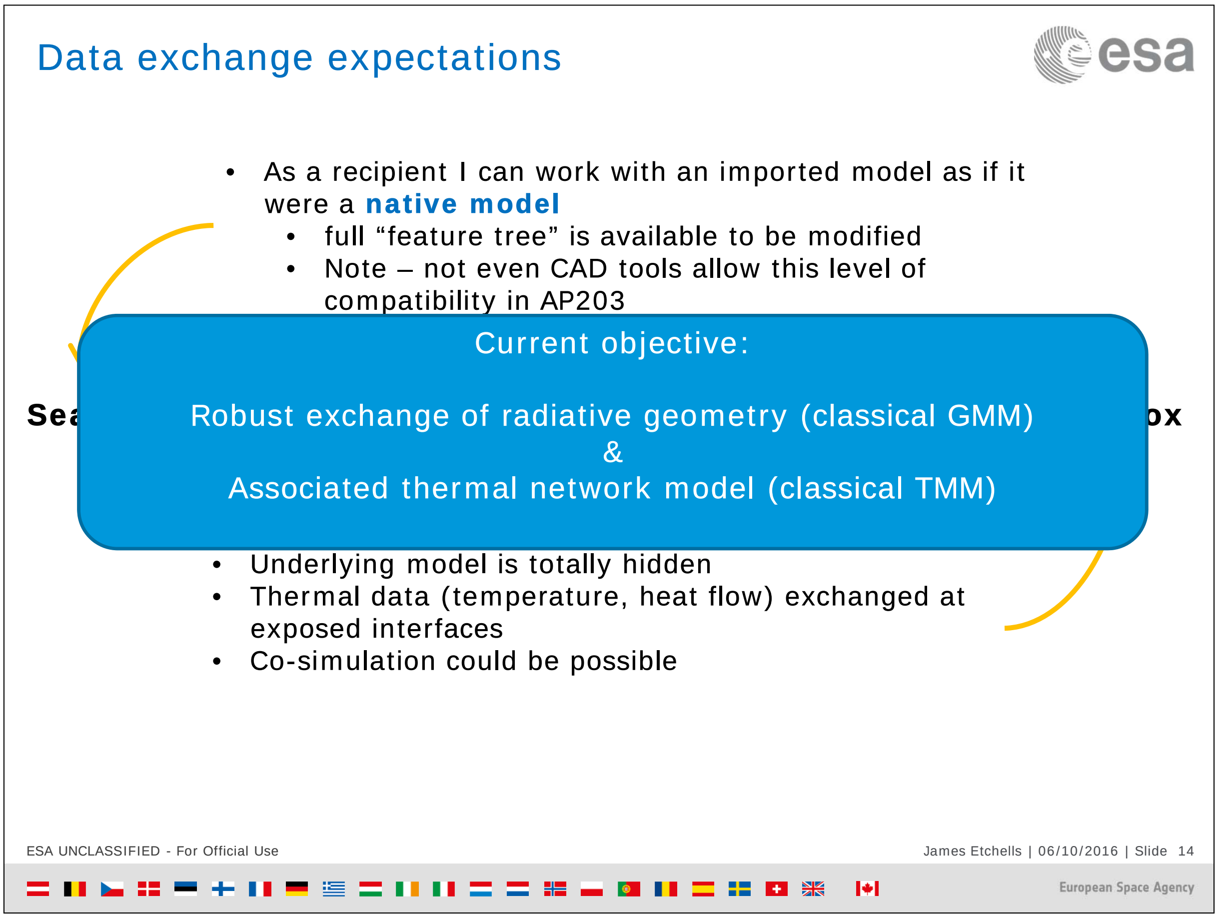
Data exchange expectations
esa
As a recipient I can work with an imported model as if it were a native model
full "feature tree" is available to be modified
Note – not even CAD tools allow this level of compatibility in AP203
Current objective:
Robust exchange of radiative geometry (classical GMM)
&
Associated thermal network model (classical TMM)
Underlying model is totally hidden
Thermal data (temperature, heat flow) exchanged at exposed interfaces
Co-simulation could be possible
ESA UNCLASSIFIED - For Official Use
James Etchells | 06/10/2016 | Slide 14
European Space Agency

Final remarks

- As end users, please:
  - try to **use** the STEP-TAS interfaces
  - **report** any issues to developers, or ESA if you're not sure
  - ESA are available to **support** where possible
  - **plan** conversions ahead, rules and guidelines to simplify model exchange may be needed
- Links:

step-tas@thermal.esa.int

http://exchange.esa.int

ICES-2016-410, A Standard for the Exchange of Thermal Analysis Data (STEP-TAS)

ESA UNCLASSIFIED - For Official Use

James Etchells | 06/10/2016 | Slide 15

European Space Agency

Appendix W

List of Participants

Alsaleh, Turki
KACST
Saudi Arabia
✉ talsaleh@kacst.edu.sa

Alvarez Copano, Miguel
Max-Planck-Institut für Sonnensystemforschung
Germany
✉ alvarez@mps.mpg.de

Baturkin, Volodymyr
DLR, Institute of Space Systems
Germany
✉ volodymyr.baturkin@dlr.de

Bayer, Ralph
German Aerospace Center (DLR)
Germany
✉ Ralph.Bayer@dlr.de

Benthem, Roel
Netherlands Aerospace Centre NLR
The Netherlands
✉ roel.van.benthem@nlr.nl

Bergmann, Kevin
RWTH Aachen
Germany
✉ kevin.bergmann@rwth-aachen.de

Bodendieck, Frank
OHB System AG
Germany
✉ frank.bodendieck@ohb.de

Bonnafous, Bastien
ESA
The Netherlands
✉ bastien.bonnafous@esa.int

Briet, Richard
CNES
France
✉ richard.briet@cnes.fr

Brouquet, Henri
ITP Engines UK Ltd
United Kingdom
✉ henri.brouquet@itp-engines.co.uk

Brunetti, François
DOREA
France
✉ francois.brunetti@dorea.fr

Bures, Nicolas
ITP Engines UK Ltd
United Kingdom
✉ nicolas.bures@itp-engines.co.uk

Caugant, Antoine
Airbus Defence & Space
France
✉ antoine.caugant@airbus.com

Cavanagh, Dominic
Thales Alenia Space UK
United Kingdom
✉ dominic.cavanagh@thalesaleniaspace.com

Cefalo, Bianca
Sonaca Space GmbH
Germany
✉ bianca.cefalo@sonaca-space.com

Checa, Elena
ESA
The Netherlands
✉ Elena.Checa@esa.int

Cheriaux, Loic
AIRBUS SAFRAN-LAUNCHERS
France
✉ loic.cheriaux@astrium.eads.net

Çokgezen, Osman Özgün
Turkish Aerospace Industries (TAI)
Turkey
✉ ozgun.cokgezen@tai.com.tr

Connil, Patrick
THALESALENIASPACE
France
✉ PATRICK.CONNIL@THALESALENIASPACE.COM

Czupalla, Markus
FH Aachen
Germany
✉ czupalla@fh-aachen.de

De Palo, Savino
ThalesAlenia Space
Italy
✉ savino.depalo@thalesaleniaspace.com

Deschamps, Severine
AIRBUS DEFENCE AND SPACE
France
✉ severine.deschamps@airbus.com

Dolce, Silvio
ESA/ESTEC
The Netherlands
✉ silvio.dolce@esa.int

Dumont, Severine
AIRBUS SAFRAN-LAUNCHERS
France
✉ severine.dumont@airbusafran-launchers.com

Ernst, Thilo
AIRBUS DS GmbH
Germany
✉ thilo.ernst@airbus.com

Etchells, James
ESA
The Netherlands
✉ James.Etchells@esa.int

Fernandez de Toro, Jorge
ATG Europe
The Netherlands
✉ jorge.fespegel@gmail.com

Fernandez Rico, German
Max Planck Institute for Solar System Research
Germany
✉ fernandez@mps.mpg.de

Fishwick, Nicholas
Airbus Defence and Space Ltd.
United Kingdom
✉ nicholas.fishwick@airbus.com

Franzoso, Alberto
CGS S.p.A. - Compagnia Generale per lo Spazio
Italy
✉ afranzoso@cgspace.it

Giardino, Marco
BLUE Engineering
Italy
✉ m.giardino@blue-group.it

Gibert, Ferran
University of Trento / INFN
Italy
✉ ferran.gibert@unitn.it

Gibson, Duncan
ESA/ESTEC
The Netherlands
✉ duncan.gibson@esa.int

Giunta, Domenico
ESA
The Netherlands
✉ domenico.giunta@esa.int

Goutagny, Guillaume
DOREA
France
✉ guillaume.goutagny@dorea.eu

Henni-mansour, Samy
Altran technologie
France
✉ samy.henni-mansour@altran.com

Holzwarth, Matthias
Airbus Safran Launchers GmbH
Germany
✉ matthias.holzwarth@airbusafran-launchers.com

Hugonnot, Patrick
THALES ALENIA SPACE FRANCE
France
✉ patrick.hugonnot@thalesaleniaspace.com

Iugovich, Stéphane
AIRBUS Defence & Space
France
✉ stephane.iugovich@airbus.com

Ivanov, Dmitri
European Space Agency
The Netherlands
✉ dmitri.ivanov@esa.int

Jurado Lozano, Pedro Jose
MOLTEK LTD c/o ESA/ESTEC
The Netherlands
✉ PEDRO.JURADO@ESA.INT

Kasper, Stefan
Jena-Optronik GmbH
Germany
✉ stefan.kasper@jena-optronik.de

Katzenberg, Joshua
Airbus Defence and Space Ltd
United Kingdom
✉ joshua.katzenberg@airbus.com

Kirtley, Chris
ITP Engines UK Ltd
United Kingdom
✉ chris.kirtley@itp-engines.co.uk

Kuhlmann, Stephan-André
OHB System AG
Germany
✉ stephan-andre.kuhlmann@ohb.de

Kurt, Ahmet
ASELSAN
Turkey
✉ AKURT@ASELSAN.COM.TR

Laine, Benoit
ESA/ESTEC
The Netherlands
✉ benoit.laine@esa.int

Jacques, Lionel
University of Liege
Belgium
✉ ljacques@ulg.ac.be

Losik, Ilia
JSC Peleng
Belarus, Republic of
✉ ilialosik@gmail.com

Lui, Jeremy
Iceye
Finland
✉ jeremy.lui@iceye.fi

Luzurier, Jerome
Airbus Defence & Space
France
✉ jerome.luzurier@airbus.com

Marach, Siarhei
JSC Peleng
Belarus, Republic of
✉ siarhei.marach@gmail.com

Mas, Guillaume
CNES
France
guillaume.mas@cnes.fr

Maschmann, Marc
Airbus Defence & Space
Germany
marc.maschmann@airbus.com

Melameka, Yannick
Alphid Ltd
United Kingdom
yannick.melameka@alphid.com

Melzack, Nicole
STFC
United Kingdom
nicole.melzack@stfc.ac.uk

Michon, Francois
MDA
Canada
francoismichon1@hotmail.com

Molina, Marco
Leonardo Spa
Italy
marco.molina@leonardocompany.com

Morgan, Scott
Airbus Defence and Space UK
United Kingdom
scott.morgan@airbus.com

Moroni, David
AVIO
Italy
david.moroni@avio.com

Muenstermann, Rolf
Airbus Safran Launchers GmbH
Germany
rolf.muenstermann@airbusafran-launchers.com

Nada, Tarek
National Authority for Remote Sensing and Space Sciences (NARSS)
Egypt
tnada@narss.sci.eg

Nadalini, Riccardo
Sonaca Space GmbH
Germany
riccardo.nadalini@sonaca-space.com

Onufrena, Aleksandra
ESA ESTEC
The Netherlands
aleksandra.onufrena@esa.int

Orgaz, David
Madrid Space
Spain
d.orgaz@madridspace.eu

Pasqualetto Cassinis, Lorenzo
ESA ESTEC
Italy
lorenzopasqualetto@gmail.com

Perez-Grande, Isabel
Universidad Politécnica de Madrid
Spain
isabel.perez.grande@upm.es

Persson, Jan
ESA
The Netherlands
Jan.Persson@esa.int

Peyrou-Lauga, Romain
ESA
The Netherlands
romain.peyrou-lauga@esa.int

Pfeiffer, Matthias
OHB System AG
Germany
matthias.pfeiffer@ohb.de

Pin, Olivier
ESA ESTEC
The Netherlands
Olivier.Pin@esa.int

Poinas, Philippe
ESA-ESTEC-TEC-MTT
The Netherlands
philippe.poinas@esa.int

Pouzin, Julien
ALTRAN
France
julien.pouzin@altran.com

Rana, Hannah
ESA
The Netherlands
hannah.rana@esa.int

Rangone, Jose
INVAP S.E.
Argentina
JRangone@invap.com.ar

Rooijackers, Harrie
ESA/ESTEC
The Netherlands
Harrie.Rooijackers@esa.int

Santoni, Massimo
Leonardo S.p.A.
Italy
massimo.santoni@leonardocompany.com

Schwarz, Christian
ESA
The Netherlands
christian.schwarz@gmail.com

Shaughnessy, Bryan
RAL Space
United Kingdom
bryan.shaughnessy@stfc.ac.uk

Sieber, Gunnar
European Space Agency
The Netherlands
gunnar.sieber@esa.int

Simonian, Samo
ATG Europe
The Netherlands
✉ samo.simonian@atg-europe.com

Smith, Charles
Iceye
Finland
✉ charles.smith@iceye.fi

Solyga, Malgorzata
Sonaca Space GmbH
Germany
✉ malgorzata.solyga@sonaca-space.com

Soriano, Timothée
Airbus Defense and Space
France
✉ timothee.soriano@airbus.com

Soto, Isabel
SENER
Spain
✉ isabel.soto@sener.es

Spalla, Alessandro
OHB-CGS S.p.A.
Italy
✉ ale.d.spalla@gmail.com

Stroom, Charles
Stremen
The Netherlands
✉ charles@stremen.xs4all.nl

Supper, Wolfgang
ESA/ESTEC
The Netherlands
✉ wolfgang.supper@esa.int

Theroude, Christophe
Airbus Defence & Space
France
✉ christophe.theroude@airbus.com

Tiedemann, Lars
HPS GmbH
Germany
✉ tiedemann@hps-gmbh.com

Tirelli, Matteo
AVIO
Italy
✉ stageprc05@service.avio.com

Tonellotto, Giulio
ESA/ESTEC
The Netherlands
✉ giulio.tonellotto@esa.int

Torralbo, Ignacio
IDR/UPM
Spain
✉ ignacio.torralbo@upm.es

Tosetto, Andrea
BLUE Engineering
Italy
✉ a.tosetto@blue-group.it

Triebig, Christoph Maximilian
OHB System AG
Germany
christoph@triebig.com

Trinoga, Martin
Airbus-Safran Launchers GmbH
Germany
martin.trinoga@airbusafran-launchers.com

Triquigneaux, Benoit
ALTRAN TECHNOLOGIE
France
benoit.triquigneaux@altran.com

Tustain, Samuel
RAL Space
United Kingdom
samuel.tustain@stfc.ac.uk

Ulfers, Hendrik
OHB
Germany
hendrik.ulfers@ohb.de

Unique, Guillaume
OHB Sweden
Sweden
guillaume.unique@ohb-sweden.se

Valentini, David
THALES ALENIA SPACE
France
david.valentini@thalesaleniaspace.com

Várhegyi, Zsolt
C3S LLC.
Hungary
zsolt.varhegyi@gmail.com

Vullings, Michiel
ATG Europe
The Netherlands
michiel.vullings@atg-europe.com

Vyas, Shubham
TU Delft
The Netherlands
S.Vyas@student.tudelft.nl

Winter, Daniel
IABG mbH
Germany
WinterD@iabg.de

Zabalza, Leire
Lidax
Spain
leire.zabalza@lidax.com

Zevenbergen, Paul
Airbus Defence & Space Netherlands BV
The Netherlands
p.zevenbergen@airbusds.nl